Metabolism of methane and propane and the role of the glyoxylate bypass enzymes in *Methylocella silvestris* BL2

Andrew Crombie

A thesis submitted to the School of Life Sciences in fulfilment of the requirements for the degree of Doctor of Philosophy

September 2011

University of Warwick
Coventry, UK

Contents

List of figures

List of tables

Declaration

I declare that the work presented in this thesis was conducted by me under the direct supervision of Professor J. Colin Murrell, with the exception of those instances where the contribution of others has been specifically acknowledged. None of the work presented has been previously submitted for any other degree. Some of the data presented in Chapters 3 and 4 have been published as part of manuscripts (Chen, Y. *et al.* Complete genome sequence of the aerobic facultative methanotroph *Methylocella silvestris* BL2. *J. Bacteriol.* **192**, 3840-3841, (2010), and Crombie, A., and Murrell, J.C. (2011) Development of a system for genetic manipulation of the facultative methanotroph *Methylocella silvestris* BL2. *Methods Enzymol* **495**: 119-133).

Andrew Crombie

Acknowlegements

I would like to acknowledge the expert guidance and generous support of my supervisor, Professor Colin Murrell. I would like to thank past and present members of the Murrell Lab, members of other research groups and the departmental support staff at the University of Warwick, for help and advice during my PhD. I am indebted to Professors Dave Hodgson (University of Warwick) and Chris Anthony (University of Southampton) for expert advice and useful discussions. I thank Vibhuti Patel, Nisha Patel, Sue Slade and the Biological Mass Spectrometry and Proteomics Group at the University of Warwick for proteomic analysis.

Abbreviations

ADH	alcohol dehydrogenase
Amp^R	ampicillin (resistance)
ANOVA	analysis of variance
ADP	adenosine diphosphate
AMP	adenosime monophosphate
ATP	adenosine triphosphate
BHR	broad-host range
BIS	*N*,*N*′-methylenebisacrylamide
BIS TRIS	2-[Bis-(2-hydroxyethyl)-amino]-2-hydroxymethyl-propane-1,3-diol
BLAST	basic local alignment search tool
bp	base pairs
BSA	bovine serum albumin
CBB	Calvin Benson Bassham cycle
CHES	2-(cyclohexylamino)ethanesulfonic acid
CTAB	cetyl trimethylammonium bromide
DAMS	dilute ammonium mineral salts
Da	Dalton
DCPIP	2,6-dichlorophenolindophenol
DH	dehydrogenase
DMF	dimethylformamide
DMSO	dimethylsulfoxide
DNA	deoxyribonucleic acid
DNase	deoxyribonuclease
DNMS	dilute nitrate mineral salts
dNTP	deoxynucleotide triphosphate
dO_2	dissolved oxygen
DTT	dithiothreitol
dw	dry weight
EDTA	ethylendiaminetetraacetic acid
EMC	ethylmalonyl-CoA
ESI	electrospray ionisation
FID	flame ionisation detector
FAD	flavin-adenine dinucleotide
g	gram / acceleration due to gravity
GC	gas chromatography
GFP	green fluorescent protein
$Gm^{(R)}$	gentamicin (resistance)
h	hour
H_4F	tetrahydrofolate
H_4MPT	tetrahydromethanopterin
HEPES	4-(2-hydroxyethyl)-1-piperazineethanesulfonic acid
ICDH	isocitrate dehydrogenase

ICL	isocitrate lyase
KDPG	2-keto-3deoxy-6-phosphogluconate
$Km^{(R)}$	kanamycin (resistance)
l	litre
LacZ	β-galactosidase
LC/ESI	liquid chromatography electrospray ionisation
LDH	lactate dehydrogenase
M	molar
MCS	multiple cloning site
MDH	methanol dehydrogenase
MES	2-(*N*-morpholino)ethanesulfonic acid
MIC	minimum inhibitory concentration
mg	milligram
min	minute
MK	myokinase
ml	millilitre
mM	millimolar
mol	mole
MOPS	3-(N-morpholino)propanesulfonic acid
mRNA	messenger RNA
MS	malate synthase
MSA	malate synthase (acetate assimilation)
MSG	malate synthase (glycolate assimilation)
MS/MS	tandem mass spectrometry
MTBE	methyl *tert*-butyl ether
NAD^+	nicotinamide adenine dinucleotide (oxidised form)
NADH	nicotinamide adenine dinucleotide (reduced form)
$NADP^+$	nicotinamide adenine dinucleotide phosphate (oxidised form)
NADPH	nicotinamide adenine dinucleotide phosphate (reduced form)
NCBI	National Centre for Biotechnology Information
ng	nanogram
NMS	nitrate mineral salts
NTC	no-template control
OD_{540}	optical density at 540 nm
orf	open reading frame
ori	origin of replication
oriT	origin of transfer
PAGE	polyacrylamide gel electrophoresis
PCR	polymerase chain reaction
PEP	phosphoenolpyruvate
PIPES	1,4-piperazinediethanesulfonic acid
PK	pyruvate kinase
PMS	phenazine methosulfate
PQQ	pyrroloquinoline quinone
PRK	phosphoribulokinase
pMMO	particulate methane monooxygenase
PrMO	propane monooxygenase
RBS	ribosomal binding site
RFLP	restriction fragment length polymorphism
RNA	ribonucleic acid

RNase	ribonuclease
rRNA	ribosomal ribonucleic acid
RT-PCR	reverse transcriptase PCR
RubisCO	ribulose 1,5-bisphosphate carboxylase-oxygenase
RuMP	ribulose monophosphate
s	seconds
SD	Shine-Dalgarno
SDIMO	soluble diiron monooxygenase
SDS	sodium dodecyl sulphate
SGAT	serine-glyoxylate aminotransferase
sMMO	soluble methane monooxygenase
TAE	tris acetate EDTA
TBE	tris borate EDTA
TCA	trichloroacetic acid / tricarboxylic acid
TCE	trichloroethylene
TE	tris EDTA
TEMED	*N*,*N*,*N*′,*N*′-tetramethyl-ethane-1,2-diamine
$TMSCHN_2$	trimethylsilyldiazomethane
Tricine	N-(2-Hydroxy-1,1-bis(hydroxymethyl)ethyl)glycine
Tris	tris(hydroxymethyl)aminomethane
v/v	volume to volume
w/v	weight to volume
X-gal	5-bromo-4-chloro-3-indoyl-β-D-galactoside

Abstract

Methylocella silvestris BL2 is a moderately acidophilic facultative methanotroph isolated from forest soil in 2003. Uniquely, it has the ability to grow on a wide range of multi-carbon compounds in addition to methane. An analysis of growth conditions identified the requirements for robust and predictable growth on a wide range of substrates. A simple and effective method of targeted mutagenesis was developed, which relies on electroporation with a linear DNA fragment, and several strains with deletions of key enzymes were constructed using this method. Deletion of isocitrate lyase demonstrated that this enzyme is required for growth on both one-carbon and two-carbon compounds. The second enzyme of the glyoxylate cycle, malate synthase, was shown to be essential for growth on two-carbon compounds. However, surprisingly, deletion of glyoxylate cycle enzymes had a dramatic effect on expression of methanol dehydrogenase. Possible causes of this effect are discussed. Surprisingly, *M. silvestris* was able to grow on propane and the presence and expression of a gene cluster encoding a putative propane monooxygenase was confirmed. This enzyme was found to be a second soluble diiron monooxygenase (SDIMO) with homology to the propane monooxygenase from *Gordonia* TY5, identifying *M. silvestris* as the first known methanotroph to contain SDIMOs from more than one group. Deletion of these enzymes in turn was used to determine the requirement for each during growth on methane or propane. The soluble methane monooxygenase (sMMO) was found to be capable of oxidising propane, whereas the propane monooxygenase (PrMO) was unable to oxidise methane. However, although a strain lacking the PrMO was capable of growth on 2.5% (v/v) propane, it was unable to grow on this gas at 20% (v/v), and at 2.5%, assimilation into biomass was less efficient in comparison to the wild-type. Evidence is presented that products of oxidation of propane by the sMMO may be toxic to the cell or inhibitory to growth in the absence of the PrMO. Both the sMMO and the PrMO were found to be capable of oxidation of a wide range of aliphatic and aromatic compounds, including xenobiotics, suggesting a possible role in bioremediation. *M. silvestris* BL2 was found to oxidise propane at both terminal and sub-terminal positions, resulting in 1-propanol and 2-propanol respectively, and biochemical methods were used to assay the enzymes of terminal and sub-terminal pathways. Assimilation of 1-propanol was found to be by the methylmalonyl-CoA pathway, and the data suggested that 2-propanol was oxidised to acetone and acetol. The final gene of the PrMO gene-cluster, predicted to encode a flavin adenine dinucleotide (FAD)-containing enzyme with homology to characterised membrane-bound D-gluconate dehydrogenase from *Gluconobacter* spp., was found to be essential for growth on 2-propanol and acetone and may be involved in the oxidation of acetol during propane metabolism by the sub-terminal pathway.

Chapter 1

Introduction

1.1 The methane budget and the significance of methane in the atmosphere

Methane occurs in the atmosphere in the highest concentration of any of the organic trace gases, and increased from about 715 ppb in pre-industrial times to 1,774 ppb in 2005. The recent values are more than double the highest of the past 650,000 years, according to ice core records (IPCC, 2007). Since methane is a much more effective greenhouse gas than carbon dioxide, (approximately 24 times mol for mol (Wuebbles and Hayhoe, 2002)), the resultant radiative forcing is about 0.48 compared to 1.66 Wm^{-2} for CO_2 (IPCC, 2007). Inclusion of indirect forcings due to formation of methane-derived stratospheric water vapour and ozone in the troposphere increases the forcing due to methane to 0.8 Wm^{-2}, approximately half the value due to CO_2 (Hansen et al., 2007). The growth rate of atmospheric methane decreased from the early 1980s until the end of the century and then remained close to zero until 2006, before resuming recently (Bousquet et al., 2006; Rigby et al., 2008; Dlugokencky et al., 2011). The short atmospheric lifetime (approximately 8 yr (Lelieveld et al., 1998)) and relatively minor imbalance between sources and sinks suggests that reduction in methane emissions would have rapid and cost-effective benefits for climate (Hansen et al., 2000). Clearly, effective mitigation strategies require a thorough understanding of the global- and regional-scale budget and knowledge of the response of source and sink elements to changing conditions. Estimates of anthropogenic and natural methane emissions total approximately 574 Tg CH_4 yr^{-1}, (Reay et al., 2010), and are shown in Figure 1.1. The major sources are biological, in particular the anaerobic conversion of substrates such as H_2, CO_2 and acetate, arising from the degradation of organic matter, by methanogenic *Archaea*, although methane is also emitted from natural gas and coal deposits, mainly during extraction processes. However, considerable uncertainties exist in respect of methane sources. Recently, a significant source term (> 60 Tg yr^{-1}) from plants was proposed (Keppler et al., 2006). Although controversial (Nisbet et al., 2009), recent research suggests that plants may emit methane either as a product of pectin degradation, by transpiration of anaerobically-produced methane in soils, or by colonisation of above-ground plant structures by methanogens (Keppler et al., 2008; Martinson et al., 2010; Rice et al., 2010). Geological sources such as macro- and micro-seeps, mud volcanoes and geothermal areas have recently been estimated at 45 - 64 Tg y^{-1}, (Kvenvolden and Rogers, 2005;

Etiope et al., 2008), whereas they had previously been ignored or identified as much less significant.

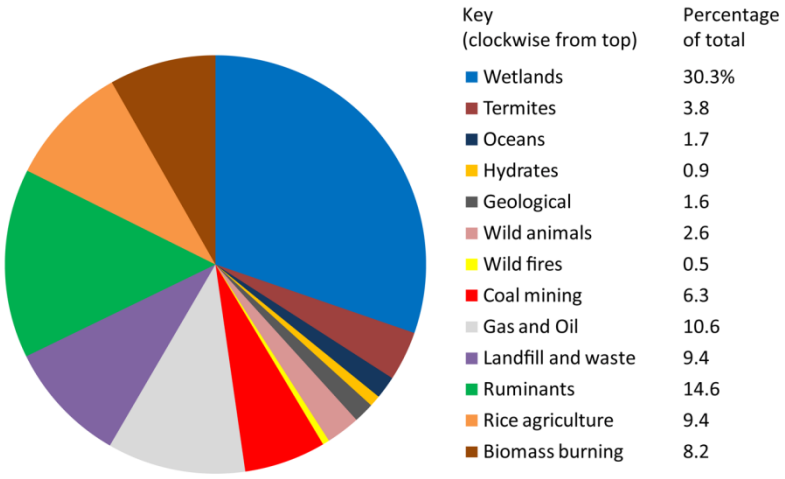

Figure 1.1. Sources of methane to the atmosphere. Compiled using data from Reay et al., (2010).

Global sinks of methane total 536 Tg CH_4 yr^{-1}, of which over 90% is atmospheric photochemical oxidation by hydroxyl radicals, predominately in the troposphere but also in the stratosphere (Lelieveld et al., 1998), and the remainder (30 Tg CH_4 yr^{-1}) is oxidation by soils. Methane produced by methanogenic bacteria during the decomposition of organic material in anaerobic conditions is oxidised in aerobic zones by methane oxidising bacteria (methanotrophs). This can result in soils constituting either a source or a sink for methane. Water-saturated or submerged soils (wetlands), ricefields and landfill sites generally comprise methane sources, whereas upland soils consume atmospheric methane and constitute around 10% of the global methane sink (Le Mer and Roger, 2001). Of course, methanotrophs are not only active in soils which constitute a net methane sink, and these soils may often be distinguished from soils which emit methane by their low levels of methane production. It has been estimated that, overall, consumption in soils is greater than total net emissions from all sources (Reeburgh, 2007). Therefore, most methane, whether of geological origin or produced in anoxic zones by methanogens, is oxidised nearer the soil surface where oxygen is present, before it reaches the atmosphere, and the soil sink term (30 Tg CH_4 yr^{-1}) represents less than 10% of total

biologically oxidised methane. The low-affinity methanotrophs responsible are well-characterised compared to their high-affinity relatives associated with methane-consuming soils (Kolb et al., 2005).

1.2 Factors influencing methane oxidation

As well as being an important greenhouse gas, methane is also subject to feedback mechanisms resulting from climate change. Anaerobic methanogenesis is highly sensitive to temperature change (Conrad, 1996), such that the sulfate aerosol produced by the 1991 eruption of Mt Pinatubo, which caused a temporary 0.5° C average global fall in temperature, is estimated to have lessened 1992 methane emissions from wetlands by 2 Tg (Lelieveld et al., 1998). Alternatively, drying of wetlands and a lowering of the water table might extend the aerobic zone in which methanotrophs operate, thereby reducing emissions to the atmosphere.

Land-use change can alter methane uptake or emission from soils (Knief et al., 2005). Addition of fertiliser often reduces uptake of atmospheric methane (Conrad, 1996), since ammonium competitively inhibits methane oxidation by methanotrophs and nitrifying bacteria (Steudler et al., 1989). Methanotroph community structure has been investigated in many environments and key active organisms identified by cultivation-independent techniques such as DNA- or RNA- stable isotope probing (SIP) (Chen and Murrell, 2010). Numerous strains have been identified and isolated since the groundbreaking work of Whittenbury and colleagues in the 1970s. However, the response of these organisms *in situ* to changing environmental conditions is hard to predict. The largest natural source of methane is wetlands. Large amounts of carbon (approximately 1000 Gt) are contained in permafrost-underlain Arctic wetlands in northern latitudes (Zimov et al., 2006), and these ecosystems are predicted to change in response to climate warming, as thawing of permafrost will release organic matter and alter water levels. Here, carbon uptake and emission are approximately balanced, but 5% of carbon is emitted in the form of methane (Anisimov, 2007). Change in the relative amounts of carbon released as carbon dioxide or methane may have very significant long-term effects on the global climate, yet the precise way in which the organisms involved (methanogens, methanotrophs, heterotrophs) will respond to moisture content, temperature, soil diffusion

characteristics, availability of alternative carbon sources and other environmental factors is not known.

1.3 Sources of short-chain alkanes

Gas emanating from the mid-ocean ridge hydrothermal systems derives from sediment-free environments and the methane from these sources may be considered abiogenic. This source is quantitatively insignificant (Schoell, 1988), and the vast majority of natural gas derives principally through either the thermal or microbial degradation of organic material. Thermogenic gas, which comprises 80% of commercial natural gas, contains, in addition to methane, C2-C4 alkanes, which can comprise 10% or more by volume (Whiticar, 1994), depending on the thermal maturity of the source rock. Microbially-produced gas is more predominantly methane, although microbial formation of ethane and propane has also been conclusively demonstrated (Fukuda et al., 1984; Oremland et al., 1987; Devai and Delaune, 1996; Marrin and Adriany, 1999; Taylor et al., 2000; Hinrichs et al., 2006). Ethane and propane flux to the atmosphere is estimated at approximately 10 Tg y^{-1} each (reported in Etiope and Ciccioli (2009), although these authors suggest this is likely to be an underestimate) but previous reports have estimated the propane flux as up to five times higher (Boissard et al., 1996). The oceans were reported to contribute 2.1 Tg y^{-1} to the flux of C2 – C4 hydrocarbons (Plass-Dülmer et al., 1995). Slightly over half of global emissions are of anthropogenic origin, and geologic (thermogenic) fluxes for ethane and propane are approximately 2 – 4 and 1 – 2.4 Tg y^{-1} respectively (Etiope and Ciccioli, 2009). The major sink, as for methane, is atmospheric oxidation by OH radicals. However, the residence times for ethane and propane are much lower than for methane, (days rather than years) leading to atmospheric mixing ratios orders of magnitude less (Clarkson et al., 1997).

As mentioned in Section 1.1, thermogenic gas emanating from the Earth's crust, mainly from macro seeps, has been largely ignored historically, but may contribute a significant proportion of the methane flux. Although terrestrial macroseeps comprise a large and sometimes dramatic source of hydrocarbons to the atmosphere, a more ubiquitous yet unnoticed source may be microseeps, which are estimated to cover up to 15% of global drylands and contribute 10 Tg y^{-1} to the methane budget (Etiope and Klusman, 2010). This gas also contains the expected non-methane low molecular mass hydrocarbons. Although some researchers have investigated microseepage in

petroleum reserves, (for example Klusman (2006)), the global extent of microseepage is subject to large uncertainties. Klusman detected high methane and other hydrocarbon concentrations in 10 m deep bore holes (up to 17% methane and 0.5% propane), and the isotopic and depth profiles indicated high rates of oxidation in the near-surface zone. Aerobic oxidation of light alkanes has also been detected in marine environments (Kinnaman et al., 2007; Valentine et al., 2010). In summary, the major sources of short chain alkanes are probably thermogenic, with an additional microbially-produced element, and, as is the case for methane (Reeburgh, 2007), no doubt the flux to the atmosphere is small compared to the amount oxidised in soils, sediments and the water column.

1.4 Methane oxidising bacteria

Methanotrophs are bacteria able to grow on methane as their sole source of carbon and energy and are a subset of methylotrophs, organisms capable of growth on one-carbon compounds such as methanol and methylated amines. These ubiquitous microorganisms are widespread in freshwater, marine and terrestrial environments (Dedysh et al., 1998). Methane oxidation is possible in both oxic and anoxic environments, but only aerobic oxidation is dealt with here. All methanotrophs use methane monooxygenase (MMO) enzymes to oxidise methane to methanol, which is further oxidised to formaldehyde (Hanson and Hanson, 1996). Methanotrophs can be broadly categorised into two groups, type I or type II, on the basis of phylogenetic, physiological and biochemical characteristics. A common feature is the presence of intracytoplasmic membranes (ICM), arranged either in bundles perpendicular to the cell envelope (type I) or around the periphery of the cell (type II). In many genera the membrane type (type I or type II) correlates with phylogeny (*γ-Proteobacteria* or *α-Proteobacteria*), GC content of DNA (43 – 60% or 60 – 67%) carbon assimilation pathway (RuMP or serine) and major phospholipid fatty acid type, although the high GC-content of species of *Methylococcus* and *Methylocaldum* led to their assignment in an intermediate group, type X. Recently, additional species have been discovered which do not fit exactly into these categories and have characteristics, including a novel arrangement of ICM comprising a single membrane stack parallel to the long axis of the cell, characteristic of the genus *Methylocapsa*, prompting the proposal of an additional type III (Dedysh et al., 2002). Recently identified thermoacidophilic methanotrophs of the genus *Verrucomicrobia* contain carboxysome-like vesicular

membranes (Op den Camp et al., 2009). Table 1.1 lists features of extant methanotrophs.

Table 1.1. Characteristics of known methanotroph genera. ND, not determined; NA, not applicable. MMO type is designated as S, soluble or P, particulate. C_1 assimilation is indicated as S, serine cycle; R, RuMP pathway. The symbols + and - indicate that the feature is present or absent in all species; ± indicates the second feature is also present in some species. Some species may also assimilate carbon via the Calvin-Benson-Bassham cycle. ICM, intracytoplasmic membranes. Data from Murrell (2010), Iguchi (2010a), Vorob'ev (2010b) and Op den Camp (2009).

Genus	Phylogeny	ICM type	MMO type	C_1 assimilation	Facultative	Features
Methylomonas	*γ-Proteobacteria*	I	P ± S	R	-	Some psychrophilic
Methylobacter		I	P	R	-	
Methylomicrobium		I	P ± S	R	-	Halotolerant; alkaliphilic
Methylosarcina		I	P	R	-	
Methylosphaera		ND	P	R	-	Psychrophilic
Methylosoma		I	P	ND	-	
Methylovulum		I	P + S	R	-	
Methylococcus		I	P + S	R + S	-	Thermophilic
Methylothermus		I	P	R	-	Thermophilic
Methylocaldum		I	P	R + S	-	Thermophilic
Methylohalobius		I	P	R	-	Halophilic
Crenothrix		I	P	ND	-	Filamentous
Clonothrix		I	P	ND	-	Filamentous
Methylacidiphilum	*Verrucomicrobia*	IV[c]	P	S[a]	-	Acidophilic
Methylosinus	*α-Proteobacteria*	II	P + S	S	-	
Methylocystis		II	P ± S	S	Some	Some moderately acidophilic
Methylocella		NA[b]	S	S	+	Moderately acidophilic
Methylocapsa		III	P	S	Some	Moderately acidophilic
Methyloferula		NA[b]	S	R + S	-	Moderately acidophilic

[a] Carbon may be assimilated via a variant of the serine cycle. [b] Contains a vesicular membrane system. [c] Carboxysome-like vesicular ICMs.

1.5 Facultative methanotrophs

Whereas the ability of non-methanotrophic methylotrophs to grow on multi-carbon compounds is common, the vast majority of the methanotrophs described in the preceding section are obligate organisms, unable to use compounds with carbon-carbon bonds as sole source of carbon and energy (although it has been shown that acetate and other multi-carbon compounds can be assimilated to a certain extent during growth on methane (Eccleston and Kelly, 1973; Patel et al., 1977)). From the first descriptions of methane-oxidising bacteria by biologists such as Söhngen at the start of the twentieth century, many examples have been described which were also said to be capable of growth on multi-carbon compounds (described and reviewed by Bushnell and Haas (1941), Zobell (1946), Theisen and Murrell (2005) and Semrau et al. (2011)). However, as verification technology and techniques improved (detailed by Dedysh and Dunfield (2011)), by the end of the twentieth century no organisms shown conclusively to be facultative methanotrophs remained in cultivation, leading to doubts regarding the verifiable existence of this trait in microorganisms. The same improvements in methodology eventually enabled the unequivocal demonstration of the facultative nature of *Methylocella* spp. by Svetlana Dedysh and co-workers (2005a), by demonstrating, *inter alia*, the concomitant increase in *mmoX* gene copies with cell numbers during heterotrophic growth. Subsequently, species of other genera have been shown to be capable of comparatively weak growth on acetate or ethanol in addition to methane, including species of *Methylocapsa* (Dunfield et al., 2010) and *Methylocystis* (Im et al., 2010; Belova et al., 2011). *Methylocella* spp., however, remain unique both in being able to grow on two-carbon compounds at similar or higher rates in comparison to methane, and also in using more complicated multi-carbon molecules as sole carbon and energy sources. Multi-carbon compounds, such as organic acids including acetate and propionate, are frequently detectable in the oxic soil horizons which comprise the habitats of methanotrophs, often reaching low millimolar concentrations (Hines et al., 2001; Strobel, 2001; Mörsky et al., 2008). The potential impact of changes in the availability of alternative carbon sources on methanotrophic activity is largely unknown; some reports have suggested that organic acids might inhibit methane oxidation (Rahman et al., 2011; Wieczorek et al., 2011) while others demonstrated that methane oxidation still occurs in the presence

of alternative carbon sources (Yoon et al., 2010; Belova et al., 2011), or that acetate may even stimulate the activity of methanotrophs (West and Schmidt, 1999).

1.6 *Methylocella* spp.

Investigation of the methane oxidising microbial communities in *Sphagnum* peat bogs identified a novel group of bacteria (McDonald et al., 1996; Dedysh et al., 1998). Isolates were obtained by growth on media at similar ionic strength, pH and temperature as the natural habitats. Subsequently, three *Methylocella* species (*M. palustris*, *M. silvestris* and *M. tundrae*) were isolated and characterised from peat, forest and tundra soils respectively (Dedysh et al., 2000; Dunfield et al., 2003; Dedysh et al., 2004), and *Methylocella* spp. have since been identified in diverse habitats ranging from hardwood forest (Lau et al., 2007) to landfill cover soils (Chen et al., 2007). Together with *Methylocapsa acidiphila,* they form a distinct 16S RNA gene phylogenetic cluster, most closely related to the heterotroph *Beijerinckia indica,* see Figure 1.2. The *Methylocella* isolates were shown to grow on acetate, pyruvate, succinate, malate and ethanol, in addition to methane, methanol and methylamine, and they contain only the sMMO (Dedysh et al., 2005a; Theisen et al., 2005). *Methylocella* are Gram negative, non-motile short rods, 0.6 – 0.8 μm in width and 1.2-1.5 μm in length. Under some circumstances they form aggregates surrounded by polysaccharide capsular material, and do not appear to form spores or other resting stages (Dunfield et al., 2003). Major PLFAs are 18:1ω7c acids, and the GC content is 60-63 mol% (Dedysh et al., 2004). *Methylocella* spp. may be of major importance in methane cycling in some environments, for example northern peatlands, where they may comprise the numerically dominant species (Dedysh et al., 2001; Dedysh, 2002).

1.6.1 The genome sequence of *M. silvestris*

During the course of this project, the genome sequence of *M. silvestris* was released by the Joint Genome Institute (Chen et al., 2010). The genome size is 4.3 Mbp with GC content 63%, and 3,917 genes and 99 pseudogenes were predicted. The data confirmed the presence of a single methane monooxygenase, but unexpectedly revealed the presence of a group of homologous genes, later identified as propane monooxygenase (discussed later). All genes for methylotrophy were identified, as were genes for nitrogen fixation and a complete TCA cycle.

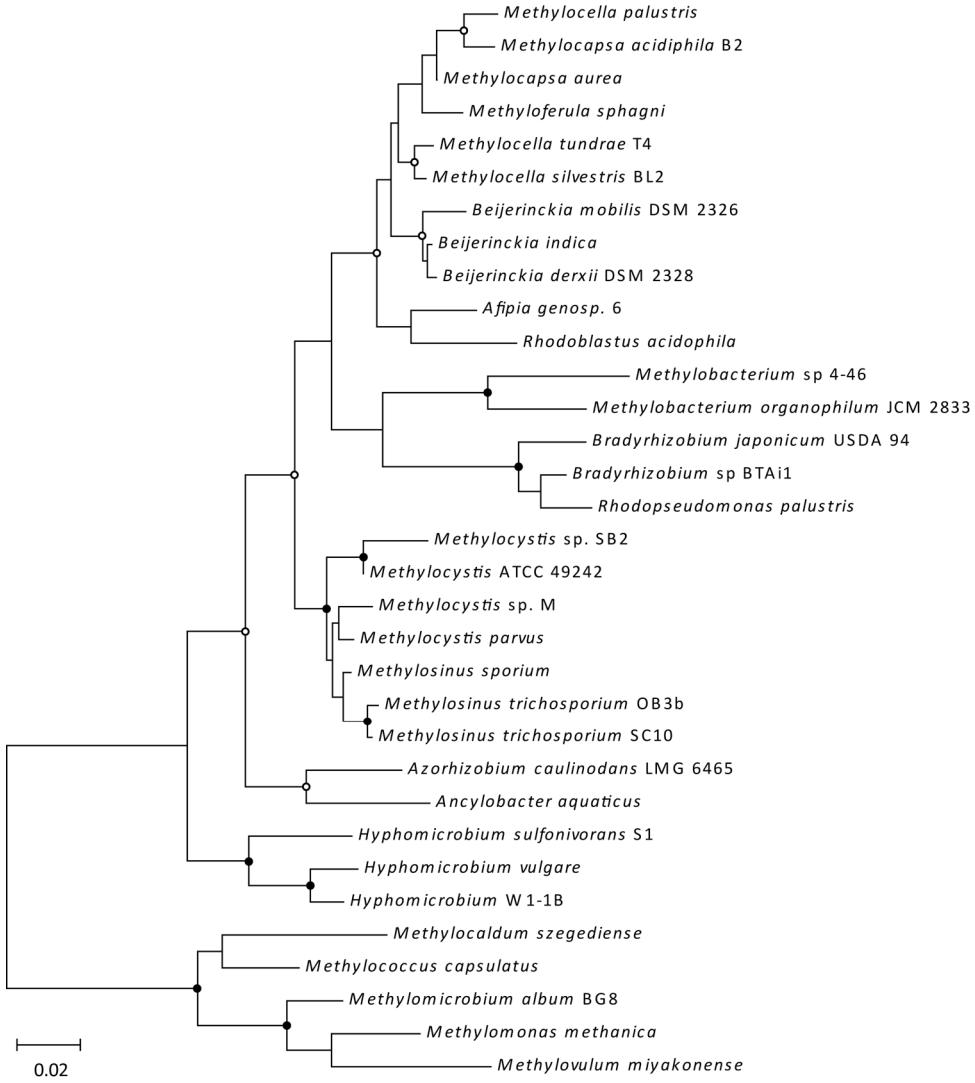

Figure 1.2. Phylogenetic relationship between *Methylocella* spp., other methanotrophs and other representative *α-Proteobacteria*. The five *γ-Proteobacterial* species at the bottom of the tree were used as an outgroup. The tree, constructed using the Maximum Likelihood method, is based on an alignment of 16S rRNA nucleotide sequences. Sequences were aligned using Clustal, positions containing gaps or missing data were eliminated, and the tree constructed with a final data set of 1049 nucleotides using Mega5 (Tamura et al., 2007). Bootstrap values (based on 500 replications) greater than 95% are shown as filled circles at nodes, and those between 75 – 95% as open circles.

1.7 Methane monooxygenase

Two forms of MMO exist. Until recently, all methanotrophs were thought to contain a copper dependent, membrane-bound particulate enzyme (pMMO), and some also to contain a soluble enzyme (sMMO) containing a di-iron centre at its active site (reviewed by Dalton (2005)). However, two genera (*Methylocella* and *Methyloferula*) are now known to contain only the sMMO (Table 1.1). In methanotrophs which contain both the pMMO and the sMMO, the reciprocal expression and activity of the

two enzymes is dependent on the copper concentration, with the sMMO only expressed at low copper to biomass ratio, controlled by as yet unexplained mechanisms (Semrau et al., 2010).

1.7.1 The particulate methane monooxygenase

The pMMO consists of three subunits encoded by the operon *pmoCAB,* encoding the γ-, β- and α-subunits respectively, which form an $(\alpha\beta\gamma)_3$ structure located in the membranes (Lieberman and Rosenzweig, 2005), including the intracytoplasmic membranes characteristic of methanotrophs containing this enzyme. It has proved difficult to purify, which has hampered biochemical analysis. The enzyme has been shown to contain copper (Balasubramanian et al., 2010), although the exact number of copper atoms and their role in the catalytic cycle remains controversial (reviewed by Semrau et al. (2010)). The pMMO has a relatively restricted range of substrates, comprising mainly straight chain $C_1 - C_5$ hydrocarbons (Elliott et al., 1997), but oxidises methane with greater efficiency than the sMMO, such that expression of the pMMO compared to the sMMO resulted in a one-third increase in the carbon conversion into biomass in *Methylococcus capsulatus* (Leak and Dalton, 1986).

1.7.2 The soluble methane monooxygenase

In contrast to the pMMO, the sMMO has been the subject of extensive study, principally the enzymes from *Methylococcus capsulatus* Bath and *Methylosinus trichosporium*, (reviewed by Trotsenko and Murrell (2008)), and comprises three components, hydroxylase, reductase and coupling protein. The hydroxylase consists of three subunits (MmoX, MmoY, MmoZ), of molecular masses 60, 45 and 19 kDa respectively (for the enzyme from *Methylosinus trichosporium*) with an $(\alpha\beta\gamma)_2$ structure, see Figure 1.3. Each α-subunit contains a di-nuclear iron centre, located in a hydrophobic pocket which forms the active site (Elango et al., 1997). The reductase MmoC (37 kDa) contains flavin adenine dinucleotide (FAD) and Fe_2S_2 prosthetic groups and transfers electrons from NADH to the hydroxylase. The coupling protein MmoB (15 kDa) which binds to the hydroxylase has a profound effect on the catalytic cycle and is important for enzyme activity and selectivity (reviewed by Dalton (2005)). An additional component, MmoD, encoded by OrfY, was identified

and proposed to play a role in the assembly of the complex (Merkx and Lippard, 2002).

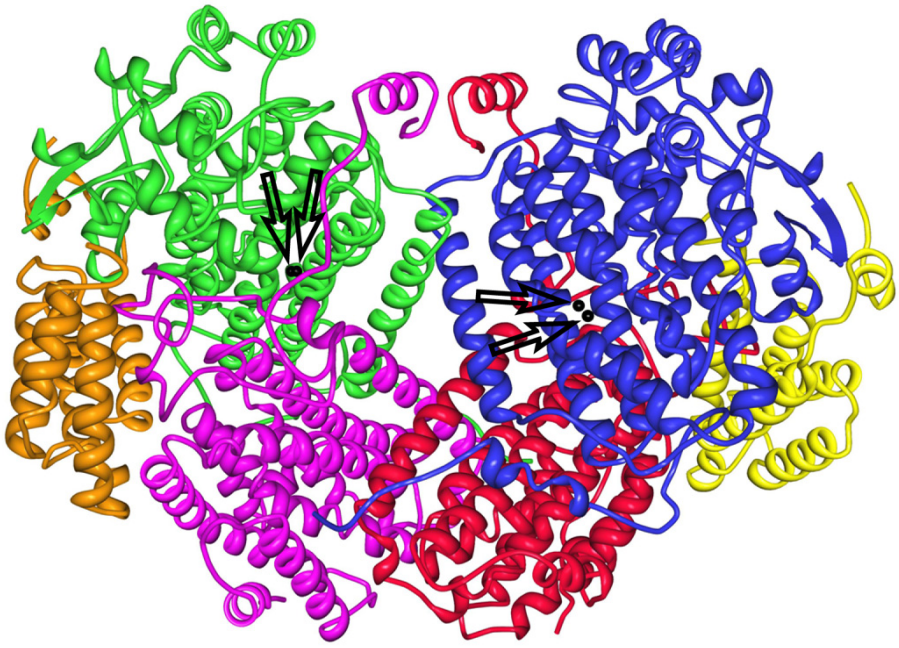

Figure 1.3. The sMMO hydroxylase from *Methylococcus capsulatus* Bath. The image shows the Protein Data Bank structure 1MTY (Rosenzweig et al., 1997), with α-subunits shown in green and blue, β-subunits in pink and red and γ-subunits in orange and yellow. The iron atoms (in black) at the active site are indicated with arrows.

Twenty years ago the genes encoding these enzymes were cloned and sequenced, (Stainthorpe et al., 1989; Stainthorpe et al., 1990; Cardy et al., 1991a, b), and later shown to be co-transcribed (Nielsen et al., 1996; Nielsen et al., 1997). The arrangement of the sMMO structural genes is the same in these two organisms and also in *Methylocystis* sp. strain M (McDonald et al., 1997) and *Methylomonas* spp. (Shigematsu et al., 1999). In these and later studies, it was established that transcription originates from a σ^{54} promoter, and two genes, *mmoG* and *mmoR,* encoding a GroEL homologue and a putative transcriptional regulator, were identified which were shown to be essential for transcription of the operon (Csaki et al., 2003; Stafford et al., 2003). However, in *Methylococcus capsulatus,* these regulatory genes are situated downstream of the structural genes (and separated from each other by two genes thought to encode two-component signal transduction proteins) whereas in *Methylosinus trichosporium* they are 5' of the structural genes.

Analysis of the sMMO operon of *Methylocella silvestris* was carried out by Theisen et al. (2005), which revealed a similar arrangement of the structural genes *mmoXYBZDC*, followed by *mmoR* and *mmoG* (separated by a short open reading frame designated *Orf2*), although in this case the entire cluster was thought to be co-transcribed. The arrangement of the sMMO genes in these organisms is shown in Figure 1.4. Transcription of the structural genes was shown to be regulated by copper in *Methylococcus capsulatus* and *Methylosinus trichosporium,* but in the case of *Methylocella silvestris,* the presence of copper was shown to have no effect on transcription (Csaki et al., 2003; Stafford et al., 2003; Theisen et al., 2005).

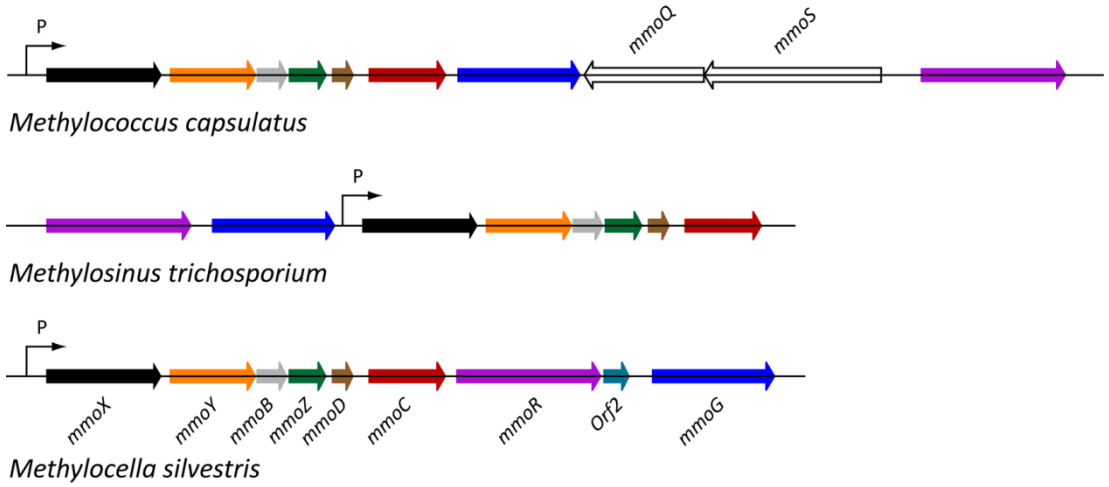

Figure 1.4. The arrangement of sMMO genes in *Methylococcus capsulatus* Bath, *Methylosinus trichosporium* OB3b and *Methylocella silvestris* BL2. Homologous genes are shown in the same colours. P: σ^{54} promoter. Data from Csaki et al. (2003), Stafford et al. (2003) and Theisen et al. (2005).

1.8 Methanol dehydrogenase

Methanol dehydrogenase (MDH) catalyses the oxidation of methanol to formaldehyde in the periplasm of methylotrophic bacteria, almost all of which possess this enzyme (except, for example, *Methyloversatilis universalis,* which possesses an alternative methanol-oxidising enzyme (Kalyuzhnaya et al., 2008)), which can constitute 15% of soluble protein (Anthony, 2000). MDH is a soluble pyrroloquinoline quinone (PQQ)-containing quinoprotein, which uses a specific cytochrome (cytochrome c_L) as electron acceptor. The X-ray structures of several MDHs have been determined, including the enzyme from *Methylobacterium extorquens* (Anthony, 2004). The enzyme is formed from two subunits (approximately 66 and 8.5 kDa respectively) arranged in an $(\alpha\beta)_2$ tetrameric

configuration. Each α-subunit forms a barrel with eight radially arranged β-sheets forming a "propellor" fold. In the tetramer the two αβ subunits are arranged approximately perpendicular to each other. Each contains the non-covalently bound PQQ prosthetic group sandwiched inside the α-subunit, together with a single Ca^{2+} ion. Affinity of MDH for methanol is very high, with K_m often less than 20 μM (Sperl et al., 1974), and the substrate specificity is broad, extending to primary alcohols up to octanol, but usually with little or no activity towards secondary alcohols (Ghosh and Quayle, 1981; Mountfort, 1990), although some of the characterised enzymes have 2-propanol activity (Goldberg, 1976; Sahm et al., 1976). Interestingly, the existence of a modifier protein has been demonstrated, whose function *in vivo* appears to be the modification of the substrate specificity to prevent formaldehyde oxidation, and which also has the effect of extending the substrate range of the enzyme to include 1,2-propanediol and 4-hydroxybutyrate (Long and Anthony, 1991), although the gene encoding this component has not been identified. The *in vitro* assay for MDH usually uses the artificial electron acceptor phenazine methosulfate (PMS) coupled to reduction of the dye 2,6-dichlorophenol indophenol (DCPIP). Under these conditions ammonia is required as activator, and the pH optimum is high (pH 9) (Anthony and Zatman, 1964). Therefore the assay conditions are quite different to those *in vivo.*

Synthesis of active MDH in the periplasm is complicated, involving processes including polypeptide translation, transport across the membrane, folding, insertion of prosthetic group and calcium ion and assembly of the subunits. In *Methylobacterium extorquens,* 25 required genes are encoded by five clusters (summarised in Zhang and Lidstrom (2003)). The largest of these, *mxaFJGIRSACKLDEHB,* contains structural genes encoding the α- and β-subunits (*mxaF* and *mxaI)* and the MDH-specific cytochrome c *(mxaG)* (Nunn and Lidstrom, 1986a, b; Nunn et al., 1989), together with four genes required for insertion of the calcium ion (Morris et al., 1995) and several essential genes of unknown function. A single upstream gene, *mxaW*, is divergently transcribed from this locus. Two clusters contain genes for PQQ synthesis *(pqqABC/DE* and *pqqFG)* (Goodwin and Anthony, 1998) and two clusters contain four genes *(mxbDM* and *mxcQE)* which, together with *mxaB,* encode regulatory genes required for transcription of the structural genes (Springer et al., 1997; Springer et al., 1998). MDH transcription is up-regulated in *M. extorquens* six-fold during growth on methanol compared to succinate (Morris and

Lidstrom, 1992). It was suggested that the MDH and PQQ biosynthesis structural genes are transcribed from σ^{70} promoters (Zhang and Lidstrom, 2003) and that, in *Methylobacterium* species, the *mxb* and *mxc* loci encode a pair of two-component response regulators that activate transcription in response to an unknown signal, possibly methanol or formaldehyde (Xu et al., 1995; Springer et al., 1997). A pair of regulators, predicted to detect formaldehyde in the periplasm and cyctoplasm respectively, is also implicated in regulation of MDH expression and formaldehyde oxidation in *Paracoccus denitrificans* (Harms et al., 1993; Harms et al., 2001).

1.9 Pathways of C_1 metabolism

Methylotrophic metabolism has been thoroughly researched, for a review see Trotsenko and Murrell (2008). Methane is oxidised via either the pMMO or the sMMO to methanol, and thence to formaldehyde, formate and carbon dioxide by the appropriate dehydrogenases, see Figure 1.5. Energy, derived in the case of the sMMO from the oxidation of NADH, is required for the initial oxidation of methane, but subsequent oxidation reactions generate energy either in the form of reducing equivalents or by passing electrons directly to the electron transport chain. Therefore part of the methane (approximately 50%) is oxidised to CO_2 to provide energy, and part is assimilated principally via one of two carbon assimilation pathways, the ribulose monophosphate (RuMP) cycle or the serine cycle.

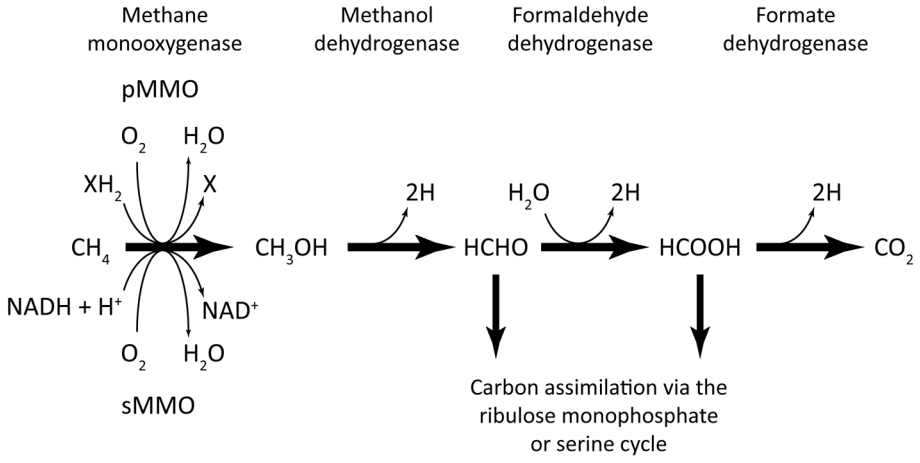

Figure 1.5. The pathway of methane oxidation. NADH is the electron donor for the sMMO, but not the pMMO. X represents the unknown electron donor for the pMMO, (recently suggested to involve the direct transfer from MDH (Myronova et al., 2006)). Modified from Murrell et al. (2000a).

Formaldehyde is produced from oxidation of methanol in the periplasm, but subsequent metabolism takes place in the cytoplasm. However, formaldehyde is extremely toxic to the cell due to its reactivity with proteins and nucleic acids, and the efficiency of its metabolism is therefore crucial. Many methylotrophs have multiple enzyme systems for its oxidation, including glutathione-, NAD^+- and dye-linked enzymes (Stirling and Dalton, 1978; Attwood, 1990; Zahn et al., 2001), reviewed by Vorholt (2002). Many methylotrophs also use pathways in which formaldehyde and other more oxidised C_1 units are bound to the carrier molecules tetrahydrofolate (H_4F) or tetrahydromethanopterin (H_4MPT), (the former is ubiquitous among life-forms as a carrier of C_1 units for biosynthetic reactions, the latter was until recently thought to be unique to *Archaea*) (Marison and Attwood, 1982; Vorholt et al., 1999). Formaldehyde condenses with H_4F or H_4MPT either spontaneously or (in the latter case) catalysed by formaldehyde-activating enzyme (Fae), and the resultant methylene-H_4F or -H_4MPT is oxidised in a series of reaction (that are reversible or irreversible in the two pathways respectively), before formate is finally released. Serine cycle organisms use the H_4F-mediated pathway primarily for assimilation of one-carbon units (as methylene H_4F), and the H_4MPT-mediated pathway for oxidation to carbon dioxide (Vorholt, 2002), although it now appears that methylene H_4F is formed both by the condensation of H_4F with formaldehyde, and also from formate following oxidation via the H_4MPT pathway in *Methylobacterium extorquens* (Crowther et al., 2008).

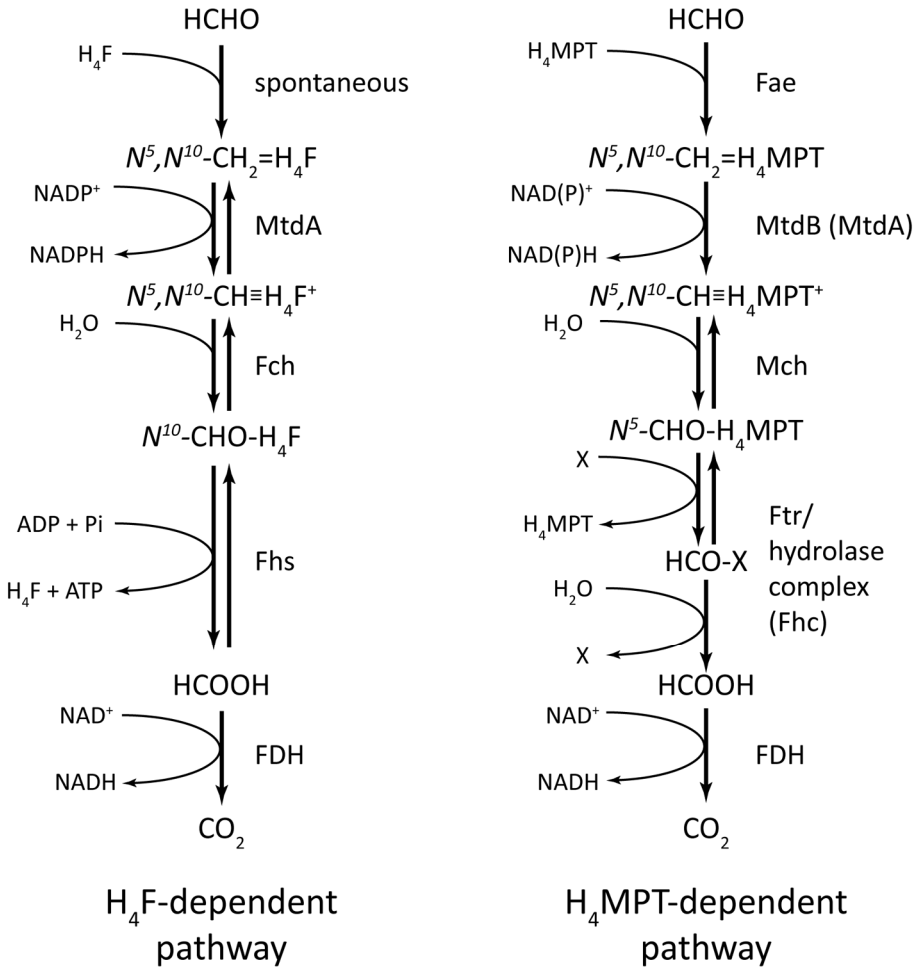

Figure 1.6. H_4F- and H_4MPT-dependent pathways of formaldehyde oxidation in *Methylobacterium extorquens* AM1. The enzymes are: MtdA, NADP-dependent methylene-H_4MPT dehydrogenase; Fch, methenyl-H_4F cyclohydrolase; Fhs, formyl-H_4F synthetase; FDH, formate dehydrogenase; Fae, formaldehyde activating enzyme; MtdB NAD(P)-dependent methylene-H_4MPT dehydrogenase; Mch, methenyl-H_4MPTcyclohydrolase; Ftr, formyltransferase; Fhc, Ftr/hydrolase complex. X is an unknown cofactor. Taken from Vorholt (2002).

Carbon is assimilated via the RuMP cycle or the serine cycle, although recent evidence suggests that the Calvin-Benson-Bassham (CBB) cycle is also wholly or partially responsible for carbon assimilation in some methanotrophs (Taylor et al., 1981; Op den Camp et al., 2009; Khadem et al., 2011) as well as methylotrophs, including members of the *Beijerinckia* (Dedysh et al., 2005b). The RuMP cycle (Figure 1.7) is prevalent among type I methanotrophs (Table 1.1), does not operate in methylotrophic *α-Proteobacteria*, and is not considered further here.

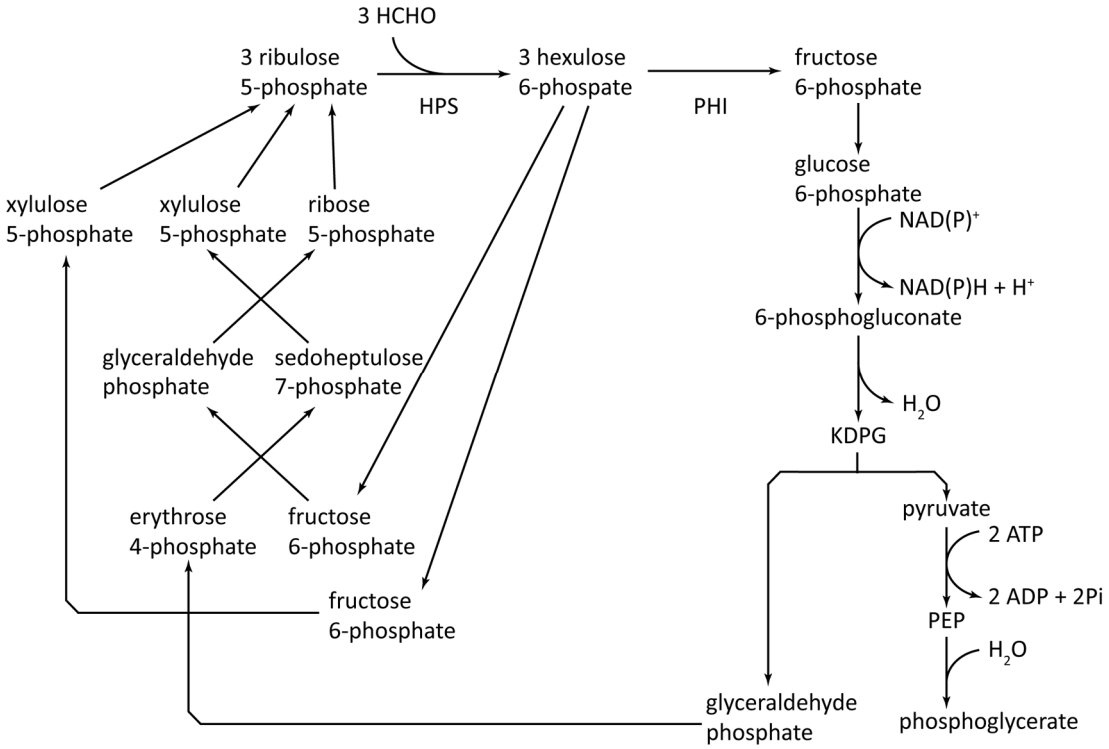

Figure 1.7. The RuMP cycle (KDPG aldolase/transaldolase variant which occurs most frequently in obligate methylotrophs), showing the formation of one phosphoglycerate from three formaldehyde molecules. KDPG, 2-keto 3-deoxy 6-phosphogluconate. Enzymes unique to the cycle, 3-hexulosephosphate synthase (HPS) and phosphohexuloisomerase (PHI), are shown. Redrawn from Anthony (1982).

The serine cycle, used by type II methanotrophs, is shown in Figure 1.8. As can be seen from the figure, the cycle as-drawn is sufficient for the biosynthesis of polyhydroxybutyrate (PHB) and other cell constituents that can be synthesised from acetyl-CoA, such as fatty acids. Removal of other intermediates from the cycle, such as 3- or 4-carbon compounds, requires the conversion of acetyl-CoA into glyoxylate, a topic discussed in Chapter 5. As mentioned above, methylene-H_4F is formed from formaldehyde either by the (spontaneous) condensation with H_4F or via formate (Vorholt et al., 1999; Crowther et al., 2008), and is a substrate for serine transhydroxymethylase. Following carboxylation of the resultant three-carbon molecule by phosphoenolpyruvate (PEP) carboxylase, acetyl-CoA is released by the cleavage of malyl-CoA. Thus, in its simplest form, the serine cycle converts formaldehyde to acetyl-CoA at the expense of 2ATP and 2NADH. The key enzymes of the serine cycle are serine transhydroxymethyltransferase, serine-glyoxylate aminotransferase, hydroxypyruvate reductase and malyl-CoA lyase, of which hydroxypyruvate reductase is the most diagnostic (Lawrence and Quayle, 1970).

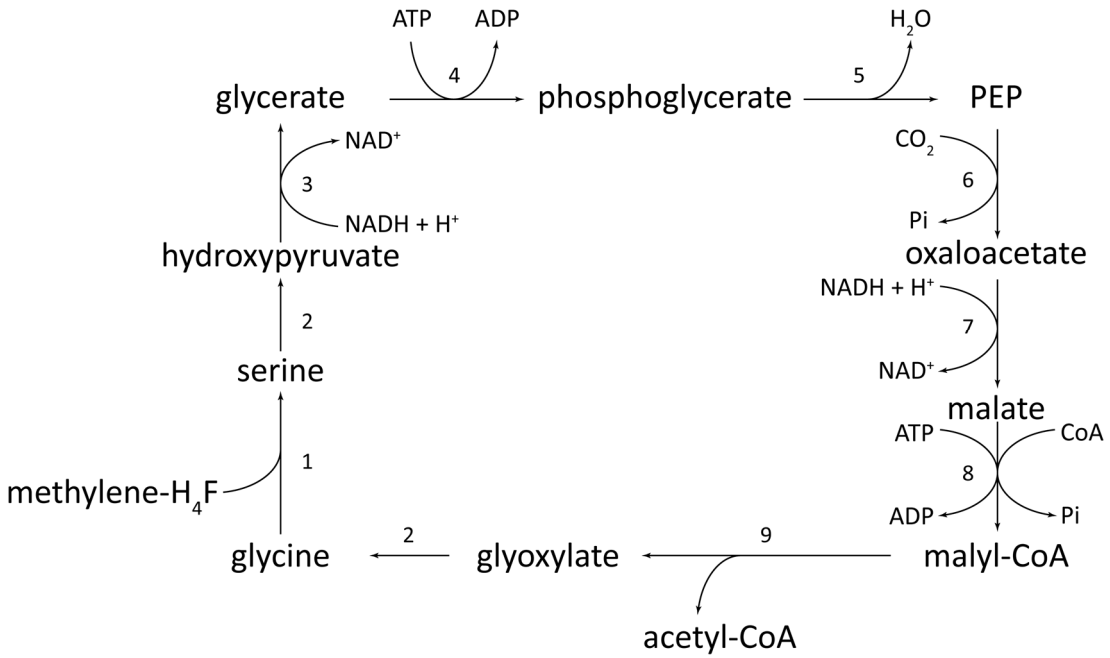

Figure 1.8. The serine cycle, showing the formation of acetyl-CoA from methylene tetrahydrofolate. The enzymes are 1, serine transhydroxymethylase; 2, serine-glyoxylate aminotransferase; 3, hydroxypyruvate reductase; 4, glycerate kinase; 5, enolase; 6, PEP carboxylase; 7, malate dehydrogenase; 8, malate thiokinase; 9, malyl-CoA lyase. PEP, phosphoenolpyruvate. From Anthony (2011).

Genes essential for methylotrophy, including those encoding the enzymes of the serine cycle, are often arranged in clusters, termed methylotrophy modules by Chistoserdova et al. (2003). In *Methylobacterium extorquens,* activities of serine-glyoxylate aminotransferase, hydroxypyruvate reductase and glycerate kinase were found to be upregulated during growth on methanol compared to succinate (Dunstan et al., 1972a) and in this organism activity of these enzymes was repressed by succinate (in the presence of methanol) but this was not the case for all facultative methylotrophs (McNerney and O'Connor, 1980). It was suggested that a product of methanol oxidation, rather than methanol itself, caused the up-regulation of the serine cycle enzymes, since mutants lacking methanol dehydrogenase activity exhibited low activities of these enzymes when induced with methanol (Anthony, 1975; McNerney and O'Connor, 1980). More recently, with the benefit of targeted genetic systems, it was shown that in *Methylobacterium extorquens,* a LysR-type regulator, (homologous to CbbR which is involved in CBB cycle regulation), controls serine cycle gene transcription and possibly responds to the intracellular level of formyl-H_4F (Kalyuzhnaya and Lidstrom, 2003; Kalyuzhnaya and Lidstrom, 2005).

1.10 Two-carbon metabolism

Aerobic utilization of ethanol requires oxidation to acetaldehyde and acetate. The first step can be catalysed by MDH in *Methylobacterium extorquens* (Dunstan et al., 1972a), by a different quinoprotein alcohol dehydrogenase in *Pseudomonas aeruginosa* (Görisch and Rupp, 1989) or by an NAD^+-dependent enzyme in *Hyphomicrobium* (Attwood and Harder, 1974). Whether exogenously supplied or formed from the oxidation of ethanol, acetate requires activation to acetyl-CoA, a reaction catalysed either by acetate kinase/phosphotransacetylase or acetyl-CoA synthetase, the latter enzyme generally being induced at low acetate concentrations (< 10 mM) (reviewed by Starai and Escalante-Semerena (2004)).

Acetate is oxidised in the tricarboxylic acid (TCA) or Krebs cycle to carbon dioxide to generate reducing equivalents, but assimilation of carbon from acetyl-CoA requires an additional cycle. The glyoxylate cycle was proposed by Hans Krebs and Hans Kornberg in 1957 (Kornberg and Krebs, 1957). This cycle shares several enzymes with the TCA cycle (both cycles are shown superimposed in Figure 1.9) and is common in prokaryotes, plants, fungi and nematodes and has been found in higher animals (Popov et al., 2005). The function is to divert the carbon flow during growth on acetate (or compounds resulting in acetyl-CoA) from the two decarboxylation reactions of the TCA cycle, (catalysed by isocitrate dehydrogenase (ICDH) and α-ketoglutarate dehydrogenase), allowing the cleavage of isocitrate into glyoxylate and succinate, and the condensation of the resultant glyoxylate with acetyl-CoA to form malate. The enzymes responsible for these two reactions are isocitrate lyase (ICL) and malate synthase (MS). Since the flux required through ICL and ICDH varies depending on carbon source, control over these enzymes is required. In enteric bacteria such as *E. coli,* flux is diverted through ICL by inactivation of ICDH by phosphorylation, mediated by isocitrate dehydrogenase kinase/phosphatase (Hurley et al., 1990). In these organisms the glyoxylate cycle genes are co-transcribed, together with *aceK* (encoding ICDH kinase/phosphorylase), in the *aceBAK* operon. However, this is not the case in all bacteria which possess these enzymes, including, for example*, Corynebacterium glutamicum, Hyphomicrobium methylovorum* GM2, *Mycobacterium tuberculosis* and *Sinorhizobium meliloti* (Reinscheid et al., 1994a; Tanaka et al., 1997; Smith et al., 2003c; Ramirez-Trujillo et al., 2007) in which the genes are either separated on the chromosome or divergently transcribed.

Transcriptional control of the glyoxylate cycle genes has been the subject of considerable study in *E. coli* and is comparatively well understood (reviewed by Cozzone (1998)). Regulatory mechanisms in other organisms are less well characterised and appear to be different in some cases; ICDH is not phosphorylated in *C. glutamicum* (Eikmanns et al., 1995) or *Bradyrhizobium japonicum* (Green et al., 1998), and the control of transcription is different in *C. glutamicum* (Gerstmeir et al., 2003). In general, ICL is induced during growth on acetate and sometimes repressed by other carbon sources such as glucose or succinate (Kornberg, 1966; Bellion and Yu, 1978; Yurkov and Beatty, 1998; Gerstmeir et al., 2003; Kretzschmar et al., 2008). There are also some reports of phosphorylation of ICL, for example in *E. coli, Acinetobacter calcoaceticus* and yeast (Hoyt et al., 1994; da Silva Cruz et al., 2011). In addition, some bacteria express different isoforms of ICL under different growth conditions, including *Aminobacter aminovorans, Mycobacterium* species and *Ralstonia eutropha* (Bellion and Woodson, 1975; Honer Zu Bentrup et al., 1999; Wang et al., 2003; Munoz-Elias and McKinney, 2005).

Malate synthase exists in two well-characterised isoforms, MSA and MSG, and some bacteria, including *E. coli, Ralstonia eutropha* and *Deinococcus radiodurans* possess both forms (Cozzone, 1998; White et al., 1999; Wang et al., 2003). In *E. coli,* MSA, encoded by *aceB*, is expressed during growth on acetate, whereas MSG, which is expressed during growth on glycolate, is encoded by *glcB* at a different location (Molina et al., 1994) although in mutants, either isozyme can replace the deleted function (Pellicer et al., 1999). Although kinetically similar, the two enzymes are structurally different, being composed of 533 and 723 amino acids respectively. High resolution structures have been published for MSA and MSG from *E. coli* and *Mycobacterium tuberculosis* (Anstrom et al., 2003; Anstrom and Remington, 2006; Lohman et al., 2008). Although sequence identity between the isoforms is low, the structural folds are similar and the difference in length is mainly due to an additional α/β domain (residues 135-262 and 296-333 in MSG from *E. coli*). This is conserved among the G isoforms and is predicted to contain a binding site with a proposed regulatory function (Lohman et al., 2008). Organisms expressing only the MSA form of the enzyme include *Yersinia pestis, Vibrio cholerae, Saccharomyces cerevisiae* and higher plants (Hartig et al., 1992; Heidelberg et al., 2000; Parkhill et al., 2001; Cornah et al., 2004).

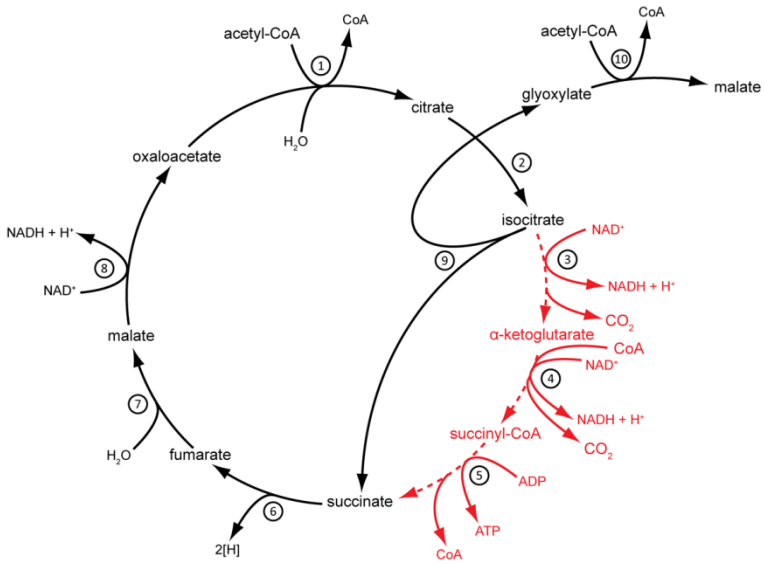

Figure 1.9. The TCA and glyoxylate cycles showing the production of one four-carbon molecule (malate) from two molecules of acetyl-CoA. During operation of the glyoxylate cycle, flux is directed away from the reactions shown in red, avoiding decarboxylation reactions. The enzymes are: 1, citrate synthase; 2, aconitase; 3, isocitrate dehydrogenase; 4, α-ketoglutarate dehydrogenase; 5, succinyl-CoA synthetase; 6, succinate dehydrogenase; 7, fumarase; 8, malate dehydrogenase; 9, isocitrate lyase; 10, malate synthase.

Organisms expressing only the MSG form (exclusive to bacteria) include *Corynebacterium glutamicum, Mycobacterium tuberculosis* and *Sinorhizobium meliloti* (Reinscheid et al., 1994a; Smith et al., 2003b; Ramirez-Trujillo et al., 2007). Although in many cases, including *E. coli,* MS is induced together with ICL, in some species of *Pseudomonas, Bradyrhizobium japonicum* and other rhizobia, MS activity is constitutive (Kornberg and Lund, 1959; Johnson et al., 1966; Green et al., 1998). *In M. tuberculosis, aceA* and *glcB* are also individually regulated. Only *aceA* transcription responds to acetate concentration, whereas *msG* is dependent on glycolate levels, suggesting a role comparable with the *E. coli* homologue (Smith et al., 2003b). Therefore a considerable diversity of expression and regulation of glyoxylate cycle enzymes exists in bacteria.

1.11 Expression of glyoxylate cycle enzymes in bacteria using the serine cycle

As mentioned in Section 1.9, synthesis of three- or four-carbon molecules in the serine cycle requires the conversion of acetyl-CoA into glyoxylate. As can be seen from Figure 1.9, this reaction is catalysed by the enzymes of the glyoxylate cycle without MS, and some bacteria possessing the serine cycle use these enzymes. However, many serine cycle methylotrophs do not possess ICL (Bellion and Spain, 1976; Anthony, 1982; Korotkova et al., 2002), and achieve this conversion by different means. The ethylmalonyl-CoA (EMC) pathway is the only fully characterised alternative (reviewed by Anthony (2011)) and is discussed in Chapter 5. Some, at least, of the organisms lacking ICL also lack MS (Cox and Quayle, 1976; Meister et al., 2005; Erb et al., 2010), although MS activity can sometimes be detected at considerable levels in extract from cells grown on one-, two-, three and four-carbon compounds (Dunstan et al., 1972b; Dunstan and Anthony, 1973; Salem et al., 1973b; Meister et al., 2005). This was found to be due to the action of the serine cycle enzyme malyl-CoA lyase operating in the reverse direction, together with a hydrolase catalysing the formation of malate from malyl-CoA (Cox and Quayle, 1976). The hydrolase was inhibited by acetyl-CoA, possibly preventing the futile cycle resulting from simultaneous activity of these enzymes and malate thiokinase.

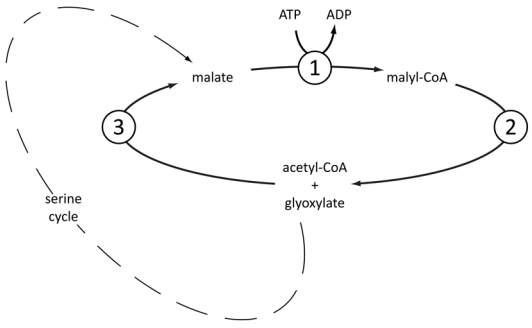

Figure 1.10. Activity of malate synthase (3) in conjunction with serine cycle enzymes malate thiokinase (1) and malyl-CoA lyase (2) would result in a futile cycle.

However, expression and activity of malate synthase would be detrimental during operation of the serine cycle, suggesting an additional regulatory requirement in serine cycle methylotrophs possessing the glyoxylate bypass. In *Aminobacter aminovorans,* malate synthase is severely repressed during growth on methylamine

(Bellion and Hersh, 1972). For this reason and due to the different roles of isocitrate lyase during one- and two-carbon growth, regulation of the glyoxylate bypass enzymes is likely to differ between facultative methylotrophs and non-methylotrophic heterotrophs.

1.12 The wider family of soluble di-iron monooxygenases

The sMMO is one of the family of soluble di-iron monooxygenases (SDIMOs), which are themselves part of a larger group of di-iron carboxylate proteins, including ferritins and rubrerythrin, the R2 subunits of ribonucleotide reductase, stearoyl-acyl carrier protein (ACP) desaturase, in addition to the hydroxylase component of the sMMO and other bacterial SDIMOs (Nordlund and Eklund, 1995). These proteins contain two adjacent iron atoms which bind molecular oxygen and whose oxidation state controls the catalytic reaction. They are coordinated by glutamate and histidine residues which are highly conserved throughout the group (Sazinsky and Lippard, 2006), see Figure 1.11. In their stable oxidation state the iron atoms are bridged by carboxylate residues and an oxo or hydroxo ligand.

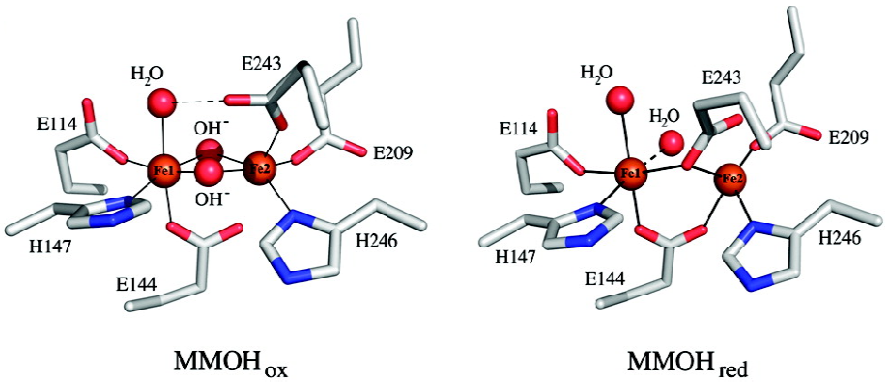

Figure 1.11. The sMMO active site in oxidised (left) and reduced form (right), showing the diiron centre and coordinating residues which are conserved throughout SDIMO groups. Oxygen atoms are depicted as red, and nitrogen as blue. Taken from Tinberg and Lippard (2011).

The sMMO is the best characterised of the SDIMOs, but subsequently di-iron carboxylate-bridged enzymes catalysing other reactions were found to have significant levels of homology, for example alkene monooxygenase from *Rhodococcus corallinus* B-276 (Gallagher et al., 1997), phenol hydroxylase from

Pseudomonas sp. CF600 (Powlowski and Shingler, 1994), toluene 4-monooxygenase from *Pseudomonas mendocina* KR1 (Pikus et al., 1996), propane monooxygenase from *Gordonia* TY5 (Kotani et al., 2003) and propane monooxygenase from *Mycobacterium* TY6 (Kotani et al., 2006). Based on phylogenetic analysis of the hydroxylase components, these enzymes were initially assigned to four, five and subsequently six subgroups (Leahy et al., 2003; Notomista et al., 2003; Coleman et al., 2006). All enzymes comprise a hydroxylase, an oxidoreductase containing NAD(P)- and FAD-binding and ferredoxin domains, and a coupling or effector protein, although members of the toluene 4-monooxygenase group (group I) contain an additional Rieske-type ferredoxin component which is essential for efficient electron transfer (Pikus et al., 1996) and are thus four component enzymes. The hydroxylase component of groups I, II and III comprise three subunits, whereas groups IV, V and VI comprise two. The three subunit hydroxylases are arranged in $(\alpha\beta\gamma)_2$ configuration (Newman and Wackett, 1995; Pikus et al., 1996; Dalton, 2005), whereas the hydroxylase of alkene monooxygenase from *Rhodococcus corallinus* B-276 was reported as a monomeric ($\alpha\beta$) configuration (Miura and Dalton, 1995). The arrangement of the genes encoding these enzymes appears to be conserved within the different groups, but differs between groups (Holmes and Coleman, 2008), as summarised in Table 1.2.

Table 1.2. The SDIMO groups as defined by Notomista et al. (2003), Leahy et al. (2003) and Coleman et al. (2006). The operon structure is given in terms of the sMMO homologues: α, hydroxylase α-subunit; β, hydroxylase β-subunit; γ, hydroxylase γ-subunit; B, coupling protein; C, reductase; D, MmoD (unknown function). F, ferredoxin; MO, monooxygenase.

Group	Example	Organism	Operon	Reference
I	Toluene 4-MO	*Pseudomonas mendocina* KR1	αFγBβC	Pikus et al. (1996)
II	Phenol hydroxylase	*Pseudomonas* sp. CF600	DβBαγC	Powlowski and Shingler (1994)
III	sMMO	*Methylosinus trichosporium* OB3b	αβBγDC	Cardy et al. (1991a, b)
IV	Alkene MO	*Rhodococcus corallinus* B-276	βBαC	Saeki and Furuhashi (1994)
V	Propane MO	*Gordonia* TY5	αCβB	Kotani et al. (2003)
VI	Propane MO	*Mycobacterium* TY6	αβBC	Kotani et al. (2006)

The genes encoding these enzymes are mostly located on the chromosome, although examples from groups I, II and IV have been reported as transcribed from linear

(Saeki et al., 1999; Krum and Ensign, 2001) or circular plasmids (Shingler et al., 1989).

1.13 Bacterial growth on short chain alkanes

Bacteria capable of growth on gaseous non-methane alkanes (C_2-C_6) are not uncommon and were first described well over half a century ago (reviewed in Fuhs (1961), Perry (1980) and Shennan (2006). Most of these are Gram-positive members of genera including *Actinomyces, Arthrobacter, Brevibacterium, Corynebacterium, Gordonia, Mycobacterium, Nocardia, Nocardioides and Rhodococcus,* while Gram-negative organisms are represented by species of *Acinetobacter, Burkholderia, Pseudomonas* and *Ralstonia* (Shennan, 2006). Enzymes capable of oxidising these compounds include the sMMO and pMMO from methanotrophs (Burrows et al., 1984), other SDIMO enzymes including the butane monooxygenase (BMO) from *Thauera butanivorans* (Arp, 1999) and the propane monooxygenase from *Gordonia* TY5 (Kotani et al., 2003), membrane non-heme alkane hydroxylase (AlkB) from *Pseudomonas putida* (van Beilen et al., 1994), cytochrome p450-family enzymes (*Mycobacterium* spp.) (van Beilen et al., 2006) and a novel membrane-associated copper containing enzyme (pBMO) from *Nocardioides* sp CF8 with homology to the pMMO (Sayavedra-Soto et al., 2011) (reviewed by Van Beilen et al. (2003)).

1.14 Bacterial growth on propane

Numerous propane-utilizing organisms have been isolated by Lukins (1963) Perry (1980), Hou (1983c), Stephens (1986) and Kotani (2003; 2006) and co-workers, among others. Until relatively recently most of the enzymes remained largely unidentified and uncharacterised, although in the case of *Rhodococcus rhodochrous* PNKb1 it was demonstrated that NADH and oxygen were required for activity, and some analysis of the polypeptides induced during growth on propane was carried out (Woods and Murrell, 1989). Kotani et al. (2003; 2006) isolated *Gordonia* and *Mycobacterium* species that use group V and group VI SDIMOs respectively to grow on propane. Recently the AlkB alkane hydroxylase has been shown capable of sustaining growth on propane in *Pseudomonas putida* GPo1 (Johnson and Hyman, 2006), whereas growth of *Nocardioides* sp CF8 on propane was shown to be due to the activity of the pMMO-like membrane associated pBMO (Hamamura and Arp,

2000; Sayavedra-Soto et al., 2011). Therefore growth on propane is possible using at least four different enzyme systems, and at least two more (the sMMO and pMMO) are capable of propane oxidation.

1.15 Organisms containing multiple SDIMOs or alkane-oxidising enzymes

It has recently become apparent that many organisms possess multiple alkane-oxidising enzyme systems. For example, *Gordonia* TY5 uses an SDIMO (a propane monooxygenase) for growth on propane and a different uncharacterised monooxygenase for growth on C_{13} – C_{22} alkanes (Kotani et al., 2003). *Methylibium petroleiphilum* contains genes encoding three SDIMOs (Kane et al., 2007), of which two are putative toluene monooxygenases (group I) and the third is a suspected propane monooxygenase (group V). This organism is capable of growth on MTBE and toluene (Nakatsu et al., 2006), and growth on MTBE was found to be dependent on an alkane hydroxylase (Schmidt et al., 2008). *Mycobacterium* NBB4, which grows on C_2 – C_4 alkenes and C_2 – C_{16} alkanes, contains genes encoding four SDIMOs (group III, two group IV and group VI), a cytochrome p450 and an alkane hydroxylase (Coleman et al., 2011a), however despite extensive analysis, it was not possible to associate particular gene products with corresponding metabolic activity. *Pseudonocardia dioxanivorans* CB1190 encodes no less than eight SDIMOs, but the activity of potential gene products remains unknown (Sales et al., 2011).

1.16 Metabolic pathways of alkane assimilation

Monooxygenase-mediated oxidation of non-methane *n*-alkanes is initiated by one of the enzymes described in the previous sections, at the terminal or sub-terminal carbon atom (reviewed by Rojo, (2009)). Terminal oxidation results in a primary alcohol, which is oxidised via alcohol and aldehyde dehydrogenases to the corresponding fatty acid, which is converted to acetyl-CoA by the β-oxidation pathway (Wegener et al., 1968; Kunau et al., 1995). Also possible is the oxidation of the terminal methyl group of the fatty acid (ω-oxidation) resulting in a dicarboxylic acid (Coon, 2005), which can also be metabolised by β-oxidation. Sub-terminal oxidation, resulting in a secondary alcohol (or occasionally an alcohol substituted at a subsequent carbon atom (Fredricks, 1967; Klein et al., 1968)), proceeds via the corresponding ketone. This is then usually oxidised by a Baeyer Villiger

monooxygenase to the ester before cleavage resulting in a primary alcohol and fatty acid (Forney and Markovetz, 1970; Van Beilen et al., 2003) which are then metabolised as described above. Propane metabolism follows this general pattern (reviewed by Perry (1980), Ashraf et al. (1994) and Shennan (2006)). The initial pathways of propane oxidation are shown in Figure 1.12. Oxidation by a dioxygenase, resulting in 1,2-propanediol, has been proposed (Hou et al., 1983a; Ashraf et al., 1994) but has not been shown to operate in propane utilising bacteria, and neither has the required 1,2-propanediol metabolising capacity been characterised. 1,2-propanediol dehydratase enzymes so far described exist in carboxysome-like structures, mostly in enteric bacteria (reviewed by Bobik, (2006)). 1,2-propanediol dehydrogenase was shown to be present in propane-grown cells of *Pseudomonas fluorescens* (Hou et al., 1983a) but it was not clear that 1,2-propanediol was the substrate *in vivo*, nor was it demonstrated that 1,2-propanediol was formed from the oxidation of propane. Dioxygenases have been shown to oxidise aliphatic alkenes, including chlorinated species such as TCE, where the products were formate and glyoxylate (Li and Wackett, 1992; Wackett, 2002). Medium-chain-length alkanes have been shown to be attacked by dioxygenases, resulting in an aldehyde via a short-live hydroperoxide (Maeng et al., 1996), but there are no reports of dioxygenase-mediated oxidation of short chain alkanes, so the involvement of a dioxygenase in propane metabolism remains in doubt. Recently additional pathways have been described for the metabolism of acetone (Hausinger, 2007), which are briefly discussed in Chapter 7, together with the metabolism of acetol.

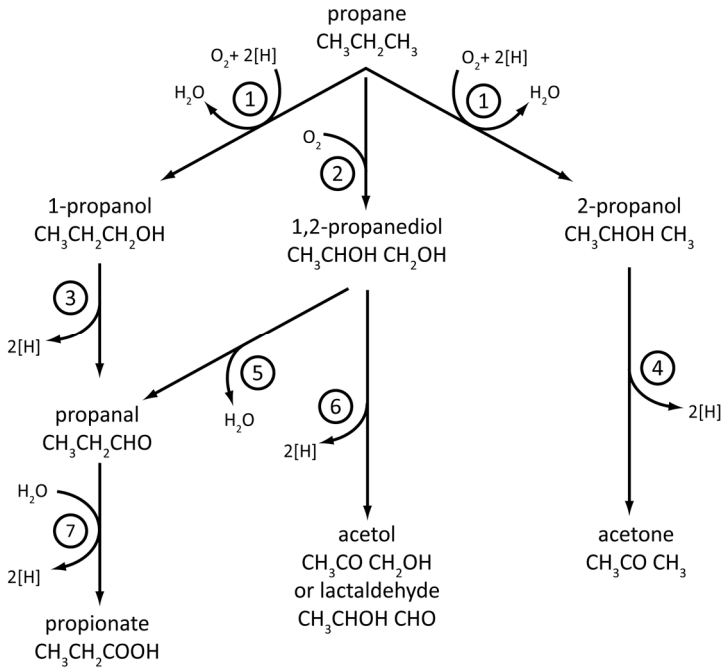

Figure 1.12. The possible pathways for the initial stages of propane oxidation. The enzymes are: 1, propane monooxygenase; 2, propane dioxygenase; 3, 1-propanol dehydrogenase; 4, 2-propanol dehydrogenase; 5, 1,2-propanediol dehydratase; 6, 1,2-propanediol dehydrogenase; 7, propanal dehydrogenase.

1.17 Regulation of alkane oxidation

In obligate methanotrophs which possess both the sMMO and the pMMO, their relative expression is regulated by copper (Murrell et al., 2000b; Hakemian and Rosenzweig, 2007), by mechanisms which are not completely understood, although it was demonstrated that *mmoR,* encoding the σ^{54} response regulator MmoR, was essential for sMMO expression in *Methylococcus capsulatus* and *Methylosinus trichosporium* (Csaki et al., 2003; Stafford et al., 2003). Previously it was shown that methane monooxygenase was expressed during growth of *Methylococcus capsulatus* and *Methylosinus trichosporium* on methanol (Linton and Vokes, 1978; Hyder et al., 1979; Best and Higgins, 1981; Yu et al., 2009), suggesting that methane itself is not directly involved in regulation in these organisms.

Similarly to the sMMO of methanotrophs, transcription of the sMMO-like butane monooxygenase (BMO) in *Thauera butanivorans* (capable of growth on C_2-C_9 *n*-alkanes), is initiated from a σ^{54} promoter (Sluis et al., 2002). Transcription was not induced by butane, but by 1-butanol or butanal, products of butane oxidation (or by the corresponding products of the oxidation of other alkane growth substrates), and

basal transcription of the BMO genes was sufficient to induce the operon in the presence of butane (Sayavedra-Soto et al., 2005). Propionate, a product of oxidation of odd-chain-length alkanes, strongly repressed BMO transcription in cells which did not contain propionate-metabolising capacity, although this capacity could be induced by addition of propionate to the growth medium, or by growth on propane or pentane (Doughty et al., 2006), which then also relieved the repression of BMO transcription. Interestingly, propionate and butyrate also irreversibly inactivated the BMO in the absence of the alkane substrates of the enzyme (Doughty et al., 2007). BmoR, (a σ^{54} transcriptional regulator homologous to MmoR) encoded by a gene upstream of the BMO operon and required for its maximal transcription, was suggested to respond to the primary alcohols capable of inducing BMO expression (Kurth et al., 2008).

Many metabolically versatile bacteria possess mechanisms to maximise use of preferred substrates when presented with alternative carbon sources, termed catabolite repression. For example, in *Pseudomonas putida* (which is capable of growth on $C_3 - C_{13}$ alkanes), the AlkS transcriptional activator responds to $C_5 - C_{10}$ alkanes (> 25 nM) and activates transcription of the alkane degradation pathway genes *alcBFGHJKL* from the *PalkB* promoter (Sticher et al., 1997). In the presence of alternative carbon sources such as amino acids, succinate or lactate, the combined effects of two regulatory systems reduce expression of AlkS and hence transcription from the *PalkB* promoter (reviewed by Rojo, (2009)). The first system, mediated by expression of the regulatory catabolite repression control protein Crc, is a global regulatory system which inhibits expression of enzymes of several metabolic pathways, whereas the second, dependent on the terminal oxidase Cyo, responds to cellular energy balance. Crc interacts with *alkS* mRNA preventing translation (and hence also transcription since AlkS is responsible for its own transcriptional activation), whereas the precise mode of action of Cyo is unknown.

Working with *Methylocella silvestris* BL2, Theisen et al, (2005), observed a lack of sMMO gene transcription or expression during growth on acetate, pyruvate or succinate, and also identified a putative MmoR regulatory protein, encoded by *mmoR*, co-transcribed with the sMMO operon, although the involvement of this gene-product in regulation of sMMO expression was not demonstrated.

These examples illustrate that expression of alkane-oxidising enzymes is carefully regulated in bacteria capable of growth on these compounds.

1.18 Applications of SDIMO enzymes in biotechnology

The increasing need for a sustainable policy regarding the use of raw materials and energy and concerns over pollution has heightened the importance of Green Chemistry, defined as the use of products and processes to minimise the production of harmful substances in chemical engineering. Biocatalysis, including the use of enzyme catalysed oxidation reactions, is an important element of this drive and is reviewed by Hollman et al. (2011). Monooxygenases, including SDIMOs, are able to catalyse useful reactions including epoxidation (Torres Pazmiño et al., 2010), which is valuable in organic synthesis because it introduces chirality. For example, using the sMMO, Xin et al. (2003) achieved the continuous co-oxidation of propene to epoxypropene by *Methylosinus trichosporium* growing on methane. The plant produced over 100 μmol day^{-1} epoxypropane from a culture volume of approximately 400 ml over a period of 53 days. The ability to engineer altered or improved enzymes for specific applications is greatly increasing the potential applications of biocatalysis (reviewed by Pollard and Woodley (2007)). An alternative approach, bioprospecting for novel enzymes with useful properties from natural environments, is also a potentially rewarding avenue for research (Holmes and Coleman, 2008).

The wide substrate specificity of SDIMOs has suggested numerous applications in bioremediation. For example, chlorinated aliphatic hydrocarbons are suspected carcinogens and common and persistent pollutants of groundwater (Vogel et al., 1987). The sMMO was shown to be able to degrade trichloroethylene (TCE) (Oldenhuis et al., 1989), achieving almost complete dechlorination, thus avoiding the toxic intermediates sometimes produced by anaerobic degradation (Lorah and Voytek, 2004). This capability is also present in propane-grown bacteria (Wackett et al., 1989), although the oxygenases responsible have not always been identified. The ability of various SDIMO-containing organisms to degrade chloroethenes has been reviewed by Mattes et al. (2010). Microcosms set up using material from a polluted aquifer at McClellan Air Force Base (California) were stimulated with methane, propane or butane in a long-term trial. Methane- and propane-stimulated (but, interestingly, not butane-stimulated) microcosms were able to degrade TCE, and in addition the propane-stimulated microcosms also degraded 1,1,1-trichloroethane, leading the authors to suggest that propane-utilisers were more suited to

cometabolism of the pollutant mix at this site (Tovanabootr and Semprini, 1998). In a similar study, Frascari et al. (2006) observed co-metabolic degradation of a range of chlorinated hydrocarbons, including 1,1,2,2-tetrachloroethane (not usually susceptible to aerobic biodegradation), in propane-supplied microcosms inoculated with indigenous microorganisms from a polluted industrial site in Italy. The potential benefits of using facultative methanotrophs for bioremediation of chlorinated hydrocarbons were illustrated by Im and Semrau (2011). A facultative *Methylocystis* strain was shown to degrade several chlorinated hydrocarbons during growth on ethanol, and the problem of the inhibition of the methane monooxygenase by the co-metabolised non-growth substrate was thus avoided, possibly leading to more rapid pollutant degradation. Propane-oxidising bacteria, including species of *Nocardia* (Steffan et al., 1997), *Mycobacterium* (Smith et al., 2003a), *Rhodococcus* (Haase et al., 2006) and *Pseudomonas* (Morales et al., 2009), were also able to degrade the toxic fuel additive methyl *tert*-butyl ether (MTBE) (reviewed by Nava et al. (2007)). A PrMO-like SDIMO was shown to be encoded by the genome of *Rhodococcus* sp. RR1, and this strain was capable of degrading the persistent environmental pollutant *N*-nitrosodimethylamine (NDMA) when induced on propane (Sharp et al., 2010). 1,4-dioxane, a probable carcinogen and groundwater contaminent, was degraded by several SDIMO-expressing strains (Mahendra and Alvarez-Cohen, 2006) including *Pseudonocardia dioxanivorans* CB1190 (which contains several SDIMOs as noted earlier) which is capable of growth on 1,4-dioxane as sole source of carbon and energy.

Other applications of organisms containing SDIMOs include production of single cell protein (Bothe et al., 2002), biopolymers (Pieja et al.) or higher value products including methanol from methane or natural gas (Lee et al., 2004), and bio-prospecting for petroleum deposits (Brisbane and Ladd, 1965).

1.19 Project aims

The aims of the work described here were:

1. To investigate the metabolic range of *Methylocella silvestris* and the potential for optimisation of growth conditions;
2. To develop a system to facilitate genetic manipulation;

3. To determine the presence and requirement for the glyoxylate bypass enzymes during growth on one- and two-carbon compounds, since previous work had failed to identify these enzymes in *M. silvestris*;
4. To investigate the requirement for the methane monooxygenase and the propane monooxygenase during growth on methane and propane, and the extent to which these two homologous enzymes are functionally redundant in the presence of each other;
5. To determine the products of propane oxidation and the pathways of propane metabolism.

1.20 Note on the proteomic analyses

During this project, use was made of the services provided by the Biological Mass Spectrometry and Proteomics Group at the University of Warwick, as described in the text. In addition, soluble extracts prepared from *M. silvestris* cells grown under different conditions were submitted for analysis as part of the development of advanced quantitative gel-free methods by Vibhuti Patel (Patel et al., 2009) and Nisha Patel (Patel et al., 2011). Some of the data generated by these researchers is mentioned in the following sections and informed the work described in this project, but did not form the basis of any of the major conclusions.

Chapter 2

Materials and methods

2.1 Materials

Analytical-grade chemicals were obtained from Sigma-Aldrich Corporation (St Louis, MO, USA), Melford Laboratories Ltd (Ipswich, UK) or Fisher Scientific UK (Loughborough UK). Gases were obtained from BOC (Manchester UK), Air Liquide UK (Birmingham UK) or Sigma-Aldrich. Methane and propane used for growth of cultures were 99.5% purity grade.

In some cases chemicals (including nicotinamide adenine dinucleotide (NAD) and nicotinamide adenine dinucleotide phosphate (NADP)) were purified of residual solvents by dissolving in a few millilitres of water and extracting several times in diethyl ether (25 – 100 ml) before drying under vacuum.

General purpose buffers and chemicals were prepared according to Sambrook and Russell (2001).

Custom oligonucleotide primers were obtained from Invitrogen (Paisley, UK).

2.2 Cultivation and maintenance of bacterial strains

All solutions and growth media were prepared with Milli-Q water and sterilised by autoclaving at 15 psi for 15 minutes at 121 ^{o}C. Solutions sensitive to autoclaving were sterilised using 0.2 μm pore-size disposable sterile filter units (Sartorius Minisart, Göttingen, Germany) and were added to cooled autoclaved media. Solid media were prepared by the addition of 1.5 % (w/v) Bacto Agar (Difco) prior to autoclaving. Bacterial strains and plasmids used in this study are shown in Table 2.1, and primers relevant to this section in Table 2.2.

2.2.1 Antibiotics

Antibiotics were filter sterilized and added aseptically to cooled, autoclaved growth medium, at the following concentrations: ampicillin 100 μg ml^{-1}; kanamycin, 25 μg ml^{-1}; gentamicin 5 μg ml^{-1}; tetracycline 10 μg ml^{-1}, except where indicated.

Table 2.1. Bacterial strains and plasmids used in this study. Abbreviations, Gm^R, gentamicin resistance; Km^R, kanamycin resistance, Tc^R, tetracycline resistance; Ap^R, ampicillin resistance; BHR, broad host range.

Strains/Plasmids	Description	Reference/source
Strains		
Escherichia coli TOP10	F– *mcrA* Δ(*mrr-hsdRMS-mcrBC*) Φ80*lacZ*ΔM15 Δ*lacX74 recA1 araD139* Δ(*ara leu*) *7697 galU galK rpsL* (StrR) *endA1 nupG*	Invitrogen
Escherichia coli JM109	*endA1*, *recA1*, *gyrA96*, *thi, hsdR17* (r_k^-, m_k^+), *relA1*, *supE44*, Δ(*lac-proAB*), [F′ *traD36*, $proAB^+$, $laqI^qZ$ΔM15]	Promega
Escherichia coli S17.1 λ*pir*	*recA1 thi pro hsdR*$^-$ RP4-2Tc::Mu Km::Tn*7* λ*pir*	(Simon et al., 1983)
Methylosinus trichosporium OB3b	Wild-type strain	Warwick culture collection
M. silvestris BL2	Wild-type strain	Warwick culture collection
M. silvestris ΔICL	*M. silvestris* BL2 with deletion of isocitrate lyase	This study
M. silvestris ΔICL pAC105	*M. silvestris* ΔICL complemented with the wild type gene on plasmid pAC105, Km^R	This study
M. silvestris ΔMS	*M. silvestris* BL2 with deletion of malate synthase	This study
M. silvestris ΔICL ΔMS	*M. silvestris* BL2 with deletions of both isocitrate lyase and malate synthase	This study
M. silvestris ΔSGAT	*M. silvestris* BL2 with deletion of serine-glyoxylate aminotransferase	This study
M. silvestris ΔMmoX	*M. silvestris* BL2 with deletion of sMMO α-subunit	This study
M. silvestris ΔPrMO	*M. silvestris* BL2 with deletion of propane monooxygenase α-subunit	This study
M. silvestris Δ1641	*M. silvestris* BL2 with deletion of Msil1641	This study
M. silvestris AC706	*M. silvestris* BL2 Δ*MmoX::*Km^R *sacB*	This study
Plasmids		
pGEM-T	Ap^R TA cloning vector	Promega
pCR2.1-TOPO	Km^R, Ap^R, TA cloning vector	Invitrogen

Table 2.1 (continued). Bacterial strains and plasmids used in this study.

Strains/Plasmids	Description	Reference/source
Plasmids		
pK18*mobsacB*	Km^R, RP4-mob, mobilizable cloning vector containing *sacB* from *B.subtilis*	(Schäfer et al., 1994)
pAC1003	pK18*mobsacB* containing upstream and downstream sequences from the *M. silvestris* malate synthase gene	This study
p34S-Gm	Source of Gm^R cassette	(Dennis and Zylstra, 1998)
pCM184	Ap^R, Km^R, Tc^R allelic exchange vector	(Marx and Lidstrom, 2002)
pCM157	Tc^R Cre expression vector	(Marx and Lidstrom, 2002)
pCM132	BHR *lacZ* vector, Km^R	(Marx and Lidstrom, 2001b)
pMHA203	BHR vector containing *M. silvestris* sMMO σ^{54} promoter and *gfp,* Km^R	(Ali and Murrell, 2009)
pAC105	pCM132 containing isocitrate lyase gene and promoter from *M. silvestris* BL2 in place of *lacZ*	This study
pAC304	pMHA203 with the sMMO promoter replaced by the PrMO promoter	This study

Table 2.2. 16S rRNA gene, sequencing and M13 primers.

Name	Sequence (5' – 3')	Reference
27F	AGAGTTTGATCMTGGCTCAG	(Lane, 1991)
1492R	TACGGYTACCTTGTTACGACTT	(Lane, 1991)
M13F	GTAAAACGACGGCCAG	Invitrogen
M13R	CAGGAAACAGCTATGAC	Invitrogen
SP6	TATTTAGGTGACACTATAG	Promega
T7	TAATACGACTCACTATAGGG	Promega

2.2.2 *Escherichia coli*

Escherichia coli strains were routinely cultivated on Luria-Bertani (or lysogeny broth) (LB) medium (Sambrook and Russell, 2001). Liquid cultures were incubated on an orbital shaker (150 - 200 rpm) at 37 ^{o}C. LB agar plates were prepared with the addition of 1.5 % (w/v) Bacto Agar (Difco) prior to autoclaving. *E. coli* strains were stored at -80 ^{o}C in the presence of 10 % (v/v) sterile glycerol.

2.2.3 Preparation and transformation of chemically competent *E. coli*

SOB medium:

The following were dissolved in 900 ml deionised water: yeast extract, 5 g; tryptone, 20 g; NaCl, 0.5 g. KCl solution (10 ml of 250 mM) was added, the pH adjusted to 7.0 with 5 M NaOH, the volume made up to 1 l with water, and the solution sterilised by autoclaving. Immediately prior to use sterile $MgCl_2$ solution (2 M) was added to 10 mM.

Inoue transformation buffer:

The following were dissolved in 800 ml deionised water: $MnCl_2.4H_2O$, 10.88g; $CaCl_2.2H_2O$, 2.2 g; KCl, 18.65 g. Piperazine-N,N′-bis(2-ethanesulfonic acid) (PIPES) buffer (10 ml of 0.5 M, pH 6.7) was added, the volume made up to 1 l with water and the solution sterilised by filtration.

SOC medium:

Glucose, sterilised by filtration, was added to SOB medium to a final concentration of 20 mM.

Chemically competent *E. coli* cells were prepared by the method of Inoue et al. (1990). A single colony from a fresh plate of *E. coli* Top10 cells was picked into 25 ml of LB medium and incubated at 37 °C with shaking. After 8 h, three 500 ml flasks containing 125 ml SOB medium each were inoculated with 1, 2 or 5 ml of this starter culture, and incubated at 20 °C with shaking overnight. The following morning, a flask was harvested as OD_{600} reached 0.55 and the other two were discarded. Cells were cooled on ice, centrifuged (2,500 × g, 10 mins, 4 °C), and the supernatant removed. Cells were re-suspended in 40 ml ice-cold Inoue buffer and centrifuged as before. Cells were re-suspended in 10 ml ice-cold Inoue buffer, and 750 µl

dimethylsulfoxide (DMSO) added gently with swirling. Following 10 min on ice, 50 µl aliquots of cells were dispensed into cooled microcentrifuge tubes, frozen in liquid nitrogen and stored at -80 ^{0}C.

For transformation, cells were thawed on ice and DNA (approximately 1 - 50 ng of plasmid DNA or ligation mix) added and gently mixed. Cells were subjected to heat shock at 42 °C for 45 s, and cooled on ice for 2 min. SOC medium (0.5 ml) was added and cells allowed to recover at 37 °C with shaking for one hour. Aliquots were spread on selective LB plates containing X-Gal and IPTG (as appropriate) and incubated at 37 °C for 18 – 24 h.

2.2.4 Preparation and transformation of electrocompetent *E. coli*

A 500 ml culture of *E. coli* was grown to an OD_{600} of 0.5 – 0.7, placed on ice for 15 min and then centrifuged at 4,000 x *g* for 15 min at 4 °C. The supernatant was removed and the cells washed, first in 500 ml, then in 250 ml of cold sterile deionised water and finally in 10 ml of cold 10% v/v glycerol, with centrifugation as above. The cells were re-suspended in 2.5 ml of cold 10 % (v/v) glycerol, dispensed in 100 µl aliquots into microcentrifuge tubes, frozen in liquid nitrogen and stored at –80 °C.

Electrocompetent cells were transformed by adding up to 2 µl of plasmid DNA or ligation mix and incubating on ice for 1 min. Cells were transferred to a chilled 0.1 cm electroporation cuvette (Plus BTX, Harvard Apparatus, Holliston, MA, USA) and an electric field pulse applied using a GenePulser Electroporation system (Bio-Rad, Hemel Hempstead, UK) set at 1.8 kV, 25 µF, 200 Ω. Cells were immediately removed into 1 ml SOC medium and allowed to recover with shaking (200 rpm) at 37 ^{o}C for 1 hour. Aliquots (50-100 µl) were spread onto selective LB agar plates.

2.2.5 *Methylocella silvestris*

A dilute nitrate mineral salts (DNMS) medium was used for growth of *M. silvestris*. Initially, medium was prepared according to Theisen (2006) using trace elements solution “A” shown below and phosphate buffer at a final concentration of 1 mM. Subsequently, a modified trace elements solution “B” and increased buffer concentration (2 mM) was used. Medium containing ammonium (DAMS medium)

was prepared using 0.1M NH_4Cl stock solution in place of solution 3, and with the addition of KCl to 1 mM final concentration.

Solution 1: Magnesium solution (100 × stock)

$MgSO_4.7H_2O$ 2.5 g

Solution 2: Calcium solution (100 × stock)

$CaCl_2.2H_2O$ 0.5 g

Solution 3: Nitrate solution (100 mM stock)

KNO_3 2.52 g

Each dissolved in 200 ml Milli-Q water and diluted to 250 ml.

Solution 4: Iron EDTA solution (10,000 × stock)

Fe-EDTA 0.38 g

Dissolved in 80 ml Milli-Q water and diluted to 100 ml.

Solution 5: Trace elements solutions (2000 × stock)

Compound	solution A (mg l^{-1})	solution B (mg l^{-1})
$ZnSO_4.7H_2O$	10	0
$ZnCl_2$	0	70
$MnCl_2.4H_2O$	3	100
H_3BO_4	30	6
$CaCl_2.6H_2O$	20	0
$CuCl_2.2H_2O$	1	2
$NiCl_2.6H_2O$	2	24
$Na_2MoO_4.2H_2O$	3	100
$CoCl_2.2H_2O$	0	100
$FeCl.4H_2O$	0	1500

Trace elements solution "A" was made by dissolving the specified compounds in 1 litre of Milli-Q water. Solution "B" was made by dissolving the $FeCl.4H_2O$ in 10 ml 25% (v/v) HCl, making up to 1 litre with Milli-Q water and then adding the remaining components. Trace element solutions were stored in the dark.

Solution 6: Phosphate buffer (0.2 M stock)

$Na_2HPO_4.2H_2O$ 7.12 g

$NaH_2PO_4.H_2O$ 5.52 g

Each dissolved separately in 150 ml Milli-Q water, diluted to 200 ml and mixed in proportion (approximately 95 ml monobasic solution + 5 ml dibasic solution) to give pH 5.5.

DNMS medium was prepared by adding 10 ml each of solutions 1, 2 and 3, 0.1 ml solution 4 and 0.5 ml solution 5 to 800 ml Milli-Q water, diluting to 1 litre and autoclaving. Following cooling, buffer was added, initially at 5 ml l^{-1}. Subsequently, as described later, buffer concentration was increased to 10 ml l^{-1}. To avoid precipitation, solutions 1 – 3 were prepared separately and medium was not stored, but prepared and autoclaved immediately prior to use. Nitrogen-fixing cultures were grown in medium without addition of a fixed nitrogen source. *M. silvestris* was routinely cultivated in 125 ml serum vials containing 25 ml DNMS medium. Flasks were sealed with grey butyl rubber seals and gassed with 20 ml (i.e. ~20 %) methane/carbon dioxide (95 %/5 % (v/v) mix). Other substrates and gas concentrations were used as described in the relevant sections. Vials were incubated at 25 ^oC with shaking at 150 rpm. *M. silvestris* was also grown in conical Quickfit flasks (250 ml or 1l) fitted with SubaSeal (Sigma-Aldrich) stoppers, although it was noted that growth with gaseous substrates was poor under these conditions, possibly due to the increased gas exchange in these flasks. For growth on solid media, agar plates were incubated in a gas-tight container under a methane/air atmosphere at room temperature, or in a methanol-rich atmosphere (achieved by addition of 1 ml of methanol to a paper tissue placed in the airtight container used for incubation of plates) or with other growth substrates as indicated. Gas or volatile substrates were replenished approximately every week.

Large scale cultivation was carried out in 4 l (LH Series 210, Stoke Poges UK), or 2 l fermenters (Fermac 300, Electrolab, Tewkesbury, UK) supplied with methane, propane (50 – 200 ml min^{-1}), or an alternative carbon source. Initially the dissolved oxygen level in the fermenter vessel was maintained above 5 % by adjusting the agitation speed and air flow rate. Subsequently it was found advantageous to limit oxygen to allow nitrogen fixation (as discussed in Chapter 3), and air flow was reduced just sufficiently to reduce the dissolved oxygen level to near zero. The pH of

the culture was maintained between 5.5 – 5.8 with the automatic addition of 0.5 M HCl or 0.5 M NaOH. Additional growth substrate or other medium components were added as required when growth slowed or analysis showed they were depleted. Growth was monitored by measuring the OD_{540} using a Beckman DU-70 spectrophotometer. DNMS medium was inoculated with 5 - 10 % (v/v) inoculum grown to mid-late exponential phase. For continuous culture, sterile medium was supplied using a previously calibrated peristaltic pump, and cells collected from the outflow in a sterile 25 l carboy.

2.2.6 Growth of *Methylosinus trichosporium* OB3b

Methylosinus trichosporium OB3b was grown in 200 ml nitrate mineral salts (NMS) medium in 1 l flasks sealed with SubaSeals and supplied with methane (20% v/v) as previously described (Oakley and Colin Murrell, 1988). Cells were harvested by centrifugation (6,000 × g, 20 min, 15 °C), washed once in growth medium (without growth substrate) and resuspended in a minimal volume of PIPES buffer (40 mM, pH 7.0). Cells were either used immediately or drop frozen in liquid nitrogen and stored at -80 °C.

2.3 Conjugation of *M. silvestris*

The transfer of plasmid DNA from *E. coli* to *M. silvestris* broadly followed the method of Martin and Murrell (1995). A 15 ml overnight *E. coli* S17.1 culture, containing the desired plasmid, and a 50 ml culture of *M. silvestris* (OD_{540} approximately 0.4) were separately centrifuged (4,000 × g, 15 min, 15 °C), washed in 25 ml DNMS medium, re-suspended in 25 ml DNMS medium, mixed together and centrifuged as before. The resultant cell pellet was re-suspended in 2 ml DNMS medium. Aliquots of the cell suspension (0.5 ml) were applied to the centre of a 0.2 µm pore-size nitrocellulose filter (Millipore, Billerica, MA, USA), placed on a DNMS agar plate containing 0.02 % (w/v) proteose peptone and incubated for 24 hours at 30 ^{o}C (with appropriate growth substrate, either 5 mM succinate contained in the plates, or in a methanol-rich atmosphere). Following incubation, the cells were washed with 10 ml DNMS medium, collected by centrifugation (4,000 x g, 15 min, 15 °C) and re-suspended in 1 ml DNMS medium. Aliquots (50-100 µl) were spread

on DNMS plates containing selective antibiotics and incubated at room temperature. Colonies formed on the plates after 3-6 weeks.

2.4 Counter-selection with sucrose

Counter-selection was applied to cultures of *M. silvestris* containing the *sacB* gene (Schäfer et al., 1994). Cells growing in liquid culture with antibiotic selection were used as inoculum for non-selective liquid DNMS medium. At mid-late exponential phase cells were diluted 1/10 or 1/100 in DNMS medium and 50 µl spread on DNMS plates containing 10% (w/v) sucrose (with an appropriate carbon source) and incubated at room temperature.

2.5 Preparation and transformation of electrocompetent *M. silvestris*

For electroporation, best results were obtained with cells grown in the fermenter using medium without fixed nitrogen, under oxygen limitation (nitrogen-fixing) conditions, which allowed growth of cells without polysaccharide slime. When necessary, it was also found possible to use flask-grown cells. Two methods for the preparation of competent cells were used. Initially, cells were prepared following the method of Kim and Wood (1998). Approximately 100 ml *M. silvestris* culture in mid - late exponential phase, OD_{540} ~ 0.5, or an equivalent amount of fermenter-grown cells in exponential phase were cooled on ice and harvested by centrifugation (3000 x g, 15 min, 4°C). Cells were washed twice in 20 ml cold 0.3 M sucrose (with centrifugation as above) followed by re-suspension in 1 ml 0.3M sucrose to which was added 75 µl of 30% PEG6000. Cells were transferred to 200 µl aliquots, frozen in liquid nitrogen and stored at -80 °C. Subsequently, the method was modified and cells were washed in cold sterile water and re-suspended in 10% (v/v) glycerol.

For transformation, cells were thawed on ice and up to 6 µl of DNA (about 20 ng -1 µg) was added to 100 µl of cell suspension and mixed gently. Cells and DNA were transferred to a chilled 0.1 cm electroporation cuvette (Plus BTX, Harvard Apparatus, Holliston, MA, USA) and an electric field pulse applied using a GenePulser Electroporation system (Bio-Rad, Hemel Hempstead, UK) set at 2.2 – 2.5 kV, 25 µF, 400 Ω. Cells were immediately washed from the cuvette with 0.5 ml DAMS medium containing a suitable carbon and energy source, transferred to 15 ml tubes and allowed to recover for 10 – 12 h at 25 °C with shaking. The cells were then

centrifuged (3000 × g, 15 °C, 10 min), washed twice and re-suspended in DAMS medium to remove sucrose or glycerol. Aliquots (50-100 µl) were spread onto selective DAMS agar plates and incubated at room temperature for 2 – 6 weeks.

2.6 Extraction of nucleic acids

2.6.1 Genomic DNA from *M. silvestris* and *Methylosinus trichosporium* OB3b

High-molecular mass genomic DNA was extracted from *M. silvestris* for use during this project, and from *Methylosinus trichosporium* OB3b for sequencing by the Joint Genome Institute (JGI), (Walnut Creek, Ca, USA) (Stein et al., 2010), essentially as Oakley and Murrell, (1988). Cells (approximately 1 – 3 g wet weight) were resuspended in 6 ml TE buffer (tris(hydroxymethyl)aminomethane (Tris) 10 mM, ethylenediaminetetra-acetate (disodium salt) (EDTA) 1 mM, pH 8.0) in 100 ml conical flasks, to which was added 1.9 ml 0.5 M EDTA (pH 8.0) and 1 ml lysozyme (50 mg ml^{-1}). Following 15 min incubation at 37 °C, 250 µl of proteinase K (20 mg ml^{-1}) and 3.1 ml 10% (w/v) sodium dodecyl sulfate (SDS) were added and mixed gently. Flasks were incubated 15 min at 37 °C and 10 min at 60 °C, sodium perchlorate (4 ml of 5 M) was added, and incubated a further 15 min at 60 °C with gentle mixing every few minutes. An equal volume of phenol/chloroform/isoamyl alcohol (25:24:1) was added and incubated at room temperature for 30 min with gentle mixing. The mixture was transferred to 50 ml centrifuge tubes. Following centrifugation (48,000 × g, 30 min, 4 °C), the aqueous phase was carefully removed using a wide-bore pipette, and two further 15 min extractions with phenol/chloroform/isoamyl alcohol and two with chloroform/isoamyl alcohol (24:1) were carried out, each followed by centrifugation (38,000 × g, 15 min, 4 °C). Salt content was adjusted by addition of NaCl to 0.1 M, followed by two volumes of cold ethanol. DNA was removed by spooling with a Pasteur pipette, dried and re-suspended in 5 ml TE buffer. In the case of *Methylosinus trichosporium* OB3b, recovery of DNA required centrifugation (48,000 × g, 15 min, 4 °C), following which the pellet was dried and resuspended in TE buffer. RNA was digested by addition of DNase-free RNase to 100 µg ml^{-1} and incubation for 30 min at 37 °C. The volume was made up to 30 ml with TE buffer and 30 g caesium chloride added and gently mixed to dissolve. Ethidium bromide was added (200 µl of 10 mg ml^{-1}) and DNA purified by density gradient centrifugation (196,000 × g, 36 h, 20 °C) in a

VTi 50 rotor (Beckman Coulter, High Wycombe, UK). DNA was visualised using UV light and removed by piercing the tube with a wide-bore syringe needle, followed by removal of ethidium bromide by several extractions with TE-saturated butanol. DNA was then dialysed (× 3) against 2 l TE buffer and quantified by agarose gel electrophoresis by comparison with a *Hin*dIII-digested Lambda-DNA ladder (Figure 2.1).

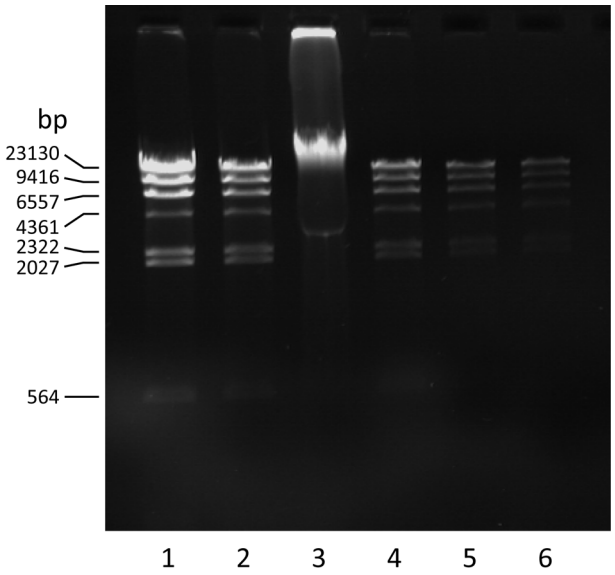

Figure 2.1. *Methylosinus trichosporium* OB3b DNA (lane 3) in comparison to *Hin*dIII-digested Lambda-DNA standards. The marker 23 kb bands contain 250, 125, 62.5, 31.2 or 15.6 ng DNA respectively in lanes 1 – 6. The mass of the >23 kbp band in lane 3 was estimated as 416 ng using GeneTools software (Syngene).

2.6.2 Extraction of small quantities of genomic DNA

For extraction of small quantities of DNA, an estimated 0.2 mg (dry weight) of cells was centrifuged (10,000 × g, 10 min, room temperature) in 1.5 ml microcentrifuge tubes. The pellet was re-suspended in 0.75 ml TE buffer, 20 µl lysozyme (100 mg ml^{-1}, Sigma) added, and tubes incubated at room temperature for 5 min. SDS (40 µl of 10% w/v) was added and mixed gently, followed by 8 µl of proteinase K (10 mg ml^{-1}) (Melford Laboratories). Tubes were mixed gently and incubated at 37 °C for 1 h, following which NaCl (100 µl of 5 M) and 100 µl of warm cetyl-trimethylammonium bromide (CTAB) (10% in 0.7 M NaCl) were added and tubes incubated at 65 °C for 10 min. Proteins and other impurities were extracted once with 0.5 ml phenol/chloroform/isoamyl alcohol (25:24:1) and once with 0.5 ml chloroform/isoamyl alcohol (24:1). Nucleic acids were precipitated from the aqueous

phase by addition of 0.6 volumes of isopropanol and 30 min incubation at room temperature. Tubes were centrifuged at maximum speed in a microcentrifuge (4 °C, 20 min), the pellet washed in 200 µl 70% v/v ethanol, dried and re-suspended in 50 µl TE buffer.

2.6.3 DNA extraction for clone library analysis

For clone library analysis, DNA was extracted from cultures using the bead-beating method of Griffiths et al. (2000).

2.6.4 RNA extraction from *M. silvestris*

For RNA work, all glassware, water and solutions were treated with diethylpyrocarbonate (DEPC) (or prepared with DEPC-treated water where appropriate) by shaking overnight at 37 °C in a 0.1% v/v solution prior to autoclaving. All plasticware, tips etc was RNase-free.

Total RNA was isolated from *M. silvestris* using the hot acid-phenol method of Gilbert et al. (2000). The quality of the RNA was checked by running a small volume on a 1% (w/v) TBE-agarose gel. DNA was removed by two treatments using Qiagen RNase-free DNase, each followed by purification using an RNeasy spin column (Quiagen, Crawley, UK) following the manufacturer's instructions. Removal of all traces of DNA was confirmed by the absence of a 16S rRNA PCR product in reactions using 1 µl or 4 µl of RNA template and 35 PCR cycles.

2.6.5 Small-scale plasmid extraction from *E. coli* (mini-prep)

Small scale plasmid preparations were carried out using 1.5 -5 ml overnight *E. coli* cultures using the Qiaprep Miniprep Kit (Qiagen) or GeneJET kit (Fermentas) according to the manufacturer's instructions.

2.7 Nucleic acid manipulation techniques

2.7.1 Quantification of DNA/RNA

DNA and RNA concentrations and purity were estimated by agarose gel electrophoresis and comparison with a known quantity of 1 kb ladder (Fermentas),

or by using an ND-1000 spectrophotometer (NanoDrop Technologies Inc., Wilmington, DE, USA)

2.7.2 Polymerase chain reaction (PCR)

Polymerase chain reactions (PCR) were conducted in a 50 µl reaction volume using a T3000 (Biometra, Goettingen, Germany) or Tetrad (Bio-Rad) thermal cycler, using recombinant Taq or DreamTaq (Fermentas) or, for high fidelity applications, *Pfu* polymerase (Promega). A typical reaction (prepared on ice) contained (in 50 µl volume) 1 × buffer, $MgCl_2$ (1.5 mM), dNTPs (0.2 mM of each), forward and reverse primer (0.4 µM) and *Taq* DNA polymerase (2.5 units). For direct amplification from colonies or cultures, DMSO (5% v/v) and BSA (0.07% w/v) were included in addition. Cycling conditions were typically: initial denaturation at 95 °C, 3 min; 25 - 35 cycles of denaturation at 95 °C, 30 s; annealing (temperature dependent on primers), 30 s; elongation at 72 °C, 1 min/kb and final elongation at 72 °C, 7 min. For PCR from colonies, the initial denaturation was increased to 10 min. Elongation was generally conducted at five degrees less than the primer melting temperature. When using *Pfu* polymerase, enzyme was added to the reaction during the initial denaturation stage at 95 °C to avoid nuclease activity (hot start). Reactions without template (no-template controls) were included in all cases.

2.7.3 DNA restriction digests

Restriction digestion of DNA was carried out with enzymes from Invitrogen or Fermentas according to the manufacturers' recommendations.

2.7.4 DNA purification

DNA fragments were routinely excised from TBE agarose gels and the DNA purified using QIAquick (Qiagen) or Nucleospin (Macherey-Nagel, Düren, Germany) Gel Extraction Kits according to the manufacturers' instructions. PCR products of well-defined size were purified using the same protocol but without excision from gels. DNA was also purified by extractions with equal volumes of phenol/chloroform and chloroform, adjustment of the salt concentration with 0.1 volumes of 3 M sodium acetate (pH 5.5), precipitation with two volumes of cold ethanol, incubation at -20 °C

overnight (or at -80 °C for 30 min), centrifugation (21,000 × g, 15 min, 4°C), washing in 70% cold ethanol, drying and re-suspension in TE buffer.

2.7.5 Preparation of linear DNA for electroporation

Linear DNA fragments for electroporation of *M. silvestris* were excised with the relevant enzymes and separated from the vector backbone in a 0.7% agarose gel, purified using a kit as described above, and eluted in sufficient TE buffer to give a concentration of 50 – 200 ng μl^{-1}. On occasion, the DNA was denatured immediately prior to electroporation using the methods of Oh and Chater (1997), but without a noticeable improvement in the efficiency of gene replacement.

2.7.6 Dephosphorylation

Prior to ligation, restriction-enzyme digested plasmid DNA was dephosphorylated using Shrimp Alkaline Phosphatase (SAP) (Fermentas) following the manufacturer's instructions.

2.7.7 DNA ligations

Ligations were typically carried out in a volume of 20 µl containing a total of 200 ng DNA, comprising vector and insert fragments in equi-molar quantities. T4 DNA ligase (Fermentas) was used according to the manufacturer's instructions.

2.7.8 Blunting of DNA

DNA fragments with overhanging 5' or 3' ends were blunted when necessary using T4 DNA polymerase (Fermentas). Reactions (20 µl final volume) containing 1 × buffer, DNA (1 µg) dNTPs (0.1 mM) and T4 polymerase (1 unit) were incubated at room temperature for 5 min and inactivated at 70 °C for 10 min.

2.7.9 Cloning of PCR products

PCR products were cloned into pCR2.1-TOPO (Invitrogen), or pGEM-T Easy (Promega, Madison, WI, USA) according to the manufacturers' instructions. Where *Pfu* polymerase was used for PCR amplification, addition of a terminal 3' adenosine was accomplished by incubating, (in a volume of 20 µl), purified PCR product, *Taq* polymerase (5 units), dATP (0.2 mM) and 1 × *Taq* buffer, at 72 °C for 20 min.

Inserts in these vectors were sequenced using primers M13F or M13R and SP6 or T7 respectively (Table 2.2).

2.7.10 Clone library construction

Clone libraries were constructed using 16S rRNA gene sequences PCR-amplified using primers 27F/1492R (Table 2.2). PCR products were cloned as described in Section 2.7.9, and 16S rRNA sequences amplified directly from colonies by PCR using primers M13F/M13R. PCR products were digested with *Eco*RI and *Msp*I and resolved by electrophoresis in 2% (w/v) agarose gel. Clones were grouped based on the pattern of restriction fragments and representatives from each group sequenced.

2.7.11 Sequencing of DNA

Purified DNA (10 – 80 ng) was combined with 5.5 pmol primer in a volume of 10 µl and submitted for Sanger sequencing at the University of Warwick Genomics Facility. Sequence data was analysed and exported using Chromas (Technelysium Pty Ltd, Brisbane Australia).

2.7.12 Reverse transcriptase PCR (RT-PCR)

Reverse transcription was performed using Superscript II or Superscript III (Invitrogen), according to the manufacturer's instructions. Either random hexamer or gene-specific primers were used as described in the relevant sections. Between 50 ng and 1 µg of RNA was used for first strand cDNA synthesis with 200 ng random hexamers or 2 pmol gene specific primer. Reactions were included in which water was used in place of reverse transcriptase as negative control, and, as described in the relevant sections, in some cases reactions were carried out without primer. Reverse transcription was carried out at 42 °C or 55 °C for Superscript II or Superscript III respectively. As indicated, in some cases RNA was digested with 2 units of *E. coli* RNaseH (Fermentas). cDNA (1 - 2 µl) was used as template in PCR reactions, alongside reactions with template in which reverse transcriptase had been omitted in cDNA-synthesis reactions and in some cases reactions where cDNA-synthesis primer had been omitted. Reactions with a DNA template were included and also no-template controls.

2.7.13 5' Rapid amplification of cDNA ends (RACE)

5' RACE was performed using the 2nd Generation 5'/3' RACE kit (Roche), following the manufacturer's instructions. Total RNA (100 ng – 1 μg) was used for cDNA synthesis. Following cDNA column-purification and polyA tailing, two rounds of nested PCR were employed using gene-specific primers in conjunction with the oligo-dT and anchor primers supplied in the kit. In most cases, a clearly size-defined PCR product resulted which was either sequenced directly, or cloned and a few of the PCR-amplified inserts from clones sequenced. Alternatively, the PCR product was excised from an agarose gel, purified, cloned and a few of the clones (those containing the largest-sized inserts) sequenced.

2.7.14 Agarose gel electrophoresis

DNA fragments were separated in 0.5 – 2 % (w/v) agarose gels in 0.5 × TBE or 1 × TAE buffer. GeneRuler 1kb DNA ladder (Fermentas) was used to estimate the sizes of DNA fragments. Ethidium bromide (0.5 μg ml^{-1}) was added to gels prior to casting. Gels were visualised on a Gene Genius transilluminator (Syngene, Cambridge, UK).

2.8 Harvesting of cells

M. silvestris cells were harvested by centrifugation (6,000 × g, 20 min, 4 °C), washed once in growth medium without growth substrate and resuspended in a minimal volume of 2-(N-morpholino)ethanesulfonic acid (MES) buffer (40 mM, pH 5.5). Cells were either used immediately or drop frozen in liquid nitrogen and stored at -80 °C. In an attempt to maximise the activity of propane-grown cells in response to propane in the oxygen electrode, cells were harvested by minimising exposure to atmospheric oxygen and using medium and buffer sparged with oxygen-free nitrogen or with propane, but it was not clear if these precautions resulted in significantly increased activity.

2.8.1 Bacterial purity checks and microscopy

All bacterial strains were handled and cultivated axenically to minimise contamination. The purity of cultures was routinely checked using phase contrast

microscopy. Purity of cultures was also checked by plating onto R2A or nutrient agar plates, which were incubated aerobically at room temperature for several days (since *M. silvestris* does not grow on rich media). In addition, from time to time small (48 or 96) 16S rRNA gene clone libraries were constructed using DNA extracted from cultures. Cultures were also checked by serial dilution and plating on DNMS plates. Following incubation with appropriate carbon sources single colonies were used for PCR amplification of functional or 16S rRNA genes which were verified by sequencing.

2.8.2 Calculation of specific growth rate, lag time and increase in biomass

For each culture, the natural logarithm of culture density (OD_{540}) was plotted against time, and a straight line (the slope of which equates to the specific growth rate) fitted to the exponential phase of growth using Microsoft Excel. Growth rate was determined for each culture from a minimum of three data points, or two data points separated by at least 48 hours. Lag time was defined as the x value of the intersection of the line fitted to the exponential growth phase with the y-value of the start density. Increase in biomass was defined as the difference between the initial and maximum densities (OD_{540}) reached by the culture.

2.9 Preparation of cell extract

Cell extract was prepared by resuspending cells in 50 mM piperazine-N,N′-bis(2-ethanesulfonic acid) (PIPES) buffer (pH 7.0) containing 1 mM benzamidine and breaking cells by three or four passages through a French pressure cell (American Instrument Company, Silver Spring, MD) at 110 MPa (on ice). Cell debris was removed by centrifugation (10,000 × *g*, 15 min, 4 °C). The resulting supernatant was used as cell-free extract, or fractionated by ultracentrifugation (140,000 × g, 4 °C, 90 min) using a SW 55Ti rotor (Beckman Coulter, High Wycombe UK). The supernatant was used as soluble fraction, and the pellet twice re-suspended and washed in 5 ml PIPES buffer (as above) followed by 45 min centrifugation as before. The pellet was finally re-suspended in a minimal volume of buffer and used as membrane fraction. Small quantities of cells were occasionally disrupted for SDS-PAGE by sonication, using a Sanyo Soniprep sonicator fitted with a 3 mm probe. Cell pellets were re-suspended in 1 ml of buffer (as above) in 1.5 ml microcentrifuge tubes

and subjected to 6 cycles, each of 15 s sonication on ice (amplitude 10 μm) followed by 20 s cooling. Cell debris was removed by centrifugation as above. Extracts were stored in aliquots following rapid freezing in liquid nitrogen.

2.10 Protein methods

2.10.1 Quantification

Total protein concentration was determined using the Bio-Rad Protein Assay (Bio-Rad Laboratories Inc., Hercules, CA, USA) according to the manufacturer's instructions, against standards prepared from bovine serum albumin (BSA).

2.10.2 Precipitation of proteins

Occasionally proteins were concentrated by precipitation. 100% Trichloracetic acid (TCA) (prepared by dissolving 500g TCA in 227 ml H_2O) was added to protein solutions to 12% final concentration and incubated 30 min on ice. Following centrifugation (26,000 × g, 20 min, 4 °C) the pellet was washed in acetone, dried and re-suspended in buffer.

2.11 SDS-PAGE

Polypeptides were separated by SDS-PAGE using an X-cell II Mini-Cell apparatus (Novex). A 4 % (w/v) stacking gel and an 8 - 12.5 % (w/v) resolving gel were used and prepared as follows, using premixed 40% (w/v) acrylamide/bis (37.5:1) (Amresco, Solon, OH, USA).

	4% Stacking gel	12.5% Separating gel
Acrylamide/bis	1.0 ml	6.25 ml *
Tris 0.5 M pH 6.8	2.5	-
Tris 3.0 M pH 8.8	-	2.5
10% SDS	0.1	0.2
10% Ammonium persulfate	0.05	0.15
TEMED (*N*,*N*,*N*′,*N*′-tetramethyl-ethane-1,2-diamine)	0.010	0.010
Water	6.3	10.9

* Separating gels of different percentages were prepared by altering the acrylamide/bis and H_2O volumes appropriately.

SDS-PAGE was performed with cell-free extract, soluble or membrane fractions, or with whole cells. Cell pellets were re-suspended in SDS-PAGE sample buffer (63 mM Tris-HCl (pH 6.8), 10 % (v/v) glycerol, 5 % (v/v) β-mercaptoethanol, 2 % (w/v) SDS, 0.00125 % (w/v) bromophenol blue) or 1/4 volume of 5 × sample buffer was added to extracts. Samples were immediately heated for 8 minutes in a boiling water bath and cooled on ice. For whole cells, cell debris was pelleted by centrifugation in a microcentrifuge (21,000 × g, 3 min, 4 °C). Approximately 10 – 60 μg protein was loaded per lane. Electrophoresis was conducted at 90V through the stacking gel and 160V during separation, using running buffer containing glycine (72 g l^{-1}), Tris base (15 g l^{-1}) and SDS (5 g l^{-1}). PageRuler Plus prestained protein ladder (Fermentas) was used as molecular mass marker.

On occasion, precast gels (Bis-Tris Novex NuPAGE gels (Invitrogen)) were used with MOPS buffer following the manufacturer's instructions. Gels were stained with Coomassie brilliant blue staining solution (0.1 % (w/v) Coomassie brilliant blue R-250 dissolved in 40 % methanol, 10 % acetic acid and 50 % water) and destained in 40 % (v/v) methanol and 10 % (v/v/) acetic acid.

2.11.1 Native gels

Native gels (7.5 or 10%) and running buffer were prepared as for denaturing gels, except without SDS. Sample buffer contained neither SDS nor β-mercaptoethanol, and samples were not heated. Gels were run at 20 mA / 40 mA through the stacking and separating gels respectively in the cold room. Gels were stained with Coomassie (as above) or in 25 mM Tris buffer pH 8 containing phenazine methosulfate (PMS) (0.7 mM), nitroblue tetrazolium (NBT) (0.2 mg ml^{-1}), NAD^+ (1 mM) and NH_4Cl (4 mM). In some cases, NAD^+ and/or ammonium were omitted, as described in the relevant sections. Following 5 min incubation (in the dark) with slow shaking at room temperature, alcohol substrates were added to 1 mM, and incubated for 10 – 30 min with shaking, before the reaction was stopped by rinsing with H_2O.

2.11.2 MS/MS analysis of polypeptides

Bands of interest from denaturing and native gels were excised from the gel using a 1 × 6 mm gel-cutting tip, cut into approximately 1.5 mm cubes, mixed with 200 μl de-ionized water and submitted for analysis by the Biological Mass Spectrometry and

Proteomics Group at the University of Warwick. Following digestion with trypsin, samples were analysed by nanoLC-ESI-MS/MS using the NanoAcquity/Synapt HDMS instrumentation (Waters). A database compiled from the predicted amino acid sequences derived from the *M. silvestris* genome sequence was used for polypeptide identifications, which were considered on the basis of at least two tryptic peptide matches.

2.11.3 Proteomic analysis by liquid-chromatography-based label-free quantitative mass spectrometry

Soluble extract was prepared as described above and submitted for proteomic analysis by Vibhuti Patel (Patel et al., 2009), Nisha Patel (Patel et al., 2011) and the Biological Mass Spectrometry and Proteomics Group at the University of Warwick.

2.12 Oxygen electrode

A Clark oxygen electrode (Rank Brothers Ltd, Cambridge, UK) was used to detect substrate-induced oxygen consumption by whole cells. Between 1 – 5 mg dw of cell suspension (as determined from OD_{540}, assuming that 1 ml of cells at OD_{540} = 1 is equivalent to 0.25 mg dw) was added to 3 ml of oxygenated 40 mM phosphate buffer (pH 5.5) in the instrument cell maintained at 25 °C using a circulating water bath (Churchill Co. Ltd, Perivale, UK). The instrument was operated and calibrated by comparison with air-saturated water as described by Green and Hill (1984). Following establishment of a stable endogenous rate of oxygen consumption, substrate (7.5 nmol – 15 μmol) was added and substrate-induced rate calculated by substracting the endogenous rate from the rate following addition of substrate. Gaseous substrates were prepared as saturated aqueous solutions in 120 ml serum vials containing 25 ml water flushed with at least ten volumes of the substrate gas, and the concentration calculated using the Henry's Law constant obtained from Sander (1999).

Frozen cells were typically used for the assays. It was found that activities of the *M. silvestris* soluble di-iron monooxygenases (SDIMOs) were extremely sensitive to oxygen, and it was necessary to thaw cells and store on ice in tubes flushed with oxygen-free nitrogen without re-suspension in buffer. Under these conditions activity of methane-grown cells in response to methane remained essentially unchanged for

several hours, whereas if cells were re-suspended in an equal volume of air-equilibrated buffer, activity was approximately halved in less than one hour. The activities of other enzymes (for example methanol dehydrogenase) were not noticeably affected.

For screening of relatively insoluble non-growth SDIMO substrates, it was found inadvisable to inject the pure compound or an excess of an aqueous solution since this was likely to damage the electrode membrane and/or leave a residue which was difficult to remove without dismantling the instrument cell. Saturated solutions were prepared and between 5 - 100 µl of the aqueous phase injected.

2.13 **Enzyme assays**

Colourimetric enzyme assays were conducted using an Ultrospec 3100pro UV/Visible Spectrophotometer (Amersham) fitted with an eight cuvette auto-changer. Reactions were conducted using 1cm path-length, 1ml disposable-plastic or quartz cuvettes (for < 320 nm) at room temperature, which was recorded. All reactions were measured against a blank, and reactions without protein and without substrate were included.

2.13.1 Naphthalene assay for sMMO

The qualitative assay of Brusseau et al. (1990) was used to detect naphthalene-oxidising activity (assumed not to be specific for the sMMO). Approximately 1 ml of active cells at OD_{540} of 0.5 was incubated with a few crystals of naphthalene for 30 min at 30 °C. A few drops of freshly prepared tetrazotized *o*-dianisidine (10 mg ml^{-1}) were added. Immediate development of a purple colour was taken as evidence of naphthalene oxidation.

2.13.2 Nitrogenase

Nitrogen-fixing cells (20 ml of culture) were removed from the fermenter and placed in 120 ml serum vials, sealed with rubber seals, and flushed with at least 10 volumes of argon. Oxygen was added (between 0.25 and 20% of headspace volume), and methanol to a final concentration of 10 mM. Vials were gently shaken at room temperature for 5 min before injection of 0.5 ml (0.5%) acetylene to the headspace. Nitrogenase-mediated reduction of acetylene to ethylene was detectable after

approximately 10 min following addition of substrate and was linear for at least 2 h. Production of headspace ethylene was monitored every 15 minutes for 90 minutes using a Pye Unicam 104 gas chromatograph at the following settings:

Column, carrier gas, detector	Porapak N, N_2 (30 ml min^{-1}), FID
Injector temp	120 °C
Column temp	100 °C (isothermal)
Detector temp	150 °C
Injection volume	100 µl

Ethylene and acetylene were quantified by comparison with standards prepared in argon at known concentrations. At these settings retention times were acetylene 1.36 min, ethylene 0.95 min. For inhibition by ammonium, 30 ml vials containing 5 ml culture were set up as before with 5% headspace oxygen (i.e. the oxygen concentration at which maximum nitrogenase activity was detected). The reaction was allowed to proceed for 30 min before injection of ammonium chloride to final concentrations of 0, 0.5 1.5 or 5 mM. Inhibition of nitrogenase activity resulted in a decrease in the rate of ethylene production.

2.13.3 Isocitrate lyase

Isocitrate lyase was assayed following essentially the method of Dixon and Kornberg (1959), adapted for a 1 ml volume. Buffer pH was varied between 6.0 and 8.0, and pH 7.0 was found to give the highest activity. The reaction mixture contained potassium phosphate buffer pH 7.0 (final concentration 100 mM), $MgCl_2$ (6 mM), phenylhydrazine HCl (4 mM) L-Cysteine HCl (12 mM) protein (50 - 200 µg) and was initiated with DL-isocitrate (trisodium salt) (8 mM). EDTA (0.7 mM) was compared with cysteine as an activator as recommended by Kennedy and Dilworth (1963) but there was no difference in activity. The increase in absorbance at 324 nm, due to the accumulation of glyoxylate phenylhydrazone, was recorded against reactions containing water instead of isocitrate. After a lag of approximately 1 – 2 min, the reaction was linear for at least 10 min. Rates were calculated using ε_{324} for glyoxylate phenylhydrazone = 1.7×10^4 $M^{-1}cm^{-1}$.

2.13.4 Malate synthase

Malate synthase activity was assayed by following the decrease in absorbance at 232 nm due to the breakage of the acetyl-CoA thio-ester bond in the presence of glyoxylate. Reactions (1 ml) contained Tris buffer pH 8.0 (final concentration 90 mM), $MgCl_2$ (3.4 mM), acetyl-CoA (sodium salt) (0.05 mM) and protein (100 µg total). Absorbance was measured for 5 min before and after addition of glyoxylate (final concentration 0.5 mM). Without substrate, change in absorbance was less than 0.0008 min^{-1}. Rates were calculated using ε_{232} for acetyl-CoA $= 4.5 \times 10^3$ $M^{-1}cm^{-1}$.

2.13.5 Aldehyde dehydrogenase

NAD(P)- dependent aldehyde dehydrogenase was assayed by following the accumulation of NADH or NADPH. Tris, tricine, glycine/NaOH and *N*-cyclohexyl-2-aminoethanesulfonic acid (CHES) buffers were compared, and the pH optimised with CHES buffer at pH 9.25, see Figure 2.2. The reaction (1 ml) contained CHES buffer pH 9.25 (50 mM), dithiothreitol (DTT) (1 mM), $NAD(P)^+$ (0.75 mM), protein (100 µg) and substrate (10 mM). Where noted, coenzyme A was included (0.1 mM). The reaction was initiated by the addition of substrate and followed by measuring absorbance at 340 nm. Activity was calculated using $\varepsilon_{340} = 6.22 \times 10^3$ M^{-1} cm^{-1}, and compared with controls both without substrate and also without protein.

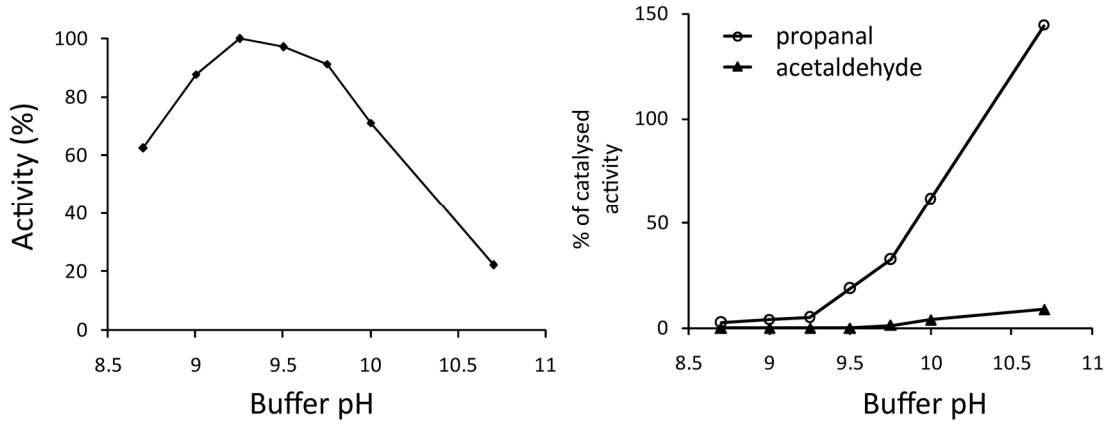

Figure 2.2. The influence of buffer pH on NAD(P)-dependent aldehyde dehydrogenase activity (left) and (right) a chemical reaction caused an increase in absorbance at 340 nm in the absence of protein. This effect was significant in reactions containing propanal and is expressed as a percentage of succinate-grown cell extract-catalysed activity in response to propanal.

There was no significant rate without substrate, but a NAD^+-dependent increase in absorbance at 340 nm in the presence of propanal (but not acetaldehyde) without protein, which increased at higher pH, was observed, see Figure 2.2. Since similar assays are frequently conducted at pH 9.5, e.g. Leal et al. (2003), this should be noted. This chemical activity was subtracted from enzyme-catalysed activity.

2.13.6 Acyl-CoA synthetase

The hydroxamate assay according to Lipman and Tuttle (1945) was used in a slightly modified form. The optimised reaction mixture (500 µl) contained potassium phosphate buffer pH 7.5 (100 mM), ATP (5 mM), $MgCl_2$ (5 mM), hydroxylamine (neutralised to pH 6.5 with KOH) (200 mM), reduced glutathione (neutralised to pH 4.5 with KOH) (5 mM), CoA-SH (0.33 mM), acetate or propionate (10 mM), and protein (100 µg). The mixture was pre-incubated at 37° C for 5 minutes before initiation of the reaction by addition of protein. Following 30 min incubation at 37° C, the reaction was stopped by addition of 500 µl acid $FeCl_3$ reagent. Production of hydroxamate was determined after 10 min, in comparison with blanks prepared without CoA-SH, by measuring the absorbance at A_{520}. Standards were prepared from known concentrations of succinic anhydride as described by Lipman and Tuttle. A continuous coupled assay as described by Horswill and Escalante-Semerena (2002) was also attempted. Reactions (1 ml) contained HEPES buffer (50 mM), phosphoenolpyruvate (PEP) (3 mM), $MgCl_2$ (5 mM), ATP (2.5 mM), CoA-SH (0.33 mM), NADH (0.4 mM), myokinase (MK) (10 units), pyruvate kinase (10 units), lactate dehydrogenase (12.5 units) protein (150 µg) and substrate (10 mM). The oxidation of NADH was followed spectrophotometrically at 340 nm. A high rate without substrate, which was not dependent on MK, made this assay unreliable and it was not pursued.

2.13.7 NAD(P)-independent alcohol dehydrogenase

Quinoprotein alcohol dehydrogenase was assayed using the artificial electron acceptor phenazine methosulfate (PMS) coupled to reduction of dichlorophenolindophenol (DCPIP) as described by Anthony (1964). Reactions (1 ml) contained Tris buffer (pH 9.0) (100 mM), PMS (1 mM), DCPIP (0.08 mM) NH_4Cl (15 mM), protein (20 µg) and substrate (10 mM). Reactions were initiated with

addition of ammonium and followed spectrophotometrically at 600 nm against a water blank. Reactions lacking ammonium or substrate were also monitored. As described by Anthony (1964), significant transient activity was noted without substrate, which was not subtracted from the substrate-induced activity (Day and Anthony, 1990). Activity was calculated using $\varepsilon_{600} = 1.91 \times 10^4\ M^{-1}cm^{-1}$ for DCPIP.

2.13.8 NAD(P)-dependent alcohol dehydrogenase

Assay reactions contained Tris buffer (25 mM, pH 9.0), NAD^+ or $NADP^+$ (1.5 mM), protein (66 – 200 µg) and substrate (20 or 40 mM). The reduction of $NAD(P)^+$ was monitored spectrophotometrically at 340 nm against a blank without substrate, and activity calculated using $\varepsilon_{340} = 6.22 \times 10^3\ M^{-1}cm^{-1}$ for NAD(P)H.

2.13.9 Reduction of ferricyanide - acetol dehydrogenase

Dehydrogenase activity coupled with the reduction of ferricyanide was assayed by colorimetric measurement of Prussian blue formed by the reaction of ferrocyanide with Dupanol reagent using a discontinuous assay (Wood et al., 1962; Shinagawa et al., 1982). The following were combined in a small test tube: 500 µl McIlvaine buffer pH 7.4 (made by mixing approximately 9.15 ml citric acid (0.1 M) with 91 ml disodium hydrogen phosphate (0.2 M)), 100 µl potassium ferricyanide (0.1M), 50 µl Triton X-100 (1% v/v), 200 µg protein, 100 µl substrate (0.2 M) and water to a volume of 1 ml. The reaction was incubated at room temperature for 10 min and stopped by the addition of 0.5 ml ferric dupanol reagent (0.5 g $Fe_2(SO_4)_3.nH_2O$, 0.3 g SDS, 9.5 ml H_3PO_4 (85%) and water to 100 ml). Water (3.5 ml) was added and the mixture incubated at 37 °C for 20 min, following which absorbance was measured at 600 nm against a blank. For quantification of ferrocyanide production, standards were made up similar to the assay reactions (except without protein and substrate), but containing, in addition, between 0 – 1 µmol of potassium ferrocyanide (with corresponding reductions in ferricyanide). These were treated identically to the assay reactions. Control reactions were conducted with no substrate, and without protein. One unit was defined as the reduction of 2nmol ferricyanide min^{-1}. The assay pH was optimised from pH 4.5 to pH 9.0, (using McIlvaine buffer for pH 4.5 to 7.4, and Tris from 7.0 to 9.0) and pH 7.4 gave the optimum activity.

2.13.10 Methylmalonyl-CoA mutase

A modification of the method of Birch et al. (1993) was used, by following the formation over time of the dimethyl derivative of succinyl-CoA in cell extracts incubated with methylmalonyl-CoA. Reactions were conducted in triplicate at each time point for each sample (growth condition). Controls with no substrate were included, as were those with no protein, also in triplicate. Reactions contained 4-(2-hydroxyethyl)-1-piperazineethanesulfonic acid (HEPES) buffer (50 mM pH 7.5), cyanocobalamin (10 µM) and cell-free extract (100 µg protein) in a volume of 180 µl. Following pre-incubation for 10 min at 30 °C, 20 µl of 10 mM methylmalonyl-CoA (trilithium salt, Sigma-Aldrich) was added and reactions incubated at 30 °C in the dark. Reactions were stopped at 0, 10, 20 and 30 min by addition of 100 µl 2M NaOH containing 1 mM glutarate as internal standard, and incubated at 55 °C for 10 min to hydrolyse thioester bonds (Corkey et al., 1981). Vials were acidified with 100 µl 15% v/v H_2SO_4 and stored on ice. The reaction mixtures were transferred to 2 ml glass vials containing 900 µl ethyl acetate and sufficient NaCl to saturate (approximately 0.3 g). Vials were mixed on a tube rotator for 30 min at room temperature, and 800 µl of the organic phase transferred to fresh 1.5 ml tubes which were evaporated to dryness using a rotary evaporator (GiroVac, North Walsham, UK). The residue was dissolved in 200 µl dimethyl formamide (DMF) containing 1/8 v/v methanol and 10 µl trimethylsilyldiazomethane ($TMSCHN_2$) was added. Tubes were mixed by rotation for 30 min at room temperature, excess $TMSCHN_2$ destroyed by the addition of 10 µl 2M acetic acid in DMF, the solution transferred to 0.3 ml glass autosampler vials and analysed using an Agilent 7890A gas chromatograph using the following settings:

Column, carrier gas, detector	JW INNOWAX, N_2 (1.8 ml min^{-1}), FID
Injector temp	250 °C
Column temp	100 °C 3 min, 100 ° to 150 °C at 10 °C min^{-1}, 150 ° to 240 °C at 50 °C min^{-1}, hold at 240 °C 3.5 min
Detector temp	250 °C
Injection volume	Injection 5 µl (50:1 split) (autosampler)

Dimethylmethylmalonate (DMM) and dimethylsuccinate (DMS), formed by the methylation of methylmalonate and succinate following hydrolysis of the thioesters, were identified by comparison of the retention times with those of the authentic

compounds obtained from Sigma-Aldrich. At the setting used, the retention times for DMM and DMS were 5.98 and 7.72 min respectively. Methylmalonyl-CoA and succinyl-CoA were quantified (assuming complete hydrolysis) by comparison with standards prepared as the reaction mixtures, except without methylmalonyl-CoA, but containing known quantities of methylmalonate and succinate. When 100 nmol succinate was added, approximately 80 nmol could be detected in the dimethylated form following extraction. Approximately 2 nmol succinate in a 200 µl reaction (10 µM) could be detected.

2.14 Measurement of substrates and metabolites

2.14.1 Quantification of headspace gases

Methane, propane, other hydrocarbons and carbon dioxide were quantified by GC using an Agilent 6890 instrument at the following settings:

Column, carrier gas, detector	Porapak Q, N_2 (20 ml min^{-1}), FID
Injector temp	150 °C
Column temp	125 °C (isothermal)
Detector temp	200 °C
Injection volume	100 µl

Standards were prepared by dilution (or serial dilution) of the pure gases in air or oxygen-free nitrogen in 120 ml serum vials sealed with Teflon coated butyl rubber stoppers. Retention times for methane and propane at these settings were 0.64 and 2.72 min respectively. Methane was detectable to approximately 1 ppmv.
For quantification of CO_2, a Methanizer catalyst (operated at 350° C) was incorporated to reduce CO_2 to CH_4, and the oven temperature reduced to 45° C. Retention times for CH_4 and CO_2 were 1.14 and 2.14 min respectively.

2.14.2 Quantification of total nitrate and nitrite in cell culture medium

Aliquots of cell culture (1.5 ml) were centrifuged to pellet cells (16,600 × g, 5 min, room temperature) and 1 ml supernatant removed to fresh tubes. Zinc dust (50 mg) was added to reduce nitrate to nitrite, and tubes mixed for 1 h on a tube rotator. Tubes were centrifuged as before and 0.5 ml supernatant transferred to cuvettes and

mixed with 0.5 ml Griess' reagant (Sigma Aldrich, UK). After 30 min incubation at room temperature, absorbance was read at 520 nm, and compared with standards prepared using potassium nitrate solution of known concentration. Limit of detection was approximately 0.5 μg ml^{-1}. Nitrite was determined in the same way but without the reduction step.

2.14.3 Quantification of ammonium in cell culture medium

Culture medium was centrifuged (16,600 × g, 5 min, room temperature) and supernatant removed and diluted as necessary to give ammonium concentration in the range 1 to 50 μM. Ammonium was determined by the method of Solórzano (1969), scaled down for a sample volume of 1 ml and measurement in a 1 ml cuvette, and using hypochlorite solution supplied by Fisher Scientific (Loughborough, UK). Standards were prepared between 0 and 50 μM using a stock solution of ammonium chloride. Ammonium was detectable to approximately 1 μM.

2.14.4 Quantification of succinate in cell culture medium

Succinate was quantified using a K-SUCC kit from Megazyme (Wicklow, Republic of Ireland), using between 100 – 500 μl of cell culture supernatant (diluted as necessary) in a coupled enzymatic reaction, following the manufacturer's instructions. The consumption of NADH was measured spectrophotometrically and the stoichiometric succinate amount in the reaction calculated using the molar extinction coefficient of NADH (ε_{340} = 6.22 × 10^3 $M^{-1}cm^{-1}$). Succinate was detectable to approximately 30 μM.

2.14.5 Quantification of acetate in cell culture medium

One millilitre aliquots of cell culture were centrifuged (16,600 × g, 5 min, room temperature) to pellet cells, and 600 μl of the supernatant removed to fresh tubes and acidified with 12 μl of 1M HCl. Acetic acid formed was extracted with an equal volume of diethyl ether by mixing on a tube rotator for 30 min. Three hundred microlitre aliquots of the organic phase were removed and transferred to 0.3 ml crimp-top vials for analysis using a Pye Unicam 104 gas chromatograph at the following settings:

Column, carrier gas, detector	Porapak N, N_2 (30 ml min^{-1}), FID
Injector temp	225 °C
Column temp	190 °C (isothermal)
Detector temp	250 °C
Injection volume	On column injection, 10 µl

Acetate (retention time 6.2 min) was quantified by comparison with standards prepared in the same way from dilutions of a known concentration sodium acetate stock solution. Acetate could be accurately quantified to approximately 1mM.

2.14.6 Quantification of propane in cell culture medium

The propane concentration of liquid medium was measured by manual injection of 0.5 µl of cell suspension into an Agilent 7890A GC, using a glass-wool containing inlet liner, at the following settings:

Column, carrier gas, detector	HP1 capillary, N_2 (1.8 ml min^{-1}), FID
Injector temp	250 °C
Column temp	45 °C (isothermal)
Detector temp	250 °C
Injection volume	Injection 0.5 µl (100:1 split) (manual injection)

Retention time for propane was 1.80 min.

2.14.7 Quantification of 2-propanol and acetone in cell culture medium

Initially, cell culture supernatant was directly analysed by GC. Two millilitre aliquots of cell culture were centrifuged (16,600 × g, 5 min, room temperature) to pellet cells, and 1.5 ml of the supernatant removed to 2 ml crimp-top glass vials for analysis using an Agilent 7890A gas chromatograph at the following settings:

Column, carrier gas, detector	HP1 capillary, N_2 (1.8 ml min^{-1}), FID
Injector temp	250 °C
Column temp	45 °C (isothermal)
Detector temp	250 °C
Injection volume	Injection 1 µl (100:1 split) (autosampler)

2-propanol and acetone (retention times 1.99 and 1.97 min) were quantified by comparison with standard aqueous solutions of a mixture of the compounds in approximately the ratio found in the samples (i.e. a molar ratio of 2-propanol to acetone of 5:1), due to the similar retention times of the two compounds. Acetone could be accurately quantified to approximately 0.5 mM in the presence of 2.5 mM 2-propanol. Subsequently, sensitivity was improved by extraction, see Section 2.14.8

2.14.8 Quantification of 1-propanol, 2-propanol, acetone and acetol in cell culture medium

Aliquots (1.5 ml) of the culture were centrifuged (16,600 × g, 5 min, room temperature) to pellet cells. Supernatant (800 µl) was added to 400 µl ethyl acetate (containing 500 ppmv 1-butanol as internal standard) and approximately 0.4 g NaCl, (sufficient to saturate the aqueous phase), in 1.5 ml tubes. Tubes were mixed for 30 min on a tube rotator, briefly centrifuged to separate phases, and 300 µl of the organic phase removed to 0.3 ml crimp top vials for analysis using an Agilent 7890A gas chromatograph at the following settings:

Column, carrier gas, detector	JW INNOWAX, N_2 (1.8 ml min^{-1}), FID
Injector temp	250 °C
Column temp	45 °C 5 min, 45 to 250 °C at 10 °C min^{-1}, hold at 250 °C 5 min
Detector temp	250 °C
Injection volume	Injection 5 µl (100:1 split) (autosampler)

Retention time for acetone was 2.40 min, 1-propanol 3.34 min, 2-propanol 5.40 min, 1-butanol 7.45 min and acetol 9.70 min. These compounds were quantified using aqueous standards extracted using the same method. R^2 values of linear standard-curve line-fitting were greater than 0.998 in all cases. Relative standard deviation of peak area measurements of the 1-butanol internal standard over a 19 day experiment was less than 1% (n=60). Detection limit was, approximately, acetone, 200 µM; 1-propanol and 2-propanol, 50 µM; acetol, 400 µM. Comparison with standards prepared directly in ethyl acetate indicated that the extraction efficiency of 2-propanol was approximately 74%.

Chapter 3

Physiology and growth

3.1 Introduction

Methylocella silvestris BL2 was isolated on nitrate mineral salts (NMS) medium diluted 1/5, and subsequently grown by Andreas Theisen in the Murrell lab on a 1/10 dilution of the same medium (Dunfield et al., 2003; Theisen, 2006), and these authors identified low ionic strength as a requirement for growth. Published reports documented the slow and sometimes unpredictable growth of *Methylocella,* with maximum density in flask culture during growth on methane about 0.1 (OD_{600} or OD_{540}) (Dedysh et al., 2005a; Theisen, 2006) or about 0.2 – 0.3 on multi-carbon compounds. *M. silvestris* was subsequently grown to high cell density in batch-fed fermenter culture on both methane and acetate (Theisen et al., 2005), albeit with a comparatively slow specific growth rate on both substrates (approximately 0.01 hr^{-1}, average of several experiments). This author also documents (Theisen, 2006) the difficulty of manipulating colonies on agar plates, during growth on which *M. silvestris*, in common with other members of the *Beijerinckiaceae,* forms tough, elastic and extremely viscous colonies. Although these previous workers developed valuable methods for the isolation and growth of this organism, and growth on sugars was tested, comparatively little work was done to investigate the full growth-substrate range of this organism, or to optimise the medium composition which had so far been used.

The purpose of the work described in this chapter was to further investigate the metabolic versatility of *M. silvestris,* to understand the factors which influence growth in the laboratory, and to optimise growth to enable genetic manipulation and biochemical characterisation to be carried out.

3.2 Growth of *M. silvestris*

At the start of this project, *M. silvestris* was grown in flasks under the conditions described by Theisen (2006). Problems encountered included the difficulty of harvesting cells by centrifugation, due to the presence of a large amount of slime, assumed to be polysaccharide, which made pelleting of cells impossible. Instead, a homogeneous jelly-like mass of cells formed in the lower half of the tube, sometimes occupying up to ¼ of the total volume, which could not be reduced in volume despite centrifugation at maximum speed (48,400 × g). Filtration in these cases also proved impossible. In some cases the failure of cultures to grow was probably linked to the

alteration of the starting pH (5.5) to approximately 4.0 or 8.0, depending on growth substrate. It was noticed that *M. silvestris* would grow on methane with shaking in 120 ml serum vials, but not in 1 l flasks, presumably due to the larger area for gas exchange. This was not the case, however, during growth on other substrates including methanol. It seemed worthwhile, therefore, to invest some time in attempting to optimise the growth of *M. silvestris* in batch culture.

3.3 Culture purity

The purity of both flask and fermenter cultures of *M. silvestris* was checked regularly by phase contrast microscopy, by serial dilutions plated onto dilute nitrate mineral salts (DNMS) plates followed by PCR amplification and sequencing of DNA from individual colonies, by plating on R2A agar plates (*M. silvestris* does not grow on R2A or similar nutrient-rich media) and from time to time by analysis of small clone libraries constructed from 16S rRNA genes PCR-amplified from DNA extracted from the cultures, as described in Materials and Methods. A representative agarose gel illustrating the RFLP pattern of 16S rRNA amplicons is shown in Figure 3.1. The cloned 16S rRNA gene was sequenced from a few examples of each library, and in every case showed high similarity to *M. silvestris* (> 99% over more than 500 bp). On one occasion an attempt was also made to amplify archaeal and eukaryotic ribosomal gene sequences from DNA extracted from fermenter-grown cells, and results were negative.

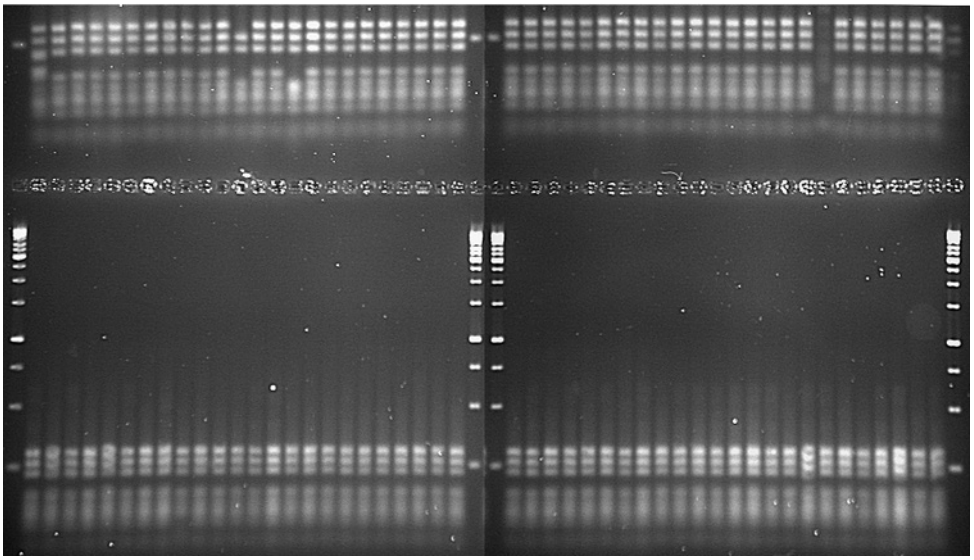

Figure 3.1. Clone library analysis of 16S rRNA genes from *M. silvestris* fermenter-grown cells. The agarose gel shows the RFLP pattern following digestion of PCR-amplified 16S rRNA genes with *Msp*I. 96 clones are shown, in two rows. A few PCR products were sequenced including all those exhibiting a RFLP profile different from the consensus. All sequences (> 500 bp) were > 99% identical to the 16S rRNA gene from *M. silvestris*.

3.4 The effect of medium composition on growth

3.4.1 Medium previously used for *M. silvestris*

It was shown previously that *M. silvestris* required a dilute medium for growth (Dunfield et al., 2003), and the medium employed previously in the Murrell lab for this organism (Theisen, 2006), and at the start of this project, was a 1/10 dilution of NMS medium (DNMS medium). However, it had not been determined if this requirement was due to overall ionic strength, or the concentration of one of the components of the medium, for example nitrate. DNMS medium contains 1 mM nitrate, therefore, without additional fixed nitrogen, would be expected to support growth to approximately 117 mg l^{-1}, assuming cellular N is 12% w/w (Madigan and Martinko, 2006). Since this corresponds to a density of only approximately OD_{540} = 0.5, an increase in the nitrogen content of the medium might be beneficial. Since the trace elements and buffer are also diluted in DNMS medium, cultures may also be limited by trace metal availability, or adversely affected by low buffering capacity. The purpose of this work was to increase understanding of the relationship between medium composition and growth, and, if possible, to alter medium composition to allow increased growth rate and culture density. Growth tests were conducted in 20 ml liquid cultures in 120 ml serum vials, with methanol (0.1% v/v) as carbon and

energy source, except where indicated. Assuming a carbon conversion efficiency for a serine cycle methanotroph growing on methanol of 53 – 56% (Anthony, 1982), this amount of methanol (0.3 g carbon l^{-1}) should support growth of approximately 0.16 g carbon l^{-1}, corresponding to an OD_{540} of 1.3 (assuming OD_{540} = 1.0 corresponds to 125 mg l^{-1} carbon).

3.4.2 Nitrate mineral salts and nitrate concentration

To evaluate the influence of mineral salts and nitrate concentration, NMS salts were varied from 0.5 to 10 times the standard DNMS concentration, and subsequently the nitrate concentration varied from 1 – 20 mM with the other components of DNMS medium unchanged, see Figure 3.2**.** There was little difference in the growth of the cultures, although in both cases the standard medium recipe resulted in the highest sustained growth rate and highest culture density. However, increased concentrations of either total salts or nitrate did not greatly inhibit the growth of *M. silvestris.*

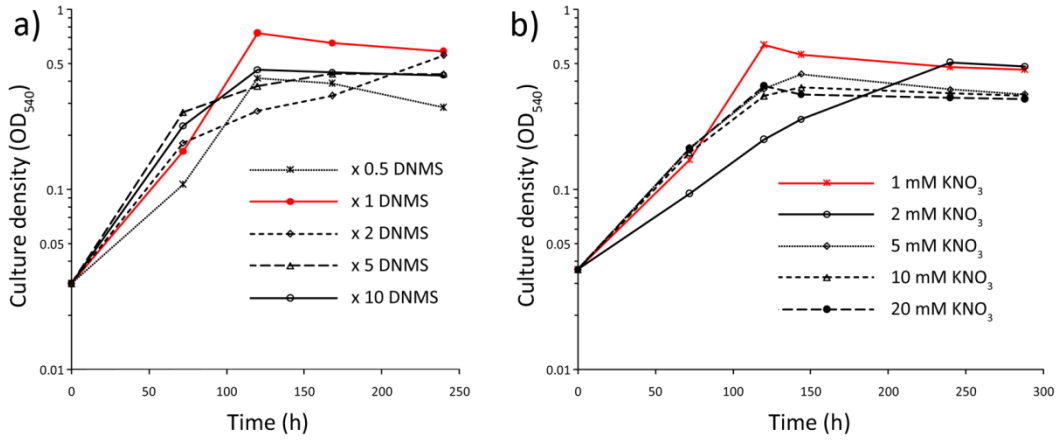

Figure 3.2. Growth of *M. silvestris,* **a)** with different concentrations of NMS salts or, **b)** with different concentrations of nitrate in DNMS medium. In both graphs the condition corresponding to the standard DNMS recipe is shown in red.

3.4.3 Nitrate versus ammonium

The effect of substituting ammonium for nitrate was investigated in three independent experiments, each consisting of replicated vials with ammonium or nitrate (1 mM or 2 mM) in DNMS medium made up without nitrate,

as shown in Figure 3.3**.** In all cases nitrate resulted in higher growth rate and culture density, but there was no significant difference between 1 and 2 mM nitrate. *M. silvestris* was able to grow well on methanol (0.1% v/v (25 mM)) or succinate (5 mM) with urea (1 mM or 5 mM) as nitrogen source, or on methylamine (5 mM) with no additional nitrogen source (data not shown). However, production of slime was not eliminated in any of these cases, demonstrating that availability of excess fixed nitrogen does not prevent polysaccharide production. Therefore the routine use of fixed nitrogen sources other than nitrate or ammonium was not investigated further.

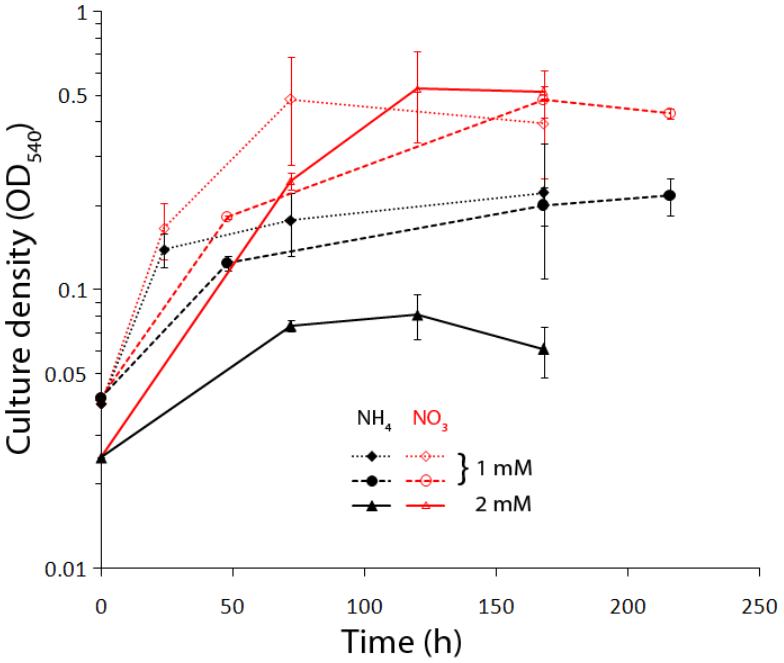

Figure 3.3. Growth with nitrate or ammonium (1 mM or 2 mM) was compared in triplicate vials. Line type (solid, dashed, dotted) distinguishes three independent experiments, and nitrate is shown in red and ammonium in black. Error bars show the standard deviation.

3.4.4 Salt concentration

The influence of ionic strength was investigated by supplementing DNMS medium with different concentrations of NaCl. Ten 20 ml cultures were grown with NaCl concentrations between 0 and 500 mM, and OD_{540} measured at five timepoints up to 240 h. Vials with up to 125 mM NaCl all grew with specific growth rate in the range 0.021 - 0.027 h^{-1} (mean 0.024, standard deviation 0.002) and reached a final density of OD_{540} between 0.41 and 0.59 (mean 0.48, standard deviation 0.06) and there was little correlation between growth rate or density and NaCl concentration (R^2 = 0.012 and 0.148 respectively), see Figure 3.4**.** However, at 500 mM NaCl, growth was

almost completely inhibited. These data demonstrate that *M. silvestris* is perhaps not as sensitive to ionic strength as initially thought, but might also explain the absence of *M. silvestris*-related sequences reported from marine environments (~ 0.6 M NaCl).

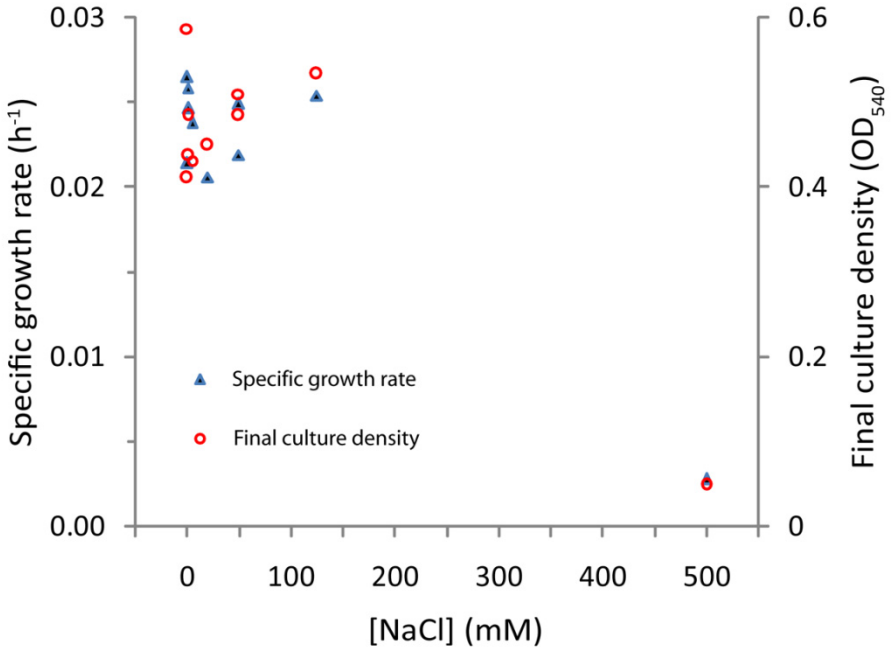

Figure 3.4. Influence of supplementation of DNMS medium with between 0 – 500 mM NaCl during growth of *M. silvestris* on 0.1% (v/v) methanol. Specific growth rates of cultures in 20 ml vials are shown as triangles and final culture densities at 240 h as open circles.

3.4.5 Trace metals

Examination of the recipe of the trace elements solution added to the medium (Table 3.1) suggested that, in the absence of additional input from impurities in other components, *M. silvestris* might be limited by lack of essential trace elements. For example, methylmalonyl CoA mutase is a vitamin B12-dependent enzyme, which requires cobalt for activity and may be required for propane metabolism (see Chapter 7), and since nitrogenase is a molybdenum-containing enzyme, nitrogen-fixing organisms have a requirement for this metal (Shah et al., 1984), which, in species of *Beijerinckia* ranges between 4 – 35 µg l^{-1} in the culture medium (Becking, 2006). Furthermore, Keifer et.al. (2009) recently demonstrated an increased requirement for trace elements, particularly cobalt, during growth of resistant strains of

Methylobacterium extorquens in the presence of antibiotics. Therefore, the original trace elements formulation may be deficient in both molybdenum and cobalt in some situations. Initially, the concentration of the previously used trace elements solution (designated Trace Elements "A") was increased up to 25 fold, while maintaining the other medium ingredients unchanged, during growth on 0.1% (v/v) methanol. There was no detectable difference between the growth of cultures with × 1, × 10 or × 25 the standard concentration, see Figure 3.5a. Since *M. silvestris* was not sensitive to increased concentration of trace metals under these conditions, a modified solution (Trace Elements "B") was formulated more similar to that commonly employed for methanotrophs, including increased amounts of molybdenum and cobalt. The compositions of trace elements solutions A and B are shown in Table 3.1. Growth was then compared using solution A (at × 1 concentration) and solution B at × 1, × 10 and × 25 concentration (Figure 3.5b). Specific growth rate was highest at the lowest concentration of solution B, but with the exception of the highest concentration of solution B, at a 95% confidence level there was no significant difference between the conditions tested. Using trace elements solution A, the influence of iron (as FeEDTA) was investigated by varying the concentration from × 0.2 to × 5, without evidence of any clear effect (data not shown). Therefore, trace elements solution B was used subsequently, with additional FeEDTA (total iron 791 μg l^{-1}).

Table 3.1. Trace elements present in DNMS medium when using two alternative recipes. Media concentrations (μg l^{-1}) are shown for trace element solutions used at × 1, assuming no addition from impurities in other components. Trace Elements "A" is the recipe previously employed, and "B" is a modified solution compared with "A" and subsequently used in the culture medium.

Element	Trace Elements "A"	Trace Elements "B"
Zn	1.5	16.7
Mn	0.4	13.9
B	2.7	0.5
Cu	0.2	0.5
Ni	0.2	3.0
Mo	0.6	19.8
Co	0.0	12.4
Fe	0*	211

*Iron is supplied separately as FeEDTA

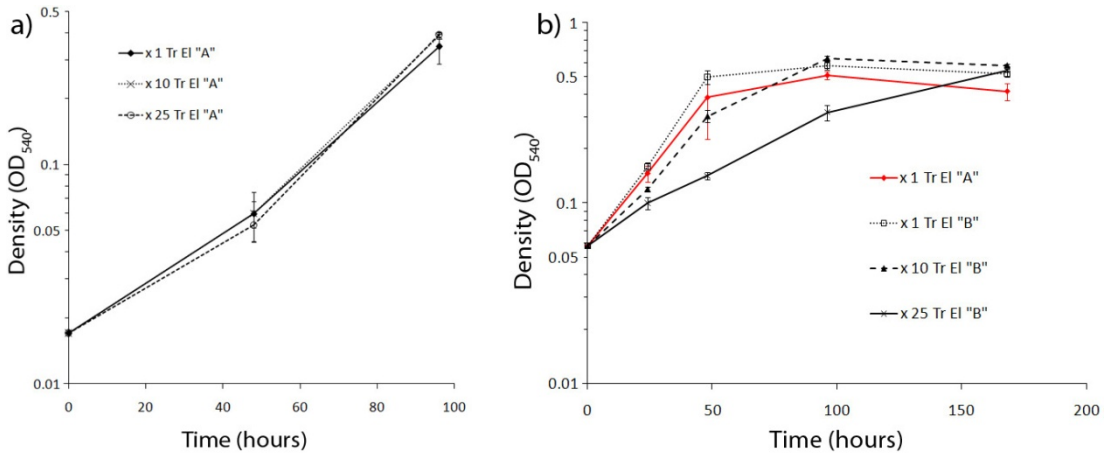

Figure 3.5. The effect of trace elements on growth of *M. silvestris* on 0.1% (v/v) methanol. **a)** The trace elements solution previously employed (Trace Elements "A") was increased to × 10 or × 25, and **b)** different concentrations of a modified solution (Trace Elements "B", in black) were compared with Trace Elements "A" (in red). All data points represent the mean of three replicates and error bars indicate the standard deviation.

3.4.6 Medium buffering capacity

The tendency of *M. silvestris* cultures to depart significantly from the initial pH of 5.5 was noted, depending on nitrogen source and substrate. For example, cultures growing on methanol (0.05%) with ammonium (1 mM) as carbon and nitrogen source respectively decreased pH to approximately 4.0 after 3 - 4 days, as did cultures growing on acetol with nitrate at the same concentrations, whereas cultures growing on acetone with nitrate remained at the initial value (pH 5.5). During growth on succinate, pH increased to approximately 8.0. Since the buffering capacity (1 mM phosphate) of the original dilute medium employed was small, the effect of increasing the concentration of phosphate buffer was investigated (Figure 3.6), during growth on methanol with 1 mM nitrate or ammonium. Under these conditions a 20-fold increase in buffer concentration did not inhibit growth, and resulted in higher biomass during growth with ammonium. pH was measured at 24, 48 and 96 hours, and remained within the range 5.3 – 6.0 in vials with nitrate at all phosphate concentrations, and with ammonium at 20 mM phosphate. At the two lower phosphate concentrations, however, pH was in the range 4.0 – 4.4 after 96 hours in vials containing ammonium. In no case did ammonium result in increase growth rate or higher culture density than nitrate.

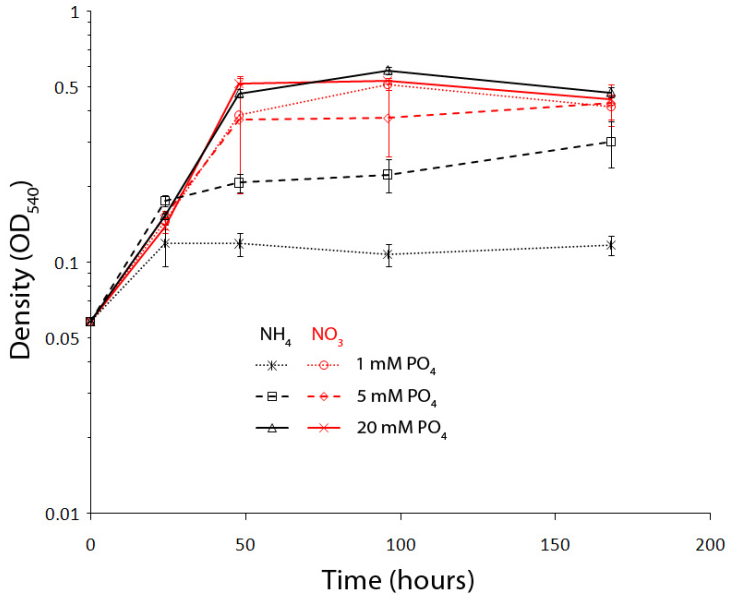

Figure 3.6. Effect of increasing the concentration of phosphate buffer during growth on methanol (0.1% v/v) with either ammonium or nitrate (1 mM) as nitrogen source. Data points represent the mean of three replicates and error bars indicate the standard deviation.

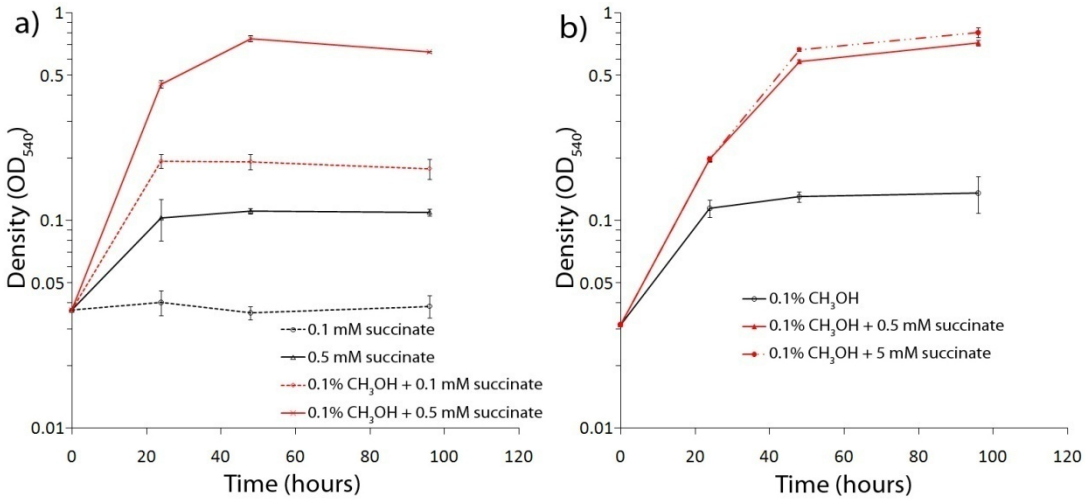

Figure 3.7. a) using ammonium (1 mM) as nitrogen source, *M. silvestris* was grown on succinate alone (0.1 mM and 0.5 mM) or succinate plus methanol. Growth was then tested **(b)** on methanol alone, or again in combination with succinate (0.5 mM or 5 mM). Data points represent the mean of three replicates and error bars indicate the standard deviation.

Since between 5 and 20 mM phosphate buffer had been shown necessary to buffer the acidification caused by 1 mM ammonium, the effect of the addition of a small amount of succinate in combination with methanol was tested. Methanol (0.1% v/v) plus 0.5 mM succinate, in medium containing 1 mM ammonium, resulted in rapid growth without pH shift to a relatively high density (Figure 3.7), in the presence of

the low buffering capacity of 1 mM phosphate. However, polysaccharide production was not prevented by these methods, illustrating that polysaccharide is not produced solely in response to pH stress.

3.5 Effect of carbon dioxide on growth

It has previously been reported that some methanotrophs have a requirement for carbon dioxide during growth on methane (Acha et al., 2002), and they have routinely been grown with the addition of carbon dioxide, see for example, Theisen (2006). To investigate this in *M. silvestris*, 20 ml cultures (in triplicate) were grown in 120 ml vials with methane (20% v/v) with the addition of 0, 0.1, 0.3, 1.0 or 3.0 (% v/v) CO_2 to the headspace. Culture density was monitored over 216 hours, and CO_2 concentrations measured twice by gas chromatography (GC) during this period. There was no difference between the specific growth rates under the different conditions (means O.022, 0.024, 0.023, 0.022, 0.020 h^{-1} respectively, single factor ANOVA, $F(4,10) = 3.05$, $p = 0.07$, $MSE = 6.72 \times 10^{-6}$), nor noticeably different lag phases. However, at 144 h, the vials with no added CO_2 had a measured CO_2 headspace concentration of 0.95% ±0.32%, clearly as a result of oxidation of substrate. To investigate this effect further, vials were set up as before, but without addition of CO_2, and containing 1 ml 10M NaOH contained in a small test tube inside the vial to remove CO_2 produced, alongside controls without CO_2 removal. No growth occurred in vials with CO_2 removal. These data are relevant to growth in fermenter culture, where a recently inoculated 4 l culture with a biomass concentration of 0.025 mg (dw) ml^{-1}, and with a specific growth rate of 0.01 h^{-1}, would be emitting CO_2 at a rate of just over 1 ml h^{-1}, a flux of 0.004% of the air supply of typically 400 ml min^{-1} (assuming half of substrate methane is oxidised to CO_2 and biomass is 50% C w/w). Under these conditions, emission of CO_2 by the growing cells would not significantly elevate the atmospheric-equilibrium CO_2 concentration in the medium, due to the sparging effect of the air supplied. Therefore for growth in fermenter culture, methane supplemented with 5% CO_2 was used as substrate (i.e. CO_2 = 0.5% (v/v) of gas inflow when supplied at 1/10 methane/air).

3.6 Substrate utilisation by *M. silvestris*

Growth on compounds of interest was investigated in liquid culture and is detailed in Table 3.2. Some of this data confirms previously published results (Dunfield et al., 2003; Dedysh et al., 2005a; Theisen et al., 2005; Theisen, 2006). Liquid-grown *M. silvestris* cells were used as inoculum (at approximately 1/10, resulting in a starting cell density of approximately OD_{540} 0.025 – 0.04) for growth in 20 ml cultures in 120 ml serum vials, supplied with the substrates shown. In the majority of cases, tests were carried out in triplicate.

3.7 Substrate-oxidising capability – oxygen electrode studies

The capacity of whole cells grown on methane to oxidise potential growth and non-growth substrates was investigated using a Clark oxygen electrode. Cells (stored frozen in pellets at -80 °C) were used in the oxygen electrode as described in Materials and Methods and oxygen consumption measured in response to addition of substrate. It was found that while a concentrated suspension of methane-grown cells retained activity in response to methane for at least 24 h when stored on ice, when resuspended in buffer at the working cell density (approximately 5 mg in 3 ml buffer) and gently stirred at room temperature for 30 min, methane-related activity was completely lost. However, these cells retained a similar level of activity to freshly thawed cells in response to methanol, possibly highlighting the instability or oxygen-sensitivity of the monooxygenase enzyme system. Initially, a range of possible substrates were tested for their ability to induce a response in *M. silvestris* methane-grown whole cells. Data are presented in Table 3.3, and show a high rate of oxidation of primary alcohols, but not secondary alcohols, typical of the substrate specificity of methanol dehydrogenase (MDH) (Anthony, 2000).

Subsequently, reactions were investigated in more detail. Kinetic data for methane and methanol are shown in Figure 3.8. Methane-grown whole cells had a k_m for methane of approximately 43 μM, (corresponding to a headspace methane concentration of 2.9%, assuming equilibrium between gas and aqueous phases). The affinity for methanol was high (k_m < 10 μM). However, in this case it was not possible to take accurate measurements at substrate concentrations approaching the k_m (i.e. < 10 μM), since the deviation (oxygen consumed) in response to addition of a few nanomoles of substrate was too small.

Table 3.2. Substrate utilisation by *M. silvestris*. Growth is indicated as ++ : growth to $OD_{540} > 0.25$, + : growth to $OD_{540} \geq 0.08$, - : growth to $OD_{540} < 0.08$. (Concentrations in % given as v/v.)

Substrate	Concentration	Growth
Formate	1 mM	-
Formate	5 mM, 40 mM	+
Formate	25 mM	++
H_2/CO_2	20% O_2, 0.5 to 10% CO_2, balance H_2	-
Methane	2.5% to 20%	++
Methanol	0.05%	++
Methylamine	5 mM	++
Acetate	5 mM	++
Ethane	20%	+
Ethene	10%	-
Ethanol	0.05%	++
Glycine	5 mM	-
Glycollate	5 mM	-
Glyoxylate	1 mM, 5 mM	-
Oxalate	1 mM, 5 mM	-
Urea	5 mM	-
1,2-propanediol	0.05%	++
1-propanol	0.01 to 0.1%	-*
2-propanol	0.05%	++
Acetol	0.05%	++
Acetone	0.05%	++
Glycerol	5 mM	++
Methyl acetate	0.05%	+
Propane	2.5% to 20%	++
Propene	10%	-
Propionate	5 mM	++
Propionate	20 mM	-
Pyruvate	5 mM	++
Butane	20%	-
Trans-2-butene	10%	-
Malate	5 mM	++
Succinate	5 mM	++
Tetrahydrofuran	0.05%	+
Pentane	0.1%	-
Gluconate	10 mM	++
Pentadecane	0.1%	-

* Data on growth on 1-propanol are presented and discussed in Chapter 7

Table 3.3. Oxygen consumption rate (nmol min^{-1} (mg dry weight)$^{-1}$) of methane-grown whole cells in response to addition of the substrates shown. Standard deviations are shown in parentheses where measurements were conducted in at least triplicate. Substrate concentrations 82 μM, except alkanes and alkenes 49 μM. N/D: not detectable.

Substrate	Rate of oxygen consumption	Substrate	Rate of oxygen consumption
methanol	22.9	butyraldehyde	11.5
ethanol	21.9 (2.4)	pentanal	4.0
1-propanol	15.0 (1.4)	benzaldehyde	11.4
1-butanol	7.4 (2.6)		
1-pentanol	12.5	formate	7.7
1-hexanol	14.4	acetate	19.6
1-heptanol	14.6	propionate	N/D
1-octanol	13.3	butyrate	N/D
benzyl alcohol	3.1	succinate	13.1
2-propanol	N/D		
2-butanol	N/D	methane	10.3 (1.8)
2-heptanol	N/D	ethane	4.7
2-methyl 2-propanol	N/D	propane	4.2
		butane	2.4
acetaldehyde	21.2	ethene	2.3
propionaldehyde	13.4	propene	3.0

3.8 Growth in fermenter culture

In order to produce sufficient high quality biomass for proteomic and biochemical investigations, cells were grown in fermenters in either 4 l or 2 l vessels on a variety of substrates. Initially, cells were grown in fed-batch mode, with addition of nutrients (and growth substrate when using liquid or solid compounds) as required. Concentrations of nitrate, nitrite (which was never detectable), ammonium and non-gaseous substrates were measured periodically as described in Materials and Methods. From time to time, cells were removed for use or for storage frozen and replaced with an equivalent volume of fresh medium.

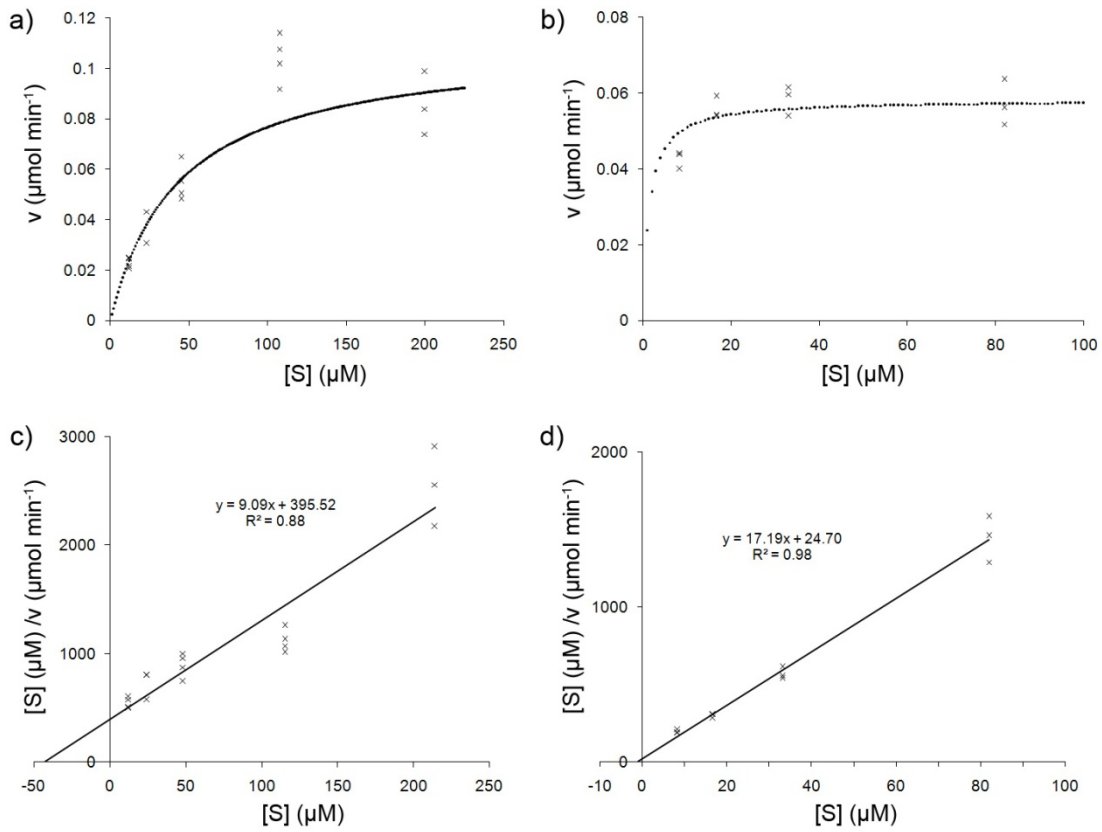

Figure 3.8. Oxygen uptake rate of *M. silvestris* whole cells as a function of methane [**a)** and **c)**] or methanol [**b)** and **d)**] concentration. The data at **a)** and **b)** are also shown as Hanes-Woolf plots at **c)** and **d)**. Data points are shown as crosses. The curves shown in **a)** and **b)** represent theoretical Michaelis-Menten kinetics, are drawn using parameters (k_m and V_{max}) derived from **c)** and **d)** and are included to illustrate the range of the data in comparison to the curve shapes.

Subsequently it was noticed that growth continued in the absence of detectable fixed nitrogen under conditions of low dissolved oxygen, and fermenters were then started on medium containing 1 mM fixed nitrogen source, and switched to N_2-fixing mode following depletion of this initial dose. Cells could then be removed and nitrogen-free medium added without interruption of growth. Operation under these conditions had the very significant advantage of allowing growth of biomass without slime, enabling harvesting by centrifugation with the formation of a compact pellet without difficulty. However, this required careful control of the culture dissolved oxygen (dO_2) level, which was maintained close to zero by adjustment of the inlet air flow. It was found that dO_2 could be stably maintained between zero and about 4% of saturation, but not between about 4% and 60%. If dO_2 was allowed to rise above a few percent, the culture oxygen consumption decreased dramatically, and the dO_2 level rose to a high level within minutes, presumably due to the reduction or

cessation of nitrogen fixation and corresponding drop in cell metabolic activity and respiration. Under these conditions growth and increase of culture density halted. Therefore the transition from initial growth with nitrogen-containing medium to nitrogen fixation required a little care to manage. The culture needed to be growing at a sufficient rate and oxygen requirement, yet at low dO_2 level, to manage the transition to nitrogen fixation. However, once in nitrogen fixing mode, the culture could be maintained, generating considerable biomass, without difficulty. A representative growth curve is shown in Figure 3.9.

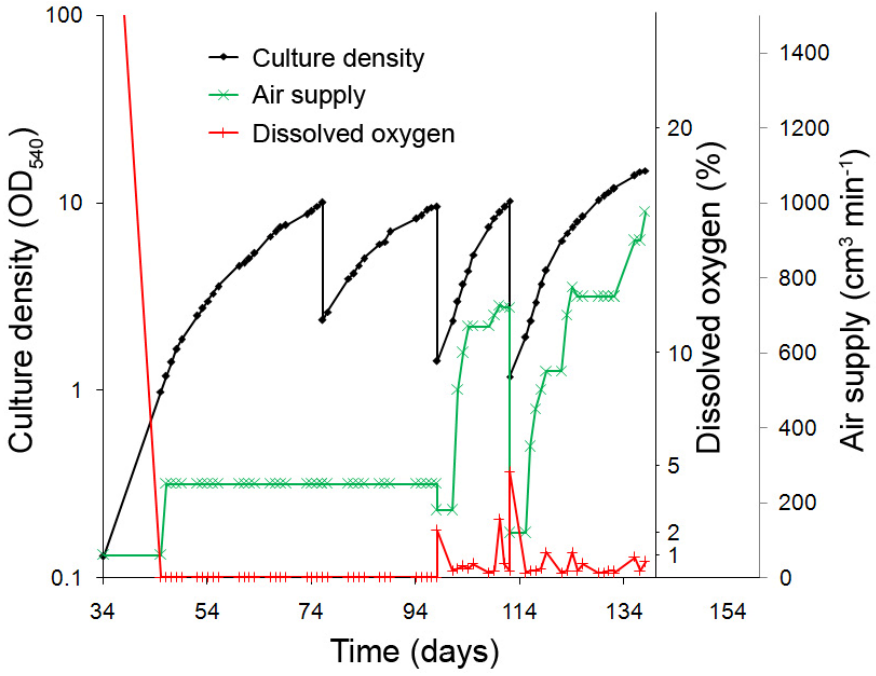

Figure 3.9. *M. silvestris* fermenter growth on methane (run 10) in nitrogen-fixing mode.

In total 12 Fermenter runs were carried out in batch mode. In some cases substrates were changed during the run. Data are summarised in Table 3.4.

3.9 Nitrogen (N_2) fixation

To confirm N_2-fixing activity, cells were removed from the fermenter and assayed for nitrogenase activity during growth on methane (run 10). The assay was carried out at different oxygen concentrations, and maximum activity occurred at approximately 5% oxygen. Ethylene production (maximum approximately 275 pmol ethylene produced (mg dw min)$^{-1}$) was linear for at least 120 min (R^2 = 0.998). No activity was detectable at atmospheric oxygen levels, see Figure 3.10a.

Table 3.4. *M. silvestris* growth in fermenter culture during this project

Run	Volume (l)	Substrate	N source	Sp. growth rate (h^{-1})
1	4	methane	nitrate	0.016
2	4	acetate	nitrate	0.043
3	4	methane	nitrate	0.022
4	4	methane	nitrate	0.014
		propane	nitrate	0.008
5	4	methanol	nitrate	0.010
6	2	propane	nitrate	0.006
		1,2-propanediol	nitrate	0.007
		acetol	nitrate	0.018
7	4	acetate	nitrate	0.016
8	4	propane	nitrate	0.010
9	2	propane	ammonium	0.011
		propane	N_2-fixing	0.006
10	4	ethanol	ammonium	0.012
		methane	N_2-fixing	0.010
		propane	N_2-fixing	0.004
11	2	succinate	ammonium	0.016
12	2	succinate	N_2-fixing	0.008

The inhibition of nitrogenase by ammonium was tested by the addition of ammonium chloride to a final concentration of between 0.5 and 5 mM in the assay vial. All concentrations tested reduced activity to about half the level without addition of ammonium, as shown in Figure 3.10b.

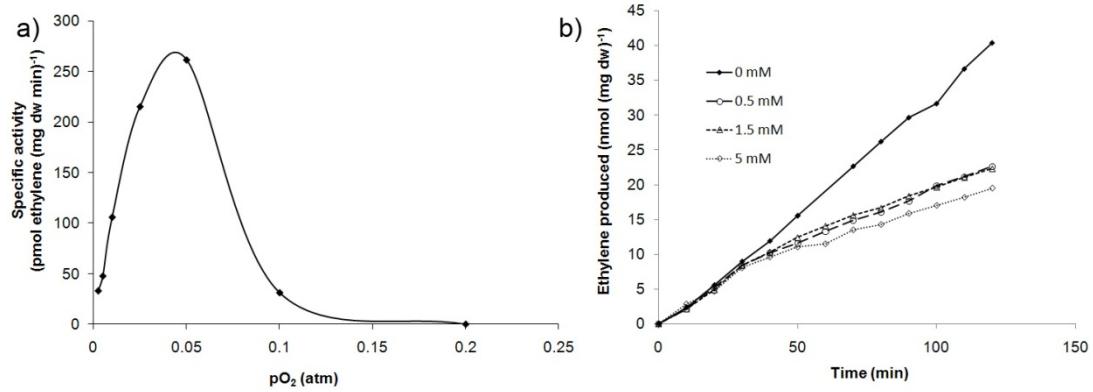

Figure 3.10. a) Nitrogenase assay during fermenter growth on methane and **b)** inhibition of nitrogenase activity by ammonium chloride. Between 0 and 5 mM (final concentration) NH_4Cl was added after 30 min.

3.10 Growth in continuous culture

Three attempts were made to grow *M. silvestris* in continuous culture, using acetate or succinate as carbon source, with ammonium as nitrogen source, or with succinate and no fixed nitrogen (nitrogen-fixing). However, it proved impossible to maintain a stable culture, even at a dilution rate of less than half the specific growth rate achieved in batch culture (Figure 3.11). Possibly ammonium was inhibiting growth when it was included in the medium, whereas when it was omitted, the culture required limitation by oxygen for nitrogen fixation, rather than by growth substrate.

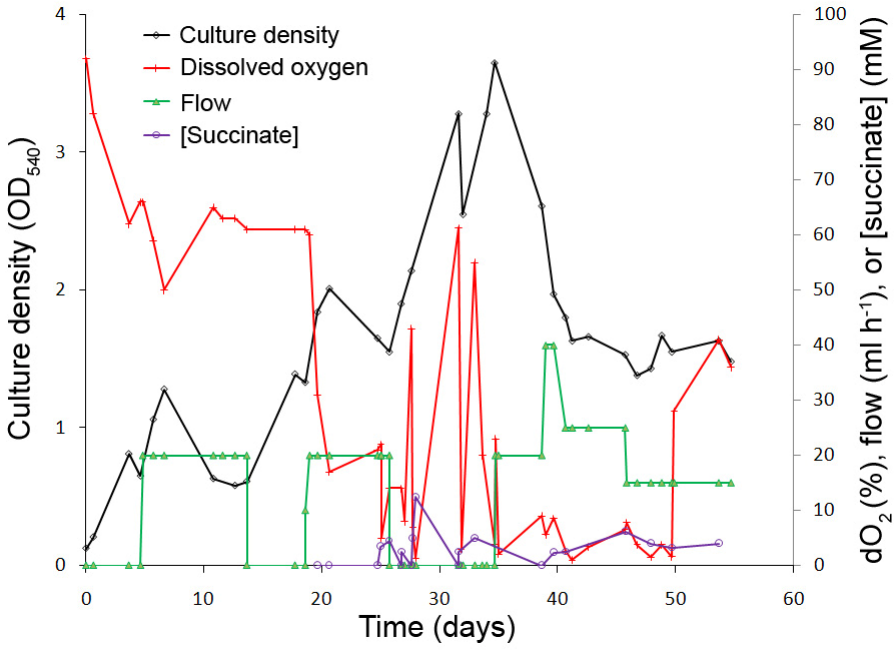

Figure 3.11. Growth in continuous culture on succinate. The medium reservoir contained dilute mineral salts medium with ammonium (2 mM) and succinate (20 mM). At day 26, ammonium was not detectable in the culture and the medium reservoir was replaced with nitrogen-free medium. Succinate concentration was measured from day 20. Cells were removed and replaced with nitrogen-free medium at day 32. Culture volume was 2.0 l and flow of 20 ml h^{-1} corresponds to a dilution rate of 0.01 h^{-1}. Additions of succinate were made to the vessel between days 25 and 34.

3.11 Antibiotic sensitivity of *M. silvestris*

M. silvestris wild type cells were tested for sensitivity to several common antibiotics during growth in liquid culture. Five millilitre cultures were set up in triplicate with methanol (0.1%) as growth substrate. Initial cell density was approximately OD_{540} = 0.05, and antibiotics were added to a final concentration of between 2 and 50 µg ml^{-1}.

Where *M. silvestris* was found to be sensitive to the antibiotic at 2 μg ml^{-1}, tests were repeated with between 0.25 and 2 μg ml^{-1} antibiotic. Growth was measured as OD_{540} at two time points and representative growth curves (for kanamycin and chloramphenicol) are shown in Figure 3.12. The data indicated that the MIC (in μg ml^{-1}) is approximately as follows. Kanamycin; < 0.25, chloramphenicol; > 50, streptomycin; 2, gentamicin; 1, spectinomycin; 5, tetracycline; 0.5, neomycin; < 2, aprimycin; < 2, nalidixic acid; > 50.

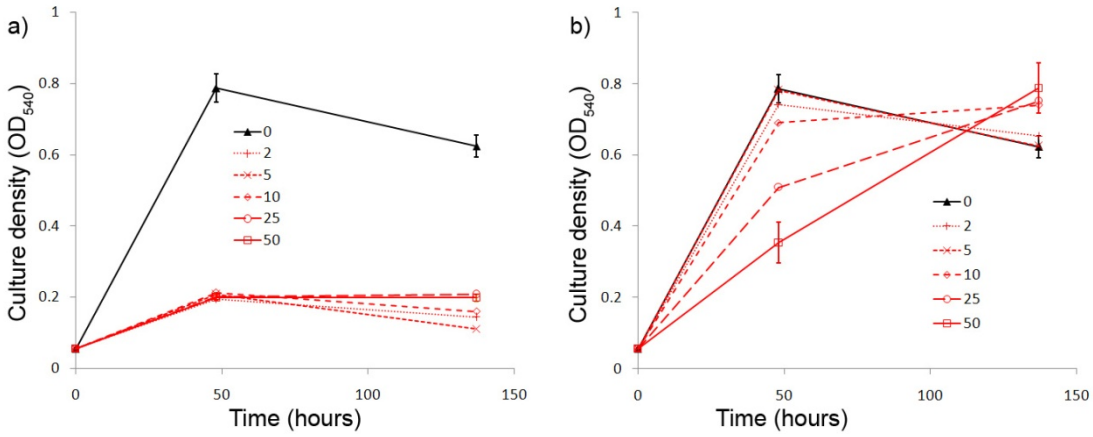

Figure 3.12. Growth of *M. silvestris* in the presence of **a)** kanamycin and **b)** chloramphenicol at the concentrations (μg ml^{-1}) shown. Each data point represents the mean of triplicate cultures, and error bars indicate the standard deviation. Most error bars are omitted for clarity, but those shown are representative.

M. silvestris was capable of growing to an OD_{540} of at least 0.15 in the presence of all concentrations of every antibiotic tested except tetracycline. It was noted that, in the presence of high concentrations of antibiotic, cultures tended to accumulate large quantities of polysaccharide slime, possibly as a method of protection for the cells. Additionally, in the case of, for example, kanamycin, probably the most suitable antibiotic for use with this organism, sensitivity continued down to the minimum concentration tested (0.25 μg ml^{-1}) – 1/100 of the concentration usually employed. These data demonstrate that it cannot be assumed that considerable growth (two doublings) of an engineered strain indicates a higher level of antibiotic resistance than that of the wild type, and highlight the necessity for careful washing of cells used as inoculum to prevent sufficient antibiotic being carried over to affect growth (for example during removal of the kanamycin cassette by electroporation of *cre* recombinase). Since *M. silvestris* was sensitive to kanamycin and gentamicin, and

since these antibiotics are relatively stable, these were considered the most suitable for routine use. DNMS agar plates were prepared containing kanamycin (2, 5, 10, 20 or 40 μg ml^{-1}). Growth occurred up to 10 μg ml^{-1}, but not at the two highest concentrations. Similarly, *M. silvestris* grew on plates containing gentamicin at up to 5 μg ml^{-1}. The ability to grow on plates at a higher antibiotic concentration than in liquid may also be related to the polysaccharide slime-producing ability of the colonies.

3.12 Proteomic analysis

Cell-free extract was produced from cells grown on acetate, succinate or methane as described in Materials and Methods. Following TCA precipitation and protein quantification, 15 μg were loaded on a 12.5% SDS-PAGE gel. Each lane of the coomassie-stained gel (Figure 3.13) was cut into approximately 1 mm thick bands and analysed by tryptic digest and LC/ESI-MS/MS by the University of Warwick Biological Mass Spectrometry and Proteomics Facility.

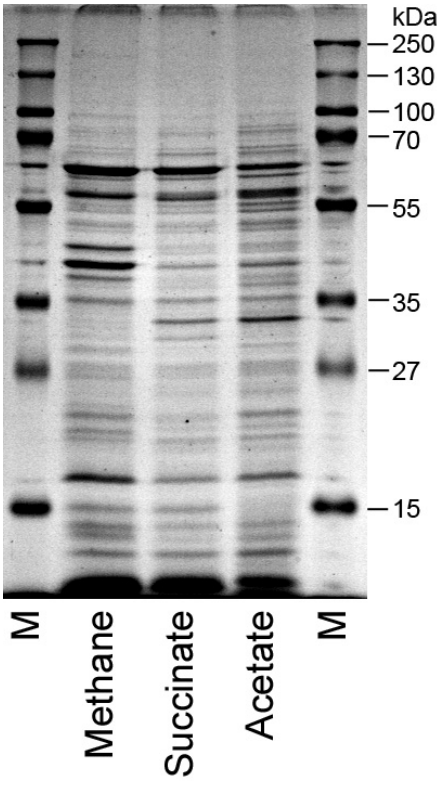

Figure 3.13. SDS-PAGE analysis of cell-free extract from *M. silvestris* cells grown on methane, succinate or acetate. M: PageRuler Plus molecular mass marker (Fermentas).

A total of 312 polypeptides were identified, 159 by two or more peptides, of which those involved in core metabolic processes are listed in Table 3.5. Single-peptide identification of polypeptides should be interpreted with caution (Veenstra et al., 2004). There is a general correlation between the abundance of a protein in a sample and the number of peptides detected (Rappsilber et al., 2002), depending on the theoretical number of peptides derived from tryptic digest of a particular polypeptide, which mainly depends on its size. Therefore, when comparing samples from different growth conditions, peptide number has been taken as an indicator of relative polypeptide abundance. Identifications were made from a database compiled from the genome sequence, which at that time was unfinished. The final genome sequence became available during the course of this project, and included many changes compared with the previous draft genome used to assign peptides identified from the gel. Re-analysis of the data using the finished genome would undoubtedly alter the results slightly, for example, the draft genome identified two isocitrate lyase genes (discussed later) to which peptides were assigned separately, but which were later shown to belong to a single open reading frame. However, time and resources precluded this computationally-intensive process. For this reason, the gene identification numbers in the table refer to the draft genome which is different to that adopted for the finished genome accessible via NCBI.

Whereas the subunits of the soluble methane monooxygenase (sMMO) were mostly only detected in methane-grown cells, methanol dehydrogenase (MDH) was present in all growth conditions. In addition, enzymes of the serine cycle for one-carbon assimilation were present during multi-carbon growth, including serine-glyoxylate aminotransferase, although hydroxypyruvate reductase was not detected. A theoretical possibility would be for *M. silvestris* to assimilate carbon via the Calvin cycle (as, for example, *Beijerinckia mobilis* during growth on formate, (Dedysh et al., 2005b)), but the two enzymes unique to this cycle, ribulose 1,5-bisphosphate carboxylase-oxygenase (RubisCO) and phosphoribulokinase (PRK), were not detected.

Table 3.5. Core metabolic gene products identified in the SDS-PAGE gel shown in Figure 3.13. Cells were grown on the substrates shown, separated by 1D SDS-PAGE and analysed by MS/MS. The figures in the columns indicate the number of peptides identified from each predicted polypeptide in each growth condition and blanks indicate that the polypeptide was not detected in that condition. Ac: acetate, Succ: succinate, MM: molecular mass (kDa).

Gene [a]	Ac	CH_4	Succ	MM [b]	Description
Methane metabolism					
1024	10	20	15	60.1	Methanol dehydrogenase alpha subunit
3901	1	13		42.5	sMMO beta subunit (MmoY)
3902		11		24.0	sMMO alpha subunit (MmoX)
3899		6	2	35.9	sMMO gamma subunit (MmoZ)
3900		5		22.6	sMMO regulatory subunit (MmoB)
1021	1		3	10.9	Methanol dehydrogenase beta subunit
3894		2		59.7	sMMO chaperone (MmoG)
3897		2		38.5	sMMO reductase (MmoC)
1025			1	8.8	Methanol dehydrogenase alpha subunit
1726	2		2	27.3	Formylmethanofuran DH, subunit C
1741	3	4	3	18.6	Formaldehyde-activating enzyme
1746	1	1	1	30.9	Methylenetetrahydromethanopterin DH
Serine cycle					
0609	7	3	3	46.0	Serine hydroxymethyltransferase
1621	7	3	3	33.4	Malate dehydrogenase, NAD-dependent
0974	5	5	3	44.9	Enolase
2256	2	1	5	42.9	Malyl-CoA synthetase, beta subunit
2258	4	4	3	42.6	Serine-glyoxylate aminotransferase
3829		2		101.8	Phosphoenolpyruvate carboxylase
2339		1		22.7	2,3-bisphosphoglycerate mutase
Central carbon metabolism					
0005	9	2	6	40.2	Acetyl-CoA acetyltransferase (β-ketothiolase)
3942	6	3	1	38.0	D-fructose 1,6-bisphosphatase
0974	5	5	3	44.9	Enolase
2946	5		1	33.4	PEP carboxykinase (ATP)
3123	4	4		35.5	Glyceraldehyde-3-phosphate dehydrogenase
3670		4		54.4	Glucose-6-phosphate dehydrogenase
2508		3		92.8	Glycogen/starch/alpha-glucan phosphorylase
2947	3		2	24.8	PEP carboxykinase (ATP)
4055	1	1	3	70.8	Acetate--CoA ligase
0605	1	1	2	27.9	Acetoacetate decarboxylase 1
3829		2		101.8	PEP carboxylase
0036	1	1	1	23.3	Acetyl-CoA:acetoacetyl-CoA transferase
0969	1		1	38.1	Pyruvate dehydrogenase
1789	1	1	1	24.8	Phosphoglycolate phosphatase
2206	1			55.7	D-3-phosphoglycerate dehydrogenase
2339		1		22.7	Phosphoglycerate mutase
3936	1		1	12.6	Fructose-bisphosphate aldolase
3937	1			21.9	Fructose-bisphosphate aldolase

Table 3.5 (contd.)

Gene [a]	Ac	CH_4	Succ	MM [b]	Description
TCA cycle					
2169	6	4	9	45.2	Isocitrate dehydrogenase, (NADP)
1620	8		8	35.0	Succinyl-CoA synthetase, beta subunit
1621	7	3	3	33.4	Malate dehydrogenase, NAD-dependent
1619	1	1	4	30.1	Succinyl-CoA ligase alpha subunit
2296	3	4	3	35.9	Citrate synthase
3412		4		101.9	Aconitate hydratase 1
1616	2		2	44.8	Dihydrolipoamide succinyl transferase
2133			2	21.9	Succinate DH / fumarate reductase
2132			1	60.7	Succinate dehydrogenase subunit
2295	1	1	1	12.7	Citrate synthase I
Glyoxylate bypass					
3298	5			34.4	Isocitrate lyase
3005	3	1	2	79.1	Malate synthase
3299	2	1		21.8	Isocitrate lyase
Nitrogen metabolism					
0721	2	16	2	42.2	Urea/short-chain amide ABC transporter
0724		8		28.2	Urea ABC transporter, ATP-binding protein
1075	4	7	3	38.8	L-glutamine synthetase
1074	4	3	2	52	Glutamine synthetase, type I
0725		3		25.8	Urea ABC transporter, ATP-binding protein
2058		3		50.2	Nitrogenase molybdenum-iron cofactor (NifN)
2059		3		14.8	Nitrogen fixation protein (NifX)
2377		3		67.7	Nitrite reductase (NAD(P)H), large subunit
3522	3			12.0	Nitrogen regulatory protein P-II
1964		2		170.1	Glutamate synthase (Ferredoxin)
1965		2		51.7	Glutamate synthase (NADH) small subunit
2040		2		48.7	Nitrogenase cofactor biosynthesis protein (NifB)
2053		2		15.6	Response regulator
2054		2		31.5	Nitrogenase reductase (NifH)
2056		2		58.2	Nitrogenase beta chain (NifK)
0113			1	20.4	Nitrogen-fixing protein (NifU)
1073	1		1	12.0	Nitrogen regulatory protein P-II
2055		1		54.8	Nitrogenase alpha chain (NifD)

[a] Gene identification numbers have since been superseded.
[b] Note that the accuracy of theoretically calculated molecular masses is dependent on correct genome sequence information.

Subunits of all enzymes of the TCA cycle except fumarase were identified, as were enzymes possibly active in the Entner Doudoroff pathway. Both enzymes of the glyoxylate bypass (isocitrate lyase and malate synthase) were identified, although (particularly the former) with low abundance in methane-grown cells. Nitrogen

scavenging systems were identified in the form of urea transporters, as well as N_2-fixing enzymes, principally in methane grown cells, possibly indicating a difference in nitrate availability between the three cultures.

3.13 Transcription of hydroxypyruvate reductase, RubisCO and phosphoribulokinase

Operation of the serine cycle requires the enzymatic activity of hydroxypyruvate reductase. Since this enzyme was not detected by proteomic analysis, *hpr* gene transcription was verified, together with that of *cbbL* and *cbbP,* encoding the RubisCO large subunit and phosphoribulokinase respectively. RNA was extracted from cells grown on methane, methanol and succinate and 100 ng used for cDNA synthesis using random hexamer primers and Superscript II enzyme as described in Materials and Methods. cDNA was used as template in PCR reactions using primers internal to *hpr, cbbL and cbbP,* and the 16S rRNA gene as positive control. Transcripts were detected, in all growth conditions, for 16S rRNA, *hpr* and *cbbP,* (Figure 3.14) but not for *cbbL* (data not shown).

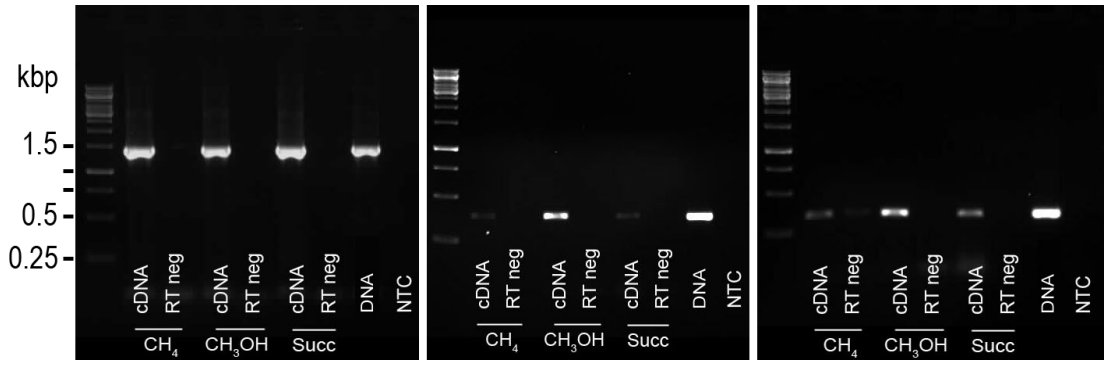

Figure 3.14. cDNA was used as template in PCR reactions to verify transcription of *hpr* (centre gel, 377 bp) and *cbbP* (right, 334 bp). The 16S rRNA-gene positive controls are shown on the left (1447 bp). PCR reactions contained, as template, cDNA synthesised by reverse transcriptase, or, labelled RT neg, the products of identical reactions where reverse transcriptase was omitted. Lanes labelled DNA contained a genomic DNA template. NTC: no template control.

3.14 Discussion

The purpose of the work described in this chapter was to develop effective methods of growing *M. silvestris*, and to gather background information on the growth-substrate range and corresponding metabolic pathways. This was essential in order to

be able to produce sufficient high quality biomass for physiological, biochemical and genetic experimentation. Initially, problems associated with large amounts of polysaccharide slime production made the harvesting and washing of cells difficult or impossible. Changes in the form or concentration of fixed nitrogen sources in the culture medium did not provide an answer, and no nitrogen source was found that provided increased growth rate or higher final culture density compared to 1 mM nitrate. For growth in the fermenter, it became apparent that reduced oxygen tension, under which conditions *M. silvestris* is capable of fixing N_2, enabled the growth of slime-free biomass, and this was achieved using several different growth substrates. It was found that *M. silvestris* is not as sensitive to ionic strength as had been assumed previously, nor were increased concentrations of trace elements toxic, allowing the formulation of an improved trace elements solution which may offer benefits under certain growth conditions. Phosphate concentrations could be considerably increased allowing better buffering and growth under conditions tending to alter pH. Whether due to improved culture conditions or gradual adaptation of the organism to laboratory conditions, methods were developed which greatly increased the ability to predictably grow cultures to comparatively high densities.

Suitable antibiotics for use in later genetic manipulations were identified as kanamycin and gentamicin, and the sensitivity of *M. silvestris* to very low levels of kanamycin and tetracycline was noted.

Oxygen electrode work identified high rates of primary but not secondary alcohol oxidation, which reflects the reported substrate specificity of MDH. SDS-PAGE demonstrated that MDH is expressed during growth on 2-carbon and 4-carbon compounds in addition to during growth on methane. It was shown that *M. silvestris* is capable of growth on ethanol, and it may be that MDH is responsible for oxidation of ethanol in *M. silvestris,* as is the case in *Methylobacterium extorquens* AM1 (Taylor and Anthony, 1976). SDS-PAGE also confirmed the expression of many key enzymes, including isocitrate lyase and malate synthase, although the low relative abundance of isocitrate lyase during growth on methane left open the possibility that this enzyme might not be essential for 1-carbon growth. The key serine cycle enzyme hydroxypyruvate reductase was not detected in the gel-based proteomic analysis, but transcription was verified by RT-PCR.

It was found that *M. silvestris* is capable of growth on propane and many of the possible metabolic products of propane oxidation, and this is the subject of a later chapter.

Chapter 4

Development of a genetic system for *M. silvestris*

4.1 Introduction

As described in Chapter 1, the discovery, isolation, characterisation and, during the course of this project, the completion of the genome sequence of *M. silvestris* identified several key questions, some of which are addressed in this work. Data acquired prior to and during this project, and the ongoing debate regarding the reasons for obligate methanotrophy (reviewed by Wood et al., 2004), suggested numerous metabolic and regulatory hypotheses which required confirmation in this organism using biochemical and genetic methods. In order to use the methods of reverse genetics, it was essential to develop an efficient method of targeted mutagenesis, which would also be a prerequisite for any attempt to engineer a strain with the aim of maximising this organism's capacity for effective bioremediation or biotransformation.

The most common method of introducing DNA into methanotrophs and methylotrophs has historically been by conjugation (Murrell, 1992), although electroporation has also sometimes been used (Kim and Wood, 1998; Toyama et al., 1998; Baani and Liesack, 2008). For marker exchange mutagenesis using homologous recombination, two recombination events are necessary, upstream and downstream of the gene of interest, to replace it with a selectable marker, for example an antibiotic cassette. When introducing DNA on a circular plasmid, the detection of the comparatively rare second recombination event, and consequent loss of the vector backbone, typically requires screening for double-crossover colonies using sensitivity to an antibiotic, resistance to which is encoded on the vector backbone, as indicator. Although the loss of the plasmid backbone may be forced by incorporation of a counter-selectable marker, for example the *sacB* gene from *Bacillus subtilis* (Schäfer et al., 1994), a (possibly large) proportion of single crossovers will revert (by recombination) to wild type unless selective pressure exists. If the intention is to construct a mutant with a deletion of two or more genes, it is convenient if the gene is deleted without incorporation of an antibiotic selectable marker. This is also desirable if the organism is destined for release into the environment, in order to prevent the possible horizontal transfer of antibiotic resistance genes (Davison, 2005). Most of the genetic methods in common use with methanotrophs therefore involve time-consuming screening and numerous transfers of colonies on plates.

The introduction of linear DNA, comprising an antibiotic resistance cassette flanked by regions homologous to sequences upstream and downstream of the gene of interest, requires two simultaneous recombination events if the organism is to gain resistance to the selective antibiotic. Thus, marker-exchange gene replacement is achieved in one operation. This approach, although common in yeast (Rothstein, 1983) has less commonly been used in bacteria, for example in *Bordetella pertussis* (Zealey et al., 1990), *E. coli* (Jasin and Schimmel, 1984; El Karoui et al., 1999), *Haemophilus ducreyi* (Hansen et al., 1992), *Methylobacterium extorquens* (Toyama et al., 1998), *Rickettsia prowazekii* (Driskell et al., 2009) and *Streptomyces coelicolor* (Oh and Chater, 1997), but in most cases the frequency of gene replacements is low (unless one of a number of methods has been used to modify the host cells to be more receptive to incoming DNA (see, for example, Murphy, 1998), a strategy usually only available with organisms already engineered for that purpose). Incorporation of specific DNA sequences adjacent to the antibiotic resistance cassette allows subsequent removal of the cassette by site-specific recombination, using, for example, the Flp-*FRT* or Cre-*loxP* recombinase systems (Ayres et al., 1993; Hoang et al., 1998), resulting in unmarked gene deletions.

4.2 Marker exchange mutagenesis using a pK18*mobsacB*-based vector introduced by conjugation

Vectors pK18*mob* and pK18*mobsacB* (Schäfer et al., 1994) have previously been used with methanotrophs to introduce genetic elements by conjugation (Murrell, 1992; Barta and Hanson, 1993; Ali and Murrell, 2009). Based on the narrow host range plasmid pBR322, these plasmids are only able to replicate in *E. coli* and closely related species. However, they include the broad host range transfer elements of plasmid RP4 (Datta et al., 1971), enabling mobilisation from *E. coli* into other bacterial genera. pK18*mobsacB* also contains the counter-selectable gene *sacB*, which is lethal when expressed in the presence of sucrose (Selbitschka et al., 1993). The use of this plasmid to introduce a modified malate synthase gene, inactivated by deletion of an internal segment, and the forcing of its incorporation into the chromosome in place of the wild type, was adopted in an attempt to engineer a strain lacking this enzyme.

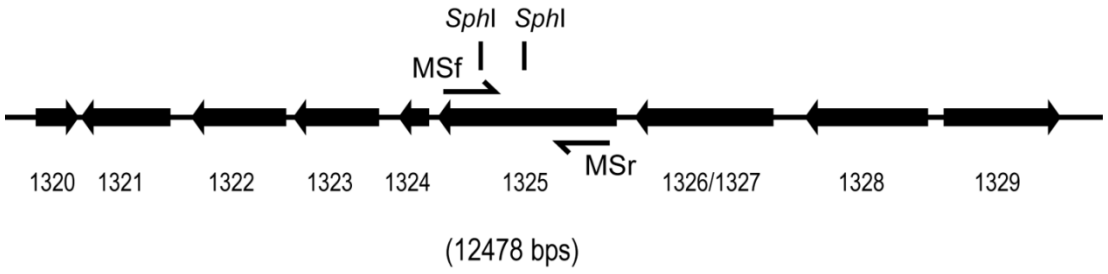

Figure 4.1. Arrangement of genes surrounding malate synthase (Msil1325) including primer sites MSf and MSr and two *Sph*I restriction sites. Open reading frames 1326 and 1327 are predicted to overlap by four nucleotides.

The genomic layout of the putative malate synthase gene (Msil1325) is shown in Figure 4.1. Primers MSf and MSr were used to amplify an internal 2011 bp sequence from 86 bp after the start codon to 71 bp before the stop codon. This fragment was cloned into vector pCR2.1 TOPO, excised and ligated into pK18*mobsacB,* followed by removal of the 526 bp *Sph*I fragment to give vector pAC1003, as shown in Figure 4.2. The PCR amplicon was checked by sequencing using primers M13F and M13R, each construct checked by restriction digest, and pAC1003 by restriction digest and PCR (data not shown). This vector was introduced into *E. coli* S17.1 λ*pir* (Simon et al., 1983) by electroporation, and this strain was used as donor in conjugations with *M. silvestris* as described in Materials and Methods. As positive control, *M. silvestris* was also conjugated with pMHA203 (Theisen et al., 2005) which comprises the promoter and upstream region of the sMMO cluster fused to *gfp,* resulting in expression of GFP in methane-grown cultures. Following conjugation, cells were spread on DNMS plates containing kanamycin with glycerol or succinate (5 mM) or methanol as carbon and energy source.

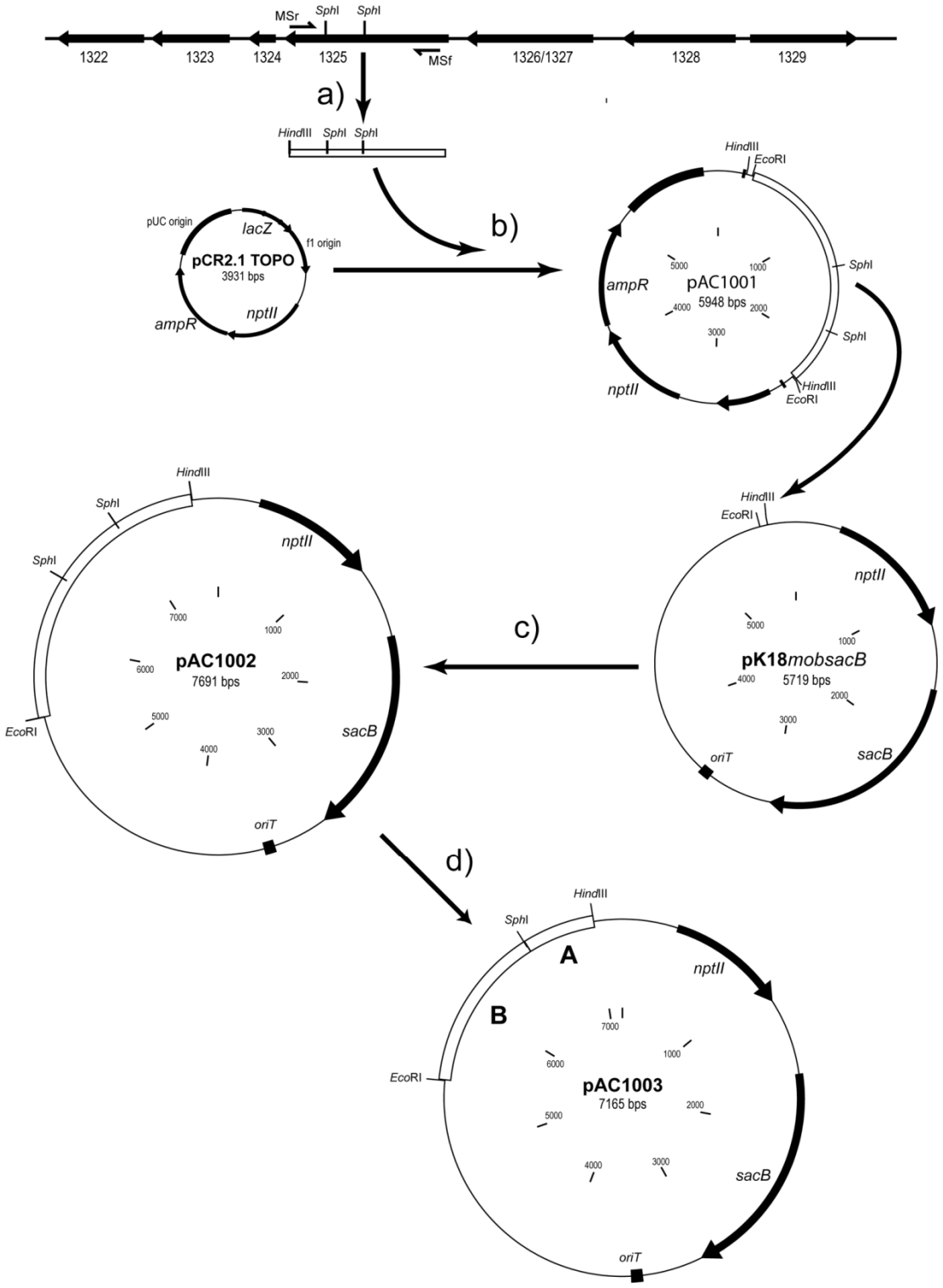

Figure 4.2. Construction of pAC1003 for mutagenesis of malate synthase in *M. silvestris.* **a)** A 2011 bp sequence was amplified from the *M. silvestris* chromosome by PCR using forward primer MSf and reverse primer MSr which introduced a 5' *Hin*dIII site. This was cloned into pCR2.1 TOPO (Invitrogen) **(b),** before excision with enzymes *Eco*RI and *Hin*dIII and ligation with pK18*mobsacB* cut with the same enzymes **(c)**. Digestion with *Sph*I and re-ligation removed a 526 bp fragment, internal to the malate synthase sequence, to give vector pAC1003, as shown at **d)**, which contains regions A and B with homology to the *M. silvestris* chromosome.

After 18 days colonies were visible on all plates, and were patched onto fresh plates and incubated with methanol. Following several transfers on plates, colonies were transferred to liquid medium containing 0.1% methanol as carbon and energy source, initially with kanamycin and then for two passages without antibiotic. Transfer from liquid back to selective plates demonstrated that the kanamycin resistance cassette was retained. Colonies and liquid cultures were monitored by PCR using primers located either side of the excised portion of the gene (Figure 4.3).

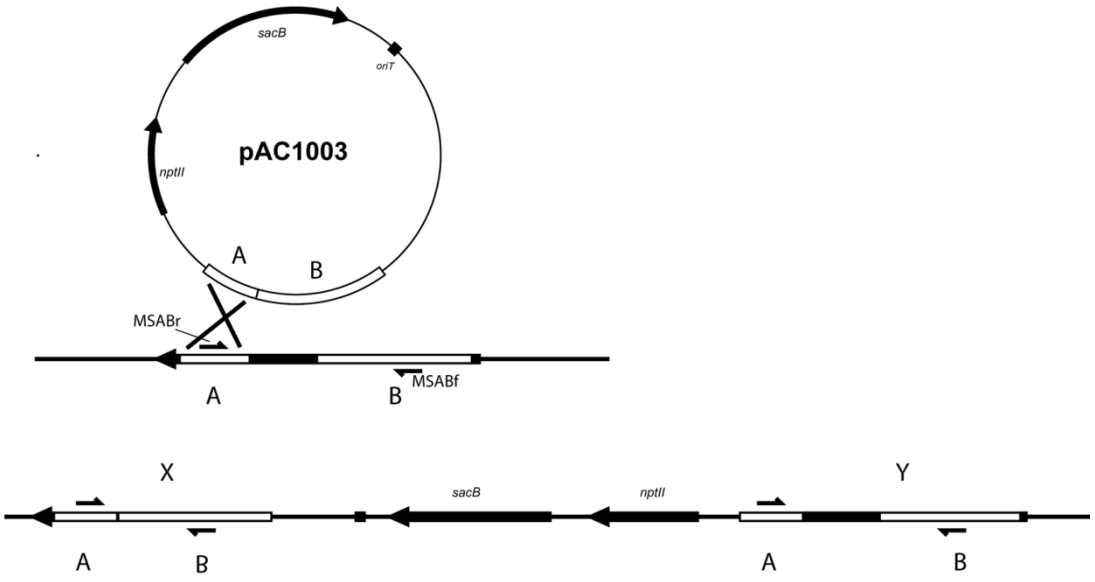

Figure 4.3. Homologous recombination between the *M. silvestris* chromosome and vector pAC1003 (top) can occur at either sequence A or sequence B, resulting in two different single-crossover molecules, only one of which is shown (below). Primers MSABf and MSABr result in two different sized amplicons (represented by X and Y) in each possible single-crossover, of which Y corresponds with the wild type.

Single crossover-mutant colonies were isolated. These retain the vector sequence incorporated into the chromosome, and have two truncated copies of the disrupted gene, one of which additionally has the central portion deleted, giving rise to two different sized amplicons in PCR reactions using primers located either side of the deleted region, see Figure 4.4. However, cells containing the single crossover mutation shown in Figure 4.3 may retain malate synthase activity due to the presence of a gene lacking only the final 70 nucleotides.

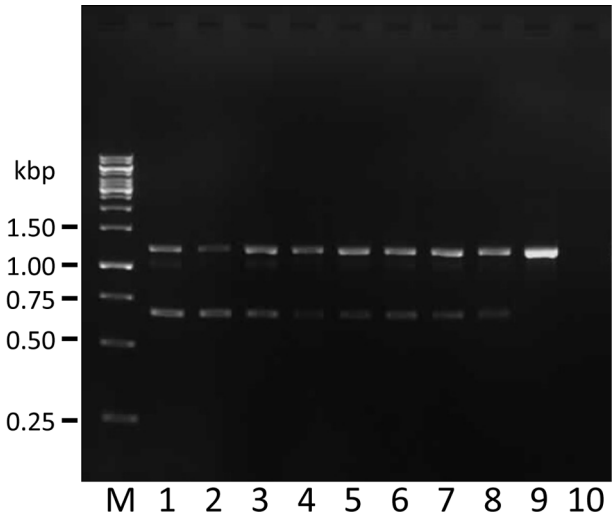

Figure 4.4. PCR using primers MSABf and MSABr, using, as template, lanes 1 and 2: cells conjugated with pAC1003 growing in liquid culture with kanamycin, lanes 3 – 8: cells growing after 2 transfers without antibiotic, lane 9: wild type culture, lane 10: no template control (NTC). M: Fermentas GeneRuler 1kb ladder. Expected sizes: single crossover mutations, 660 bp and 1186 bp; wild-type, 1186 bp.

Eventually cells were diluted (10^{-2} or 10^{-3}) and spread on DNMS plates containing succinate or malate (5 mM) or methanol and sucrose (10% w/v) in order to force a second recombination event. Approximately 200 colonies were tested by PCR for recombination at the second locus which would result in a deletion mutant, however all colonies were wild type, suggesting that either there is selective pressure to retain the malate synthase gene, or possibly that recombination is more common at one of the sites, perhaps due to the difference in size of the homologous sequences. Both these issues could be addressed by the incorporation of an antibiotic cassette in place of the deleted gene fragment, but this would have the disadvantage of leaving the selectable marker permanently in the mutated chromosome. However, since no single crossover mutants were detected following sucrose selection, this demonstrated that the SacB system is effective in *M. silvestris.*

Difficulties were experienced with this method; numerous transfers of colonies were required, both to remove the donor *E. coli* cells, and to identify kanamycin-resistant transconjugants, but it was exceedingly difficult to remove the colonies from the plates. Colonies were tough, sticky and adhered to the agar. Difficulty was experienced in successfully transferring cells from solid medium to liquid, and cultures frequently did not grow when, eventually, a colony was successfully placed in liquid medium. Due to the slow growth of *M. silvestris,* problems were

encountered with contamination by fungi, which the addition of cycloheximide did not fully alleviate. Finally, all colonies tested had reverted to wild type. For these reasons, progress was slow. Therefore, an alternative method was sought that would not involve a donor organism, and that would reduce the transfers between plates.

4.3 DNA introduction by electroporation in *M. silvestris*

Introduction of DNA into *M. silvestris* by electroporation would offer several advantages over conjugation, including avoiding the difficulty of removal of contaminating *E. coli* cells, which at the minimum requires several transfers on plates. To test the potential of this method, plasmid pMHA203 (Ali, 2006) was once again chosen. Competent cells were prepared following the method of Kim and Wood (1998), by washing and resuspending cells in 0.3 M sucrose, as described in Materials and Methods. Electroporation was carried out in 1 mm cuvettes, with conditions as detailed in Table 4.1. Following recovery overnight in DNMS medium containing methanol (0.05% v/v) at 25 °C, cells were spread on selective DNMS plates and incubated with methanol.

Table 4.1. Electroporation of *M. silvestris* with pMHA203 plasmid DNA

Vial	V (kV)	R (Ω)	C (μF)	DNA (μg)	Time constant (ms)	Selection	Colonies
1	2.0	200	25	0	4.7	kan^{25}	0
2	1.5	200	25	5	4.6	kan^{25}	34
3	2.0	200	25	20	4.4	kan^{25}	68
4	2.5	400	25	5	8.7	kan^{25}	92
5	2.0	400	25	30	6.7	kan^{25}	96
6	-	-	-	10	-	kan^{25}	0
7	2.0	200	25	0	4.7	None	Thick lawn

Colonies appeared after approximately 3 weeks, which, when patched onto fresh plates and incubated with methane, fluoresced brightly with excitation at 395 nm, demonstrating the uptake of DNA by cells.

4.4 Gene deletion by electroporation with linear DNA

Having demonstrated the ability of electroporation to introduce DNA, an attempt was made to use this method for chromosomal genetic manipulation of *M. silvestris*. For this experiment, a different approach was adopted than previously, using vector

pCM184 (Marx and Lidstrom, 2002). This vector possesses two multiple cloning sites on either side of a kanamycin resistance cassette. Therefore, this facilitates the amplification of sequences upstream and downstream of the gene of interest and the cloning of these fragments separately into the two sites. The vector also incorporates *loxP* sites flanking the kanamycin cassette, enabling later removal of the antibiotic resistance marker.

Isocitrate lyase, encoded at locus Msil3157, was chosen for deletion. Approximately 500 bp of chromosomal DNA were amplified by PCR, from regions upstream and downstream of the gene, using *M. silvestris* genomic DNA as template and primers 3157Af/3157Ar and 3157Bf/3157Br (Table 4.3). In most cases primers were designed to incorporate restriction sites. These fragments were cloned separately into pCR2.1 TOPO (Invitrogen). Following sequencing using primers M13f and M13r to check that the PCR had not introduced unwanted mutations, the upstream and downstream fragments were excised from pCR2.1 and ligated separately into pCM184 to give pAC104, as shown in Figure 4.5**.** This plasmid was introduced into *M. silvestris* cells by both conjugation and electroporation. Both transconjugant and electro-transformed colonies appeared on selective DNMS plates containing succinate (5 mM). However, cells were also electroporated with the linear *Eco*RI/*Sac*I fragment digested from pAC104, prepared as described in Materials and Methods. Colonies appeared on selective plates spread with cells transformed with linear DNA. Since incorporation of the antibiotic resistance cassette in this case should require two simultaneous and independent recombination events leading to gene deletion in a single step (Figure 4.6), these colonies were investigated further. After several transfers on selective plates, colonies were transferred to liquid culture with succinate (5 mM) as carbon and energy source and kanamycin (25 μg ml^{-1}). Following two subcultures in liquid containing antibiotic, cells were transferred to liquid culture without antibiotic. After two transfers, a 50 ml culture was used to prepare competent cells as described previously.

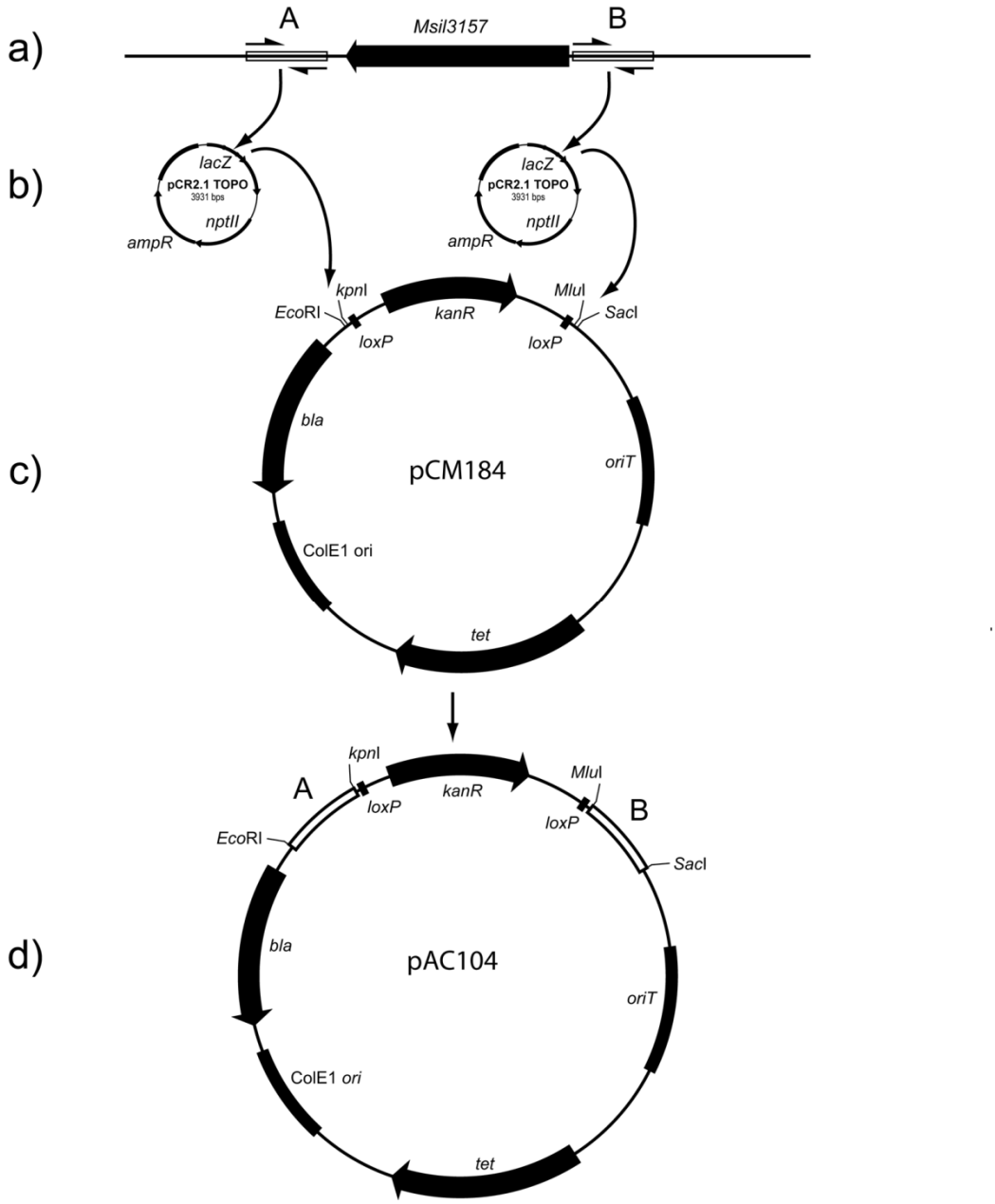

Figure 4.5. Cloning of regions upstream and downstream of *M. silvestris* isocitrate lyase for marker exchange mutagenesis. Approximately 500 bp sequences of chromosomal DNA (A and B) upstream and downstream of the putative isocitrate lyase coding sequence were amplified by PCR (**a**) and cloned into pCR2.1 TOPO (**b**). These fragments were excised using enzymes *Eco*RI and *Kpn*I or *Mlu*I and *Sac*I respectively, and ligated sequentially into pCM184 cut with the same enzymes (**c**), resulting in pAC104 (**d**).

These cells were electroporated with pCM157 (Marx and Lidstrom, 2002), and spread on DNMS plates containing succinate (5 mM) and tetracycline (10 μg ml^{-1}). This plasmid contains the *cre* gene under the control of the *E. coli lac* promoter, and expression of Cre mediates recombination between *loxP* sites and consequent loss of the kanamycin cassette.

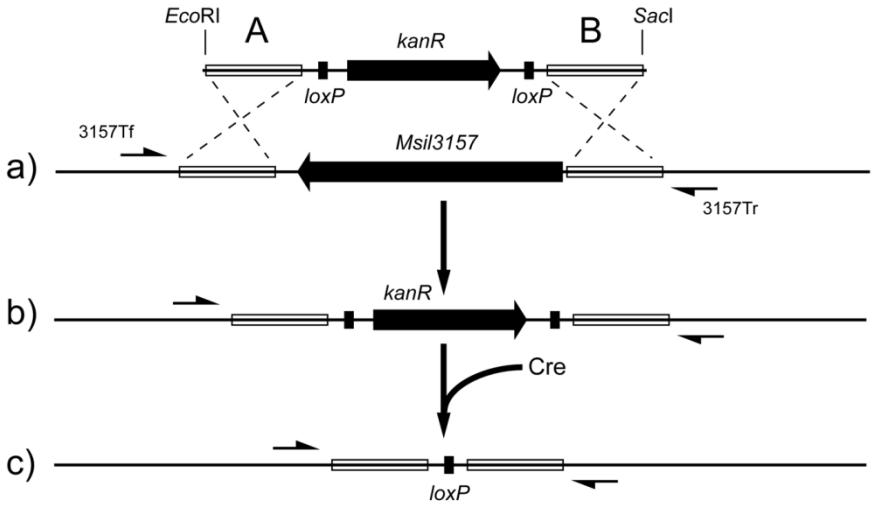

Figure 4.6. Recombination with linear DNA. The *Eco*RI/*Sac*I fragment digested from pAC104 was electroporated into competent *M. silvestris* cells (**a**). Two recombination events resulted in gene deletion, shown at **b**). Subsequently, Cre recombinase was expressed transiently from plasmid pCM157, resulting in the excision of the kanamycin cassette (**c**).

Colonies appeared after 14 – 20 days, with a transformation efficiency of approximately 10^3 cfu (μg DNA)$^{-1}$. After one further transfer onto selective plates, colonies were picked onto plates without selection to allow the plasmid to be cured.

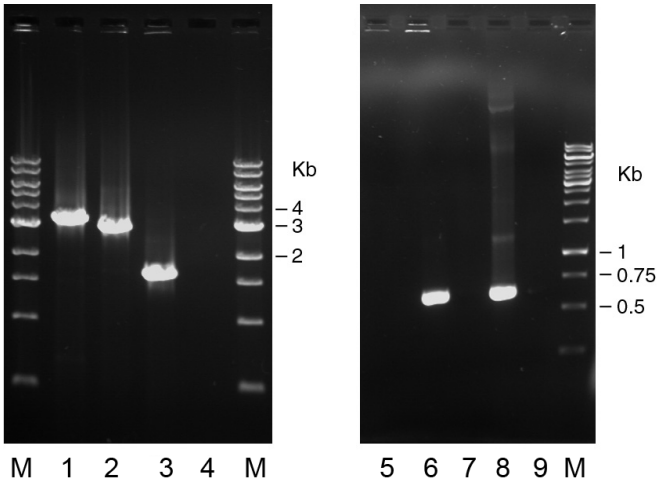

Figure 4.7. Primers 3157Tf and 3157Tr (Figure 4.6) were used to monitor replacement and deletion of isocitrate lyase in *M. silvestris* (left hand gel). Removal of sequences containing binding sites for primers KanF and KanR (kanamycin resistance) is shown in the right hand gel. Lanes 1 & 5: wild type, 2 & 6: *Msil3157::kan*^{R}, 3 & 7: *Δ3157* following electroporation with pCM157, 4 & 9: NTC, 8: pCM184 vector DNA, M: Fermentas GeneRuler 1 kb ladder.

Replacement of the isocitrate lyase gene with the kanamycin resistance cassette, and the subsequent loss of the marker following expression of Cre, were monitored by

PCR using primers 3157Tf and 3157Tr, which bind to the *M. silvestris* chromosome further upstream and downstream of the regions initially amplified and used for cloning, and also with primers internal to the kanamycin cassette, see Figure 4.7. Subsequently, colonies were found to be sensitive to both kanamycin and tetracycline, additionally confirming the curing of plasmid pCM157.

Primers 3157Tf and 3157Tr were also used to sequence the intervening chromosomal region, revealing the removal of 1,694 bp including the entire isocitrate lyase coding region, and the insertion 100bp consisting of small fragments of plasmid DNA flanking one *loxP* site, see Figure 4.8.

GGTACCATGGATGCATATGGCGGCCGCATAACTTCGTATAGCATACATTATACGAAGTTATGGATCCAGCTT
ATCGATACCGCNGGNNNCTACGTACGCGT

Figure 4.8. Sequencing using primers 3157Tf and 3157Tr revealed the sequence shown inserted between chromosomal positions 3470071 and 3471766, representing a deletion of 1694 bp. A single *loxP* site (shaded) is flanked by short sequences of vector pCM184. The palindromic sequences are underlined.

4.5 Application and optimisation of gene deletion

The strain with a deletion of isocitrate lyase described in the previous section was designated *M. silvestris* strain ΔICL. In total, six strains were constructed with single gene deletions using this method. In some cases the restriction enzymes employed (shown in Table 4.3) were varied to avoid sites in the regions of homology that were cloned, and methanol was used as carbon source where the deleted gene was not expected to be required for the metabolism of this substrate. In all other respects the method employed was identical, and construction of these mutants is therefore not described in detail. A double mutant, with a deletion of malate synthase (MS) in addition to isocitrate lyase, was constructed by applying the described method to the deletion of MS, and electroporating competent cells prepared from strain ΔICL, demonstrating the advantage of the removal of the antibiotic resistance cassette.

These strains are described in the relevant chapters, and summarised in Table 4.2

Table 4.2. Summary of mutant strains constructed using the methods described in this chapter. Chromosome positions and locus tags refer to GenBank accession number CP001280. Headings "A frag" and "B frag" indicate the length of the cloned sequences for homologous recombination. Strain ΔICLΔMS was also constructed, with deletions of both isocitrate lyase and malate synthase, in which both regions shown were deleted.

Strain	Locus tag (Msil)	Coding sequence	A frag (bp)	B frag (bp)	Chromosome region deleted (bp)
ΔICL	3157	3470137 – 3471765 (R)	509	573	3470072 - 3471765 (1694)
ΔMmoX	1262	1357783 – 1359363 (F)	525	544	1357807 - 1359337 (1531)
ΔMS	1325	1423900 – 1426065 (R)	632	597	1423969 - 1426024 (2056)
Δ1641	1641	1774764 – 1776332 (R)	548	591	1774759 - 1776408 (1650)
ΔPrMO	1651	1785113 – 1786771 (R)	681	696	1785072 - 1786838 (1767)
ΔSGAT	1714	1863161 – 1864351 (R)	564	512	1863316 - 1864340 (1025)

In every case, 10 – 20 colonies which appeared on selective plates following electroporation were tested, and all were found to be double crossover mutants with a deletion of the expected gene, as determined by PCR and sequencing using primers outside the manipulated region. In each case, following removal of the kanamycin cassette, the inserted sequence corresponded to that shown in Figure 4.8, with minor differences in the length of vector sequence on either side of the single *loxP* site, depending on the choice of restriction enzyme employed.

Following growth in liquid, mutant cultures were diluted in medium and spread on DNMS or DAMS plates with a suitable carbon source. Colonies were counted to relate colony forming units to the density of the originating culture, and PCR used to check the genotype of approximately 12 colonies. In all cases, 100% of colonies tested gave rise to the expected PCR amplicon size. A representative gel is shown in Figure 4.9.

A modified method of preparing competent cells, washing twice in ice cold water and re-suspending in 10% (v/v) glycerol, was compared with the previously described method of Kim and Wood (1998). Electroporation with circular plasmid DNA (repeated in two separate experiments) resulted in more than 10 times as many colonies using the new method, which was then used to prepare competent cells to assess the frequency of gene replacement, using a construct designed to replace gene Msil1641, downstream of the propane monooxygenase gene cluster.

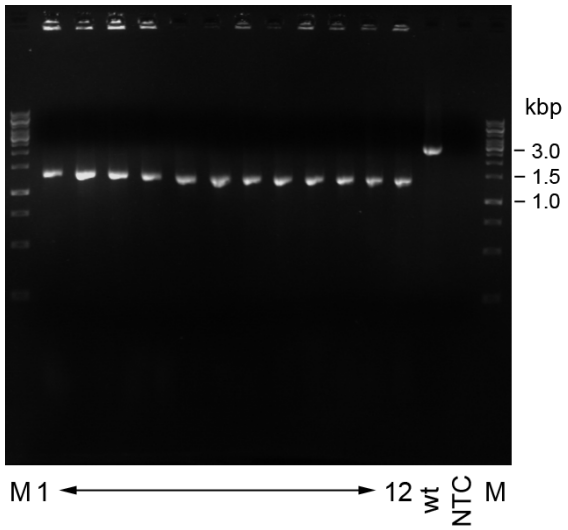

Figure 4.9. A *mmoX* deletion strain growing in liquid was diluted $1/10^6$ and 100 µl spread on DAMS plates and incubated with methanol, resulting in an average of 21 cfu $plate^{-1}$, corresponding to a culture density of 2.1×10^8 cfu ml^{-1}. Colony PCR using primers mmoXTf and mmoXTr resulted in amplicons of the expected size (1,265 bp) compared to the wild type (2,692 bp). Lanes 1 – 12: ΔmmoX colonies, wt: wild type, NTC: no template control, M: Fermentas GeneRuler 1 kb ladder.

The rationale and effect of the deletion of Msil1641 are described in Chapter 7. Following the scheme described in Section 4.4, upstream and downstream sequences of 591 and 548 bp respectively were amplified either side of a 1,650 bp segment targeted for deletion. A linear fragment of 2,548 bp was used for electroporation, with between 12.5 and 348 ng DNA per reaction. Plates were incubated with methanol, and colonies tested by PCR, using, as before, primers outside the manipulated region. All colonies tested (21/21) gave the expected amplicon size, one of which was sequenced, confirming gene deletion, and all colonies were therefore assumed to be the deletion strain. Figure 4.10 shows gene replacements (colonies) per ng of DNA included in the electroporation reaction, suggesting that, in this case, 100 ng of linear DNA would be sufficient to produce 400 colonies, all of which would be expected to possess the desired genotype.

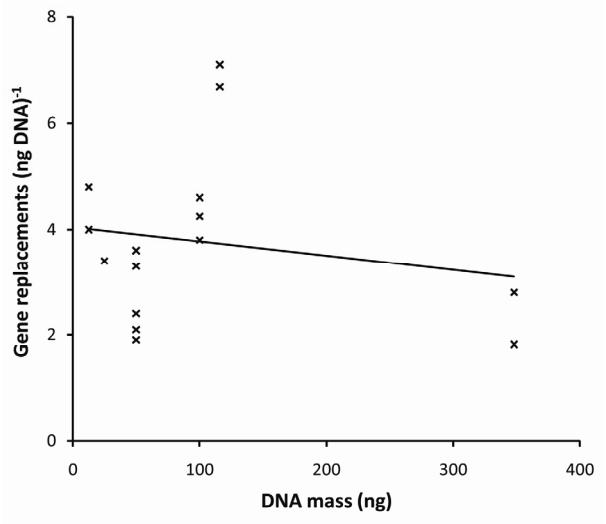

Figure 4.10. Efficiency of gene replacement by electroporation with linear DNA, as a function of DNA mass per reaction.

4.6 Apparent recombination between *loxP* sites

It was noticed that in mutant strains, prior to electroporation with pCM157 for Cre expression, two bands were often visible in PCR reactions using primers spanning the gene-exchange regions. This was noted during the construction of most mutant strains, and is illustrated, in the case of strain ΔPrMO, in Figure 4.11. The relative amount of this minor band, which was approximately 1 kb smaller than the major band, varied somewhat but did not become noticeably more abundant when cultures were grown without antibiotic. The three bands shown arrowed in Figure 4.11 were cut from the gel, purified and re-amplified by PCR using the same primers, see Figure 4.12. Two of these PCR products (corresponding to the major bands from the wild-type and ΔPrMO strains) were analysed by restriction digest (Figure 4.12), resulting in fragments of the expected sizes for sequences containing the PrMO coding sequence and the kanamycin cassette, respectively. The minor band from the mutant culture was sequenced using primers PrmTf and PrmTr. Analysis of the sequences showed the absence of the kanamycin cassette, with upstream and downstream *M. silvestris* sequences flanking a single *loxP* site. The presence of this amplicon (prior to Cre-mediated removal of the kanamycin cassette) is likely to be due to an artefact of the PCR, or possibly indicates the spontaneous removal (and replacement) of the region by recombination between *loxP* sites.

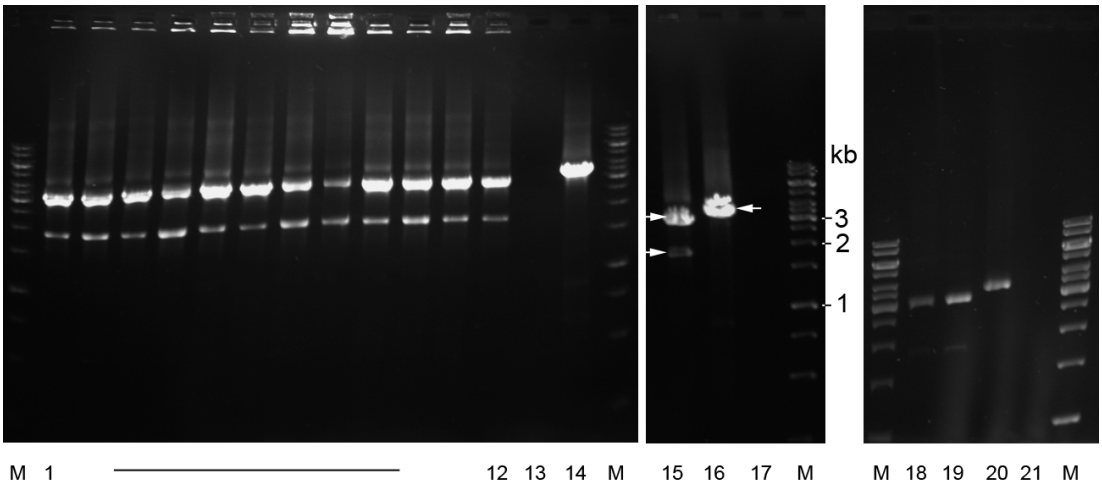

Figure 4.11. Primers PrmTf and PrmTr were used to amplify the mutated region from colonies (left hand gel) and liquid culture (centre and right hand gels) of strain ΔPrMO and the wild-type. A less abundant PCR product was visible in mutant strains with a size approximately 1 kb smaller than the major product. Growth without antibiotic (right hand gel, lane 19) did not increase the relative amount of the minor band. All colonies from mutant strain ΔPrMO show two bands in the gels (lanes 1 – 12, 15, 18 and 19), whereas wild-type colonies result in a single band of larger size (lanes 14, 16 and 20). Lanes 13, 17 and 21: no template control. M: Fermentas GeneRuler 1 kb ladder. The bands shown arrowed (centre gel) were excised from the gel and re-amplified.

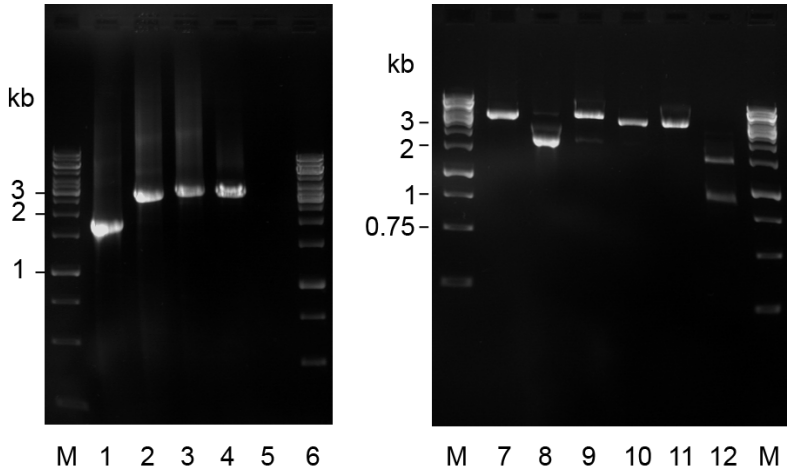

Figure 4.12. Left-hand gel: Bands shown arrowed in Figure 4.11 were re-amplified in a second round of PCR using the same primers. Lanes 1 and 2: the two amplicons from strain ΔPrMO (two bands cut from lane 15 in Figure 4.11). Lane 3: the wild-type amplicon (band cut from lane 16). Lane 4: wild-type DNA template. Lane 5: no template control. M: Fermentas GeneRuler1 kb ladder.
Right hand gel: PCR products from lanes 2 and 3 were analysed by restriction digest. Lanes 7 – 9: digest of wild-type PCR product (shown in lane 3), lanes 10 – 12: digest of strain ΔPrMO PCR product (shown in lane 2). Lanes 7 and 10: uncut, lanes 8 and 11: digested with *Sal*I, lanes 9 and 12: digested with *Kpn*I and *Mlu*I. A *Sal*I site is located in the PrMO coding sequence, while *Kpn*I and *Mlu*I sites flank the kanamycin cassette. Expected sizes, lanes 7 and 9: 3,492 bp, lane 8: 1,722 and 1,770 bp, lanes 10 and 11: 3,118 bp, lane 12: 880, 847 and 1,391 bp.

4.7 Construction of *M. silvestris* strain AC706

The method described proved effective at deleting genes of choice from the chromosome of *M. silvestris.* However, it would also be useful to be able to introduce novel or mutated genes, and a method was devised to accomplish this, making use of the counter-selectable *sacB* gene already described and shown to operate effectively in Section 4.2. Although strain ΔMmoX (with a deletion of the the α-subunit of the soluble methane monooxygenase) was constructed using the method described in Section 4.5 above, an additional strategy (shown in Figure 4.13) was developed to insert the *sacB* gene and a kanamycin resistance cassette into the *M. silvestris* BL2 chromosome in place of *mmoX,* encoding MmoX. The presence of *sacB* in this locus should permit the replacement of the inserted elements with any gene(s) of interest, by the electroporation of the required sequence flanked by regions homologous to the *M. silvestris* chromosome, and selection on plates containing sucrose.

To construct a strain containing kan^R and *sacB,* approximately 500 bp sequences were amplified from the *M. silvestris* BL2 chromosome using primers 1262Af/1262Ar (incorporating *Sac*I and *Mlu*I sites respectively) and 1262Bf/1262Br (incorporating *Mun*I and *Eco*RI sites respectively) from locations upstream and downstream respectively of *mmoX*.

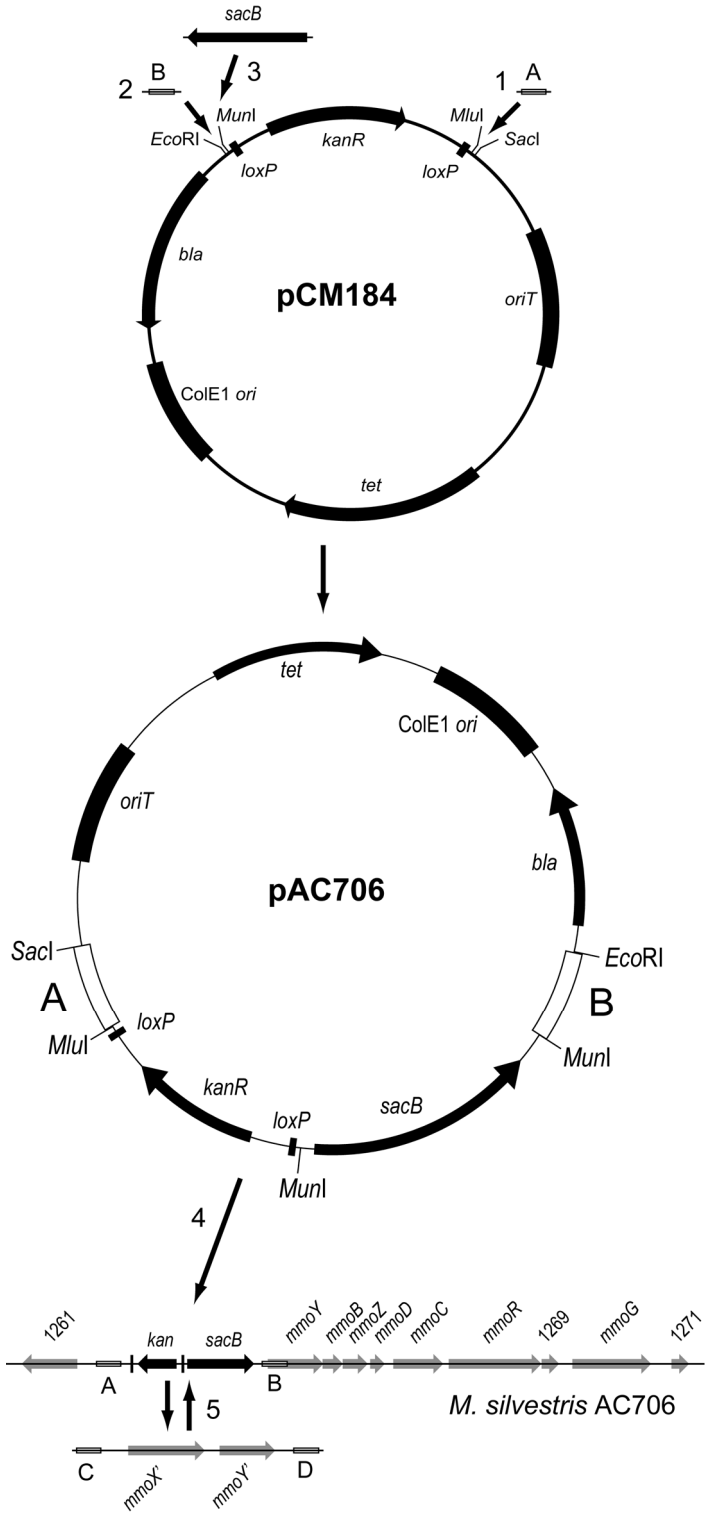

Figure 4.13. Construction of *M. silvestris* strain AC706. Sequences A and B, PCR-amplified from upstream and downstream of *mmoX,* were cloned (in reverse order) sequentially into pCM184 (as shown at 1 and 2). The *sacB* gene was then ligated into the *Mun*I site (3), resulting in pAC706. Following digestion with *Sac*I and *Eco*RI, the linear fragment containing the kanamycin cassette and *sacB* was used to electroporate *M. silvestris* BL2 (4), resulting in strain AC706. It should now be possible to replace this construct by electroporation with a gene or genes of interest, shown here as modified versions *mmoX'* and *mmoY',* by electroporation with the linear fragment containing regions of homology C and D (5), followed by counter-selection on plates containing sucrose.

These fragments were cloned into pGEM-T Easy (Promega), released by digestion with the respective enzymes, and cloned sequentially into pCM184, resulting in pAC704. The *sacB* gene was PCR-amplified from pK18*mobsacB* using primers SacBf2/SacBr2 (both incorporating *Mun*I sites), cloned into pGEM-T Easy, and released by digestion with *Mun*I. This fragment was then ligated into pAC704 digested with the same enzyme, resulting in pAC706. All sequences were checked by sequencing and the orientation of the fragments was verified by restriction digest and PCR. Vector pAC706 was digested with *Sac*I and *Eco*RI, purified from an agarose gel, and the 4652 bp linear fragment containing Kan^R and *sacB* was used to electroporate electrocompetent *M. silvestris* BL2 cells which were spread on DNMS plates with kanamycin. After several weeks, colonies appeared which were transferred to liquid DNMS/succinate medium containing kanamycin. After several transfers, cells were diluted $1/10^5$ and 100 µl spread on DNMS/succinate selective plates. A single colony was transferred to liquid culture without selection. DNA from this culture was amplified by PCR using primers Kanf/Kanr, SacBf2/SacBr2 and 1262Tf/1262Tr. It was possible to amplify sequences from both the kanamycin cassette and *sacB*, and sequence data verified the insertion of these elements at the expected position in the *M. silvestris* chromosome. Competent cells were prepared from a 200 ml culture and stored at -80 °C. Unfortunately, due to constraints of time, it was not possible to complete this experiment and demonstrate the replacement of the inserted elements. This would require electroporation of a linear fragment containing a gene of interest, (perhaps an *mmoX* gene from a different methanotrophs), flanked by regions homologous to the *M. silvestris* chromosome, followed by counter-selection on plates containing sucrose. It should be possible, of course, to replace DNA, of length only restrained by the decrease in the efficiencies of recombination and electroporation with longer fragments.

4.8 Conclusions and future perspectives

The method developed in this chapter uses the Cre-*loxP* system, the components of which are derived from phage P1, for removal of the antibiotic cassette. However, bacteria naturally have an analogous system which allows segregation of chromosomes during cell division (Rappsilber et al., 2002), raising the possibility of removal of the antibiotic cassette without expression of a recombinase *in trans*, by

using the cells own recombination machinery. This has been demonstrated in *E. coli* and *Bacillus subtilis* (Bloor and Cranenburgh, 2006) and, in *E. coli,* relies on the XerC and XerD recombinases which mediate recombination between 28 bp *dif* sites naturally present in the chromosome. Engineering these sites either side of an antibiotic cassette during marker exchange mutagenesis allows removal of the marker when selective pressure is removed, in a similar way to the Cre-*loxP* system, but without the necessity for expression of an exogenous recombinase. A survey of the *dif*/Xer recombinase system in the proteobacteria (Carnoy and Roten, 2009) identified a *dif* consensus sequence, which was used as query in a search of the *M. silvestris* genome. A region of the chromosome located in a non-coding region with close similarity to the consensus sequence was identified, see Figure 4.14. Homologues of *xerC* and *xerD* were identified (Msil1177 and Msil1847, with 36% and 43% identity at the amino acid level, to XerC and XerD from *E. coli* K-12). This suggests that incorporation of *dif* sites instead of *loxP* sites might enable automatic removal of an antibiotic cassette, thus simplifying the gene deletion procedure by avoiding the necessity for expression of Cre *in trans.*

Figure 4.14. The sequence at position 598970 of the *M. silvestris* chromosome compared with the consensus *dif* sequence of Carnoy and Roten (2009), who identified as most conserved the nucleotides shown in upper case. Binding sites for XerC and XerD are shown in boxes.

The work described in this chapter has established a system for gene deletion in *M. silvestris*, which, although not rapid, is reliable and straightforward. This has demonstrated the genetic amenability of *M. silvestris* and was an essential tool for unravelling the metabolic pathways of this unique organism. The methods described here were used in the following chapters and make possible the engineering of strains with innovative bioengineering potential.

Table 4.3. Primers used in the work described in this chapter. Restriction sites are shown underlined.

Name	Description	Sequence 5' – 3'	Enzyme
Deletion of Msil1325 malate synthase *(ms)* (pK18*mobsacB* strategy)			
(Unsuccessful)			
MSf	Upstream primer	TCAAGGCGGACCAGTTCTGGAC	
MSr	Downstream primer	AAGCTTTCCTCGCGGCCCTTGAAGATG	*Hin*dIII
MSABf	Detection of crossover	AGCCACAAGGACGTCATCAG	
MSABr	Detection of crossover	GCGGGATCGTCAGAATATCG	
Deletion of Msil3157 isocitrate lyase *(icl)*			
Strain ΔICL			
3157Af	Upstream region	TCACTGTGCGGCGACTATG	
3157Ar	Upstream region	TATCGGTACCCGTTGAGGACCGCCTCAAG	*Kpn*I
3157Bf	Downstream region	TATCACGCGTTGCGTCTGCCTTGTTCAGTC	*Mlu*I
3157Br	Downstream region	TATCGAGCTCCCAGCGCCAGCTGTTCTTC	*Sac*I
3157Tf	Detection of gene deletion/substitution	AAGTCTCGGCTTCATGCTAGCG	
3157Tr	Detection of gene deletion/substitution	CGTCGATCTCGTCCGACATTTC	
Deletion of Msil1641 (gluconate dehydrogenase)			
Strain Δ1641			
1641Af	Upstream region	ATCAGAGCTCAAAGCACGGCCGCTATCG	*Sac*I
1641Ar	Upstream region	ATCAACGCGTGCGCTTTCGCCCTGATAACC	*Mlu*I
1641Bf	Downstream region	ATCAGGTACCCGTCATTGGGCAACGATAAG	*Kpn*I
1641Br	Downstream region	GAAACCGCCAATGCATCTC	
1641Tf	Detection of gene substitution/deletion	GCCGATTGGAGCTAAACTTC	
1641Tr	Detection of gene substitution/deletion	GGCGAGATTCTTCTTCGTTC	
Deletion of Msil1651 propane monooxygenase *(prmA)*			
Strain ΔPrMO			
1651Af	Upstream region	GATCGAGCTCTAGTCGGCTACGGCTATTATGG	*Sac*I
1651Ar	Upstream region	GAGAACGCGTGGCGCCTAACGAACTTTCTTTG	*Mlu*I
1651Bf	Downstream region	GATCGGTACCTCATGGGAGGCGATGGATTG	*Kpn*I
1651Br	Downstream region	GTCCGCTGACGGTGACTTTG	
1651Tf	Detection of gene substitution/deletion	AAGGCCGCGTCCGATACAAG	
1651Tr	Detection of gene substitution/deletion	CAGAACAAATCGGCCTGGGTCC	
Deletion of Msil1714 serine-glyxoxylate aminotransferase *(sga)*			
Strain ΔSGAT			
1714Af	Upstream region	ATCAAGATCTGCAGCGGAACCTTGTTGG	*Bgl*II
1714Ar	Upstream region	ATCAGGTACCGCGACCTCAACGAACTGATG	*Kpn*I
1714Bf	Downstream region	ATCAACGCGTCGGCCCGGCATTATGTATCC	*Mlu*I
1714Br	Downstream region	ATCAGAGCTCATCTCGGGCGGCGAAACCAC	*Sac*I
1714Tf	Detection of gene substitution/deletion	GACACGGTAACGCCATGAGC	
1714Tr	Detection of gene substitution/deletion	CTCGCCAATGACATCGAGGG	

Table 4.3 (continued).

Name	Description	Sequence 5' – 3'	Enzyme
Deletion of Msil1325 malate synthase *(ms)*			
Strain ΔMS			
1325Af	Upstream region	ATCAGTTAACGCCGTGTCGACGCTTATC	*Hpa*I
1325Ar	Upstream region	ATCAGAGCTCCAACCCAGACGCCAAATG	*Sac*I
1325Bf	Downstream region	ATCAAGATCTGCCAAGCTGGCGTTACCC	*Bgl*II
1325Br	Downstream region	ATCAGGTACCCGAACGGCTACACGGAAGG	*Kpn*I
1325Tf	Detection of gene substitution/deletion	TCAGGAGCTGGAGCGTATTC	
1325Tr	Detection of gene substitution/deletion	CGCAACCCAGACGCCAAATG	
Deletion of Msil1262 methane monooxygenase *(mmoX)*			
Strain ΔMmoX			
1262Af	Upstream region	GATCGAGCTCCGACACGGAAACAACCTATC	*Sac*I
1262Ar	Upstream region	GATCACGCGTTTCGTCGCGGTGCTTAATGC	*Mlu*I
1262Bf	Downstream region	GATCCAATTGTCGCCGATCCGCTCGCAG	*Mun*I
1262Br	Downstream region	GATCGAATTCCGATCGAGCGCACAGCTCC	*Eco*RI
1262Tf	Detection of gene substitution/deletion	CCCAGTTCCATTCGTAAGAC	
1262Tr	Detection of gene substitution/deletion	GTATTCGCTGAACAGCAAGG	
Kanf	Kanamycin cassette forward	GCGATAATGTCGGGCAATCAG	
Kanr	Kanamycin cassette reverse	AAACTCACCGAGGCAGTTCC	
SacBf2	Amplification of *sacB*	GATCCAATTGCAGCGCATCGCCTTCTATCG	*Mun*I
SacBr2	Amplification of *sacB*	GATCCAATTGATGAGCCTGTCGGCCTACC	*Mun*I

Chapter 5

The glyoxylate cycle and the role of isocitrate lyase in the serine cycle

5.1 Introduction

5.1.1 The glyoxylate cycle and the ethylmalonyl-CoA (EMC) pathway

Organisms able to grow on acetate, or on substrates such as fatty acids which are metabolised through acetyl CoA, face a particular problem in generating multi-carbon biosynthetic precursors, and avoiding the decarboxylation steps of the TCA cycle. In most life forms, with the exception of mammals, this is accomplished by the glyoxylate cycle, shown in Figure 5.1a. In this pathway, enzymes isocitrate lyase (ICL) and malate synthase (MS) provide a route that bypasses the oxidative steps of the TCA cycle, catalysed by isocitrate dehydrogenase and α-ketoglutarate dehydrogenase (Kornberg, 1966).

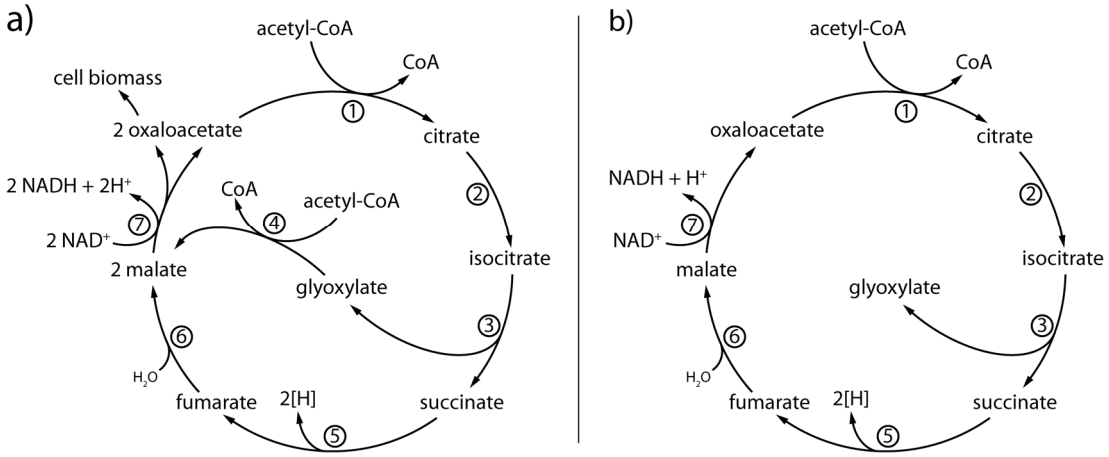

Figure 5.1. a) The glyoxylate cycle showing the production of one four-carbon molecule (oxaloacetate) from two molecules of acetyl-CoA (modified from Erb et al., 2007). Enzymes, 1: citrate synthase, 2: aconitase, 3: isocitrate lyase, 4: malate synthase, 5: succinate dehydrogenase, 6: fumarase, 7: malate dehydrogenase. b) In the isocitrate lyase pathway, the same enzymes, without malate synthase, function to convert acetyl-CoA into glyoxylate during the serine cycle.

However, it has become apparent that this pathway does not operate in all aerobic bacteria able to grow on two-carbon compounds, including many methylotrophs (Anthony, 1982), or for example *Rhodospirillium rubrum* or *Rhodobacter sphaeroides* (Kornberg and Lascelles, 1960). Recent research has uncovered two alternative pathways for the prokaryotic assimilation of acetyl-CoA, the ethylmalonyl-CoA (EMC) pathway shown or expected to operate in *Methylobacterium extorquens, Rhodobacter sphaeroides* and streptomycetes (Erb et

al., 2009; Okubo et al., 2010) and the methylaspartate cycle of Haloarchaea (Khomyakova et al., 2011). Both these pathways incorporate a (different) series of reactions which convert acetyl-CoA into glyoxylate, which is the reaction accomplished (together with enzymes of the TCA cycle) by ICL. The EMC pathway is illustrated in Figure 5.2. The product, glyoxylate, then combines with another molecule of acetyl-CoA to give malate, which can be assimilated into biomass following well established biosynthetic reactions. The EMC pathway uses enzymes from previously characterised pathways, including polyhydroxybutyrate metabolism, the 3-hydroxypropionate cycle and propionate assimilation, but includes three enzymes, crotonyl-CoA carboxylase/reductase, (2*R*)-ethylmalonyl-CoA mutase and (2*S*)-methylsuccinyl-CoA dehydrogenase, which are unique to this pathway.

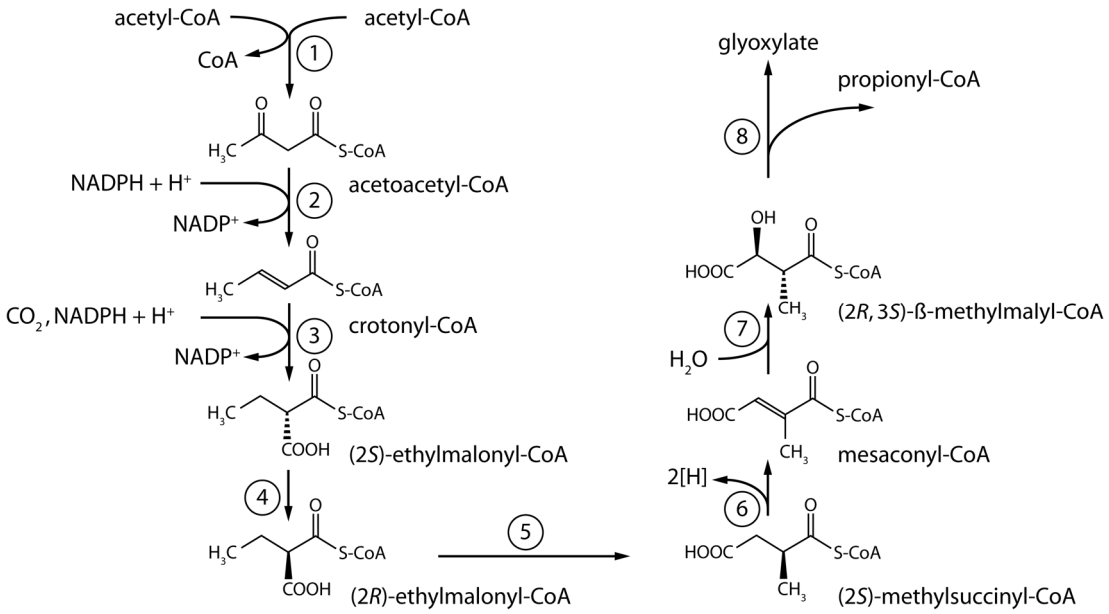

Figure 5.2. The ethylmalonyl-CoA pathway, showing the conversion of two molecules of acetyl-CoA and one CO_2 into glyoxylate and propionyl-CoA (modified from Erb et al., 2009). Enzymes, 1: β-ketothiolase, 2: acetoacetyl-CoA reductase, 3: crotonyl-CoA carboxylase/reductase, 4: ethylmalonyl-CoA/methylmalonyl-CoA epimerase, 5: ethylmalonyl-CoA mutase, 6: methylsuccinyl-CoA dehydrogenase, 7: mesaconyl-CoA hydratase, 8: β-methylmalyl-CoA/malyl-CoA lyase.

5.1.2 The serine cycle

The serine cycle, which *Methylocella silvestris,* in common with other type II methanotrophs, uses to assimilate carbon, is shown in Figure 5.3. However, an intermediate of the serine cycle is acetyl-CoA, which is subsequently converted to glyoxylate. Thus a series of reactions, which may be catalysed by ICL and enzymes of the TCA cycle (Figure 5.1b, which is described as the isocitrate lyase pathway in this work), also occurs in the serine cycle (Figure 5.1b), but many methylotrophs growing methylotrophically do not contain ICL, and instead use the enzymes of the ethylmalonyl-CoA pathway to accomplish this conversion or "glyoxylate regeneration", as has been demonstrated recently for *Methylobacterium extorquens* during growth on methanol (Peyraud et al., 2009).

5.1.3 The distribution of the EMC pathway

As noted above, most methylotrophs do not contain isocitrate lyase, and the mechanism by which glyoxylate is formed from acetyl-CoA has been the subject of intensive research for more than 30 years (Dunstan et al., 1972a; Korotkova et al., 2002). In a survey of 1215 fully sequenced bacterial genomes Erb et al. (2009) screened for the presence of isocitrate lyase, and for the genes specific to the EMC pathway. Isocitrate lyase homologues were found in 28% of species from 34% of genera, whereas EMC gene homologues were present in 5% of species from 8% of genera, suggesting that this pathway has considerable environmental relevance. Interestingly, nine organisms (nearly 1%) appeared to harbour both capabilities, raising the possibility that the relevant enzymes may be expressed under different conditions. For example, *Paracoccus versutus* expressed ICL during anaerobic denitrifying growth, but this enzyme activity was not detectable during aerobic growth on acetate (Claassen and Zehnder, 1986).

It was notable that Dunfield and co-workers (2003) detected neither isocitrate lyase nor malate synthase activity in cell extracts of *M. silvestris*. It was therefore important to establish the pathways of two-carbon assimilation and the mode of operation of the serine cycle in the first facultative methanotroph isolated in laboratory culture.

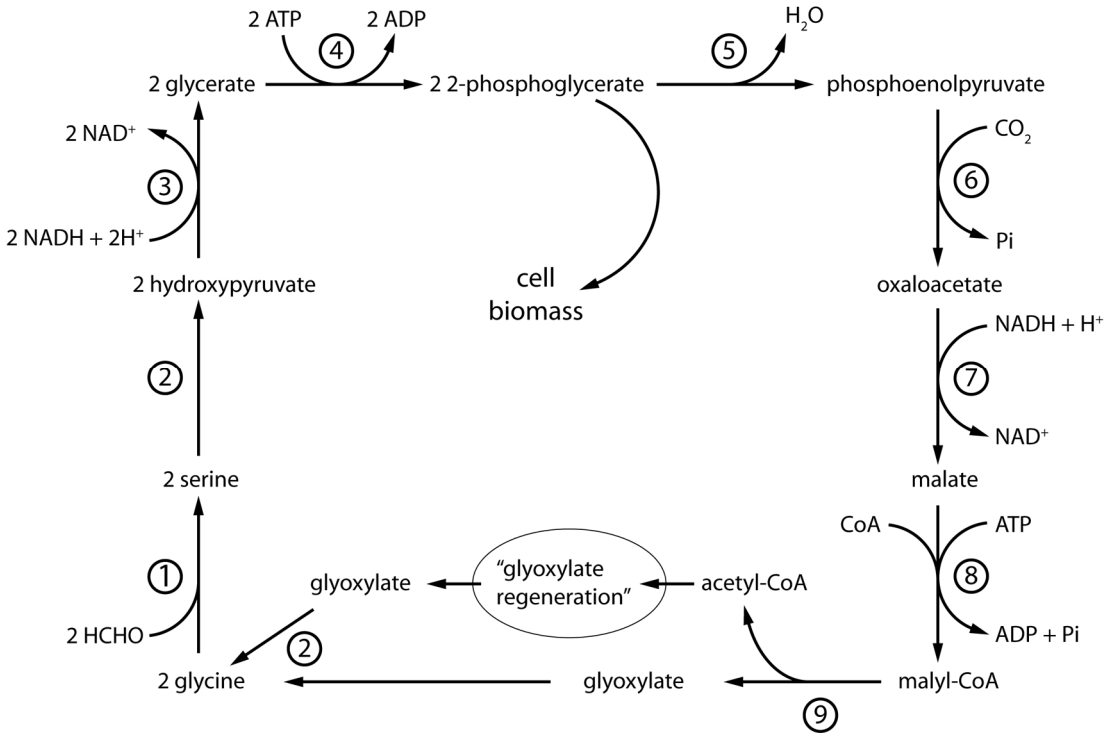

Figure 5.3. The serine cycle. During the cycle acetyl-CoA molecules need to be oxidised to glyoxylate by a series of reactions shown as "glyoxylate regeneration". This is performed either by isocitrate lyase and enzymes of the TCA cycle (Figure 5.1b), or by the EMC pathway (Figure 5.2). The figure shows the isocitrate lyase positive version, and the carbon balance is slightly different in the two variations. Enzymes, 1: serine transhydroxymethylase, 2: serine-glyoxylate aminotransferase, 3: hydroxypyruvate reductase, 4: glycerate kinase, 5: enolase, 6: phosphoenolpyruvate carboxylase, 7: malate dehydrogenase, 8: malate thiokinase, 9: malyl-CoA lyase. Modified from Anthony (1982).

5.2 *M. silvestris* homologues to genes of the EMC pathway

In order to investigate the genetic potential for the operation of the EMC pathway in *M. silvestris,* genes encoding enzymes of the EMC pathway (Figure 5.2) from *Rhodobacter sphaeroides,* which have been biochemically characterised, were used as query sequences in a search of the *M. silvestris* genome, in order to locate possible homologues. In contrast to genes also involved in other pathways (polyhydroxybutyrate metabolism, propionate metabolism), the genes encoding enzymes specific to the EMC pathway (*ccr, ecm, mcd*) had no close homologues, nor were the low-similarity candidates clustered together. In particular, the same gene was identified in the *M. silvestris* genome in response to searches for homologues to both *ecm* and *mcm,* encoding ethylmalonyl-CoA mutase and methylmalonyl-CoA mutase respectively. However, the gene identified (Msil3784) has a much higher

similarity to *mcm*, suggesting that methylmalonyl-CoA may be its true substrate. The alternative, that this enzyme converts both the methyl- and ethyl-substituted compounds, would be contrary to the specificity reported for ethylmalonyl-CoA mutase (Erb et al., 2008) (although the respective compounds use the same epimerase in *Rhodobacter sphaeroides* and *Methylobacterium extorquens*). It is therefore doubtful that *M. silvestris* contains the genes necessary for the operation of this pathway.

Table 5.1. *M. silvestris* genome BLAST hits to ECM pathway genes from *Rhodobacter sphaeroides.* The ECM pathway genes (column 1) corresponding to the enzymes identified by numbers in Figure 5.2 (column 2) were used as query sequences at the amino acid level. *pccA, pccB and mcmA,* which encode propionyl-CoA carboxylase and methylmalonyl-CoA mutase (α-subunit), predicted to be also involved in propionate metabolism, and which recycle propionyl-CoA to glyoxylate and acetyl-CoA, are not shown in the figure.

ECM p/w gene	Fig. ref.	*M. silvestris* locus tag	% identity	E value
phaA	1	Msil_2996	73	7e-170
phaB	2	Msil_2997	75	5e-104
ccr	3	Msil_3002	28	2e-17
epi	4	Msil_2934	76	3e-54
ecm	5	Msil_3784	39	2e-106
mcd	6	Msil_1741	27	2e-20
mch	7	Msil_3435	37	2e-18
mcl-1	8	Msil_1719	57	2e-99
pccA	-	Msil_3786	60	0.0
pccB	-	Msil_3787	72	0.0
mcmA	-	Msil_3784	65	0.0

5.3 Arrangement and annotation of genes encoding glyoxylate bypass enzymes – draft genome

The draft *M. silvestris* genome (available prior to 20 June 2008) identified two open reading frames with homology to isocitrate lyase genes, or3298 and or3299 located on contig 17. (The "or-" gene-identification prefixes have since become "Msil-", and in addition all gene numbers have been changed.) A putative malate synthase gene (or3005) was identified on contig 28. Examination of the *M. silvestris* isocitrate lyase homologues showed similarity to different regions of other isocitrate lyase genes. For example, the translation of or3298 (311 amino acids) shares 79% identity with residues 1 – 300 of isocitrate lyase from *Pseudomonas aeruginosa* PA1 (532 amino

acids) (Díaz-Pérez et al., 2007) and or3299 (197 amino acids) shares 84% identity with residues 335 – 531. Therefore it seemed likely that either this was a pseudogene with no physiological function, or that a sequencing error had resulted in mis-annotation.

5.3.1 RT-PCR

RNA was extracted from cells grown on methanol using the hot acid-phenol method as described in Materials and Methods. cDNA was synthesised from 100 ng RNA using Superscript II reverse transcriptase (Invitrogen) and random hexamer primers in 100 µl reactions alongside identical reactions except without the addition of reverse transcriptase, and 2 µl used as template in PCR reactions using primers located in or3298, or3299 and or3005, and also with a forward primer located in or3298 and reverse primer in or3299, see Figure 5.4. This demonstrated transcription in all cases, and showed that the two isocitrate lyase open reading frames are transcribed as a single molecule, suggesting that a sequencing error may have resulted in misannotation of this region.

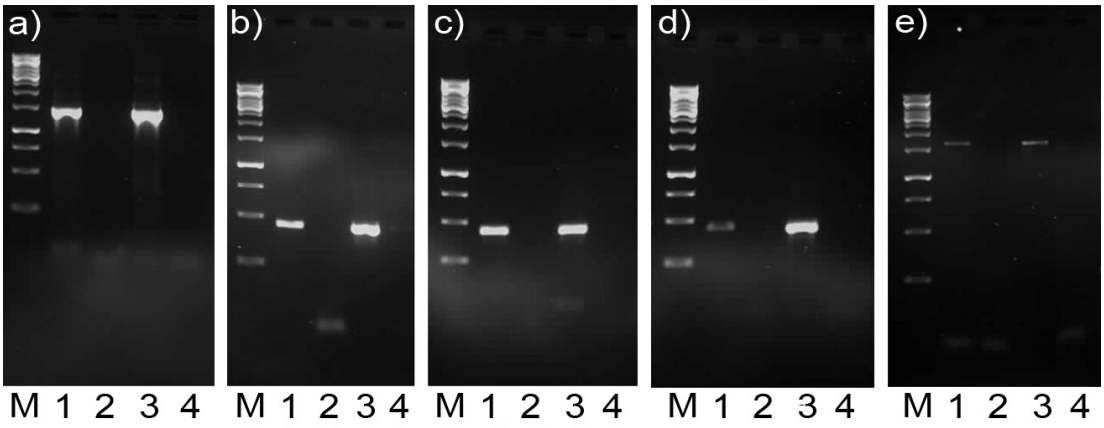

Figure 5.4. RT-PCR was used to identify transcription of a) 16S rRNA gene (1.5 kbp fragment), b) isocitrate lyase or3298 (440 bp) and c) or3299 (391 bp), d) malate synthase or3005 (~ 420 bp) and e) both isocitrate lyase genes as one mRNA molecule (1660 bp). Lanes, 1: cDNA template, 2: reverse transcriptase negative, 3: DNA template, 4: NTC, M: GeneRuler 1kb ladder (Fermentas).

5.4 Arrangement of glyoxylate bypass genes – finished genome

The finished genome (released 20 June 2008, GenBank accession number CP001280 (Chen et al., 2010)) confirmed the existence of a single open reading frame with homology to characterised isocitrate lyase genes from other organisms. Malate synthase is located in a different location on the chromosome, see Figure 5.5. The SWISS-PROT/TrEMBL database was interrogated with translated sequences of these genes and results are shown in Table 5.2. These data do not reveal any nearby genes whose products are expected to be directly involved in the same metabolic pathways as malate synthase or isocitrate lyase.

The 500 bp sequences upstream of the predicted start codons of malate synthase and isocitrate lyase were scanned for promoter sequences using the Berkeley Drosophila Genome Project Neural Network Promoter Prediction online tool (http://www.fruitfly.org/seq_tools/promoter.html). This identified possible promoter sequences with transcription start sites 103 bp and 91 bp upstream of the predicted start codons respectively (scores 0.94 and 0.91). A promoter was also predicted downstream of malate synthase, 53 bp upstream of Msil1324 (score 0.53). These data, together with the relative orientation of the surrounding genes, are consistent with transcription of malate synthase and isocitrate lyase as monocistronic units.

Figure 5.5. Gene layout of malate synthase Msil1325 (upper) and isocitrate lyase Msil3157 (lower). For gene identities refer to Table 5.2. Genes Msil1326 / Msil1327 and Msil3153 / 3154 are predicted to overlap by 4 (phase 2 overlap) and 11 (phase 1 overlap) nucleotides respectively. The intergene space 3155 – 3157 contains a pseudogene, consisting of frame-shifted fragments of a putative transport protein sequence (304/419 amino acid identity to YP_001523349.1 from *Azorhizobium caulinodans* ORS 571).

5.4.1 Phylogenetic relationships of *M. silvestris* glyoxylate bypass genes

The translated sequence of the *M. silvestris* putative isocitrate lyase gene was aligned against isocitrate lyase sequences from other organisms, including those for which structural and biochemical data exist such as *E. coli* (Britton et al., 2001), *Mycobacterium tuberculosis* (Sharma et al., 2000), *Corynebacterium glutamicum* (Reinscheid et al., 1994b), *Hyphomicrobium methylovorum* (Tanaka et al., 1997), *Pseudomonas aeruginosa* (Kretzschmar et al., 2008), *Cupriavidus necator* (Wang et al., 2003) and *Colwellia maris* (Watanabe and Takada, 2004), as well as plants and fungi. The alignment was used to construct the phylogenetic tree shown in Figure 5.6. The *M. silvestris* sequence grouped separately from the sequences of many well characterised bacterial enzymes, adding to Subfamily 3 as defined by Watanabe and Takada (2004), which contains the sequences of *H. methylovorum, P. aeruginosa, Cupriavidus necator* and *Colwellia maris*, although the functional significance of this is unclear.

The translated sequence of the putative malate synthase had no extremely high-similarity sequences in the databases. A search of the non-redundant protein sequences (nr) database identified the sequence from *Methylobacterium nodulans* (64% identity) as the closest match. All high-similarity hits were to the MSG isoform and compared to well characterised enzymes the *M. silvestris* sequence displayed 60%, 58% and 57% identity to MSG from *Mycobacterium tuberculosis, Corynebacterium glutamicum* and *E. coli* respectively.

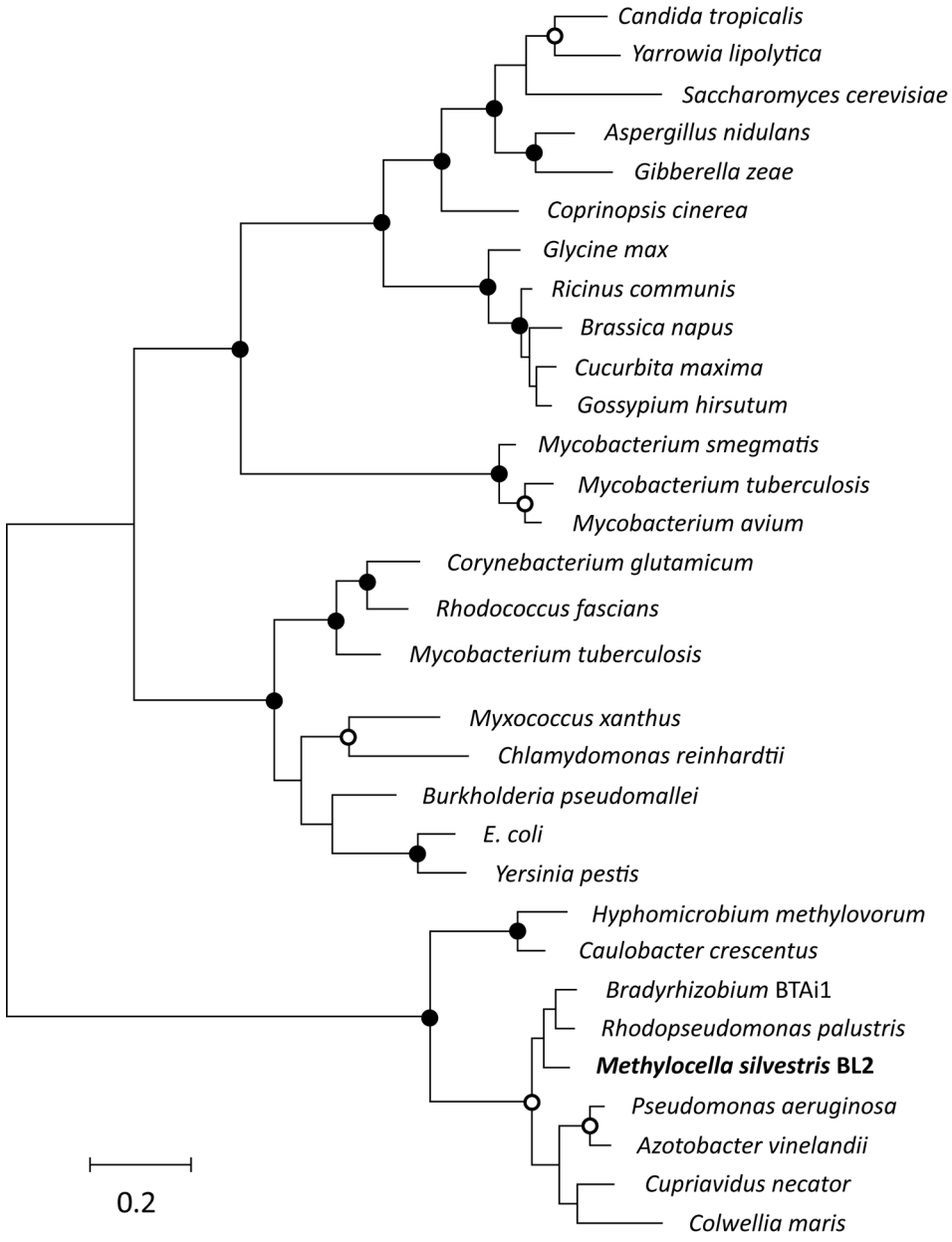

Figure 5.6. Unrooted phylogenetic tree showing the relationship of the putative *M. silvestris* isocitrate lyase with homologous enzymes from other organisms. The tree, constructed using the Maximum Likelihood method, is based on amino acid sequences aligned using Clustal. Positions containing gaps or missing data were eliminated, and the tree constructed with a final data set of 380 amino acids using Mega5 (Tamura et al., 2007). Bootstrap values (based on 500 replications) greater than 95% are shown as filled circles at nodes, and those between 75 – 95% as open circles. Accession numbers: *Yarrowia lipolytica*, P41555.3; *Candida tropicalis*, P20014.1; *Saccharomyces cerevisiae* ACEA, NP_010987.1; *Aspergillus nidulans*, XP 663238.1; *Gibberella zeae*, XP 390072.1; *Coprinopsis cinerea*, O13439.1; *Glycine max* ACEA1, P45456.1; *Ricinus communis*, P15479.1; *Brassica napus*, P25248.1; *Cucurbita maxima*, P93110.1; *Gossypium hirsutum*, P17069.1; *Mycobacterium smegmatis*, YP 888007.1; *Mycobacterium tuberculosis*, P46831.2; *Mycobacterium avium*, NP 960577.1; *Corynebacterium glutamicum*, P42449.2; *Rhodococcus fascians*, P41554.1; *Mycobacterium tuberculosis*, CAE55284.1; *Myxococcus xanthus*, AAB97828.1; *Chlamydomonas reinhardtii*, Q39577; *Burkholderia pseudomallei*, pdb|3I4E; *E. coli*, P0A9G6.1; *Yersinia pestis,* NP 667361.1; *Hyphomicrobium methylovorum*, BAA23678.1; *Caulobacter crescentus*, NP 420572.1; *Bradyrhizobium* BTAi1, YP 001240153.1; *Rhodopseudomonas palustris*, YP 780327.1; *Methylocella silvestris*, YP_002363427.1; *Pseudomonas aeruginosa*, NP 251324.1; *Azotobacter vinelandii*, YP 002799989.1; *Cupriavidus necator*, AF499030.1; *Colwellia maris*, BAB62107.1.

Table 5.2. Top BLAST hits to SWISS-PROT/TrEMBL database and protein annotation of translated sequences of open reading frames surrounding malate synthase (Msil1325) and isocitrate lyase (Msil 3157).

ORF	Annotation	Organism	aa	% id
1320	Uncharacterised protein	*Methylobacterium extorquens* DM4	173	47
1321	Uncharacterised protein	*Rhodopseudomonas palustris* BisB5	361	30
1322	Uncharacterised protein	*Rhodopseudomonas palustris* BisB5	382	34
1323	K^+ transporter	*Caulobacter crescentus*	346	50
1324	Uncharacterised protein	*Beijerinckia indica*	123	75
1325	Malate synthase G	*Methylobacterium nodulans*	721	64
1326	Fmu (Sun) domain protein	*Beijerinckia indica*	439	65
1327	Uncharacterised protein	*Nitrobacter hamburgensis*	129	47
1328	Inosine 5' monophosphate DH	*Beijerinckia indica*	496	83
1329	Drug resistance transporter	*Beijerinckia indica*	472	63
3150	Ton B receptor	*Beijerinckia indica*	807	50
3151	Histidine kinase sensor	*Aurantimonas* SI85-9A1	453	34
3152	Uncharacterised protein	-	94	-
3153	Uncharacterised protein	-	105	-
3154	Uncharacterised protein	-	64	-
3155	Trans. reg., MarR family	*Agrobacterium tumefaciens*	132	56
3157	Isocitrate lyase	*Beijerinckia indica*	542	87
3158	Trans. reg., XRE fam	*Sphingomonas* sp. SKA58	472	72
3159	5-carboxymethyl-2-hydroxymuconate delta-isomerase	*Methylibium petroleiphilum*	255	60
3160	DNA polymerase IV	*Aurantimonas* SI85-9A1	359	73

5.5 5' RACE

Rapid amplification of cDNA ends (RACE) was used in an attempt to empirically determine the isocitrate lyase transcription start site, using a 2nd Generation 5'/3' RACE kit (ROCHE, Basel, Switzerland), as described in Materials and Methods. RNA was extracted from cells grown on acetate, and cDNA synthesised using antisense primer IclRa1 located at +346 relative to the start codon (see Table 5.13 for primer sequences). Using a cDNA template, a single-sized PCR amplicon was generated using PCR primer IclRa2 (position +310), see Figure 5.7.

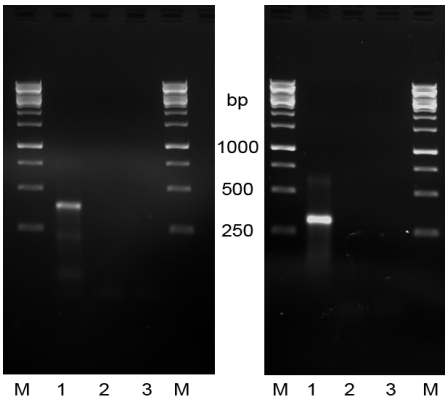

Figure 5.7. First-round (left) and nested second round (right) PCR amplification of cDNA synthesised from RACE primer IclRa1. Lane 1: cDNA template, lane 2: control reaction without reverse transcriptase, lane 3: no template control (NTC). M: GeneRuler 1 kb ladder (Fermentas).

A second round of PCR using nested primer IclRa3 (position +239) was employed to increase specificity. The 71 nt difference in the binding sites of primers IclRa2 and IclRa3 resulted in DNA bands on the gels differing in size by the corresponding amount. Sequencing of both the PCR product directly and the cloned PCR product indicated that the mRNA terminated 32 bp 5' of the start codon (position -32). PCR amplicons corresponding to the predicted transcription start (position -88) would be distinguishable on the gel from the visible band, indicating that few or no cDNA molecules were synthesised which extended to this point. However, the -10 and -35 sequences upstream of the experimentally determined transcription start site displayed relatively low levels of similarity to the *E. coli* consensus sequences.

```
----TTGACA-----------------TATAAT-------
      -35                   -10
---AATCTTTACATCATTACAATCATTTTTTGTAAAGTATGACATCTTTGCTTCGCTCC
   CTCTGCACAGAGAGGGATTTGCTGTGGTAGGGGTGCCTCACAAATGTCTTCGACTG
   AACAAGGCAGACGCAAATG---
```

Figure 5.8. Isocitrate lyase upstream sequence. The predicted promoter sequence is shown boxed, and the predicted and experimentally determined transcription start sites shown underlined. Possible -35 and -10 sequences upstream of the experimentally determined transcription start site are shown shaded. The start codon is shown in red. The consensus *E. coli* σ^{70} sequence (Harley and Reynolds, 1987) is shown above, in green, for comparison.

Interestingly, isocitrate lyase is flanked on either side by regulatory genes, transcribed in the opposite orientation, both of which have homologues in other

organisms known to be involved in response to environmental stimuli such as xenobiotic chemicals. Any involvement of these genes in the regulation of isocitrate lyase transcription was not investigated.

5.6 Operation of the glyoxylate bypass in *M. silvestris* during growth on 2-carbon compounds

5.6.1 Assay of isocitrate lyase and malate synthase

The activities of isocitrate lyase and malate sythase were assayed in soluble cell extract prepared from cells grown on acetate, methane, propane or succinate, as described in Materials and Methods, including killed controls consisting of extract form acetate-grown cells inactivated by boiling for 15 min. The pH optimum was determined as 7.0, and EDTA was compared with cysteine as an activator, as suggested by Kennedy and Dilworth (1963), as described in Materials and Methods. Data are presented in Table 5.3. Minimum activity required to account for the observed growth rate (μ) on acetate of the cells used for the assay (0.043 h^{-1}, Table 3.4), can be calculated considering only the assimilatory pathway, since acetate is oxidised to CO_2 without the involvement of isocitrate lyase. The specific rate of substrate (S) consumption dS/dt = (μ/A).B, where A represents the growth yield (approximately 24 g of biomass formed per mol of carbon assimilated), and B represents the biomass in g (1 g of protein corresponds to approximately 2 g of cell dry weight). Therefore, during growth on acetate, the carbon assimilation rate dS/dt = (0.043/24) *2 mol h^{-1} g^{-1} = 59.7 nmol min^{-1} mg^{-1}.

For every isocitrate molecule split by isocitrate lyase, one four carbon molecule is generated in the glyoxylate cycle. Therefore, the minimum activity of this enzyme is approximately 15 or 20 nmol min^{-1} mg^{-1} depending on whether carbon is assimilated as a four carbon molecule or decarboxylated to a three carbon molecule (Anthony, 1982). Since between approximately 15 – 30% of expressed proteins are membrane located (Schneider, 1999), activity in the soluble fraction as assayed should be correspondingly higher. Therefore the isocitrate lyase activity assayed is just sufficient to support growth on acetate.

Malate synthase activity was high in all growth conditions, and is comparable with reported activities in other organisms able to assimilate acetate using the glyoxylate

bypass, for example *E. coli* (500 nmol min^{-1} mg^{-1}) (Kornberg, 1966) or *Haloferax volcanii* (230 nmol min^{-1} mg^{-1}) (Khomyakova et al., 2011).

Table 5.3. Activity of isocitrate lyase and malate synthase in soluble extract of *M. silvestris*. Enzyme specific activity (nmol min^{-1} (mg protein)$^{-1}$) is given ± standard deviation of at least three replicates. N/A, not assayed. Strain ΔICL is described in Section 5.6.2.

Strain, growth substrate	Isocitrate lyase	Malate synthase
Wild type, acetate	23.2 ± 3.3	424 ± 59
Wild type, methane	0.52 ± 0.02	277 ± 40
Wild type, propane	0.3 ± 0.03	367 ± 20
Wild type, succinate	2.2 ± 0.39	243 ± 78
Strain ΔICL, succinate	0.40 ± 0.40	N/A

5.6.2 Deletion of isocitrate lyase

In order to establish definitively the role of isocitrate lyase, *M. silvestris* strain ΔICL was constructed as described in Chapter 3, involving the deletion of the entire coding sequence and 65 bp downstream, and replacement with approximately 100 bp containing a single *loxP* site. Due to the removal of the antibiotic marker and the genomic context (Figure 5.5) this was unlikely to have a polar effect on transcription of nearby genes. Assay of ICL in succinate-grown cells of strain ΔICL did not detect activity above background (Table 5.3). Growth of *M. silvestris* strain ΔICL was evaluated in 20 or 25 ml cultures in 120 ml serum vials in triplicate, and growth on acetate, ethanol, pyruvate and succinate is compared with growth of the wild-type in Figure 5.9. Growth data are summarised in Table 5.4, and Figure 5.10 shows specific growth rate and biomass increase of the mutant strain as a percentage of wild type growth on the same substrate.

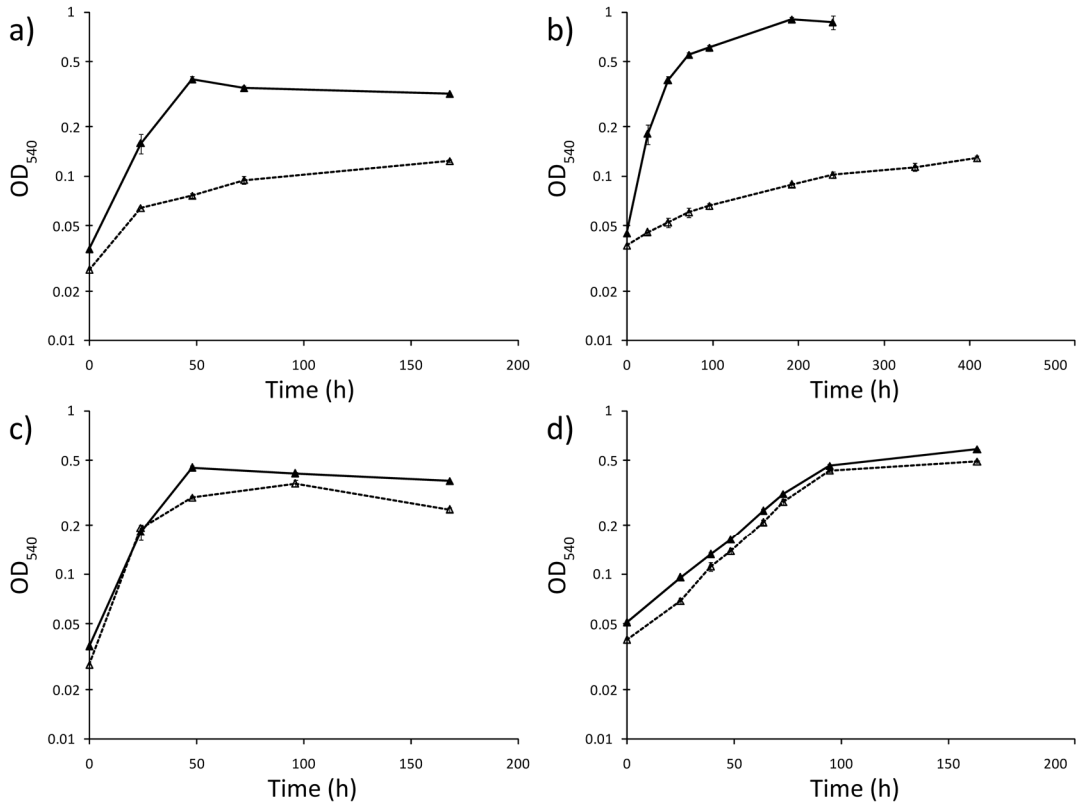

Figure 5.9. *M. silvestris* wild-type (solid lines) and strain ΔICL (dashed lines) growth on a) acetate, b) ethanol, c) pyruvate and d) succinate. Data points show the mean of at least three replicates and error bars indicate the standard deviation.

Strain ΔICL was able to grow on succinate and pyruvate similarly to the wild type, but growth on acetate and ethanol were severely restricted. These data suggest that isocitrate lyase is active during growth on two-carbon compounds during the operation of the glyoxylate cycle. (It is also worth noting here that the ability of strain ΔICL to grow on pyruvate implies a difference from the situation in *Methylobacterium extorquens* AM1, which has been shown to assimilate pyruvate via decarboxylation to acetyl-CoA (Bolbot and Anthony, 1980b).)

Table 5.4. Growth of *M. silvestris* BL2 wild type and strain ΔICL on one-, two-, three- and four-carbon compounds. Figures are the mean of at least three replicates ± standard deviation. Substrate concentrations: 5 mM, except methane: 20% (v/v), ethanol and methanol: 0.1% (v/v). Growth on one-carbon compounds is discussed in Section 5.7.

Growth substrate	Specific growth rate (h^{-1})		Lag time (h)		Increase in biomass (OD)	
	BL2	ΔICL	BL2	ΔICL	BL2	ΔICL
Methane	0.016 ± 0.002	0.001 ± 0.001	76 ± 27	-	0.48 ± 0.05	0.02 ± 0.02
Methanol	0.049 ± 0.003	0.003 ± 0.001	0 ± 0	-	0.58 ± 0.03	0.03 ± 0.01
MMA	0.037 ± 0.006	0 ± 0	51 ± 5	-	0.35 ± 0.01	0.00 ± 0.00
Ethanol	0.045 ± 0.001	0.007 ± 0.001	0 ± 1	0 ± 1	0.86 ± 0.03	0.09 ± 0.01
Acetate	0.050 ± 0.001[a]	0.022 ± 0.001[a]	0 ± 1	0 ± 0	0.35 ± 0.02	0.10 ± 0.00
Pyruvate	0.052 ± 0.001	0.049 ± 0.000	0 ± 1	0 ± 0	0.38 ± 0.01	0.33 ± 0.02
Succinate	0.025 ± 0.001	0.027 ± 0.001	0 ± 1	0 ± 2	0.48 ± 0.06	0.42 ± 0.04

[a] Growth of strain ΔICL occurred at a rate of 0.036 ± 0.0004 h^{-1} for the first 24 h. The tabulated figures refer to growth between 0 – 48 h

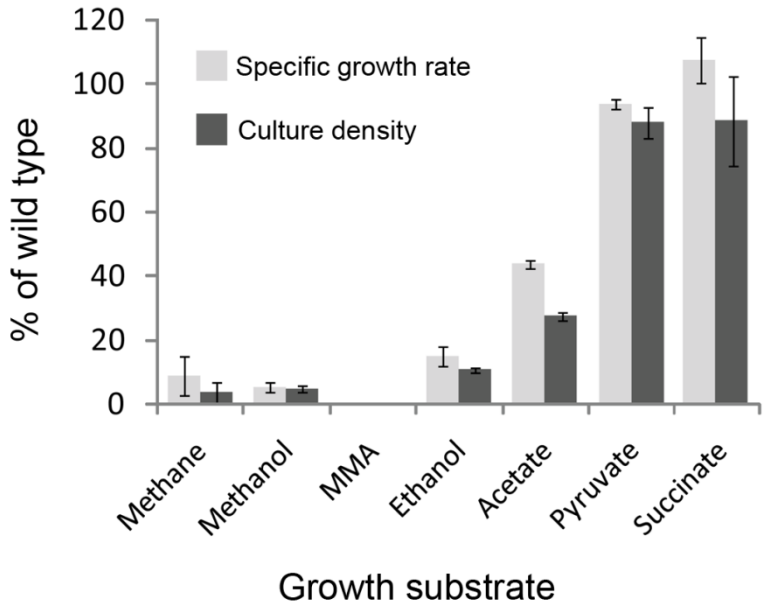

Figure 5.10. Specific growth rate and increase in biomass (as measured by OD_{540}) of strain ΔICL, expressed as a percentage of the wild-type growth rate and biomass increase under the same conditions. Calculated from data for at least three replicates, error bars indicate the standard deviation.

5.6.3 Deletion of malate synthase

Strain ΔMS was constructed with a deletion of Msil1325, encoding malate synthase. The same procedure was adopted as previously described, resulting in a marker-less deletion of 2056 bp, consisting of almost the entire coding sequence, from 40 bp

after the start codon to 69 bp before the stop codon, and its replacement with 105 bp containing a single *loxP* site.

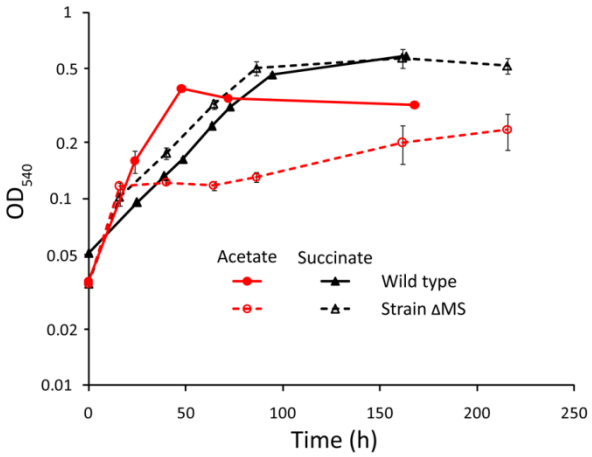

Figure 5.11. Growth of wild-type *M. silvestris* (solid lines) and strain ΔMS (dashed lines) on succinate (black) and acetate (red).

Strain ΔMS was able to grow on succinate similarly to the wild type, but growth on acetate was severely restricted, see Figure 5.11 and Table 5.5. Strain ΔMS was able to grow on formate (25 mM, duplicate vials, data not shown).

Table 5.5. Growth of *M. silvestris* strain ΔMS on one-, two- and four-carbon compounds. Figures are the mean of at least six replicates ± standard deviation. Substrate concentrations: 5 mM, except methanol: 0.1% (v/v). Growth on methanol is discussed in Section 5.10.

Strain	Substrate	Sp growth rate (h^{-1})	Lag time (h)	Increase in biomass (OD)
ΔMS	Methanol	0.028 ± 0.007	38 ± 23	0.74 ± 0.06
ΔMS	Acetate	0.005 ± 0.001 [a]	-	-
ΔMS	Succinate	0.028 ± 0.001	0 ± 6	0.48 ± 0.07

[a] Refers to the latter phase of growth after approximately 60 h.

However, interestingly, strain ΔMS was able to grow on acetate to a density of 0.15 at a rate similar to the wild type, in contrast to strain ΔICL. Eventually, after approximately 50 hours, during which no further growth occurred, growth of strain ΔMS resumed at a low rate. This experiment was repeated with almost identical results (data not shown). The fast initial growth could be explained by the ability of strain ΔMS to use a cellular storage compound, the identity of which is unknown, which is not available to strain ΔICL.

The data presented in Section 5.6 strongly support the hypothesis that *M. silvestris* uses the glyoxylate cycle during growth on two-carbon compounds.

5.7 Operation of an isocitrate lyase positive serine cycle in *M. silvestris* during 1-carbon growth

5.7.1 Carbon assimilation via alternatives to the serine cycle

Serine cycle enzymes hydroxypyruvate reductase and serine-glyxoylate aminotransferase were assayed by Dunfield et al. (2003), and data suggested that *M. silvestris* assimilates carbon during methylotrophic growth using the serine cycle. However, *M. silvestris* also contains a complete set of Calvin cycle genes located in a cluster (Msil1191 - Msil1198), including those encoding key enzymes ribulose 1,5-bisphosphate carboxylase-oxygenase (RubisCO) and phosphoribulokinase (PRK) (87% and 76% identity to *cbbL* and *cbbP* from *Bradyrhizobium japonicum* respectively). Previous reports have suggested that *Beijerinckia mobilis,* an organism relatively closely related to *M. silvestris,* may assimilate carbon using both the Calvin and the serine cycles (Dedysh et al., 2005b).

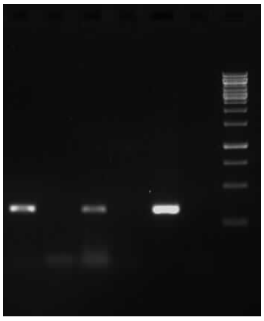

Figure 5.12. RT-PCR using cDNA synthesised from cells grown on methanol (lanes 1 and 2) or succinate (lanes 3 and 4) and primers located in *cbbP*. Lanes 2 and 4 are controls in which cDNA synthesis reactions were conducted without reverse transcriptase enzyme. Lane 5, DNA template, lane 6, NTC. M: Generuler 1kb marker (Fermentas).

RNA was extracted from cells grown on methanol and succinate and used for cDNA synthesis using Supercript II reverse transcriptase and random hexamer primers, as described in Materials and Methods. RT-PCR was carried out using a cDNA

template and primers located in the putative *cbbL* and *cbbP* coding sequences. Whereas a PCR product was obtained for *cbbP* with cDNA from both conditions (Figure 5.12), no *cbbL* amplicons could be obtained (not shown). RNA was extracted from cells grown on formate, but due to the poor growth on this substrate and the synthesis of a large amount of slime, RNA quality (as determine by the University of Warwick Molecular Biology Service Agilent Bioanalyser) was low, and cDNA sythesis was not attempted.

5.7.2 Deletion of serine-glyoxylate aminotransferase

Confirmation of the operation of the serine cycle during one-carbon growth of *M. silvestris* was obtained by construction of strain ΔSGAT, involving the deletion of serine-glyoxylate aminotransferase, encoded by *sgaA*, locus tag Msil1714. This gene bears 66% identity (at the amino acid level) to *sgaA* from *Methylobacterium extorquens,* which was shown to be essential for operation of the serine cycle (Chistoserdova and Lidstrom, 1994), and in *M. silvestris* forms part of a cluster of five genes including those predicted to encode glycerate kinase, hydroxypyruvate reductase and formate-tetrahydrofolate ligase, see Figure 5.13 and Table 5.6. The method of deletion is described in Chapter 4.

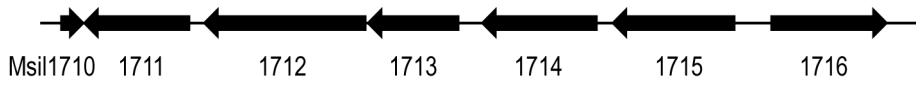

Figure 5.13. The *M. silvestris* gene cluster including Msil1714, annotated as serine-glyoxylate aminotransferase.

Table 5.6. Top BLAST hits to the SWISS-PROT/TrEMBL database, and associated annotation of translated sequences of open reading frames surrounding serine-glyoxylate aminotransferase (Msil1714).

ORF	Annotation	Organism	aa	% id
1711	Uncharacterised	*Rhodopseudomonas palustris* BisA53	363	46
1712	Formate-tetrahydrofolate ligase	*Methylibium petroleiphilum* PM1	558	78
1713	2-hydroxyacid dehydrogenase	*Methylobacterium nodulans*	313	73
1714	Serine-glyoxylate aminotransferase	*Methylobacterium* strain 4-46	396	71
1715	Glycerate kinase	*Methylibium petroleiphilum* PM1	421	70

Strain ΔSGAT was unable to grow on one-carbon compounds, whereas growth on acetate and succinate was unaffected, see Figure 5.14 and Table 5.7.

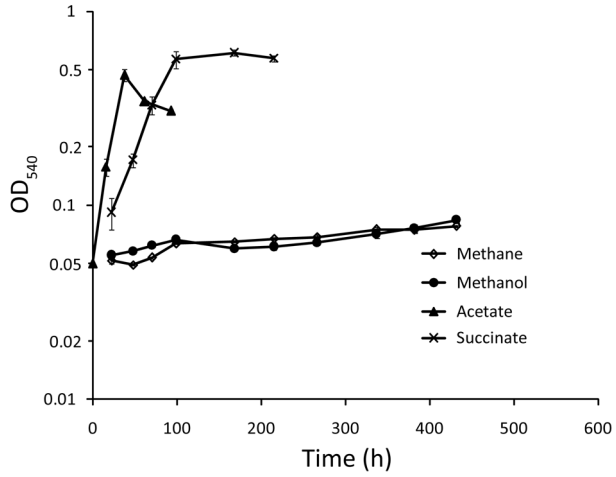

Figure 5.14. Growth of *M. silvestris* strain ΔSGAT on one-, two- and four-carbon compounds. Data points are the mean of three replicates, and error bars show the standard deviation.

Table 5.7. Growth of *M. silvestris* strain ΔSGAT on one-, two- and four-carbon compounds. Figures are the mean of at least three replicates ± standard deviation, except formate, in duplicate. Substrate concentrations: acetate, succinate: 5 mM, formate: 25 mM, methane: 20% (v/v) and methanol: 0.1% (v/v).

Strain	Substrate	Specific growth rate (h^{-1})	lag time (h)	increase in biomass (OD)
ΔSGAT	Formate	No growth	-	-
	Methane	0.001 ± 0	-	0.03 ± 0
	Methanol	0.001 ± 0	-	0.03 ± 0
	Acetate	0.059 ± 0.002	0 ± 0	0.42 ± 0.03
	Succinate	0.024 ± 0.001	0 ± 8	0.56 ± 0.02

These data confirm that *M. silvestris* uses the serine cycle for one-carbon assimilation.

5.7.3 Assay of isocitrate lyase

Low isocitrate lyase activity was detected in methane-grown cells, see Table 5.3. The isocitrate lyase positive variant of the serine cycle can generate one three-carbon molecule for assimilation into biomass, for the lysis of each isocitrate molecule (Anthony, 1982), therefore, using the same assumptions as Section 5.6.1, but the specific growth rate for methane-grown cells (0.01-0.022 h^{-1}, Table 3.4), minimum

enzyme activity would be expected to be in the range 5 – 10 nmol min^{-1} mg^{-1}, which is ten times the activity detected. In assay reactions where methane-grown extract (1145 µg protein) was added to acetate-grown extract (57.5 µg protein) the activity detected was approximately the sum of the activities separately, demonstrating that methane-grown extract did not contain components that inhibited the assay. Therefore methane-grown cell extract did not appear to contain sufficient isocitrate lyase activity to support the measured growth rate.

5.7.4 Growth of strain ΔICL on 1-carbon compounds

Strain ΔICL was unable to grow on methane, monomethylamine (MMA) or methanol, see Figure 5.15, Table 5.4 and Figure 5.10. In duplicate vials, growth was also not observed with formate (25 mM, data not shown).

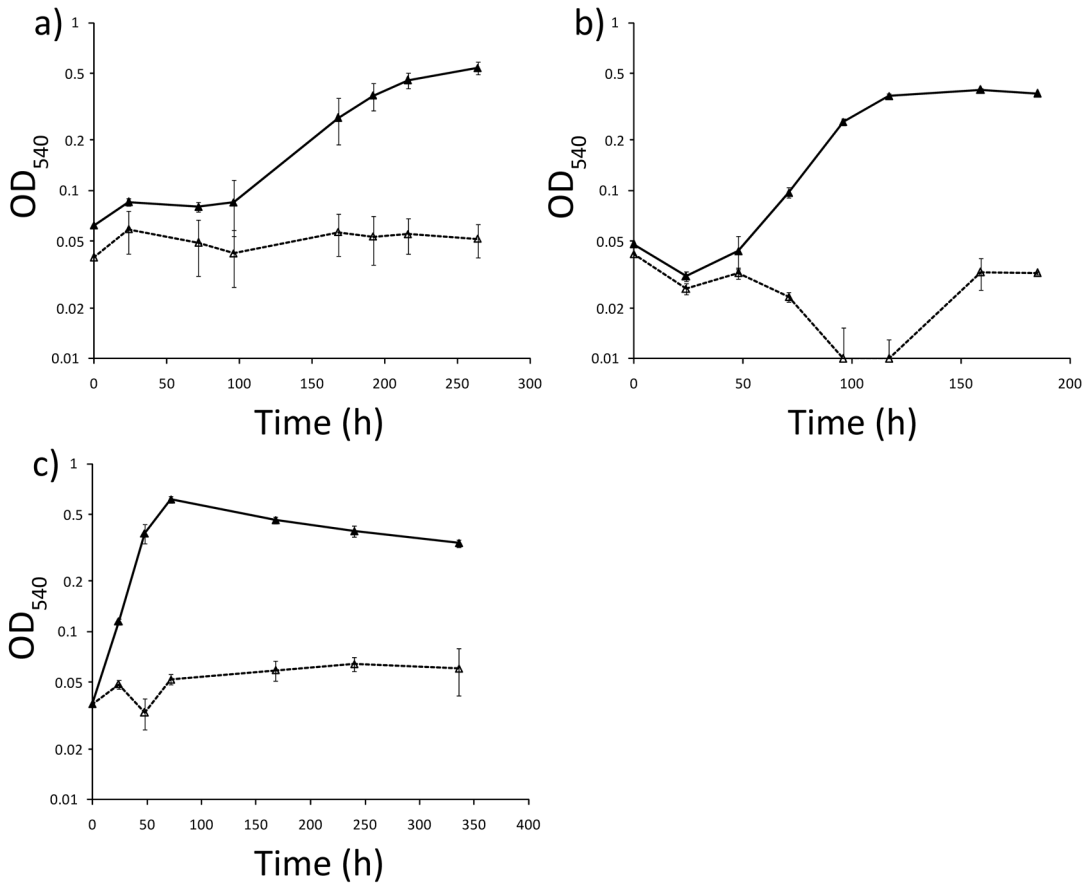

Figure 5.15. Growth of *M. silvestris* wild-type (solid lines) and strain ΔICL (dotted lines) on a) methane, b) MMA and c) methanol. Data points show the mean of three replicates and error bars indicate the standard deviation.

These data demonstrate that isocitrate lyase is essential for one-carbon assimilation in *M. silvestris,* and support the hypothesis that an ICL^+ variant of the serine cycle is employed.

5.7.5 Rescue of C1 growth of strain ΔICL by glyoxylate

M. silvestris is unable to grow on glyoxylate (Table 3.2), but since this is the product of the isocitrate lyase reaction in the serine cycle, strain ΔICL was tested for growth on methanol (5 mM) plus glyoxylate (2.5 mM). Mutants of *Methylobacterium extorquens* AM1 defective in C_1 metabolism are able to grow on methanol supplemented with glyoxylate (Dunstan et al., 1972a). There was no detectable growth for at least 7 days, but after 4 weeks, vials had become turbid. These cultures were therefore used as inoculum for a repeat experiment using 10 mM methanol (~0.04% v/v) plus 5 mM glyoxylate. The rationale for these concentrations was based on the assumption that one glyoxylate would be required for each one-carbon unit assimilated, comprising approximately 50% of the supplied methanol, and that higher glyoxylate concentrations might be toxic. Controls were included, supplied with methanol alone and glyoxylate alone. Strain ΔICL was able to grow on methanol (0.04% v/v) plus glyoxylate at 70% of the wild type growth on methanol (0.1% v/v) alone, whereas there was little or no growth on either glyoxylate or methanol alone (Table 5.8). These data demonstrate that, in the mutant strain, exogenously supplied glyoxylate is able to replace that generated by isocitrate lyase, albeit with a lag phase not present in wild type cells during growth on methanol.

Table 5.8. Growth of strain ΔICL on glyoxylate, methanol, or methanol plus glyoxylate. Data are the mean of three replicates ± standard deviation.

Substrate	specific growth rate (h^{-1})	Lag time (h)	Increase in biomass (OD)
Glyoxylate	0.00 ± 0.003	-	0.01 ± 0.00
Methanol	0.006 ± 0.000	33 ± 16	0.06 ± 0.00
Methanol + glyoxylate	0.033 ± 0.008	62 ± 14	0.36 ± 0.01

5.8 Complementation of strain ΔICL

M. silvestris strain ΔICL was complemented by expression of the wild type isocitrate lyase gene (Msil3157) encoded on vector pAC105. For this construct, broad host

range promoter probe vector pCM132 (Marx and Lidstrom, 2001a) was modified by removal of *lacZ* and replacement with the isocitrate lyase gene and promoter from *M. silvestris*. Primers C-Iclf and C-Iclr (Table 5.13) were used to amplify the Msil3157 coding sequence and 183 bp upstream and 186 bp downstream, using wild-type genomic DNA as template and proofreading enzyme *pfu* (Promega). This fragment was cloned into pCR2.1 TOPO, excised with *Kpn*I and *Sma*I, and purified from an agarose gel. Vector pCM132 was cut with *Sph*I, blunted using T4 polymerase, cut with *Kpn*I, de-phosphorylated, gel purified, and ligated with the *Kpn*I *Sma*I fragment (Figure 5.16). This vector therefore has sequences of 183 bp and 121 bp homologous to the chromosome of strain ΔICL upstream and downstream respectively of Msil3157. It was assumed that this level of homology would be unlikely to result in spontaneous re-integration of the deleted sequence into the chromosome.

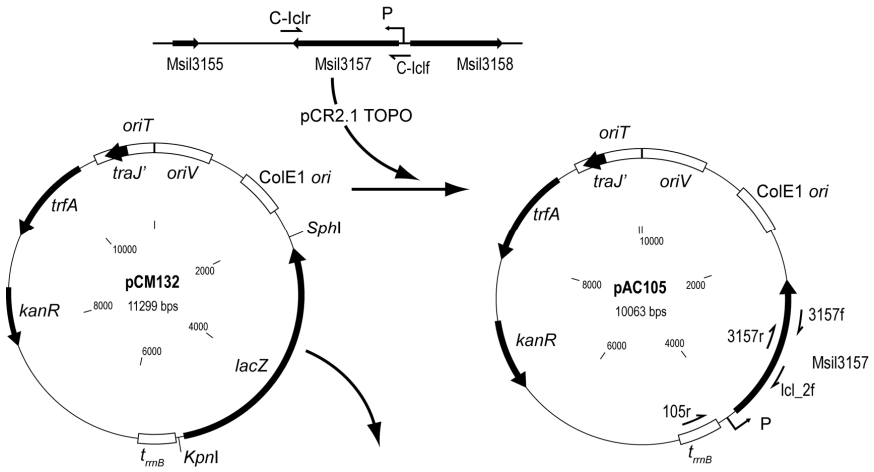

Figure 5.16. Vector pAC105 for complementation of strain ΔICL was constructed by replacing *lacZ* in pCM132 with the Msil3157 coding sequence and promoter, PCR-amplified from the *M. silvestris* wild-type chromosome using primers C-Iclf and C-Iclr. Primers 3157f, 105r, 3157r and Icl_2f were used to screen transformed strain ΔICL-pAC105.

Accuracy of vector pAC105 was verified by sequencing, and *M. silvestris* strain ΔICL was transformed by electroporation. Cells containing the vector were selected on DAMS plates containing kanamycin. PCR reactions with various combinations of primers binding to positions in the wild type chromosome, the deleted coding sequence and the vector backbone sequence demonstrated the presence of the

complementing vector in cells, and the lack of stable re-integration (see Figure 5.17 and Table 5.9).

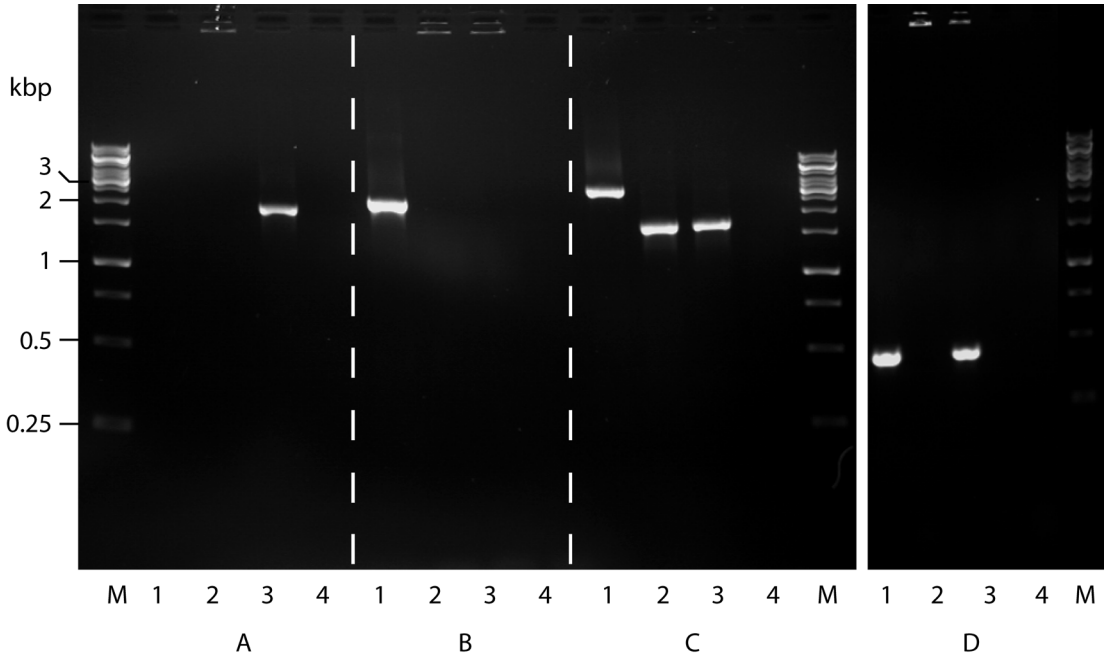

Figure 5.17. PCR was used to verify strain ΔICL complemented with pAC105, using four primer sets, A, B, C and D, as shown in Table 5.9. Lanes 1: wild-type, 2: strain ΔICL, 3: complemented strain ΔICL-pAC105, 4: NTC.

Table 5.9. Primer pairs used in PCR reactions shown in figure Figure 5.17. Primer locations are shown in Figure 5.16, except 3157Tf and 3157Tr, which are located upstream and downstream of Msil3157, beyond the regions originally cloned during the gene deletion procedure, as described in Chapter 4. w-t: wild type, ΔICL: strain ΔICL, C- ΔICL: strain ΔICL complemented with vector pAC105.

	Primer pair	Primer location		Amplicons (bp)		
		Fwd primer	Rev primer	w-t	ΔICL	C-ΔICL
A	Icl_2f/105r	Deleted region	pAC105 vector	-	-	1891
B	Icl_2f/3157Tr	Deleted region	Chromosome	2224	-	-
C	3157Tf/3157Tr	Chromosome	Chromosome	3259	1660	1660
D	3157f/3157r	Deleted region	Deleted region	451	-	451

Complementation largely restored the ability of strain ΔICL-pAC105 to grow on acetate and methanol, see Table 5.10. When growing with antibiotic, growth was reduced in comparison to the wild type, but during growth on methanol without antibiotic, growth rate and increase in biomass approached that of the wild type. Complemented cultures exhibited a lag phase not present in the wild type cultures.

Table 5.10. Growth of complemented strain ΔICL-pAC105 on acetate (5 mM), succinate (5 mM) or methanol (0.1% v/v) with or without kanamycin (25 μg ml^{-1}).

Substrate	Kanamycin (+/-)	specific growth rate (h^{-1})	Lag time (h)	increase in biomass (OD)
Acetate	+	0.024 ± 0.0004	2 ± 0	0.22 ± 0.00
Succinate	+	0.018 ± 0.0003	20 ± 6	0.46 ± 0.00
Methanol	+	0.019 ± 0.001	43 ± 5	0.50 ± 0.02
Methanol	-	0.037 ± 0.0004	11 ± 3	0.56 ± 0.03

5.9 Metabolism of methanol in strain ΔICL

Proteomic analysis demonstrated expression of methanol dehydrogenase during wild-type growth on succinate, both by analysis of bands cut from a 1D gel (Chapter 3, Table 3.5), and also by quantitative analyses of soluble extract performed by Vibhuti Patel (Patel et al., 2009) and subsequently by Nisha Patel (Patel et al., 2011) and the University of Warwick Biological Mass Spectrometry and Proteomics Facility. The latter study quantified MDH as 9.3% of the soluble protein in succinate-grown soluble extract, (in comparison to 0.18% for isocitrate lyase in the same extract). Therefore the ability of *M. silvestris* to metabolise methanol during growth on succinate was investigated by analysis of growth on a mixture of succinate (5 mM) and methanol (0.05% v/v) (Figure 5.18). Whereas the wild-type grew at a faster rate and to a higher final density, strain ΔICL was repressed by the presence of methanol. Although the mutant is unable to assimilate one-carbon compounds into biomass due to a disabled serine cycle, it might be expected that it would be able to oxidise methanol to produce energy, thus enabling more succinate to be diverted into biomass production.

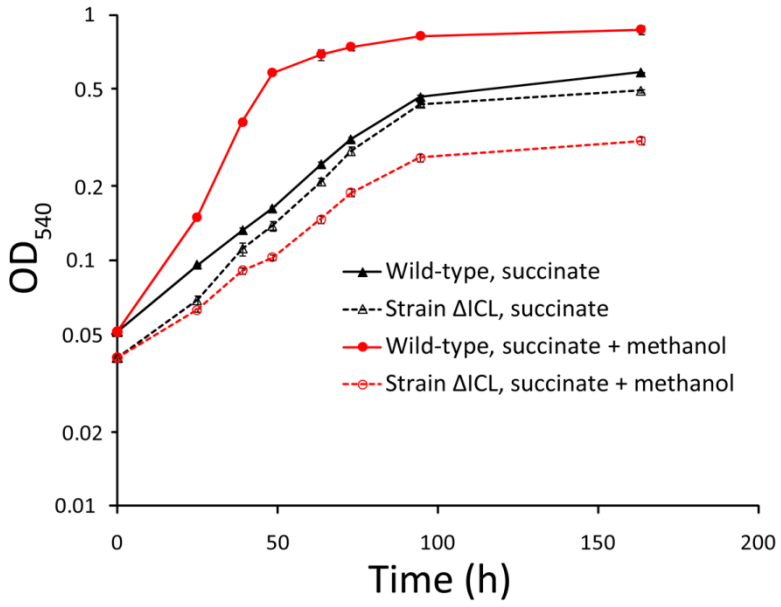

Figure 5.18. Growth of *M. silvestris* wild type (solid lines) and strain ΔICL (dashed lines) on succinate (black, solid or open triangles) or succinate (5 mM) plus methanol (0.05% v/v) (red, solid or open circles). Data points represent the mean of triplicate vials and error bars indicate the standard deviation.

5.9.1 Analysis of substrate-stimulated oxygen uptake in strain ΔICL

Since there was no benefit to strain ΔICL of the addition of methanol to succinate-containing growth medium, the ability of this strain grown on succinate in 125 ml vials to oxidise methanol was tested in a Clark oxygen electrode. These cells showed oxygen uptake in response to the addition of succinate, but no detectable response to methanol (data not shown). In order to investigate this more fully, strain ΔICL was grown on succinate in a 2 l batch culture in a fermenter, and cells were used for comparison with the wild-type. Substrates (2.5 nmol except succinate, 5 nmol and formate, 12.5 nmol) were added to whole cells (5 mg, calculated from OD readings assuming 1 ml at OD_{540} = 1.0 is equivalent to 0.25 mg dw) in the oxygen electrode, and data are shown in Figure 5.19. Oxygen consumption rate was similar in response to succinate, acetate and formate, but there was no detectable response to methanol or ethanol by the mutant cells, in contrast to wild-type cells which exhibited high activity in response to these alcohols. Formaldehyde-stimulated oxygen consumption was also highly down-regulated in strain ΔICL.

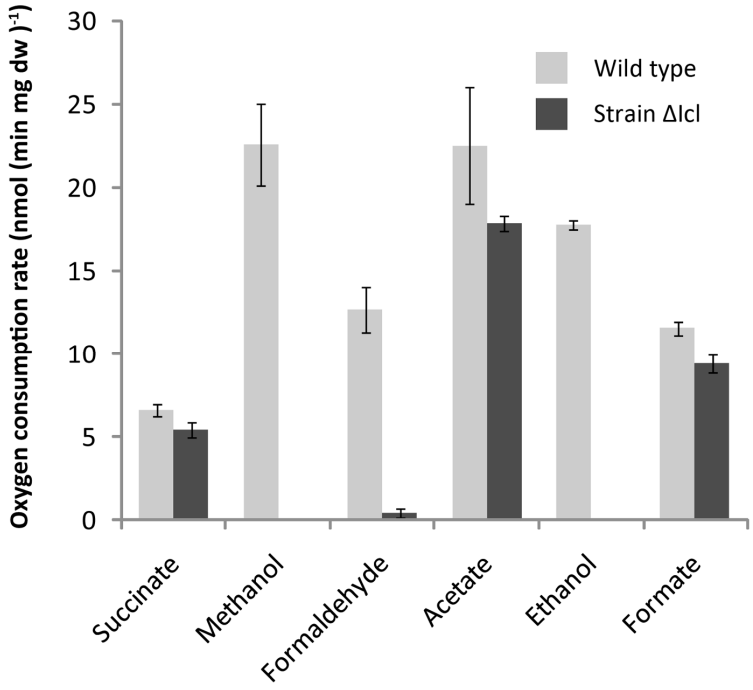

Figure 5.19. Oxygen-uptake rates of *M. silvestris* wild-type and strain ΔICL, grown on succinate in a fermenter, in response to addition of the substrates shown. Error bars show the standard deviation of a minimum of three measurements.

5.9.2 Methanol dehydrogenase activity and expression in strain ΔICL

Since there was no detectable response to methanol or ethanol with succinate-grown strain ΔICL in the oxygen electrode, methanol dehydrogenase (MDH) activity was assayed in the soluble fraction of cell extract from the same cells, using the standard PMS/DCPIP linked assay as described in Materials and Methods. High levels of activity were detected in wild type cells in response to methanol, formaldehyde and ethanol (Table 5.11), but activities were very low or not detectable in extract from strain ΔICL. However, complemented strain ΔICL-pAC105 exhibited over half of the wild type activity with methanol, demonstrating that the lack of activity in strain ΔICL was not caused by unexpected non-reversible disruption of MDH-expression related sequences in the genome. The simultaneous absence of methanol, ethanol and formaldehyde activity in strain ΔICL suggests that MDH is responsible for the measured activity with all three substrates in wild-type extract.

Table 5.11. Assay for PQQ-containing dehydrogenase conducted using soluble fraction of *M. silvestris* cell extract, from fermenter-grown cells. Specific activity (nmol (min mg)$^{-1}$) is shown as the mean of three replicates ± standard deviation, except ethanol (as substrate), mean of duplicate reactions. Hyphens indicate that the assay was not carried out.

	Assay substrate		
Strain / growth-substrate	Methanol	Formaldehyde	Ethanol
Wild type / methane	936 ± 14	-	-
Wild type / succinate	1142 ± 36	1060 ± 23	1197
ΔICL / succinate	0 ± 5	7 ± 1	0
ΔICL-pAC105 / methanol	590 ± 56	488 ± 6	-

These findings were corroborated by SDS-PAGE using the same soluble extracts, see Figure 5.20. The size of the arrowed band was estimated as 64 -66 kDa, in agreement with the predicted MDH size of 65.7 kDa. A discrete band corresponding to isocitrate lyase (predicted size 59.8 kDa) could not be identified in the gel, reflecting its relatively low abundance. A band (from a different gel) corresponding to the band shown arrowed was subsequently excised and the identity (MDH) confirmed by mass spectrometric analysis (see Figure 6.14, Chapter 6).

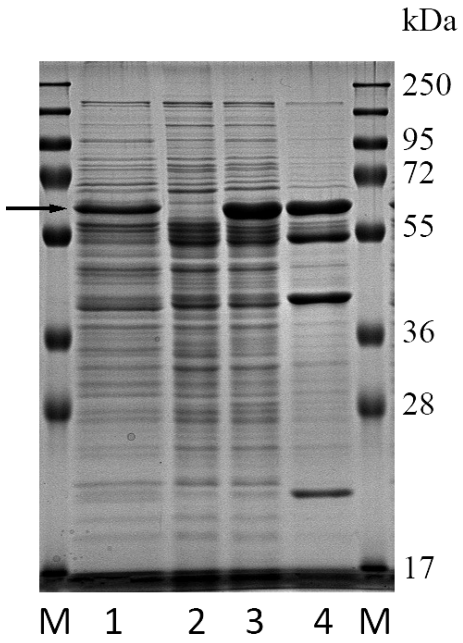

Figure 5.20. 12.5% SDS-PAGE demonstrated lack of expression of MDH in *M. silvestris* strain ΔICL (lane 2), whereas complementation restored expression in strain ΔICL-pAC105 (lane 1). Lane 3: wild type (succinate-grown) and lane 4: methane-grown. M: PageRuler Plus prestained marker (Fermentas). The arrow indicates MDH large subunit.

5.9.3 Transcription of isocitrate lyase and *mxaF*

RNA was extracted from fermenter-grown *M. silvestris* wild type and strain ΔICL grown on succinate and also from complemented strain ΔICL-pAC105 grown in volumes of 20 ml in 125 ml vials on succinate (5 mM) or methanol (0.1% v/v), using the hot phenol method as described in Materials and Methods. Superscript II reverse transcriptase (Invitrogen, UK) was used with 500 ng total RNA and random hexamers to synthesise cDNA as described in Materials and Methods. cDNA (1 µl) was used as template in PCR reactions together with genomic DNA for comparison. Control reactions were also included, identical except that no reverse transcriptase enzyme was added during cDNA synthesis. To analyse transcription of Msil3157, primers 3157f/3157r were used targeting the gene coding sequence. In addition, primers MxaFf/MxaFr and CytCf/CytCr for two genes located in the MDH operon, *mxaF*, encoding the α-subunit, and *cytC,* encoding the MDH-specific cytochrome C (Anthony, 1992) were included, together with primers for *hpr* (Hpr2f/Hpr2r) encoding hydroxypyruvate reductase and 16S rRNA gene primers 27f /1492r.

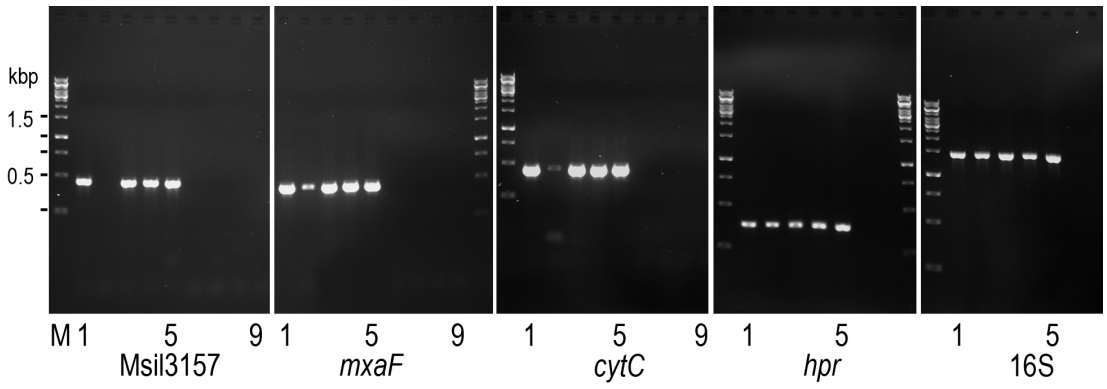

Figure 5.21. RT-PCR reactions using cDNA synthesised from RNA extracted from wild type (lanes 1), strain ΔICL (lanes 2) and strain ΔICL-pAC105 grown on succinate (lanes 3) or methanol (lanes 4). Lanes 6 – 9 as lanes 1 – 4 except using template prepared without reverse transcriptase. Lanes 5, DNA template. 30 PCR cycles, except *hpr* and 16S, 21 cycles. M: GeneRuler 1 kb ladder (Fermentas). For *hpr* and 16S, negative reactions shown correspond to wild-type cDNA synthesis without reverse transcriptase and NTC only. Expected sizes: Msil3157: 451bp, *mxaF*: 430 bp, *cytC:* 447 bp, *hpr:* 377 bp, 16S: 1447 bp.

As expected, Msil3157 was not transcribed in strain ΔICL, but transcription was restored in complemented strain ΔICL-pAC105. Genes *mxaF* and *cytC,* although transcribed in all strains, appeared to be transcribed at a lower level in strain ΔICL than in the wild type or complemented strains. Transcription of *hpr* was unaffected

by deletion of Msil3157 in strain ΔICL. The similar amplicons generated from 16S rRNA cDNA templates (when PCR cycles were reduced to 21) suggests that comparison between transcripts in the other reactions is valid.

5.9.4 Comparison of MDH expression in flask-grown wild-type and strain ΔICL

Since much of the work described in Sections 5.9.2 and 5.9.3 relied on fermenter-grown cells, *M. silvestris* wild-type and strain ΔICL were grown in 200 ml volumes under identical conditions in 1 l flasks on succinate (5 mM). Cells were harvested at late exponential phase and cell-free extract prepared. This was used for SDS-PAGE and PMS-linked enzyme assays, see Figure 5.22. Although some MDH activity was present in cell-free extract of strain ΔICL, it was less than 15% of the wild type strain, and the polypeptide band corresponding to the α-subunit was also much less prominent. However, under these conditions MDH expression was not completely eliminated in the mutant strain.

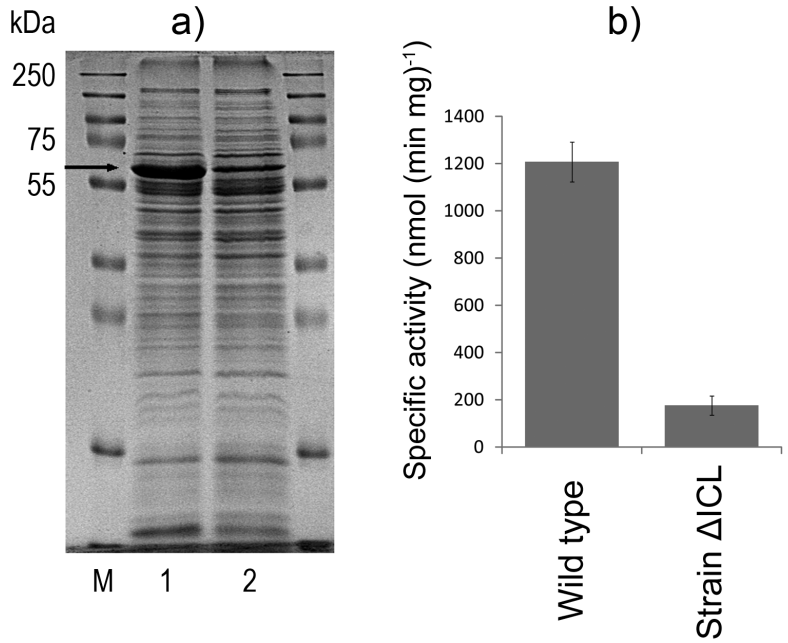

Figure 5.22. Strain ΔICL exhibited reduced MDH expression and activity in comparison to the wild-type when grown on succinate in flasks. a) SDS-PAGE of cell-free extract, lane 1: wild type, lane 2: strain ΔICL. The band corresponding to the MDH α-subunit is indicated with an arrow. M: PageRuler Plus prestained protein ladder (Fermentas). b) PMS-linked methanol dehydrogenase assay of cell-free extract. Error bars indicate the standard deviation of three replicate measurements.

5.9.5 Effect of glyoxylate and hydroxypyruvate on MDH expression

It seemed possible that differences in the level of intracellular metabolites caused the unexpected change in expression of MDH in strain ΔICL compared to the wild type, and that MDH expression might be induced by one of the products of isocitrate lyase. During growth on succinate, the glyoxylate bypass is not essential (Table 5.4), but the activity of isocitrate lyase might result in significant intracellular levels of glyoxylate or one of the products of its metabolism. To test this, cultures of strain ΔICL (20 ml, in 120 ml vials) were grown on succinate supplemented with either glyoxylate or hydroxypyruvate. The latter is the product of the next enzyme in the serine cycle, serine-glyoxylate aminotransferase. Glyxoylate or hydroxypyruvate were included at between 0 and 2 mM, together with 5 mM succinate. Growth was inhibited in vials with 0.5 and 2 mM glyoxylate and the latter did not produce sufficient biomass and was not included in proteomic analysis. Cells were harvested after 7 days at late exponential or stationary phase at OD_{540} between 0.46 and 0.49, disrupted by sonication and centrifuged to remove debris as described in Materials and Methods.

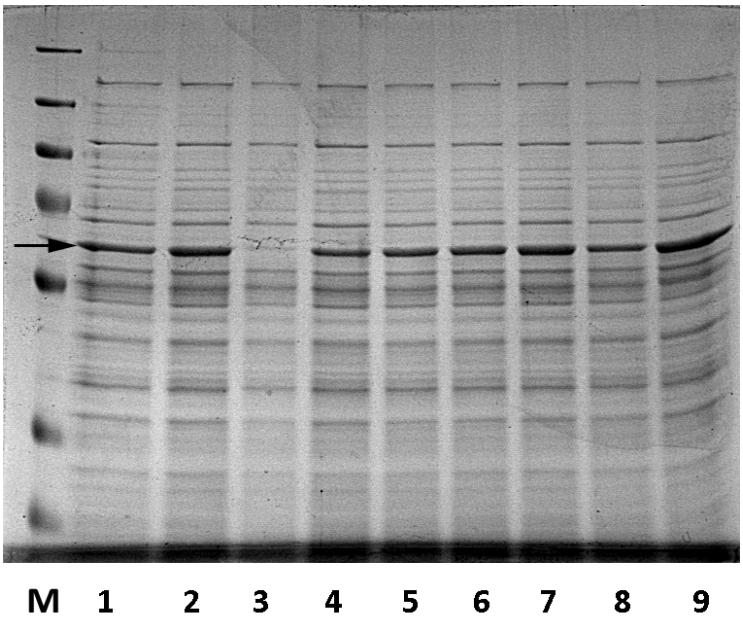

Figure 5.23. Strain ΔICL was grown on succinate (5 mM) with glyxoxylate or hydroxypyruvate. Lanes 1-4: glyoxylate at 0, 25, 100, 500 μM, lanes 5 – 9 hydroxypyruvate at 0, 25, 100, 500 and 2000 μM respectively. M: PageRuler Plus prestained protein marker (Fermentas). The band corresponding to MDH (68.5 kDa) is indicated with an arrow.

Protein was quantified and 5 – 10 µg loaded on a 10% SDS-PAGE gel, see Figure 5.23. Unexpectedly, MDH was expressed at similar levels under all conditions, except for the vial with 100 µM glyoxylate (lane 3), where expression seemed considerably reduced.

The genotype of the cultures was confirmed by PCR reactions using two primer pairs; 3157Tf/3157Tr which are located outside the deleted region and give different product sizes in the two strains, and 3157f/3157r which are located in the coding region and therefore give a product in the wild type but not in strain ΔICL. Results (not shown) were as expected.

5.9.6 Expression of MDH in strain ΔICL under different growth conditions

Strain ΔICL was grown on succinate in flasks with nitrate or ammonium as nitrogen source and harvested at mid- or late-exponential phase in an effort to identify growth conditions resulting in differences in MDH expression. SDS-PAGE revealed a uniformly low level of MDH expression and did not identify any correlation with the growth conditions tested (not shown).

5.10 Growth of strain ΔMS on methanol

Strain ΔMS grew on methanol at a specific growth rate of 0.28 ± 0.007 h^{-1} (Table 5.5), slightly over half the rate of the wild-type. In addition, this strain exhibited a considerable and highly variable lag phase (7 – 76 h, mean 38 h, standard deviation 23 h, n = 9), which was not present in the wild type under these growth conditions. This experiment was repeated with the same results, see Figure 5.24. Following routine methods employed to check culture purity, cells of a vial of methanol-grown strain ΔMS, which exhibited a short lag phase, were used as inoculum for growth on succinate, which was then used as inoculum for a repeat of the growth experiment on methanol and acetate. The growth phenotype was confirmed on both substrates, although with a more uniform (long) lag phase on methanol as shown in the figure. Cells were also serially diluted from the succinate culture, spread on DNMS succinate plates, and colonies used to check the gene deletion by PCR using primers 1325Tf and 1325Tr (Table 4.3). All colonies tested (12/12) displayed the mutant genotype (not shown).

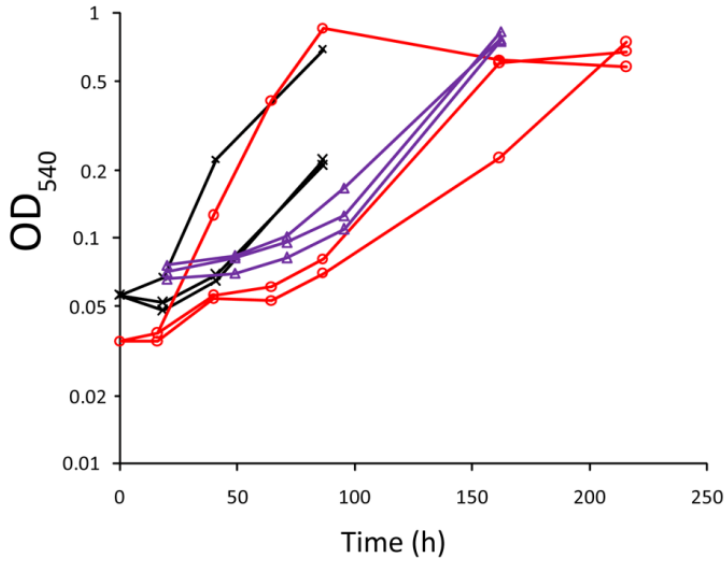

Figure 5.24. Growth of strain ΔMS on methanol. Curves represent growth of nine individual vials in three separate experiments (shown in black, red, or purple) including vials (purple) using inoculum from a vial exhibiting a short lag phase, as described in the text.

These data demonstrate that deletion of malate synthase had an effect on methanol metabolism in strain ΔMS, and are consistent with the hypothesis that altered levels of intracellular metabolites influenced regulatory elements controlling methanol metabolism.

5.11 Expression of MDH in wild-type *M. silvestris* BL2

Transcription, expression and activity of MDH in wild-type *M. silvestris* grown on succinate was conclusively demonstrated as described in Section 5.9. However, production of 3-carbon molecules, required as precursors for synthesis of cellular components (for example amino acids cysteine, glycine, phenylalanine, serine, tryptophan and tyrosine), would require a decarboxylation reaction (for example the activity of PEP carboxykinase, the expression of which was identified in succinate-grown cells, Table 3.5). Enzymes such as isocitrate lyase or PEP carboxykinase which are involved in anaplerotic or catabolic processes would be expected to be tightly and co-ordinately regulated (Sauer and Eikmanns, 2005). Therefore, to investigate MDH expression during growth that does not require the activity of these enzymes, *M. silvestris* was grown on glycerol and D-gluconate, and analysed by SDS-PAGE, in order to test the hypothesis that under these growth conditions MDH

might not be expressed. As shown in Figure 5.25, MDH was expressed under all conditions tested.

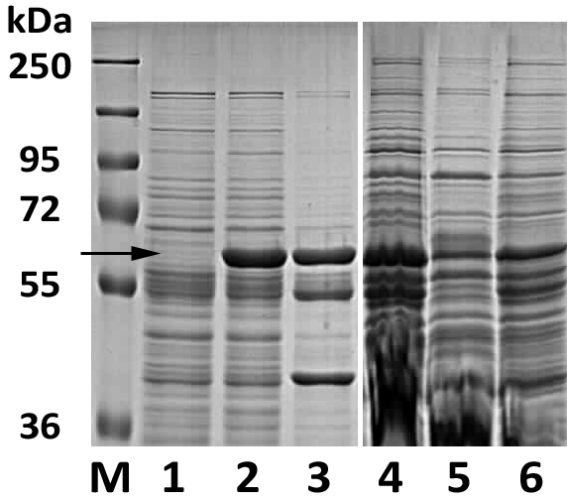

Figure 5.25. Expression of MDH was evaluated in cells grown on different substrates. Lanes 2, 3, 4, 6: wild type growth on succinate, methane, gluconate and glycerol respectively. Also, for comparison, lanes 1 and 5, strain ΔICL, grown on succinate and methanol plus glyoxylate respectively. M: PageRuler Plus pre-stained protein marker (Fermentas). The band corresponding to MDH is shown arrowed.

5.12 Growth phenotype of strain ΔSGAT

Data presented in Sections 5.9 and 5.10 demonstrate that deletion of the genes encoding the enzymes of the glyoxylate bypass had an effect on MDH expression. However, data presented in Sections 5.7.5 and 5.8 show that this was not caused by a polar effect of the gene deletion, or unintended disruption of MDH genes. Therefore, it seemed possible that an alteration in the intracellular level of metabolites moderated by the glyoxylate bypass resulted in the differences in MDH expression and activity observed. Since glyoxylate, a product of isocitrate lyase, is a substrate of serine-glyoxylate aminotransferase, strain ΔSGAT was investigated in respect of methanol metabolism and MDH expression.

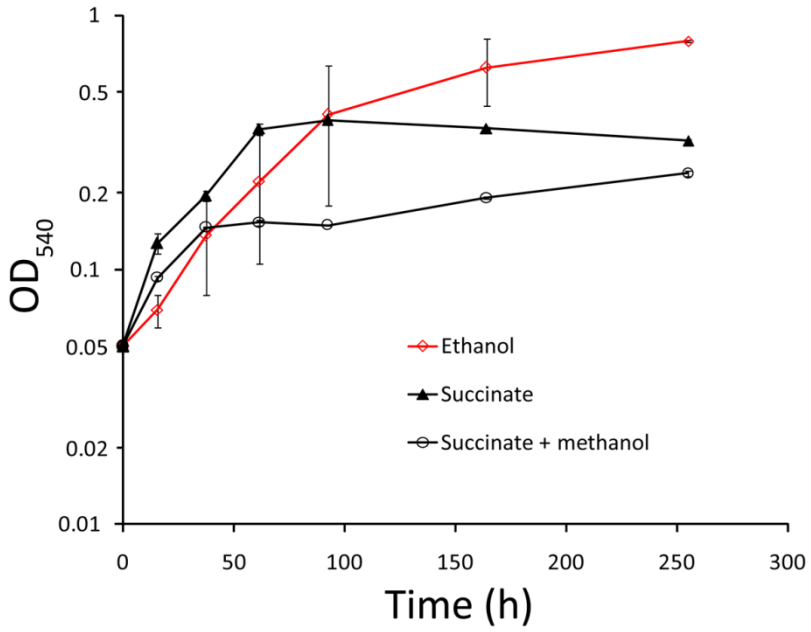

Figure 5.26. Growth of strain ΔSGAT on ethanol (in red), succinate or succinate plus methanol. Data points show the mean of three replicates and error bars indicate the standard deviation.

Strain ΔSGAT grew on ethanol with a specific growth rate of 0.019 h^{-1}, (Figure 5.26, Table 5.12) in comparison to the wild type rate of 0.045 h^{-1} (Table 5.4), and exhibited a similar variation in lag phase as observed for strain ΔMS during growth on methanol. Strain ΔSGAT did not benefit from the addition of methanol during growth on succinate and growth was repressed after a short initial period, see Figure 5.26. However, strain ΔSGAT was able to grow on acetate similarly to the wild type (Figure 5.14, Table 5.7), demonstrating that serine-glyoxylate aminotransferase is not involved in metabolism of this compound.

Table 5.12. Growth of strain ΔSGAT on ethanol, succinate or succinate plus methanol. Data are the mean of three replicates ± standard deviation. Substrate concentrations, ethanol: 0.1% (v/v), succinate: 3 mM, succinate plus methanol: 3 mM + 0.05% (v/v).

Strain	Substrate	Specific growth rate (h^{-1})	Lag time (h)	Increase in biomass (OD)
ΔSGAT	Ethanol	0.019 ± 0.003	0 ± 25	0.74 ± 0.01
	Succinate	0.030 ± 0.001	0 ± 1	0.34 ± 0.00
	Succinate plus Methanol	0.028 ± 0.000 (0.003 ± 0.000)[a]	0 ± 0	0.19 ± 0.01

[a] Growth resumed after 92 h at a reduced rate

5.12.1 Expression of MDH in strain ΔMS and strain ΔSGAT during growth on succinate

Cells of *M. silvestris* wild-type, strain ΔMS and strain ΔSGAT were grown in flasks on 5 mM succinate, and harvested at mid-exponential and stationary phase. Cell-free extract was prepared and analysed by SDS-PAGE. As shown in Figure 5.27, MDH was expressed under all conditions tested.

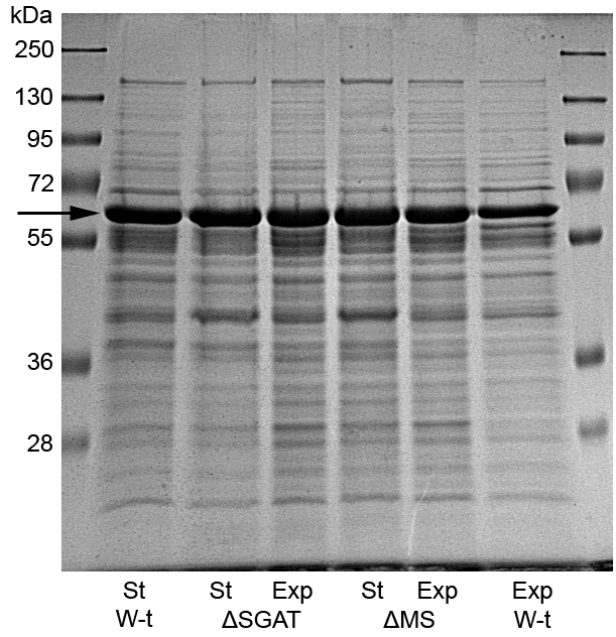

Figure 5.27. SDS-PAGE demonstrating that MDH was expressed in strains ΔMS and ΔSGAT during growth on succinate at both mid-exponential (Exp) and stationary (St) phases. W-t: wild-type. The band corresponding to MDH is indicated with an arrow.

5.13 Construction of an isocitrate lyase – malate synthase double mutant

Strain ΔICLΔMS was constructed with a deletion of both isocitrate lyase and malate synthase. This strain was able to grow on succinate, but not on methanol or acetate, as expected, and was not investigated further.

5.14 Discussion

5.14.1 Operation of the glyoxylate cycle in *M. silvestris*

Enzyme activity detected in soluble extract from cells grown on acetate was sufficient to support the observed growth rate. No doubt there is scope for further

optimisation of the activity assay, and the true enzyme activity may be somewhat higher. Deletion of each of the glyoxylate bypass genes demonstrated highly disabled phenotypes during two-carbon growth, whereas growth on succinate was unaffected. These data provide good evidence for the operation of the glyoxylate cycle during two-carbon growth.

5.14.2 The operation of an ICL$^+$ variant of the serine cycle in *M. silvestris*

Strain ΔSGAT, with a deletion of a key serine cycle enzyme, serine-glyoxylate aminotransferase, was unable to grow on one-carbon compounds, demonstrating the operation of the serine cycle in *M. silvestris*. The only fully documented and characterised alternative to isocitrate lyase and enzymes of the TCA cycle for the conversion of acetyl-CoA to glyoxylate in the serine cycle is the EMC pathway. However, *M. silvestris* does not appear to have the necessary genes for expression of the enzymes unique to this pathway. On the other hand, isocitrate lyase activity detected in assays of soluble extract of cells grown on methane was extremely low, casting doubt on the role of this enzyme during one-carbon growth.

Deletion of isocitrate lyase abolished growth on methane and methanol in strain ΔICL, initially appearing to demonstrate conclusively the role of this enzyme in the serine cycle. During growth on succinate, the wild-type strain is able to benefit from the addition of methanol. There is no suggestion of biphasic growth, implying that methanol is either oxidised for energy, or assimilated into biomass, or both, during metabolism of succinate. It seemed logical to imagine that strain ΔICL might also be able to benefit from oxidation of methanol to CO_2 although it may be unable to assimilate methanol-derived carbon into biomass. However, strain ΔICL did not grow faster or to a higher OD in the presence of methanol, implying either that this strain is unable to oxidise methanol, or that some other factor is inhibiting growth, for example the build-up of a toxic intermediate (e.g. formaldehyde), or that there is no benefit from generation of additional reducing equivalents. Analysis of strain ΔICL during growth on succinate conclusively demonstrated a lack of, or decrease in, transcription and expression of MDH in comparison to the wild type under the same conditions. Analysis of gene transcription, and complementation with the wild-type gene carried on a plasmid, supplied confidence that the observed phenotype was not caused by inadvertent disruption of sequences directly required for transcription of

the genes responsible for methanol oxidation. This change in MDH expression in strain ΔICL may have been caused either by a change in the intracellular level of metabolites as a result of removal of flux through isocitrate lyase, for example glyoxylate or a product of the metabolism of glyoxylate, or by a change in the redox balance of the cell caused by the deletion of this gene, which in turn might control MDH expression. The latter implies that isocitrate lyase plays a role in maintaining redox status, perhaps by diverting flux away from the energy-generating steps of the TCA cycle. The fact that no difference in the succinate growth-phenotype was discernable in strain ΔICL suggests that this effect must be subtle if it exists, although either hypothesis does imply some flux through isocitrate lyase during growth on succinate.

The realisation that expression of MDH was affected in strain ΔICL suggested that the failure to grow on methane and methanol might be due not to inactivation of the serine cycle, but simply by the inability to oxidise methanol. However, strain ΔICL was also unable to grow on monomethylamine or formate, which are not oxidised via MDH, demonstrating that one-carbon growth was disabled by more than the absence or reduced expression of MDH. It remains a theoretical possibility that expression of methylamine- and formate-oxidising enzymes is affected in strain ΔICL in a similar way to MDH, but constraints of time did not permit investigation of this. Taken together, these data suggest that the isocitrate lyase-positive variant of the serine cycle operates in *M. silvestris.* There is no satisfactory explanation for the low level of enzyme activity detected in methane-grown cells, but proteomic analysis of methane-grown cell extract did detect isocitrate lyase, both by mass-spec analysis of bands cut from a 1D gel (Table 3.5) and by the quantitative gel-free analyses mentioned earlier (isocitrate lyase, methane-grown cell extract, 0.19% of soluble protein, succinate-grown extract, 0.18%), although, of course, the presence of protein does not imply active enzyme.

5.14.3 Alcohol-growth phenotype of strains ΔMS and ΔSGAT

Strain ΔMS grew at a comparatively low rate on methanol (strain ΔMS 0.028 ± 0.007 h^{-1}, wild-type 0.049 ± 0.003 h^{-1}, Table 5.4 and Table 5.5), although removal of glyoxylate due to flux through MS would be expected to prevent the operation of the serine cycle, suggesting that there should be little or no flux through MS during wild-

type methylotrophic growth. In addition, the normally highly predictable growth was disrupted in strain ΔMS growing on methanol and cultures displayed a highly variable lag phase.

A similar situation was recorded in the case of strain ΔSGAT during growth on ethanol, which grew at less than half the wild type rate, despite similar growth to the wild-type on acetate. Again, ethanol-grown cultures exhibited a variation in lag phase. Since ethanol can be assumed to be assimilated via acetyl-CoA, this is a surprising finding.

The reduced growth of strain ΔMS on methanol and strain ΔSGAT on ethanol may most easily be explained by postulating reduced expression of MDH in strain ΔSGAT, perhaps caused by a similar mechanism to that shown to reduce MDH expression in strain ΔICL, since ethanol is probably oxidised by MDH in *M. silvestris* (Section 5.9.2), as is the case in, for example, *Methylobacterium extorquens* (Dunstan et al., 1972b). Once again, the possibility that alteration of redox balance is responsible cannot be discounted. It was not possible to investigate these issues further in the time available.

Growth of strain ΔSGAT on succinate was inhibited by the addition of methanol (Figure 5.26), which cannot be explained by reduced MDH expression. Glyoxylate is inhibitory to *M. silvestris* as noted in Section 5.9.5, and known to be toxic to *M. extorquens* (Okubo et al., 2010). Possibly, intracellular accumulation of glyoxylate caused by the blocking of flux through serine-glyoxylate aminotransferase is responsible for this growth reduction. This would imply some flux through MDH under these conditions, but does not supply further evidence of the relative levels of MDH expression.

5.14.4 Malate synthase activity in methane-grown cells

A relatively high level of malate synthase activity was detected in extract from cells grown on all substrates tested (Table 5.3). However, during operation of the serine cycle, not only would removal of glyoxylate, substrate of malate synthase, prevent operation of the cycle, but malate synthase activity would constitute a futile cycle (Chapter 1, Figure 1.9). Apparent malate synthase activity has been detected previously in organisms that use the serine cycle or the EMC pathway, but do not possess malate synthase (Large and Quayle, 1963; Salem et al., 1973a; Meister et al.,

2005), due to the combined activities of malyl-CoA lyase (in reverse) and a hydrolysing enzyme (recently identified as malyl-CoA thioesterase in *Rhodobacter sphaeroides* (Erb et al., 2010)). It was suggested that this reaction is prevented *in vivo* by inhibition of the hydrolase by acetyl-CoA (Cox and Quayle, 1976), and a similar mechanism might operate in *M. silvestris,* although this topic deserves further investigation.

5.14.5 An alternative to malate synthase in *M. silvestris*

Recently Okubo and co-workers (2010) have shown that, in *Methylobacterium extorquens,* an additional pathway operates for the consumption of glyoxylate during two-carbon growth. Glyoxylate is converted to glycine, decarboxylated by the glycine cleavage enzymes into methylene-tetrahydrofolate, and assimilated by combination with a second glycine in the usual serine cycle reactions. This pathway could theoretically operate in *M. silvestris* during two-carbon growth. The inability of strain ΔMS to grow normally on acetate, and the lack of any phenotype during growth on acetate in strain ΔSGAT, suggest that this pathway does not operate to any major extent in *M. silvestris.*

5.15 Conclusions

The data presented in this chapter strongly suggest that *M. silvestris* assimilates carbon during two-carbon growth using the glyoxylate cycle, and that the isocitrate lyase pathway is an essential component of the serine cycle. No evidence was found that suggest that the EMC pathway operates in *M. silvestris* during either one- or two- carbon growth.

Interesting effects of the deletion of the glyoxylate bypass enzymes on MDH expression were observed, possibly caused by an alteration of intracellular levels of metabolites, or a change in the redox balance of the cell, but without clear evidence for the causes or mechanisms. In the absence of additional data speculation is probably inappropriate.

Glyoxylate is positioned at a metabolic branch point in *M. silvestris*, with flux directed to the serine cycle during methylotrophy and via malate synthase during two-carbon growth. The regulation of the enzymes involved, and also of MDH,

which has been shown to be affected by the gene deletions described, would provide considerable scope for continued research.

Table 5.13. Primer sequences used in this chapter

Name	Sequence 5' – 3'	Restriction site
IclRa1	CCATCCAGCCGGA CAGATAG	
IclRa2	TCGTGCCGAAATGCTTCTTG	
IclRa3	TGGGTGTAAAGGGCCGAATC	
C-Iclf	ATCAGGTACCGAGGCTCCGCGCTGTTTC	*Kpn*I
C-Iclr	ATCACCCGGGATCTGCCGGCGTTCTTTG	*Sma*I
3157f	GATCATGCGCAAAGACATGG	
3157r	TTTCTTGGCGAGGAGATACG	
MxaFf	TCGGACAGATCAAGGCCTAC	
MxaFr	GCAAACTCGCCGAGATTCAC	
CytCf	GGAGCTTTCGCACAAACAAC	
CytCr	AAAGTGCGCTTTCTCCTCTG	
Hpr2f	TTGGCCTATGACGTCTTTCC	
Hpr2r	TTGTCGATCAACTGGTCAGC	
27f	AGAGTTTGATCMTGGCTCAG	
1492r	TACGGYTACCTTGTTACGACTT	
105r	GCCGAACTCAGAAGTGAAACG	
Icl_2f	AGAGGCGTGCCGTCATAATCG	

Chapter 6

Oxidation of methane and propane

6.1 Introduction

Soluble di-iron monooxygenase (SDIMO) enzymes, of which the soluble methane monooxygenase (sMMO) is an example, have been classified on the basis of their phylogeny into six groups, and the substrate utilisation of the microorganisms using these enzymes broadly follows this categorisation (Leahy et al., 2003; Coleman et al., 2006; Holmes and Coleman, 2008). Of these, groups I and II are largely associated with aromatic substrates (phenol, toluene), group III contains the methane and butane monooxygenases, group IV the alkene monooxygenases, group V propane and tetrahydrofuran and group 6, propane monooxygenases. The sMMO has been extensively characterised, and has a well-defined and broad substrate specificity (Burrows et al., 1984; Green and Dalton, 1989), suggesting that the barrier to growth of obligate methanotrophs on short chain alkanes is lack of downstream metabolic capability (Wood et al., 2004). The propane monooxygenase (PrMO), in contrast, is less well-characterised. Although numerous propane-utilising bacteria have been isolated (Foster, 1962; Vestal and Perry, 1969; Ashraf et al., 1994) the enzymes responsible have not until recently been identified. The first unequivocal demonstration of bacterial propane oxidation by an SDIMO was claimed by Kotani et al (2003), and the substrate specificity of propane-oxidising enzymes is less well investigated, although propane-utilisers were shown to co-metabolise pollutants such as trichloroethylene (TCE) (Wackett et al., 1989) and methyl tert-butyl ether (MTBE) (Steffan et al., 1997).

Soon after the start of this project, inspection of the *Methylocella silvestris* genome sequence identified a second SDIMO enzyme in addition to the sMMO. The discovery that *M. silvestris* was capable of growth on propane prompted exploration of the metabolic roles of these two enzyme systems. Since it seemed likely that the *M. silvestris* sMMO can oxidise propane, at least to some extent, and the substrate specificity of the PrMO was unknown, the purpose of the work described in this chapter was to identify the requirement for and role of these enzymes during growth on methane or propane, and the conditions under which they are expressed. The relative roles of different SDIMOs have been little studied in the relatively small group of organisms known to contain more than one of these enzymes. *Mycobacterium chubuense,* for example, contains four SDIMOs, including a Group III enzyme, and can grow on a range of alkenes and alkanes including propane (but

not methane) (Coleman et al., 2011b). This sMMO-like enzyme was shown to be transcribed during growth on propane, but its function in the oxidation of this gas was not demonstrated.

During this project useful data would have been generated by the successful separation and purification of the *M. silvestris* SDIMOs, and analysis of the kinetic properties of the reconstituted functional enzymes. This approach, however, might have been less than straightforward. It might well have proved difficult to design an assay capable of distinguishing between the enzymes *in vitro*, causing difficulties during their separation. In addition, the instability of SDIMOs during purification, and the loss of activity *in vitro*, has been reported in some cases (Dubbels et al., 2007). Thiemer et al. (2001), for example, were unable to detect any activity in cell free extract when working with the group V enzyme from *Pseudonocardia* sp. strain K1. Furthermore, by working with the enzymes in their intracellular context, which includes aspects such as the diffusion or transport of substrate across the cell membranes, it should be possible to predict more accurately the organism's response in environmental situations. For these reasons, the approach adopted here was to investigate growth and substrate consumption in wild-type and deletion mutant strains, together with some analysis of gene transcription and expression.

6.2 Soluble di-iron monooxygenase (SDIMO) enzymes in *M. silvestris*

6.2.1 Phylogenetic relationships of the *M. silvestris* SDIMOs

BLAST searches of the *M. silvestris* genome using, as query sequence, the amino acid sequence of the α-subunit of the well-characterised sMMO from *Methylosinus trichosporium* OB3b identified two homologous open reading frames, Msil1262 (86% identity over 526 amino acids) and Msil1651 (30% identity over 528 amino acids). Alignment of the amino acid sequence of the gene product of Msil1651 with representative sequences of hydroxylase α-subunits from SDIMOs from other groups, including those for which enzyme structures have been determined (the sMMO and toluene 4-monooxygenase from *Pseudomonas stutzeri* OX1), identified the highly conserved SDIMO-characteristic residues (E114, E144, H147 and E209, E243 H246 in *Methylococcus capsulatus* Bath) which coordinate the iron atoms (Rosenzweig et al., 1993), as shown in Figure 6.1. Phylogenetic analysis of the translated amino acid sequence of the two *M. silvestris* genes, together with the sequences of characterised

methane, short chain alkane and alkene and related monooxygenases, clearly assigned Msil1262 to the sMMO subgroup of SDIMOs, whereas Msil1651 aligned with *prmA* genes from propane utilising organisms including *Gordonia* TY5, *Rhodococcus jostii* RHA1 and *Pseudonocardia* TY-7, see Figure 6.2. Taken together with the gene organisation, (hydroxylase α-subunit, reductase, hydroxylase β-subunit, coupling protein), this suggests that the latter gene-cluster encodes a member of the propane monooxygenases (SDIMO subgroup V) as defined by Leahy (2003), Coleman (2006) and co-workers.

```
                          *  *                  :       :** **             :.
B8EK59_M. silvestris BL2  PEISAARSMAMLGRLAPGDELRTGFTMQMVDEFRHSTIQMNLKKWYMENYIDPAGFDITE  164
Q768T5_Gordonia TY5       PEISAARAMPMAIDAVPNPEIHNGLAVQMIDEVRHSTIQMNLKKLYMNNYIDPAGFDITE  155
Q9F3V6_Pseudonocardia K1  AEAAATRCMGMLVDALDDPELQNAYYIQQLDEQRHTAMQMNLYRWYMKNMPEPVGWNLGL  163
Q53027_Rhodococcus B276   AEYQAVAGCGMIISAVENQELRQGYAAQMLDEVRHAQLEMTLRNYYAKHWCDPSGFDIGQ  153
P22869_M. capsulatus Bath GEYNAIAATGMLWDSAQAAEQKNGYLAQVLDEIRHTHQCAYVNYYFAKNGQDPAGHNDAR  172
O87798_Pseudomonas OX1    EEYAASTAEARMARFAKAPGNRNMATFGMMDENRHGQIQLYFPYANVKR---SRKWDWAH  159
P19732_Pseudomonas CF600  LEYQAFQGFSRVGRQFSGAGARVACQMQAIDELRHVQTQVHAMSHYNKHFDGLHDFAHMY  167

                                                  : .  *  :**  ::     *.   *
B8EK59_M. silvestris BL2  AA-FGKCYATTIGRQFGEAFLTGDAVTAANIYLQVVAESAFTNTLFVAMPSEAARNGDYA  223
Q768T5_Gordonia TY5       KA-FANNYAGTIGRQFGEGFITGDAITAANIYLTVVAETAFTNTLFVAMPDEAAANGDYL  214
Q9F3V6_Pseudonocardia K1  QA-VGGDSILVAAQNLTGSFMTGDPFQAA-VALQVVVETAFTNTILVAFPDVAVRNHDFA  221
Q53027_Rhodococcus B276   RG-LYQHPAGLVSIGEFQHFNTGDPLDVI-IDLNIVAETAFTNILLVATPQVAVANGDNA  211
P22869_M. capsulatus Bath RTRTIGPLWKGMKRVFSDGFISGDAVECS-LNLQLVGEACFTNPLIVAVTEWAAANGDEI  231
O87798_Pseudomonas OX1    KAIHTNEWAAIAARSFFDDMMMTRDSVAVSIMLTFAFETGFTNMQFLGLAADAAEAGDHT  219
P19732_Pseudomonas CF600  DR----VWYLSVPKSYMDDARTAGPFEFL-TAVSFSFEYVLTNLLFVPFMSGAAYNGDMA  222

                            :.  * ::** **   *   :     :   .    :  :    *     .    *
B8EK59_M. silvestris BL2  LPTVFLSVQSDESRHIGNGHSFLMSVLNNP-DNHLLLERDIRYAFWQNHGIVDAAVGTIV  282
Q768T5_Gordonia TY5       LPTVFHSVQSDESRHISNGYSILLMALADE-RNRPLLERDLRYAWWNNHCVVDAAIGTFI  273
Q9F3V6_Pseudonocardia K1  LPTVMNSVQSDEARHINNGYATLLYLLQEP-ENAPLLEQDIQQMFWTVHAFVDAFMGILV  280
Q53027_Rhodococcus B276   MASVFLSIQSDEARHMANGYGSVMALLENE-DNLPLLNQSLDRHFWRAHKALDNAVGWCS  270
P22869_M. capsulatus Bath TPTVFLSIETDELRHMANGYQTVVSIANDP-ASAKYLNTDLNNAFWTQQKYFTPVLGMLF  290
O87798_Pseudomonas OX1    FASLISSIQTDESRHAQQGGPSLKILVEN--GKKDEAQQMVDVAIWRSWKLFSVLTGPIM  277
P19732_Pseudomonas CF600  TVTFGFSAQSDEARHMTLGLEVIKFMLEQHEDNVPIIQRWIDKWFWRGYRLLT-LIGMMM  281
```

Figure 6.1. Partial sequence alignment of deduced amino acid sequence of the hydroxylase α-subunits from SDIMOs of different groups. Included are the putative propane monooxygenase from *Methylocella silvestris* BL2, propane monooxygenase from *Gordonia* TY5 (Kotani et al., 2003), tetrahydrofuran monooxygenase from *Pseudonocardia* K1 (Thiemer et al., 2003), alkene monooxygenase from *Rhodococcus rhodocrous* B276 (Saeki and Furuhashi, 1994), sMMO from *Methylococcus capsulatus* Bath (Rosenzweig et al., 1993), toluene/*o*-xylene monooxygenase from *Pseudomonas stutzeri* OX1 (Sazinsky et al., 2004) and phenol hydroxylase from *Pseudomonas* CF600 (Nordlund et al., 1990). Residues important in the coordination of the iron atoms are shown shaded. Identical residues are shown with asterisks, highly conserved with colons, and conserved residues with single dots.

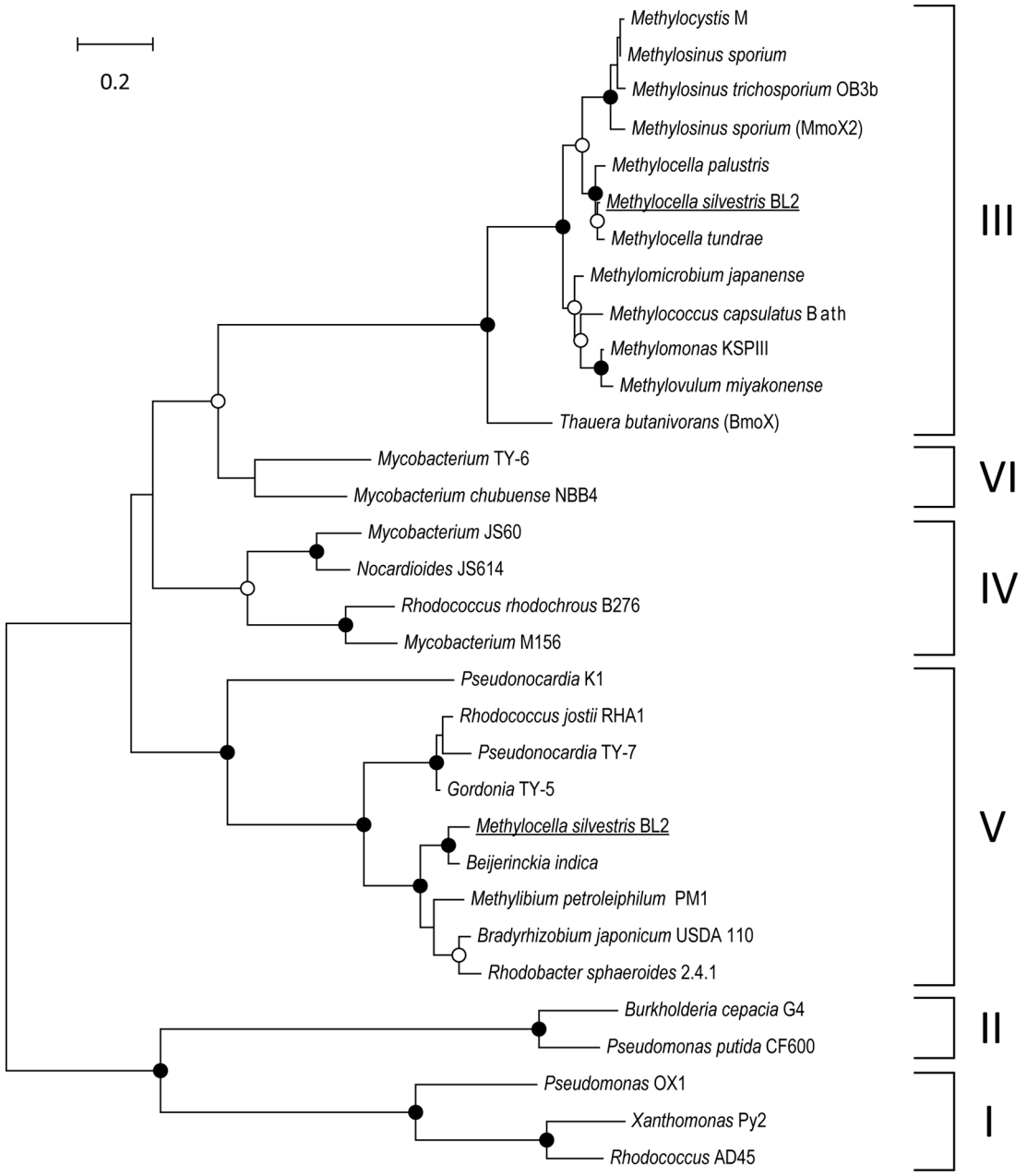

Figure 6.2. Phylogenetic relationships between the two *M. silvestris* SDIMOs (underlined) and other representative enzymes. The tree, constructed using the Maximum Likelihood method, is based on an alignment of amino acid sequences of the α-subunit of the hydroxylases. Sequences were aligned using Clustal, positions containing gaps or missing data were eliminated, and the tree constructed with a final data set of 356 amino acids using Mega5 (Tamura et al., 2007). Bootstrap values (based on 500 replications) greater than 95% are shown as filled circles at nodes, and those between 75 – 95% as open circles. The SDIMO subgroups (Leahy et al., 2003; Coleman et al., 2006) are indicated on the right of the figure. GenBank accession numbers (in order from top): AAC45289.1, ABD46892.1, ZP_06887019.1, ABD46898.1, CAD30366.1, YP_002361593.1, CAD88243.1, BAE86875.1, YP_113659.1, BAA84751.1, BAJ17645.1, AAM19727.1, BAF34294.1, ACZ56324.1, AAO48576.1, YP_919254.1, BAA07114.1, AAS19484.1, CAC10506.1, YP_700435.1, BAF34308.1, BAD03956.2, YP_002361961.1, YP_001834443.1, YP_001020147.1, NP_770317.1, YP_352924.1, AAL50373.1, P19732.1, AAT40431.1, YP_001409304.1, CAB55825.1.

6.2.2 Gene layout of the propane monooxygenase

Msil1262 encodes the hydroxylase α-subunit of the sMMO investigated previously by Theisen et al. (2005). The sMMO gene layout and that of the PrMO cluster are shown in Figure 6.3, and the closest relatives to the propane monooxygenase genes present in the SWISS-PROT/TrEMBL database are shown in Table 6.1.

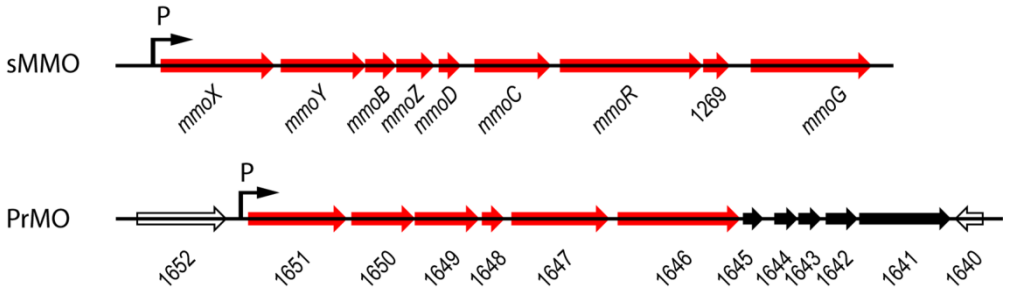

Figure 6.3. The sMMO and PrMO gene clusters. The genes previously shown, or expected, to be essential for expression of the functional monooxygenases are shown in red. Genes downstream of the PrMO, transcribed in the same direction, are shown in black. P, σ^{54} promoter.

Table 6.1. Top BLAST hits to the SWISS-PROT/TrEMBL database and protein annotations of translated sequences of the PrMO gene cluster and adjacent genes shown in Figure 6.3.

Locus tag Msil	Annotation	Organism	aa	% id
1652	Uncharacterised protein	*Methylocella silvestris*	505	50
1651	Methane monooxygenase	*Beijerinckia indica*	552	90
1650	Oxidoreductase	*Beijerinckia indica*	351	82
1649	Methane/phenol/toluene hydroxylase	*Beijerinckia indica*	357	75
1648	Phenol 2-monooxygenase	*Beijerinckia indica*	118	82
1647	60 kDa chaperonin	*Beijerinckia indica*	547	71
1646	σ^{54} transcriptional regulator	*Beijerinckia indica*	689	66
1645	Siderephore biosynthesis-like protein	*Beijerinckia indica*	117	70
1644	Cytochrome C	*Beijerinckia indica*	133	64
1643	Glyoxylase-like protein	*Beijerinckia indica*	131	77
1642	Uncharacterised	*Beijerinckia indica*	182	67
1641	Gluconate 2-dehydrogenase	*Beijerinckia indica*	522	82
1640	Transcriptional regulator *AsnC* family	*Rhizobium loti*	154	77

As can be seen from the table, all genes of the PrMO cluster have, as closest relatives, genes from *Beijerinckia indica,* although in this organism the downstream genes

(corresponding to Msil1645 – Msil1641) are located in a different area of the chromosome and do not cluster with the PrMO genes.

6.2.3 The PrMO promoter and determination of the transcription start site

The sMMO σ^{54} promoter and transcription start site (98 bp upstream of the *mmoX* start codon) were previously identified by Theisen et al. (2005). No σ^{70} promoters were obvious upstream of the PrMO, so presuming that the PrMO may also be under the control of a σ^{54} promoter, the upstream sequences of both monooxygenases were scanned using the online σ^{54} promoter prediction tool Promscan (http://molbiol-tools.ca/promscan/), which correctly identified the experimentally determined sMMO promoter, and also predicted a PrMO promoter and transcription start site 119 bp upstream of the start codon of Msil1651, as shown in Figure 6.4.

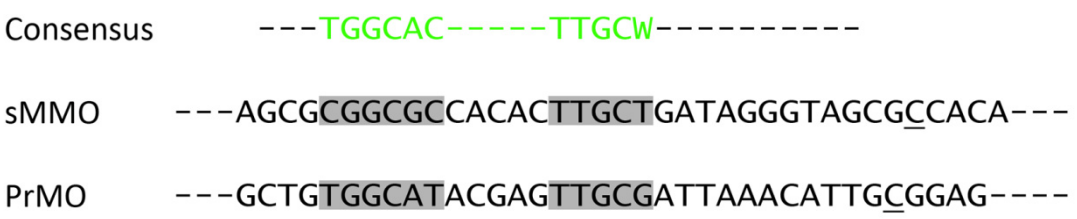

Figure 6.4. σ^{54} promoters identified upstream of the sMMO and PrMO gene clusters using the online tool Promscan. The σ^{54} consensus sequence compiled by Barrios et al. (1999) is shown in green, the predicted transcription start sites are underlined, and the conserved -12 and -24 regions are shown shaded.

Rapid amplification of cDNA ends (RACE) was used to empirically determine the PrMO transcription start site, using a 2nd Generation 5'/3' RACE kit (ROCHE, Basel, Switzerland), as described in Materials and Methods. RNA was extracted from cells grown on propane, and cDNA synthesised from 100 ng RNA using antisense primer 51Ra1 located at +643 relative to the predicted transcription start site (see Table 6.8 for primer sequences). Using a cDNA template, a first round of PCR with reverse primer 51Ra2 (position +545), followed by a second round of PCR using nested reverse primer 51Ra3 (position +317) (together with the forward primers supplied in the ROCHE kit) resulted in an amplicon of the expected size, see Figure 6.5. The PCR product was cloned and two clones were sequenced. Both sequences identified the transcription start site as 120 nucleotides upstream of the start codon, consistent with the predicted promoter sequence shown in Figure 6.4.

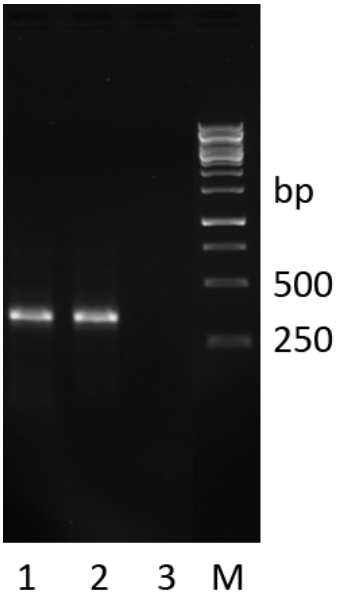

Figure 6.5. PCR amplicons generated using RACE and nested PCR using reverse primers 51Ra2 followed by 51Ra3. PCR template was 1 µl of the first round PCR either undiluted (lane 1) or using a 1/10 dilution (lane 2). Lane 3: no-template control. M: Generuler 1 kb ladder (Fermentas). Band size 355 bp.

6.2.4 Promoters located internally in the PrMO gene cluster

In order to locate other promoters from which PrMO-cluster genes may be transcribed, the entire cluster (15 kb) was scanned for σ^{70} promoter sequences using the Berkeley Drosophila Genome Project Neural Network Promoter Prediction online tool (http://www.fruitfly.org/seq_tools/promoter.html). This identified 18 possible promoter sequences (scores 0.80 to 0.98, data not shown). Of these, only one was not located in a predicted open reading frame, lessening the likelihood of transcription being controlled from these sequences. The inter-gene site, with a relatively low score of 0.8, was predicted to direct transcription from a site 91 bp upstream of the start codon of Msil1646. Since this gene encodes a σ^{54} transcriptional regulator, expression of which is assumed to be required for transcription of the PrMO cluster, separate transcription of this gene, possibly at a low level, would seem likely.

RACE was used in an attempt to identify transcription from this site. However, cDNA synthesised from propane-grown RNA, using primer 46Ra1, was found to extend into the preceding open reading frame, further upstream than the predicted transcription start site (data not shown). It is possible that Msil1646 is co-transcribed

both as part of the entire PrMO gene cluster, induced under the appropriate conditions, and also constitutively from its own promoter. Perhaps the existence of long transcripts, originating from the promoter upstream of the start of the PrMO cluster, prevented detection of low abundance transcripts originating from a promoter in this region. In this case, the use of RNA extracted from cells grown on a different substrate, under conditions in which the PrMO is not transcribed, might detect low level constitutive transcription from this site, but time did not allow further investigation of this topic.

6.2.5 Inter-gene RT-PCR

A considerable amount of time and effort was expended attempting to determine the extent of co-transcription of the PrMO gene cluster, using inter-gene PCR amplification of cDNA synthesised from mRNA extracted from propane-grown cells. Three slightly different methods were used, but all were ultimately inconclusive. Since this work has potential implications for the use of this technique, it is described in detail.

6.2.5.1 cDNA synthesis using random hexamer primers and Superscript II enzyme

Initially, cDNA was synthesised from approximately 60 ng total RNA in 20 µl reactions using Superscript II enzyme (Invitrogen) and random hexamer primers, using the procedures and quality checks as described in Materials and Methods. Using this method, transcripts were detected across all inter-gene spaces from Msil1651 to Msil1641 (Figure 6.6 and data not shown). However, an amplicon was also obtained in a control reaction employing primers located outside the region expected to be co-transcribed (i.e. spanning the region Msil1640 – Msil1641, since these genes are predicted to be transcribed in opposing directions), suggested that the presence of mRNA corresponding to this region is due either to the continuation of transcription for a considerable distance beyond the end of the coding sequence, and/or to the presence of an mRNA molecule transcribed from the opposite strand, see Figure 6.6, which shows reactions targeting the region downstream of Msil1647. It was found that PCR products up to approximately 2 kbp could be successfully amplified from cDNA templates, above which size efficiency diminished.

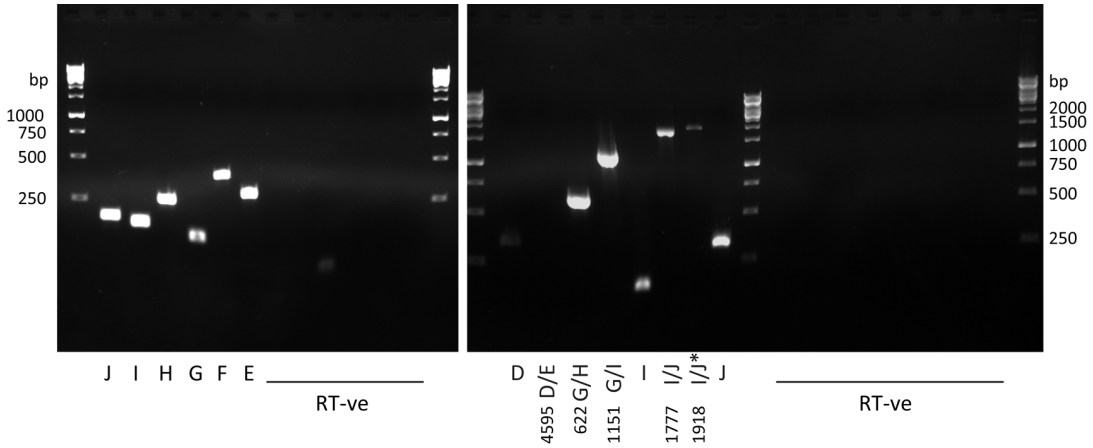

Figure 6.6. PCR spanning the inter-gene regions of the PrMO gene cluster using a cDNA template, synthesised using random hexamer primers. Lanes are identified by the letters corresponding to the PCR primers shown in Figure 6.7, which also shows the expected product sizes for these primers. Where other primer combinations have been used the expected amplicon size is shown below. Controls using cDNA synthesis reactions omitting the reverse transcriptase enzyme are identified as RT-ve, and correspond with the reactions to the left. DNA marker lanes (unlabelled) contain GeneRuler 1kb ladder (Fermentas). PCR reactions using DNA templates generated amplicons of the same sizes, and are not shown.

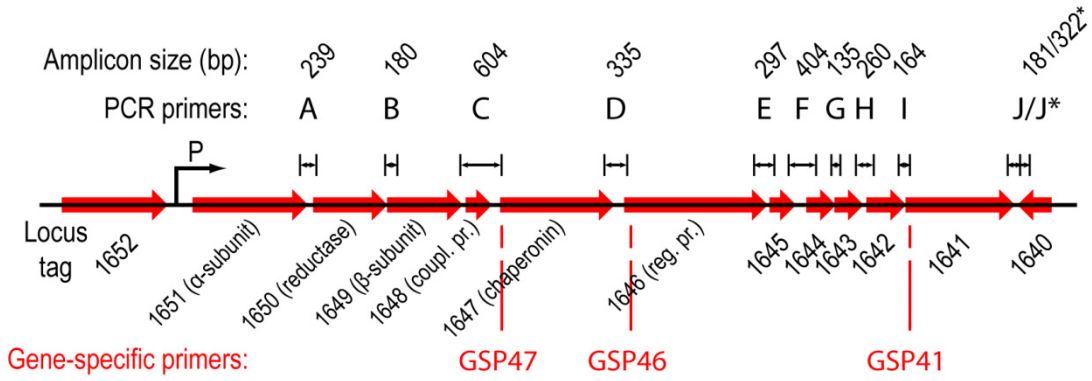

Figure 6.7. The PrMO gene cluster, showing locations of inter-gene PCR using a cDNA template, and primers designed to generate amplicons labelled A – J. The sizes of the PCR amplicons are shown above. Position J used one of two alternative reverse primers, resulting in products differing in size by 141 bp, of which the larger is indicated with an asterisk. cDNA synthesis used either random hexamer primers, or gene-specific primers GSP41, GSP46 or GSP47, indicated in red. In some cases PCR reactions were also included using combinations of primers, for example forward primer G combined with reverse primer H, identified as G/H in gel photographs. P, σ^{54} promoter; coupl. pr., coupling protein; reg. pr., regulatory protein.

6.2.5.2 cDNA synthesis using gene-specific primers

Since discrimination between mRNA molecules transcribed from opposing strands is not possible using random hexamer primers, this experiment was repeated using gene-specific anti-sense primers for cDNA synthesis. Three primers were used (GSP41, GSP46 and GSP47), located as shown in Figure 6.7.

As before, cDNA was synthesised using approximately 60 ng total RNA in 20 µl reactions using Superscript II reverse transcriptase (Invitrogen). Once again, PCR products were obtained using primers spanning all inter-gene spaces, although primers spanning Msil1646 and Msil1647 generated a very weak product just visible on the gels, and only when using cDNA synthesised from the nearby gene-specific primer, see Figure 6.8. However, products were also obtained using primers downstream of the gene-specific primer used to synthesise cDNA (product J with GSP41 and product E with GSP46, see Figure 6.7). Since cDNA is synthesised by reverse transcriptase directionally, there should be no cDNA template in these reactions. In attempting to identify the cause of these apparent artefacts, non-specific binding of the PCR primers was ruled out since well-defined products were obtained using both DNA and cDNA templates, both of which corresponded to the predicted sizes. Contamination of RNA with DNA was ruled out since not only was no product obtained with 16S rRNA PCR reactions using an RNA template, including with increased template amount and an increased number of cycles (see Materials and Methods), but no product was obtained in any case where reverse transcriptase was omitted from otherwise identical cDNA-synthesis reactions. Other sources of contamination were ruled out by the use of different batches of reagents, and by the use of RNA extracted on different occasions. However, initially, non-specific binding of the gene-specific primer during cDNA synthesis was considered a possibility, since Superscript II reverse transcriptase operates at the relatively low temperature of 42° C, raising the possibility of annealing of the primer to non-target sequences.

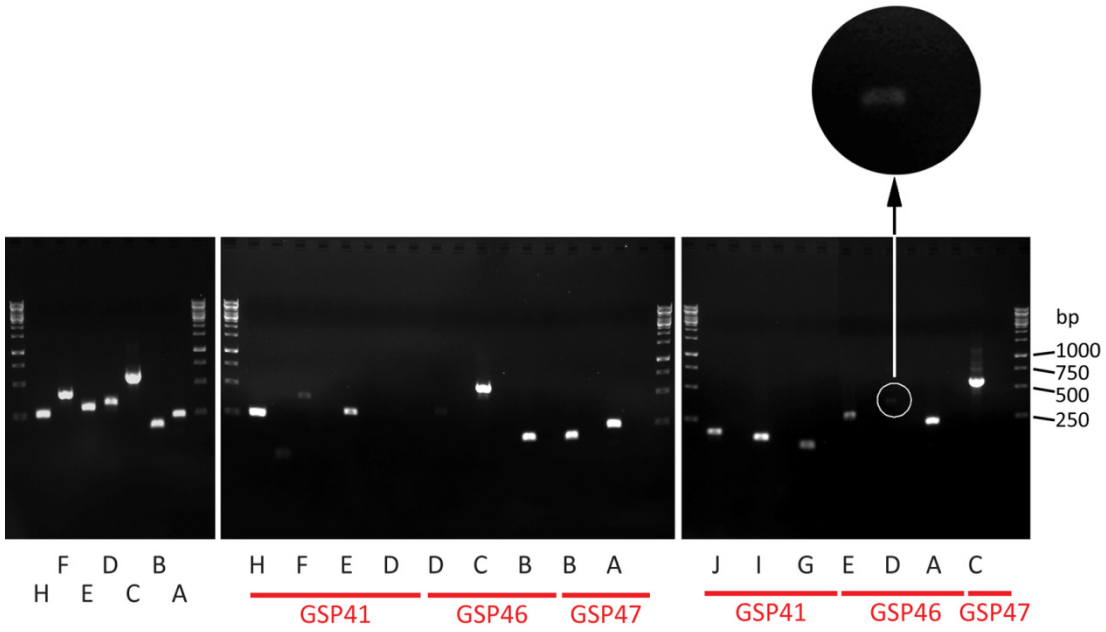

Figure 6.8. PCR spanning PrMO-cluster inter-gene regions using DNA (left-hand gel) or cDNA templates (centre and right-hand gels), where cDNA was synthesised using the gene-specific primers indicated below (in red). Lanes are identified by the primer locations shown in Figure 6.7, which also indicates expected PCR amplicon sizes. Corresponding controls (using cDNA-synthesis reactions omitting reverse transcriptase) are immediately to the right of each labelled lane. Products J and E in the right-hand gel imply cDNA synthesis downstream of the gene-specific primer employed. DNA marker lanes (unlabelled) contain GeneRuler 1kb ladder (Fermentas). The feint band in lane D (right-hand gel) is shown enlarged for clarity.

6.2.5.3 Use of gene-specific primers, Superscript III enzyme, and controls without primer during cDNA synthesis

In order to reduce non-target primer binding during cDNA synthesis, reactions were carried out using 1 µg total RNA in 20 µl reactions to provide an increased ratio of target:primer molecules, and by the use of Superscript III reverse transcriptase at 55° C. In addition, RNase H was used to remove traces of RNA following reverse transcription. As before, cDNA-synthesis reactions were included, identical except without the addition of reverse transcriptase, and additional controls were included in which cDNA synthesis reactions did not contain any primer (no primer controls, NPC), as recommended by Guacucano et al. (2000) and Zhou and Yang (2006). Transcripts were detected for all inter-gene spaces, see Figure 6.9 and Figure 6.10.

Increased sensitivity due to the increased amount of RNA used for cDNA synthesis resulted in increased intensity of PCR amplicons spanning Msil1647 to Msil1646.

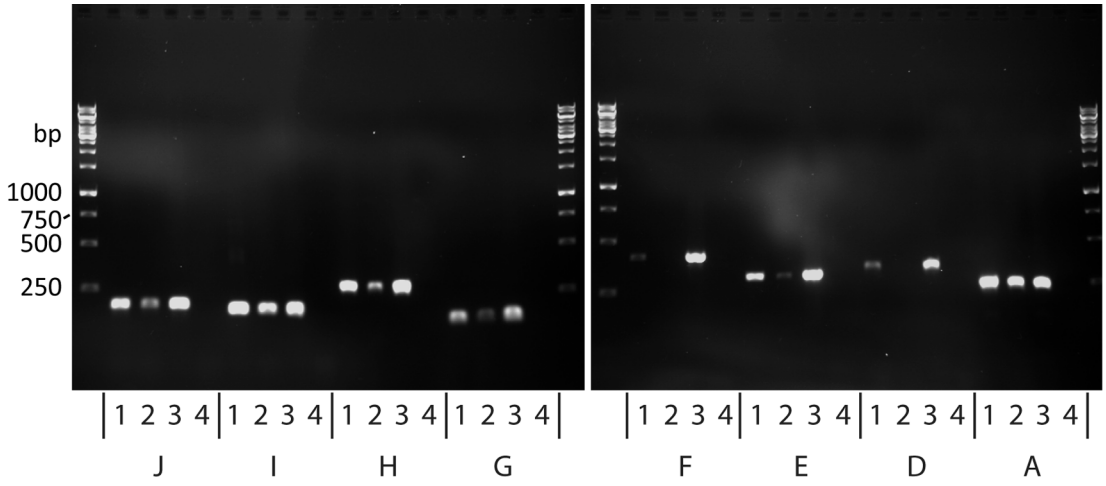

Figure 6.9. PCR spanning PrMO-cluster inter-gene regions. Each group of four lanes used PCR primers identified by letters A – J as shown in Figure 6.7, which also indicates expected PCR amplicon sizes. Lanes, 1: cDNA template synthesised with gene-specific primer GSP41, 2: control with no primer in the cDNA synthesis reaction (NPC), 3: DNA template, 4: control without reverse transcriptase in cDNA synthesis reaction. DNA marker lanes (unlabelled) contain GeneRuler 1kb ladder (Fermentas).

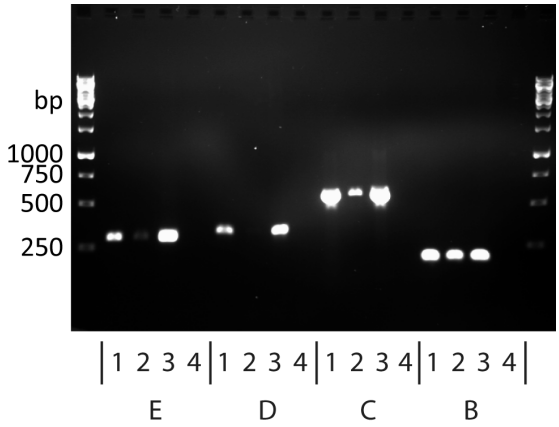

Figure 6.10. As Figure 6.9, except gene-specific primer GSP46 used for cDNA synthesis.

However, the control reactions in which no primer was included during cDNA synthesis resulted in transcripts covering most of the inter-gene regions. In only two cases, when using PCR primer pairs D and F, was no product obtained in these control reactions, although in all cases less PCR product was obtained. This was consistent between replicated reactions, and revealed a variation in the level of PCR amplification obtained depending on the primer pair used, additionally arguing against contamination as the cause. Guacucano et al. (2000) also generated PCR

amplicons using cDNA templates synthesised without primers, and suggested that this was an artefact caused by self-priming of the mRNA molecules. This has long been recognised as a problem in the field of virology, where virus detection frequently requires strand differentiation (McGuinness et al., 1994; Tuiskunen et al., 2010). It is however difficult to account for the variability of PCR product obtained from self-primed cDNA synthesis compared to reactions with primer included. Therefore it is difficult to draw definite conclusions from these data. It seems highly likely that transcripts exist where PCR products were obtained. If this is the case, then there are two unanswered questions; how does cDNA synthesis occur without inclusion of a primer, and which DNA strand does the transcript originate from? Recent studies have highlighted the detection of long (up to 1000s of nucleotides) and medium length anti-sense RNA molecules, including those partially or completely overlapping protein coding regions (reviewed by Thomason and Storz (2010)). Many of these occur in same region as transcriptional regulators, and play a role in the control of protein expression. The existence of anti-sense RNA molecules in this area of the *M. silvestris* chromosome, which might contribute towards self-priming and thus help to explain the results presented, cannot be discounted, but clearly, if this is the case and antisense transcription is being detected, this cannot be used as evidence of gene co-transcription. Possible future approaches would include the use of a different method, for example Northern blots, or inclusion of a unique tag included at the 5' end of the gene-specific primer used for cDNA synthesis, which could subsequently be used as primer binding site for PCR amplification, such that only cDNA synthesised from the tagged primer was able to act as PCR template. Lack of time prevented further investigation of this topic.

6.2.6 Transcription of the propane monooxygenase

Qualitative assessment of transcription from the propane monooxygenase σ^{54} promoter was made by construction of a promoter probe vector. As starting point, pMHA203 (Ali, 2006) was selected for modification. This vector contains the promoter region of the *M. silvestris* sMMO fused to *gfp,* encoding green fluorescent protein (GFP), so that cells containing this vector express GFP under conditions that lead to transcription of the sMMO gene cluster. Primers PrPf and PrPr, incorporating *Mun*I and *Sac*I sites respectively, were used to amplify the 1112 bp promoter-containing region extending upstream from 44 bp 5' of the predicted start codon of Msil1651, encoding the PrMO hydroxylase α-subunit, see Figure 6.11. The PCR product was cloned into pCR2.1 TOPO, and excised by digestion with *Mun*I and *Sac*I. The *mmoX* promoter region of pMHA203 was removed by digestion with *EcoR*I and *Sac*I, followed by its replacement with the compatible *Mun*I / *Sac*I fragment containing the PrMO promoter region. This vector, and also pMHA203, were introduced into *M. silvestris* by electroporation and selection on DNMS kanamycin plates with methanol as growth substrate.

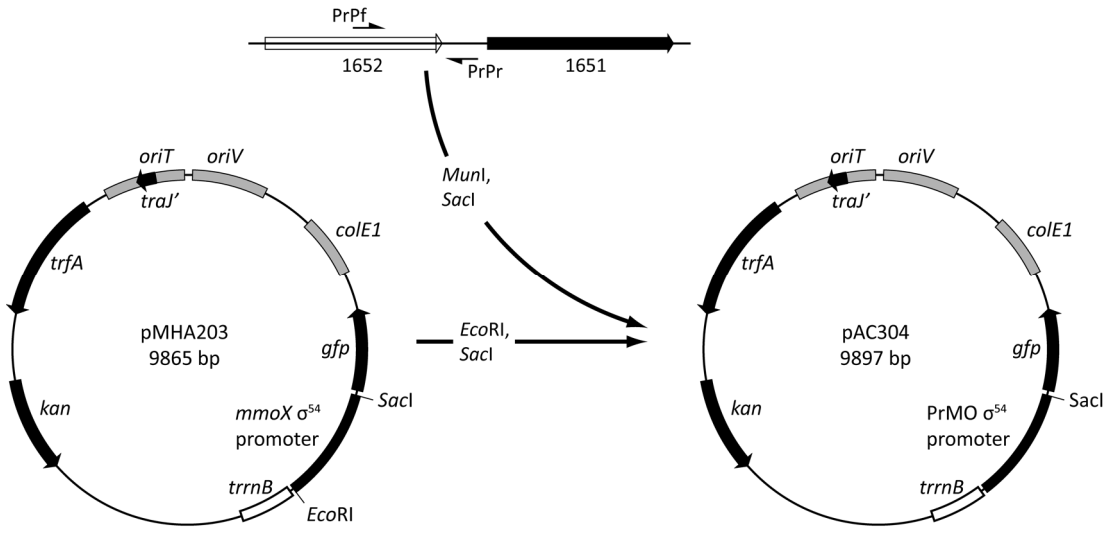

Figure 6.11. Construction of promoter probe vector pAC304 by modification of pMHA203. Primers PrPf and PrPr were used to amplify a sequence containing the PrMO promoter, which replaced the *mmoX* promoter-containing *Eco*RI / *Sac*I region in pMHA203.

Kanamycin-resistant colonies were transferred into liquid culture and grown on methanol (0.1% v/v), methane (20% v/v) or propane (20% v/v). At late exponential phase, cells were visualised by fluorescence microscopy. Whereas both methane- and

propane-grown cells containing pMHA203 were fluorescent, in cells containing pAC304, fluorescence was only visible with propane as substrate, see Figure 6.12. No fluorescence was visible with methanol-grown cells containing either plasmid. This provided evidence that transcription of the sMMO occurs in response to either methane or propane, and that transcription of the PrMO is activated by propane but not by methane.

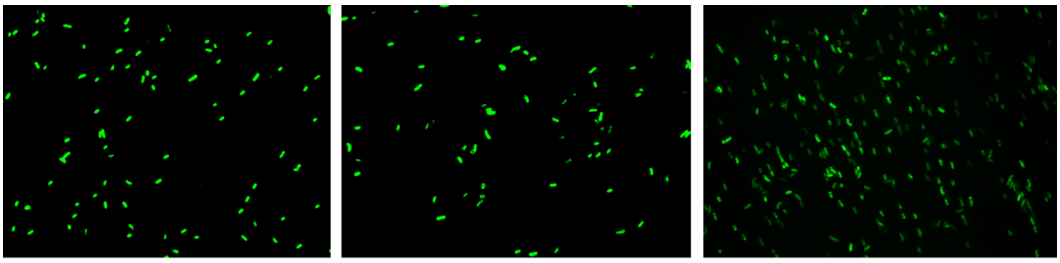

Figure 6.12. *M. silvestris* cells containing plasmid pMHA203 or plasmid pAC304 were grown on methane, propane or methanol. Fluorescent cells containing pMHA203 were present during growth on both methane and propane, but fluorescent cells containing pAC304 were exclusive to propane-supplied cultures. No fluorescent cells were observed in cells containing pAC304 grown on methane, or on methanol-grown cells containing either plasmid. The figure shows pseudocoloured GFP-expressing cells.

6.3 Growth on methane and propane

6.3.1 Gas purity

Methane and propane used for growth were assessed for purity by gas chromatography as described in Materials and Methods. CO_2 present in the CH_4/CO_2 gas mix used for growth in flasks was determined to be 3% v/v. Impurities were identified by comparison of their retention time with standards prepared from the authentic compounds. Ethane (approx 67 ppmv) was the only impurity detected in methane. Methane was detected at an extremely low level in propane. In the absence of standards in this range (below atmospheric concentration), the methane impurity in propane (1.28 ± 0.38, n = 6) was compared with atmospheric air (3.88 ± 0.50, n = 6) and oxygen-free nitrogen (British Oxygen PLC) (1.07 ± 0.65, n = 9) on the basis of peak area (± standard deviation). These data show that the methane content of the

propane used was less than that of atmospheric air. An unidentified impurity with a peak area approximately 0.3% of the propane peak area eluted at approximately 6 min, (compared with propane at 2.7 min at the settings employed). This was not ethane, butane, ethene, propene, acetylene, methanol, 1-propanol, 2-propanol, acetone, acetol or methyl acetate and did not diminish as a component of headspace gas as cultures grew.

6.3.2 Growth of *M. silvestris* on methane and propane

M. silvestris was able to grow with either methane or propane as sole source of carbon and energy in fermenter culture as outlined in Chapter 3. Specific growth rate was similar and nitrogen fixation was possible in both cases. *M. silvestris* was grown in 20 ml volumes in 120 ml serum vials in triplicate with 20% (v/v) methane or 20% (v/v) propane. Specific growth rate (± standard deviation) was similar in both cases (methane 0.013 h^{-1} ± 0.003, propane 0.015 h^{-1} ± 0.002).

6.4 Expression of the sMMO and PrMO during growth on methane and propane

6.4.1 SDS-PAGE

One-dimension denaturing PAGE was used to examine the expression of the methane and propane monooxygenase subunits during growth on methane, propane and a mixture of these substrates. Soluble extract was prepared from fermenter-grown cells and from cells (200 ml) grown in 1 l flasks on propane or a mixture of methane and propane (all 10% v/v). Protein was quantified and 12 - 20 µg loaded on 10% or 15% (w/v) SDS-PAGE or 10% bis-tris NUPAGE gels (Invitrogen), together with soluble extract prepared from succinate-grown cells, see Figure 6.13.

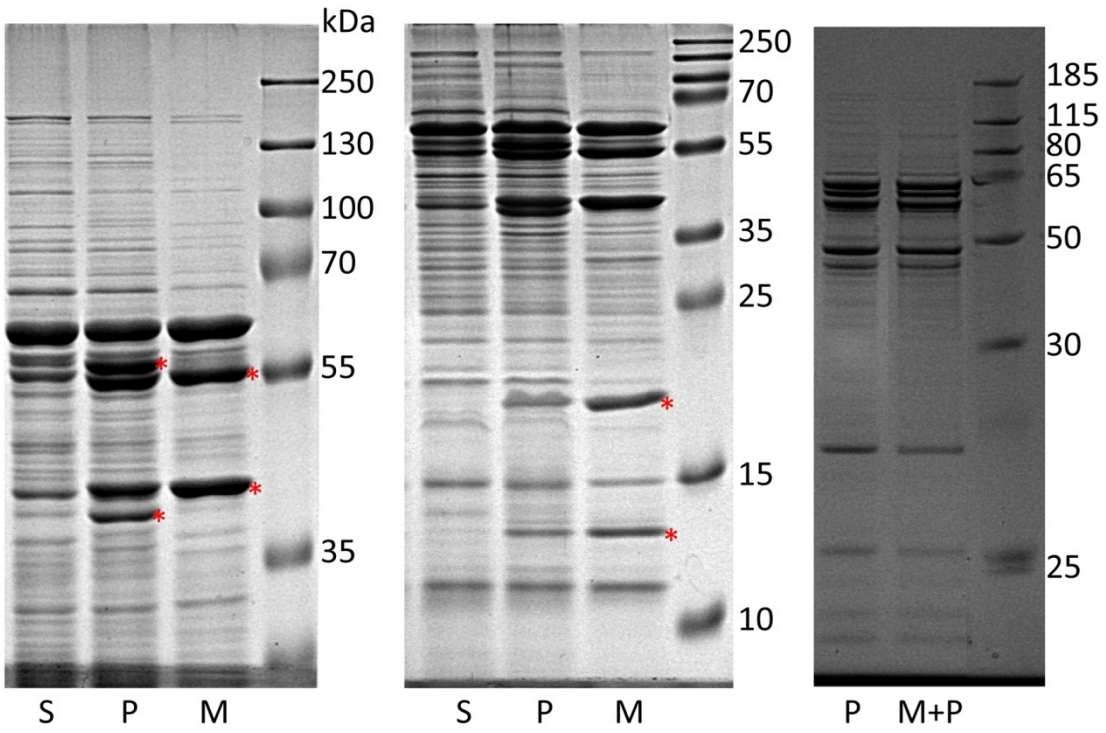

Figure 6.13. Left-hand gel: 10% SDS-PAGE, centre: 15% SDS-PAGE and right: 10% NUPAGE gels loaded with soluble extract of cells grown on succinate (S) propane (P) methane (M) or a mixture of methane and propane (M+P). Prominent bands present in extract from growth on methane or propane but absent from the succinate-grown lanes are marked with asterisks. Molecular mass marker: PageRuler Plus prestained protein ladder (Fermentas).

Four bands (marked with asterisks in the figure) were visible in the lanes corresponding to methane-grown cells that were either absent or much less prominent in succinate grown cells. The molecular mass of these bands corresponded approximately with the known sizes of the sMMO subunits from purified enzymes from characterised methanotrophs (54.4, 43.0, 22.7, 39.7 and 15.8 kDa for the α-, β-, γ-subunits, reductase and coupling protein, respectively for the enzyme from *Methylosinus trichosporium* OB3b (Fox et al., 1989)). Two prominent bands in the propane-grown lanes did not appear in the methane or succinate lanes. This suggested that the prominent bands present in methane- and propane- grown cells might correspond with the subunits of the respective monooxygenases. The bands shown in Figure 6.14 were excised from the gels and submitted to the Proteomics and Mass Spectrometry Facility of the University of Warwick for tryptic digest and analysis by nanoLC/ESI-MS/MS. It was also apparent that the major bands present in the methane growth condition, but not in succinate, also occur in the propane-grown

lanes, whereas the bands unique to the propane lanes are not present in methane. There are also few, if any, detectable differences between the lanes corresponding to propane and propane plus methane. Mass spectrometric results confirmed that the expected bands corresponded to four of the subunits of the sMMO and to the two subunits of the PrMO hydroxylase. Only sMMO subunits were identified in soluble extract from methane-grown cells, whereas in the propane-grown condition, components of both monooxygenases were detected. Neither SDIMO was expressed in succinate-grown cells. These data confirm that the PrMO is not expressed at high level (if at all) during growth on methane, whereas both monooxygenases are expressed during growth on propane. The prominent band at approximately 60 kDa in lanes from all growth conditions was confirmed to be methanol dehydrogenase (MDH).

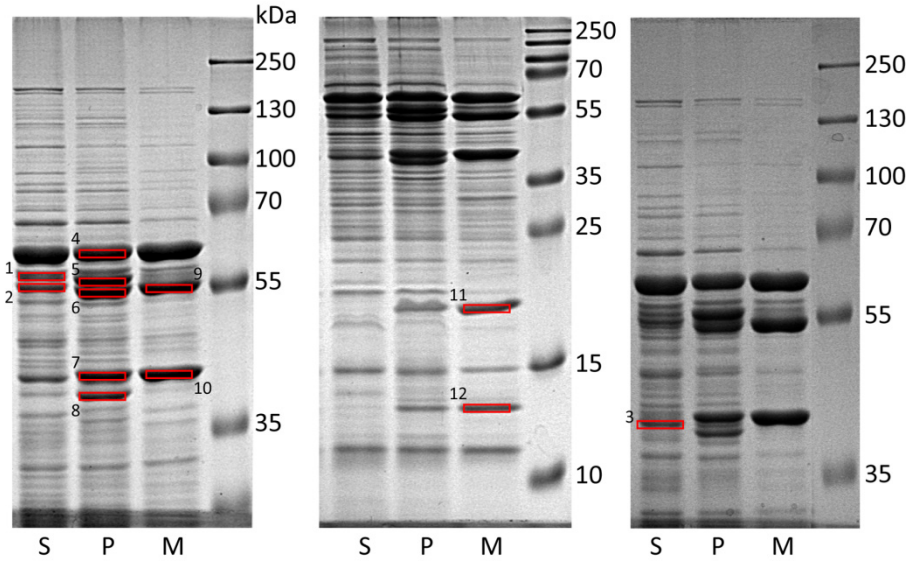

Figure 6.14. Bands from the 10% and 15% SDS-PAGE gels shown in Figure 6.13, and an additional 10% gel (right) were selected for analysis. The red rectangles identify bands which were excised and identified by tryptic digest and mass-spectrometric analysis. Band-identifying numbers refer to Table 6.2. Gels were loaded with soluble extract from cells grown on succinate (S), propane (P) or methane (M).

Table 6.2. Polypeptide identifications of the gel bands shown in Figure 6.14. For each band, the four most abundant polypeptides are shown except where less than four were detected. In addition, in the case of lanes loaded with propane or methane extract, all polypeptides identified with at least three peptides are included, but including all polypeptides encoded by genes of the sMMO and PrMO clusters irrespective of the number of peptides used for identification. Other polypeptides identified are not shown. The number of peptides detected and used to identify each polypeptide is shown. The total number of peptides detected from all polypeptides identified in each band is shown for comparison. MM: theoretical molecular mass, DH: dehydrogenase.

Band	Growth condition	Locus tag Msil	Annotation	Peptides	Total peptides	MM kDa
1	Succinate	0795	Chaperonin	20	119	57.6
		3763	Hydrogenase	16		59.9
		3631	Nitrogenase s/u	12		58.2
		3630	Nitrogenase s/u	11		58.2
2	Succinate	2342	Aldehyde DH	17	46	55.6
		3881	Aldehyde DH	8		53.3
		2301	Unknown function	4		55.8
		1608	FeS assembly protein	3		54.3
3	Succinate	2996	Acetyl CoA acetyltransferase	15	29	40.2
		0082	GDP mannose 4,6-dehydratase	5		39.5
		1354	Hypothetical protein	4		43.2
		0471	MDH α-subunit	3		68.5
4	Propane	0471	MDH α-subunit	33	33	68.5
5	Propane	1651	PrMO α-subunit	18	59	64.2
		1641	Gluconate dehydrogenase	9		56.7
		0795	Chaperonin GroEL	7		57.6
		1375	PEP carboxykinase	6		58.2
		1647	Chaperonin (PrMO cluster)	3		57.3
		2506	Dihydrolipoyl dehydrogenase	3		49.4
		0162	Fumarase	3		58.6
		1262	MmoX	2		59.8
6	Propane	1262	MmoX	20	48	59.8
		2342	Aldehyde dehydrogenase	12		55.6
		1651	PrMO α-subunit	5		64.2
		0410	Beta-lactamase	5		52.4
		3881	Aldehyde dehydrogenase	3		53.3
		1263	MmoY	3		44.9
7	Propane	1263	MmoY	23	49	44.9
		2007	Urea transporter	9		43.4
		3698	NADH flavin oxidase	5		39.2
		1267	MmoC	5		38.5
		2996	Acetyl-CoA acetyl transferase	3		40.2
		1262	MmoX	2		59.8
8	Propane	1649	PrMO β-subunit	11	22	40.2
		1263	MmoY	5		44.9
		2400	Formylmethanofuran DH	4		39.2
		1265	MmoZ	2		19.5
9	Methane	1262	MmoX	22	28	59.8
		1263	MmoY	4		44.9
		2342	Aldehyde dehydrogenase	2		55.6

Table 6.2 (continued).

Band	Growth condition	Locus tag Msil	Annotation	Peptides	Total peptides	MM kDa
10	Methane	1263	MmoY	25	27	44.9
		1262	MmoX	2		59.8
11	Methane	1265	MmoZ	12	18	19.5
		2360	Type VI secretion protein	3		19.9
		1262	MmoX	3		59.8
12	Methane	1264	MmoB	7	17	15.3
		3206	UspA domain protein	3		16.0
		1263	MmoY	3		44.9
		1265	MmoZ	2		19.5
		1262	MmoX	2		59.8

6.4.2 Naphthalene assay

Both methane-grown and propane-grown cells gave a positive naphthalene assay result. However, since the sMMO and SDIMOs in general are known to possess wide substrate specificity (Colby et al., 1977), these data did not provide any evidence as to which enzyme was responsible. For the same reason, enzyme assays based on measuring, for example, the epoxidation of propene, would not enable the two enzymes to be distinguished, and were not attempted.

6.5 Substrate utilisation during growth on methane and propane

6.5.1 Wild type growth on 2.5% methane and propane

M. silvestris was grown in 25 ml volumes in 120 ml serum vials on a mixture of 2.5% (v/v) methane and propane. The Henry's law constants for methane and propane are similar ($K_H = 1.3 \times 10^{-3}$ and 1.4×10^{-3} M atm^{-1} respectively (Mackay and Shiu, 1981)) so at equilibrium this would result in similar concentrations in the aqueous phase. These gas concentrations allowed measurement of substrate uptake by gas chromatography. The cultures used the two gases in an extremely co-ordinated manner, whether the inoculum was from succinate-grown or methane and propane-grown cells, see Figure 6.15.

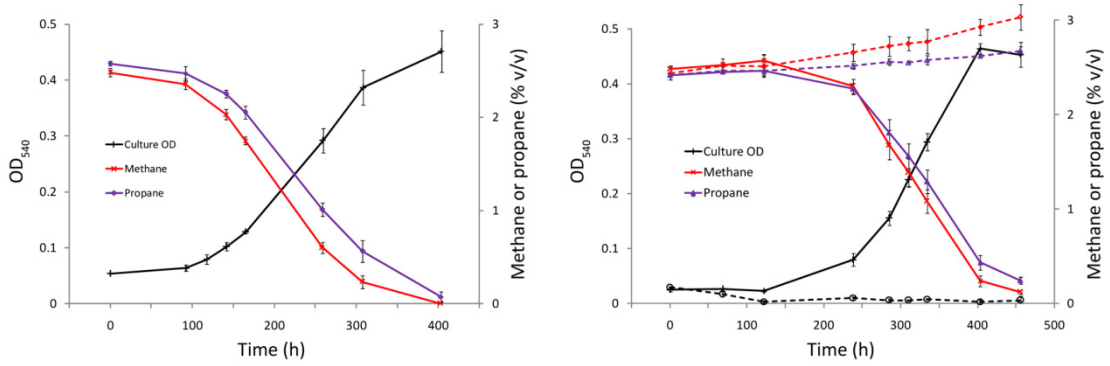

Figure 6.15. Growth (black lines) and gas consumption of *M. silvestris* during growth on a mixture of methane (red) and propane (purple) (2.5% v/v each). The experiment illustrated in the left-hand graph used succinate-grown inoculum, while that on the right used inoculum grown on a mixture of methane and propane. Dashed lines represent killed control vials. All data points are the mean of three replicates and error bars indicate the standard deviation.

The equivalent rates of gas consumption, which imply a three fold higher carbon consumption originating from propane, and the relatively linear growth rate at culture densities over OD_{540} ~ 0.15, suggest either that substrate oxidation may be limited by some factor such as mass transfer from the gas to the liquid phases, and/or that the kinetic properties of the enzymes concerned are equivalent for the two substrates. Therefore, these data do not shed light on the relative rates of methane and propane oxidation by the sMMO and PrMO.

6.5.2 Deletion of the α-subunit of the propane monooxygenase hydroxylase

Strain ΔPrMO, with a deletion of Msil1651, encoding the α-subunit of the propane monooxygenase hydroxylase, was constructed as described in Chapter 4. The result (confirmed by sequencing) was the deletion of the entire Msil1651 coding sequence together with 67 bp upstream and 41 bp downstream, and the insertion of 100 bp of vector sequence containing a single *loxP* site. This strain grew on methanol (0.05% v/v), ethanol (0.05% v/v) or acetate (5mM) indistinguishably from the wild-type, see Figure 6.16.

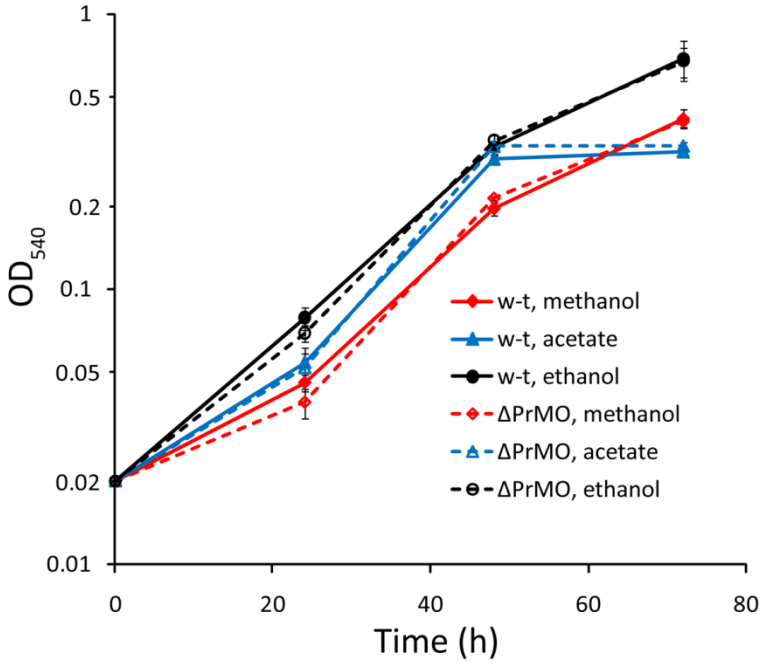

Figure 6.16. Growth of *M. silvestris* strain ΔPrMO (dashed lines and open symbols) on methanol (red), ethanol (black) or acetate (blue lines), in comparison with the wild-type strain (solid lines and filled symbols). Data points represent the mean of readings from triplicate flasks and error bars indicate the standard deviation.

6.5.3 Growth of strain ΔPrMO on 20% v/v methane or propane

Strain ΔPrMO grew on methane (20% v/v) similarly to the wild-type, but was completely unable to grow on propane (20% v/v), as shown in Figure 6.17 and in tabular form in Table 6.3.

Table 6.3. Growth of *M. silvestris* wild-type and strain ΔPrMO on methane or propane (20% v/v). Data show the mean of triplicate cultures ± standard deviation.

Substrate	Strain	Specific growth rate (h^{-1})	Lag time (h)	Increase in OD_{540}
methane	Wild-type	0.013 ± 0.003	63 ± 11	0.48 ± 0.05
	ΔPrMO	0.019 ± 0.005	60 ± 22	0.48 ± 0.06
propane	Wild-type	0.015 ± 0.002	199 ± 30	0.28 ± 0.02
	ΔPrMO	0	-	0

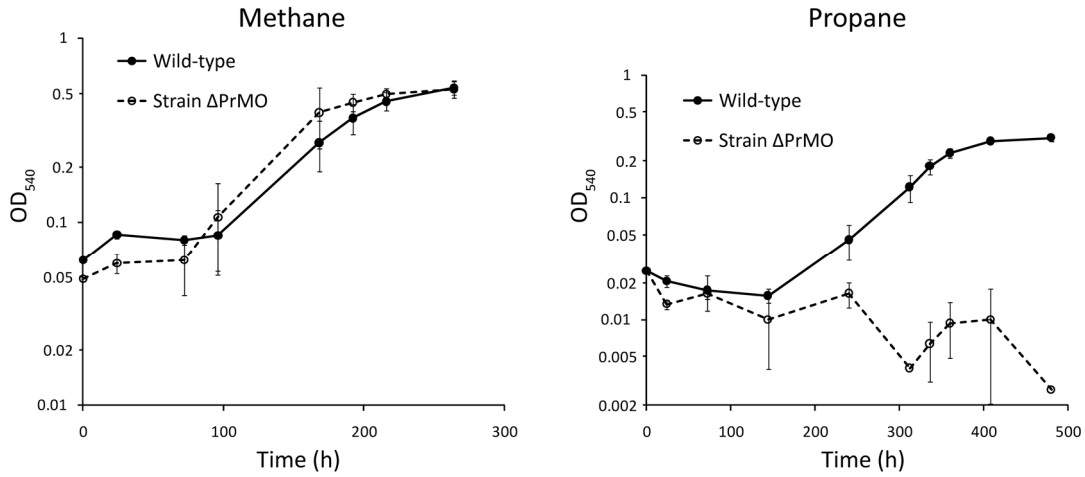

Figure 6.17. Growth of *M. silvestris* wild-type (solid lines and filled symbols) and strain ΔPrMO (dashed lines, open symbols) on methane (left) or propane (right) (both 20% v/v). Data points represent the mean of readings from triplicate flasks and error bars indicate the standard deviation.

6.5.4 Growth of strain ΔPrMO on 2.5% (v/v) methane and propane

Surprisingly, despite deletion of the propane monooxygenase hydroxylase α-subunit and the inability of strain ΔPrMO to grow on 20% (v/v) propane, during growth on a mixture of 2.5% (v/v each) methane and propane, strain ΔPrMO both grew and consumed the gases similarly to the wild type, as shown in Figure 6.18, in comparison with Figure 6.15. To eliminate the possibility that these cultures were contaminated with wild-type cells, serial dilutions were made from the cultures, and spread on DNMS plates and incubated with methanol. Colonies grew, indicating a culture density of 1.8×10^8 cfu ml^{-1} (corresponding approximately with the measured OD), of which 12 were tested by PCR using primers 1651Tf/1651Tr, revealing the deletion genotype in all cases (data not shown).

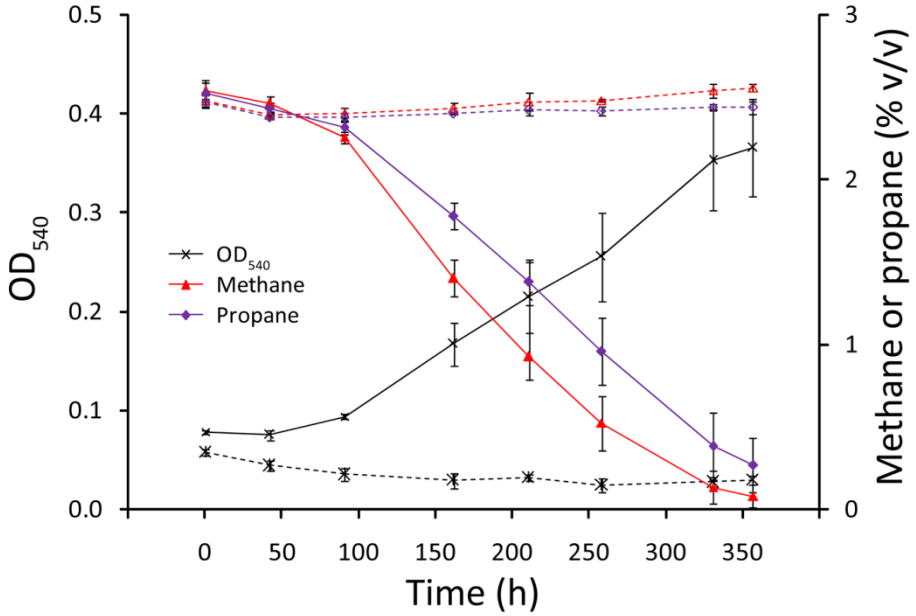

Figure 6.18. Growth of strain ΔPrMO on a mixture of methane and propane (2.5% v/v each). Control vials, containing cells killed by autoclaving, are shown as dashed lines. Data points represent the mean of readings from triplicate flasks and error bars indicate the standard deviation.

Growth on 2.5% v/v gas was then repeated, using this concentration of each gas either alone or as a mixture, in strain ΔPrMO alongside the wild-type. Strain ΔPrMO was able to grow not only on 2.5% v/v methane, but also, at a reduced specific growth rate, on 2.5% v/v propane, as shown in Figure 6.19 and Table 6.4. Growth on the gas mixture replicated data shown in Figure 6.18, but allowed additional comparison with the wild-type and with growth on each gas alone. In contrast to growth on propane alone, growth rate and biomass increase on the gas mixture approached that of the wild-type, although 75% of carbon consumed was in the form of propane, see Figure 6.20.

Table 6.4. Specific growth rate, lag time and increase in biomass of *M. silvestris* wild-type and strain ΔPrMO during growth on methane, propane, or a mixture (all at 2.5% v/v). Data show the mean of triplicate cultures ± standard deviation.

	Specific growth rate (h^{-1})		Lag time (h)		Biomass increase (OD_{540})	
	Wild-type	ΔPrMO	Wild-type	ΔPrMO	Wild-type	ΔPrMO
Methane	0.011 ± 0.001	0.013 ± 0.003	112 ± 23	71 ± 16	0.07 ± 0.01	0.06 ± 0.01
Methane plus propane	0.012 ± 0.000	0.011 ± 0.002	90 ± 3	108 ± 22	0.42 ± 0.01	0.38 ± 0.01
Propane	0.007 ± 0.000	0.004 ± 0.001	123 ± 15	177 ± 19	0.33 ± 0.01	0.23 ± 0.03

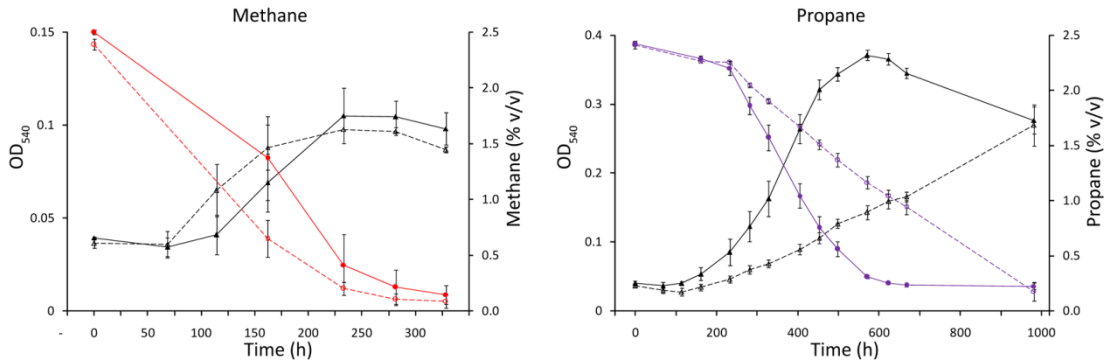

Figure 6.19. Growth of *M. silvestris* wild-type (solid lines and filled symbols) and strain ΔPrMO (dashed lines and open symbols) on 2.5% v/v methane (left, in red) or propane (right, in purple). Data points represent the mean of readings from triplicate flasks and error bars indicate the standard deviation.

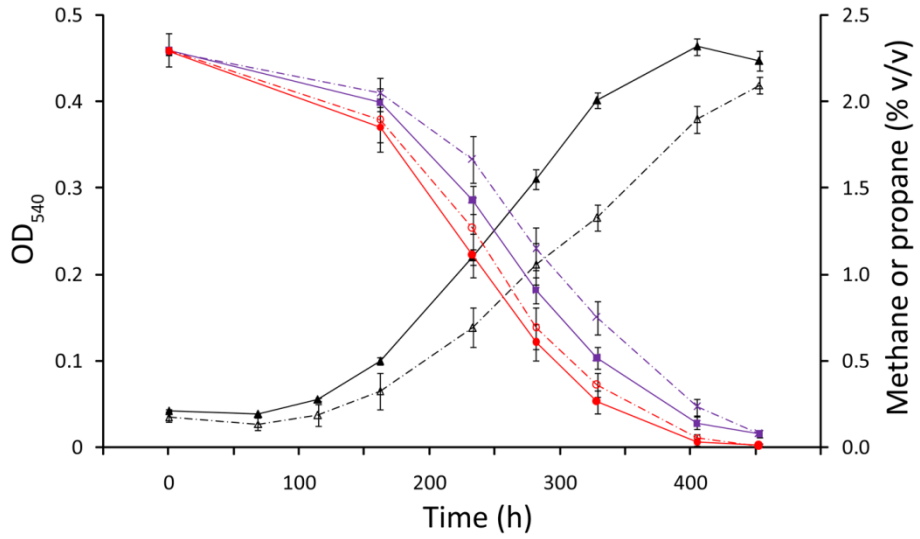

Figure 6.20. Growth of *M. silvestris* strain ΔPrMO (dashed lines and open symbols) on a mixture of methane (red) and propane (purple) (2.5% v/v each) was repeated alongside the wild type (solid lines and filled symbols). Data points represent the mean of readings from triplicate flasks and error bars indicate the standard deviation.

6.5.5 Conversion of substrate carbon into biomass

Measurement of gas consumption allowed comparison of the relative conversion of substrate carbon into biomass. Data from experiments using 2.5% v/v substrate concentration (shown in Figure 6.15 and Figure 6.18 - Figure 6.20) are presented in Figure 6.21 as a percentage of substrate carbon converted into biomass as cellular dry weight. The data are presented in this form by assuming that an OD_{540} of 1.0 corresponds to 0.25 mg dw ml^{-1}. Although the true conversion factor may depart

somewhat from this estimate, this does not affect comparison between strains, and the data could equally well be presented in terms of culture densities rather than biomass. Comparison of the wild-type and strain ΔPrMO under each condition using Student's t-test confirmed that while there was no difference during growth on methane ($t_{(4)} = 0.3$, $p > 0.05$), carbon assimilation was less efficient in strain ΔPrMO during growth on methane plus propane ($t_{(13)} = 4.4$, $p < 0.01$) and propane alone ($t_{(4)} = 15.8$, $p < 0.01$). These data highlight the inessential but beneficial role of the PrMO during growth on this concentration of propane, and confirm that this enzyme is not required for oxidation of methane.

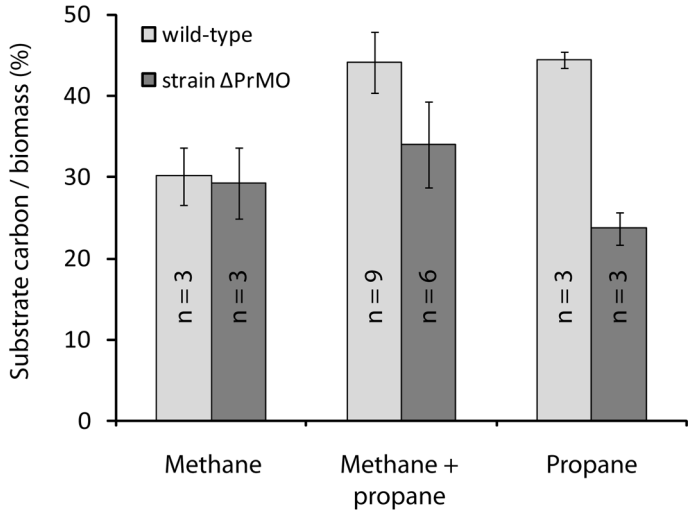

Figure 6.21. Growth and substrate consumption of *M. silvestris* wild-type and strain ΔPrMO on the gases shown (2.5% v/v) were used to compare the conversion of substrate carbon into biomass. Data are the mean of the number of replicates shown and error bars indicate the standard deviation.

6.5.6 Growth on 20% v/v methane and 10% v/v methane plus propane

Growth was compared between 20% v/v methane and a 10% v/v (each) mixture of methane and propane in the wild-type and strain ΔPrMO, see Figure 6.22. Whereas wild-type growth was similar in the two conditions, strain ΔPrMO exhibited a prolonged lag phase on the gas mixture compared to on methane alone (171 ± 12 h and 66 ± 3 h respectively (mean of three replicates ± standard deviation)), suggesting that at this propane concentration the gene deletion is detrimental to growth of strain ΔPrMO.

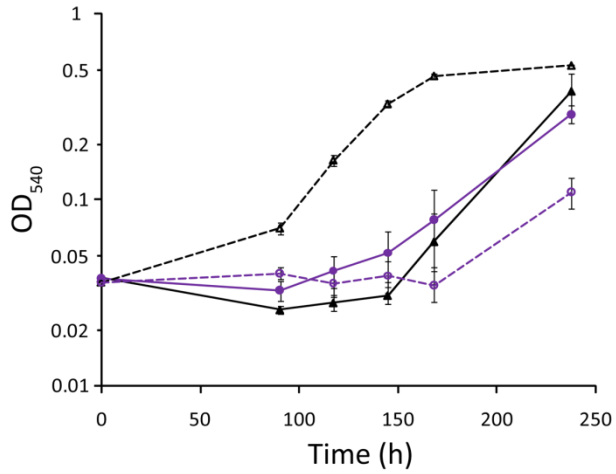

Figure 6.22. Growth on 20% v/v methane (black lines) was compared with growth on 10% v/v (each) methane and propane (purple lines) in *M. silvestris* wild-type (solid lines) and strain ΔPrMO (dashed lines). Whereas growth of the wild-type did not differ between conditions, strain ΔPrMO exhibited an extended lag phase during growth on the mixture. This illustrates a difference (an extended lag phase during growth on the mixture) between the two conditions in the mutant strain, which was not detectable in the wild-type. Data points represent the mean of readings from triplicate flasks and error bars indicate the standard deviation.

6.5.7 Summary of the growth phenotype of strain ΔPrMO

Strain ΔPrMO was able to grow on methane, methanol, ethanol and acetate indistinguishably from the wild-type. However, this strain was totally disabled for growth on 20% propane. Surprisingly, strain ΔPrMO was able to grow on 2.5% v/v propane at slightly over half the specific growth rate of the wild type, and at nearly the wild-type rate on a mixture of the gases (2.5% v/v each). The similar rates of gas consumption observed in the wild-type were mirrored during growth of strain ΔPrMO, suggesting that the ability of this strain to oxidise propane under these conditions is little affected. However, analysis of the conversion of substrate into biomass suggested that, at these concentrations, the deletion of the PrMO, while not fatal, is deleterious to strain ΔPrMO. During growth on a 10% (v/v each) mixture, strain ΔPrMO was inhibited in comparison to growth on methane alone. Thus, while the propane-oxidising ability of strain ΔPrMO was little affected, deletion of the PrMO had an increasingly serious effect on *M. silvestris* as propane concentration was increased.

6.6 Analysis of transcription and expression of PrMO subunits

M. silvestris wild-type and strain ΔPrMO were grown in 30 ml medium in 120 ml serum vials with a mixture of approximately 2.5% v/v (each) methane and propane, harvested at late exponential phase and RNA extracted as described in Materials and Methods. The purified RNA (200 ng) was used for cDNA synthesis using random hexamer primers and Superscript III reverse transcriptase (Invitrogen). Transcription was detected by PCR using primers internal to the coding sequences of Msil1651 (1651f/r) and Msil 1649 (1649f/r), encoding the propane monooxygenase α- and β-subunits, and Msil1641 (1641f/r), the final gene in the propane monooxygenase gene cluster (Figure 6.3). As expected, no transcription of Msil1651 could be detected in strain ΔPrMO, but the other genes were transcribed at seemingly similar levels in both strains, demonstrating (within the limitations of this method) that the gene deletion did not exert a polar effect on downstream genes, see Figure 6.23. Other studies (for example Pomerantsev et al. (2009)) have also shown that insertion of the *LoxP* sequence into an operon does not prevent transcription of downstream genes.

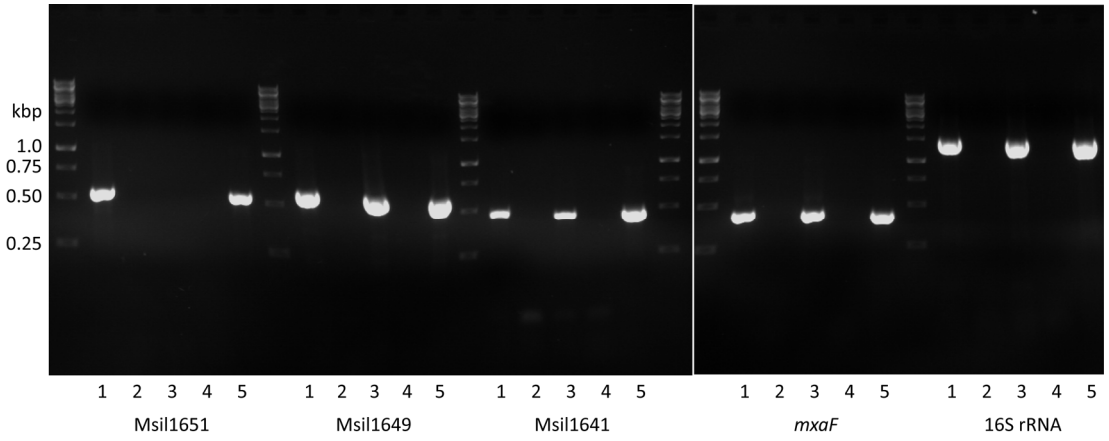

Figure 6.23. Presence or absence of transcription of the PrMO hydroxylase α- and β-subunits (Msil1651 and Msil1649) and the final gene of the cluster (Msil1641) was verified in *M. silvestris* wild-type and strain ΔPrMO, together with *mxaF* (encoding methanol dehydrogenase) and the 16S rRNA gene as positive controls. Lane 1: wild-type, cDNA template, lane 2: wild-type, negative control without reverse transcriptase, lane 3: strain ΔPrMO, cDNA template, lane 4: strain ΔPrMO, negative control without reverse transcriptase, lane 5: wild-type DNA template. Band sizes, Msil1651: 543 bp, Msil1649: 587 bp, Msil1641: 468 bp, *mxaF:* 430 bp, 16S rRNA: 1447bp.

Protein production was analysed by 1D SDS-PAGE. Cells, grown on a mixture of methane and propane (2.5% v/v each), were used to prepare cell-free extract, and 15 μg protein loaded on a 10% SDS-PAGE gel, see Figure 6.24.

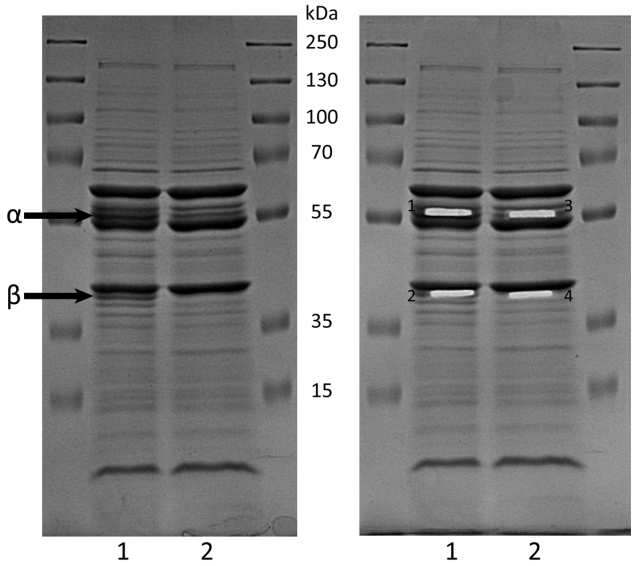

Figure 6.24. Left-hand gel: SDS-PAGE analysis of cell-free extract of wild-type (lane 1) and strain ΔPrMO (lane 2) grown on a mixture of methane and propane (2.5% v/v each). The α- and β-subunits of the PrMO hydroxylase are shown arrowed. The same gel is shown on the right, after excision of corresponding bands in the two lanes, for analysis by tryptic digest and mass spectrometry.

Bands previously identified as corresponding to the α- and β-subunits of the PrMO hydroxylase were excised from the lane loaded with wild-type extract, and from the corresponding positions from the lane loaded with extract from strain ΔPrMO, and analysed by tryptic digest and mass spectrometry by the Proteomics and Mass Spectrometry Facility of the University of Warwick. Identities of the polypeptides detected are shown in Table 6.5. Both the α- and β-subunits of the PrMO were identified in the lane derived from the wild-type extract, but neither was detected in the lane from strain ΔPrMO, not only demonstrating that there is, as expected, no expression of the deleted α-subunit, but also suggesting that although the β-subunit is transcribed, it is either not expressed in the absence of the α-subunit, or that under these conditions it is unstable.

Table 6.5. Polypeptide identifications of bands excised from the gel shown in Figure 6.24. For each band, the most abundant six polypeptides are shown, based on the number of peptides detected. Neither of the PrMO hydroxylase subunits was detected in the lane loaded with extract of strain ΔPrMO. The number of peptides detected and used to identify each polypeptide is shown. The total number of peptides detected from all polypeptides identified in each band is shown for comparison. MM: theoretical molecular mass.

Band	Strain	Locus tag Msil	Annotation	Peptides	Total peptides	MM kDa
1	w-t	0795	Chaperonin GroEL	16	84	57.6
		1647	Chaperonin GroEL	13		57.3
		1262	MmoX	13		59.8
		1651	PrMO α-subunit	10		64.2
		1641	Gluconate dehydrogenase	9		56.7
		2912	Trigger factor	6		50.6
2	w-t	1649	PrMO β-subunit	17	58	40.2
		1263	MmoY	11		44.9
		1267	MmoC	6		38.5
		1714	Serine-glyoxylate aminotransferase	5		42.6
		2996	Acetyl-CoA acetyl transferase	4		40.2
		0832	Acetylornithine acetyl transferase	4		41.8
3	ΔPrMO	1262	MmoX	15	79	59.8
		1641	Gluconate dehydrogenase	10		56.7
		3763	Hydrogenase α-subunit	9		59.9
		0795	Chaperonin GroEL	9		57.6
		2342	Aldehyde dehydrogenase	8		55.6
		1375	PEP carboxykinase	7		58.2
4	ΔPrMO	1263	MmoY	14	68	44.9
		2996	Acetyl-CoA acetyl transferase	9		40.1
		1714	Serine-glyoxylate aminotransferase	7		42.6
		1262	MmoX	7		59.8
		0471	MDH	6		68.5
		1267	MmoC	5		38.5

6.7 Deletion of the α-subunit of the sMMO hydroxylase

Strain ΔMmoX, with a deletion of Msil1262, encoding the α-subunit of the hydroxylase of the methane monooxygenase, was constructed as described in Chapter 4. The result (confirmed by sequencing) was the deletion of 1531 bp including almost the entire Msil1262 coding sequence, from 24 bp after the start codon to 26 bp before the stop codon, and the insertion of 104 bp of vector sequence containing a single *loxP* site. This strain was able to grow on succinate and methanol similarly to the wild-type (data not shown and Figure 6.25).

6.7.1 Growth on 20% and 2.5% (v/v) methane or propane

Strain ΔMmoX was able to grow on 20% (v/v) propane similarly to the wild-type, but at this concentration there was no growth on methane (Figure 6.25). Simultaneously, vials (120 ml, containing 25 ml medium) were set up in triplicate to test growth on 2.5% (v/v) methane, propane, or a mixture, as for strain ΔPrMO. The cultures did not grow in any of the three conditions, see Figure 6.26.

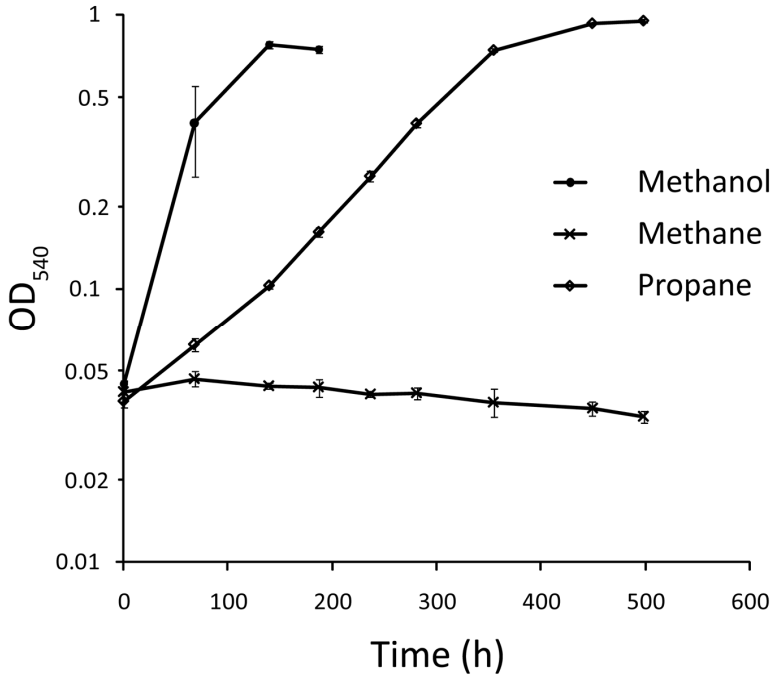

Figure 6.25. Growth of *M. silvestris* strain ΔMmoX on methanol (0.1% v/v) (filled circles), propane (open diamonds) or methane (crosses) (both 20% v/v). Data points represent the mean of readings from triplicate flasks and error bars indicate the standard deviation.

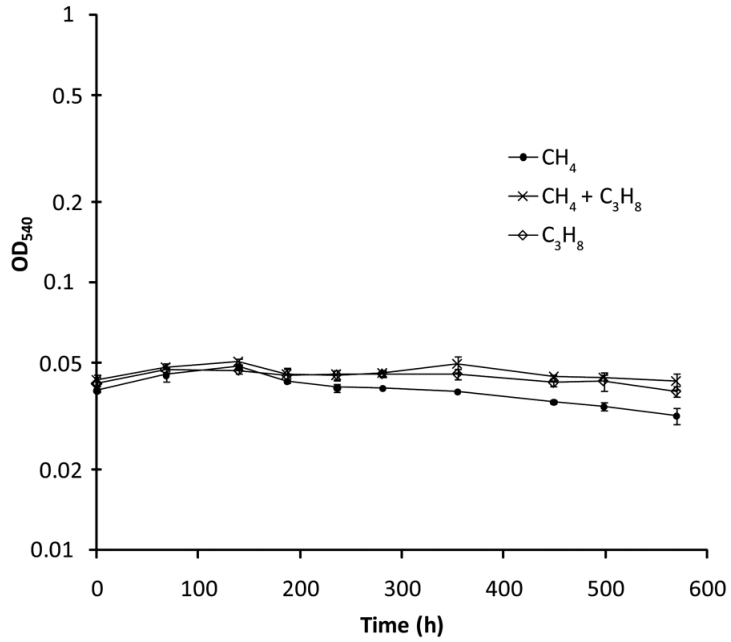

Figure 6.26. Growth of *M. silvestris* strain ΔMmoX on methane, methane plus propane, or propane (all at 2.5% v/v). Data points represent the mean of readings from triplicate flasks and error bars indicate the standard deviation.

6.7.2 The capacity of strain ΔMmoX to oxidise methane

In order to assess the ability of the PrMO to oxidise methane, *M. silvestris* wild-type and strain ΔMmoX were grown on a mixture of 20% (v/v) propane and 2% (v/v) methane. Whereas the wild-type consumed methane and propane proportionally to their concentrations, methane was not consumed in strain ΔMmoX, see Figure 6.27.

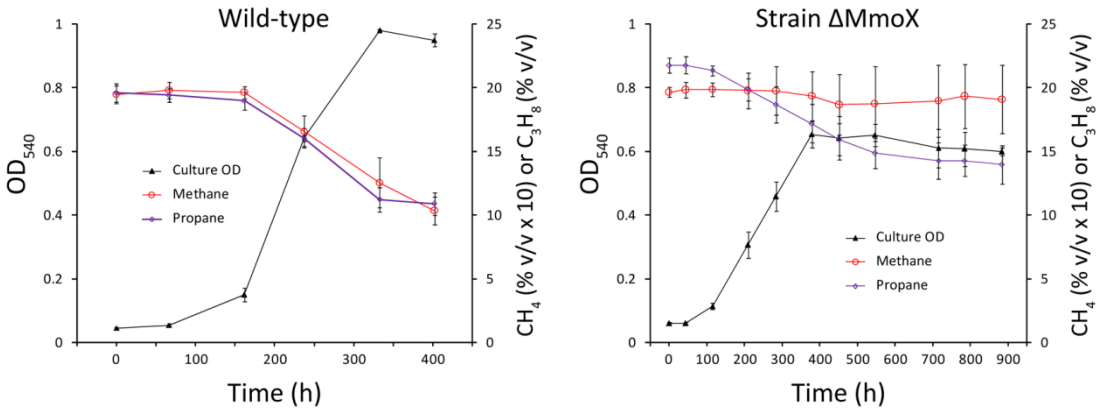

Figure 6.27. Consumption of methane and propane in *M. silvestris* wild-type (left) and strain ΔMmoX (right) when supplied with approximately a 1:10 v/v ratio of gases. Methane concentrations are shown as % v/v ×10 on the y-axis.

6.8 Substrate oxidation range of *M. silvestris*

6.8.1 Methane- and propane-oxidising ability of cells grown on these substrates

A Clark Oxygen electrode was used to determine the substrate-oxidising capabilities of methane- and propane-grown *M. silvestris* wild-type whole cells. Cells grown on methane exhibited high activity in response to methane, but a relatively low level response (approximately 5% of the rate with methane) in response to propane. Cells grown on propane, surprisingly, consumed oxygen at a higher rate when stimulated with methane than with propane. However, the activity in response to methane was less than half that of methane-grown cells, whereas the activity in response to propane was more than double, so the ratio of the propane to methane activities increased from 5% in methane-grown to 28% in propane-grown cells, as shown in Table 6.6. There was no detectable rate with succinate-grown cells in response to these substrates. The activity in response to methane of propane-grown cells may be due to the expression of the sMMO in these cells, shown to occur during growth on propane (see Section 6.4). This hypothesis is supported by the inability of strain ΔMmoX to oxidise a significant amount of methane when growing on propane (20% v/v) and methane (2 % v/v), in contrast to the wild-type (Figure 6.27). The up-regulation of propane-oxidising capability in propane-grown cells suggests, however, that the propane-related activity is due mostly to the PrMO.

Table 6.6. Methane- and propane-induced specific oxygen consumption rate (nmol min^{-1} (mg $dw)^{-1}$) of *M. silvestris* whole cells grown on methane, propane or succinate as determined by oxygen electrode studies. Data are the mean of three measurements (± standard deviation).

Substrate for oxidation	Growth substrate		
	Methane	Propane	Succinate
Methane	49.0 ± 1.2	21.1 ± 2.1	Not detectable
Propane	2.5 ± 0.5	5.9 ± 0.8	Not detectable

6.8.2 Affinity of *M. silvestris* for propane

The affinity of *M. silvestris* wild-type propane-grown whole cells for propane was measured using the oxygen electrode, by determining oxygen uptake rate in response to a range of substrate concentrations. The apparent K_m of whole cells for propane

was 19 μM, as shown in Figure 6.28. This concentration corresponds to a headspace propane concentration of approximately 1.4% v/v assuming equilibrium between the gas and liquid phases. If, as suggested in the previous section, at saturating concentrations of propane the PrMO is largely responsible for propane oxidation, it follows that the K_m reported above largely refers to the activity of this enzyme (assuming Michaelis Menten kinetics).

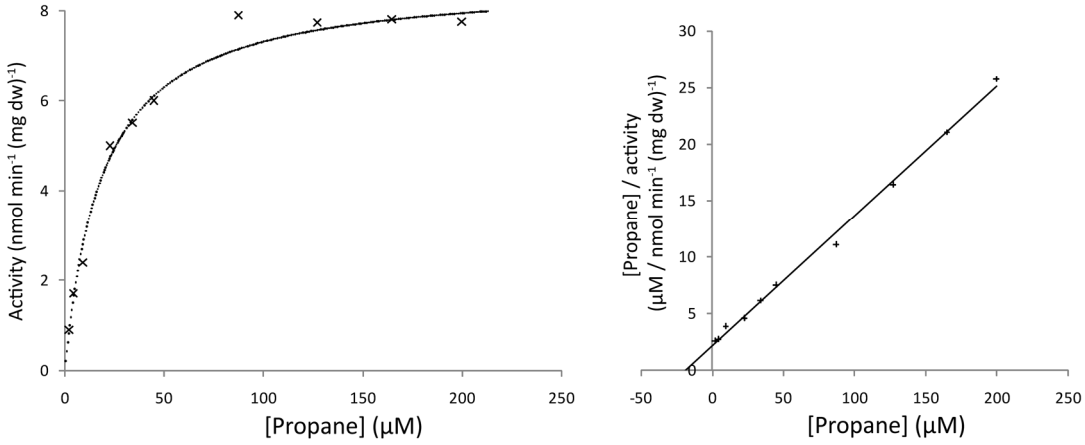

Figure 6.28. Activity, defined as oxygen uptake rate, of propane-grown cells in response to addition of various amounts of propane in the oxygen electrode, is shown as crosses in the left-hand graph, which also shows the theoretical Michaelis-Menten curve generated using parameters (K_m, V_{max}) derived from the Hanes-Woolf plot (right-hand graph) drawn using the same data.

6.8.3 Potential ability to metabolise or co-metabolise alternative substrates

Examples of substrates previously described as having the potential for oxidation by the sMMO (Colby et al., 1977; Patel et al., 1982; Burrows et al., 1984) were tested for their ability to induce oxygen up-take in the oxygen electrode, using cells grown on methane or propane. Investigators such as Oldenhuis et al. (1989) and Stirling and Dalton (1979) investigated the co-metabolism of similar compounds using whole cells of methanotrophs, and found that the addition of co-substrate (formate or formaldehyde) was necessary to provide the reductant (NADH) required by the monooxygenase, since most of the compounds tested cannot be further metabolised

to regenerate reducing power. This approach was not possible using the oxygen electrode, since the oxidation of additional formaldehyde or other alternative sources of reducing power would mask any effect due to the substrate of interest. Therefore, only intracellular reserves were available to cells. In contrast to methods which measure depletion of substrate or accumulation of product, and which rely on the oxidation of significant quantities of substrate, the high sensitivity of the oxygen electrode is such that these reserves are sufficient to indicate the potential for substrate oxidation. Substrates tested are listed in Table 6.7, together with specific rates of oxygen consumption. It was found necessary to add all substrates as aqueous solutions, in most cases saturated, and in the case of low-solubility substrates the amount added was necessarily extremely low. Two methods were adopted to determine if a saturating amount of substrate was added; the addition of further substrate and the recording of any consequent increase in rate, and secondly the subsequent addition of methane during oxidation of the co-metabolised substrate. The absence of increased rate in response to methane indicated saturation or inhibition (or inactivation) of the SDIMO responsible for methane oxidation, further providing evidence that the co-metabolised substrate was oxidised by these enzymes. No additional rate or a much reduced rate in response to methane under these conditions was recorded for all substrates except octane, pentadecane, cyclohexane, biphenyl, anthracene and phenanthrene. The aqueous solubility of all these compounds except cyclohexane is extremely low (between 8 mg L^{-1} for biphenyl to 0.05 mg L^{-1} for anthracene, (Silverman and Shideler, 1958; Sarraute et al., 2004; Kuramochi et al., 2006), and the small amount necessarily added to cells in the oxygen electrode may have been insufficient to detect a response, or, alternatively, these compounds are not oxidised at high rates by the *M. silvestris* SDIMOs. The solubility of cyclohexane is approximately 63 mg L^{-1} (de Hemptinne et al., 1998), suggesting that the affinity for this compound is low or it is not a particularly good substrate for these enzymes.

Table 6.7. Oxidation of non-growth substrates by *M. silvestris* grown on methane or propane. Specific oxygen consumption rates (nmol min^{-1} (mg dw)$^{-1}$ are shown as ± standard deviation where measurements were conducted in at least triplicate. n.d.: not determined.

Substrate for oxidation	Growth substrate	
	Methane	Propane
pentane	1.1	n.d.
octane	0.0	n.d.
pentadecane	0.0	n.d.
cyclohexane	0.0	n.d.
1,2-dichloroethane	3.6	4.3
propene	2.9 ± 0.1	5.8 ± 0.6
isoprene	3.2 ± 0.1	9.2
trans-2-butene	4.2	8.0
trichloroethylene	4.1	5.7
cyclohexene	0.7	1.0
benzene	2.5	3.7
phenol	2.4	4.1
toluene	2.7	1.2
p-xylene	1.0	n.d.
p-cresol	2.3	n.d.
ethyl benzene	1.2 ± 0.5	0.6
styrene	4.0	n.d.
anthracene	0.0	n.d.
phenanthrene	0.0	n.d.
biphenyl	0.0	n.d.

6.8.4 Relative substrate specificities of the sMMO and PrMO

Propane-grown cells displayed higher activity towards propane, propene and other alkenes than methane grown cells. Although some or all of the activity towards methane of propane-grown cells may be due to expression of the sMMO, which may also contribute to co-metabolism of the compounds shown in Table 6.7 by propane-grown cells, the relatively higher rates recorded suggest that the PrMO may have higher activities with alkenes than the sMMO. Lack of time prevented the repeat of these experiments with strains ΔMmoX and ΔPrMO.

6.9 Inhibition of the *M. silvestris* SDIMOs

Wild-type *M. silvestris* cells were grown in 120 ml serum vials containing 25 ml medium supplied with methane and propane (2.5% v/v each). At mid-exponential phase acetylene (1.5 ml, equivalent to an aqueous concentration of approximately 0.4 mM) was added, and growth and gas consumption recorded. Compared to un-amended control vials, acetylene completely inhibited both growth of the cultures and consumption of gases, as shown in Figure 6.29. It should be noted, however, that deletion of the sMMO was sufficient to prevent growth on propane and methane at this concentration (Section 6.7.1), so these data do not necessarily imply inhibition of the PrMO.

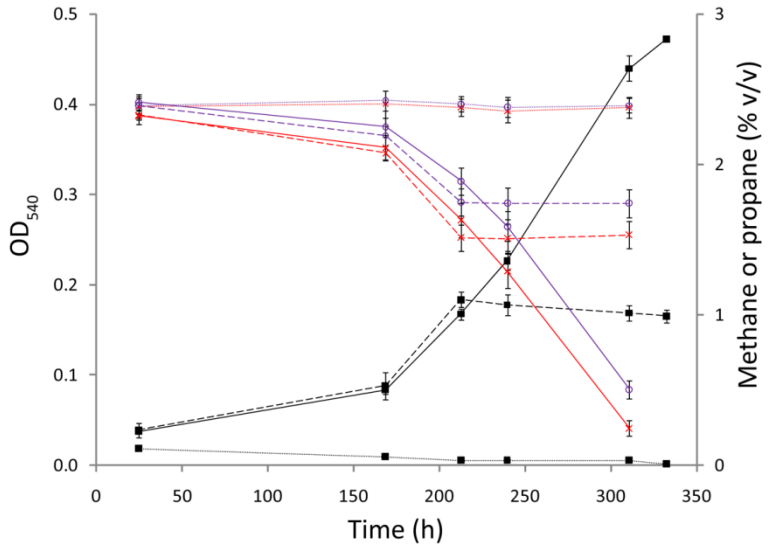

Figure 6.29. Acetylene was added to culture growing on methane and propane and completely inhibited both growth and substrate gas oxidation. Black lines: culture OD_{540}, red: methane headspace concentration, purple: propane headspace concentration. Solid lines: control cultures without addition of acetylene, dashed lines: cultures inhibited with acetylene, dotted lines: killed controls. Error bars show the standard deviation of triplicate vials.

6.10 Oxidation of low levels of methane

It was noticed during the course of these experiments that *M. silvestris* growing on a mixture of methane and propane was capable of reducing the methane concentration to low levels. In particular, the methane concentration in the vials shown in Figure 6.20 (wild-type and strain ΔPrMO supplied with a mixture of methane and propane)

was approaching, or below, atmospheric levels after 980 h (data not shown). To test the relative consumption of methane and propane with dissimilar concentrations of the two gases, vials (120 ml containing 25 ml medium) were inoculated with wild-type *M. silvestris* and supplied with approximately 2.5% v/v propane and 0.3 % v/v methane. Gas concentration was monitored at 14 time-points over 910 h, and additional propane (2 ml) added at 350 and 740 h, when the concentration dropped below approximately 0.5% v/v, see Figure 6.30. Oxygen (5 ml) was added at 570 h. Methane was reduced to 72 ± 20 ppmv over this time period (mean of three vials ± standard deviation). Gas consumption rates were approximated by dividing the gas consumed between consecutive time-points by the time interval. Figure 6.31 shows the (log transformed) relative rates of consumption of the gases as a function of their relative headspace concentrations. A linear relationship was observed over a 40 fold difference in their relative concentrations and methane was consumed at approximately 1.7 times the relative rate for propane, suggesting that the kinetic parameters for methane and propane consumption are fairly similar under these conditions.

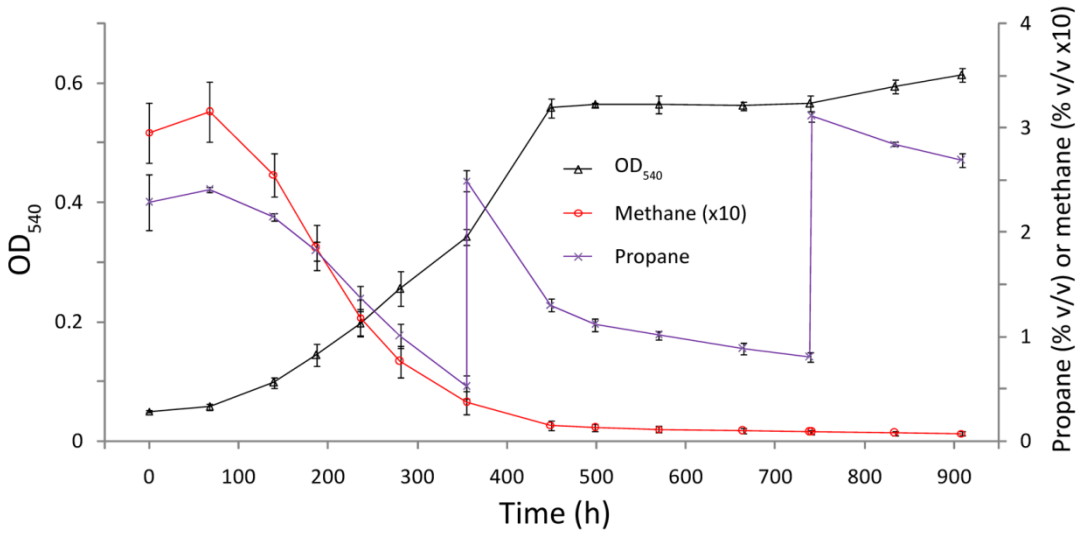

Figure 6.30. Growth and gas concentrations of wild-type *M. silvestris* supplied with a mixture of methane and propane at dissimilar concentrations. Methane is shown as % v/v ×10 on the y-axis.

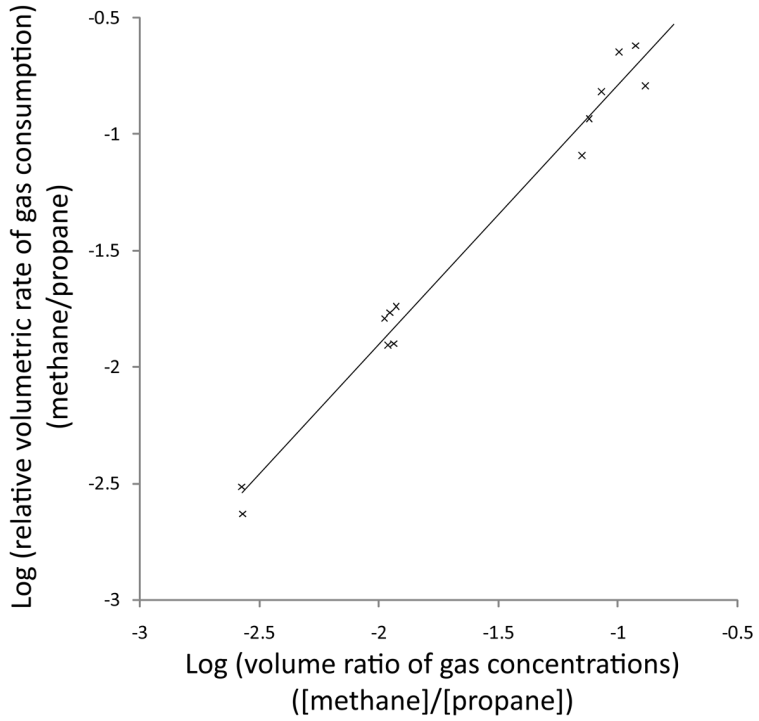

Figure 6.31. The relative rates of methane and propane consumption plotted relative to their headspace concentrations (both log transformed), during the growth of wild-type *M. silvestris* on methane and propane shown in Figure 6.30. Methane concentration dropped from 3000 to 72 ppmv over the course of the experiment, and propane concentration was maintained at between 0.5 and 3% v/v.

6.11 Discussion

6.11.1 The PrMO promoter and gene cluster

5' RACE was successful at identifying transcription of the PrMO from a σ^{54} promoter, with transcription start site located 119 bp upstream of the hydroxylase α-subunit. Although it is highly likely that the genes of this cluster are co-transcribed as an operon, and no experimental evidence was obtained that argues against this, inter-gene PCR conducted on cDNA synthesised from mRNA extracted from propane-grown cells was inconclusive, due to the amplification of cDNA synthesised from control reactions without primers. This can most readily be explained by self-priming of mRNA strands, in which case the presence of PCR amplicons does demonstrate the existence of RNA transcripts, although the sense of the transcript cannot be determined. Many studies use a similar inter-gene PCR method to determine operon extent, for example Borodina et al. (2004), Zhang and Lidstrom (2003), Roback et al.

(2007). None of these examples document the use of control reactions without cDNA-synthesis primer, but, as advised by Zhou and Yang (2006), this precaution would seem to be wise.

6.11.2 Transcription and expression of the *M. silvestris* SDIMOs

Using promoter-probe vectors and proteomic analysis, both transcription and expression of the two SDIMOs were analysed during growth on methane and propane. It was conclusively demonstrated that during growth on methane, only the sMMO is transcribed, whereas during growth on propane, both monooxygenases are transcribed and expressed. This finding has implications for the regulation of gene expression which are briefly discussed in the following chapter.

6.11.3 Construction of mutant strains lacking the sMMO and PrMO

Mutant strains were constructed with deletions of the α-subunits of the hydroxylases of the two *M. silvestris* SDIMOs. The possibility that subunits of the alternative enzyme could complement this deletion cannot be discounted. However, several lines of evidence argue against this possibility. Firstly, due to the considerable differences in enzyme structure (three- versus two-subunit hydroxylases) and extensive α-subunit divergence (31% identical and 48% similar residues) between the sMMO and the PrMO, interchangeability between subunits seems very unlikely. Very few studies have investigated the possibility of reconstituting active enzymes using components from different SDIMOs. Champreda et al. (2006) replaced the coupling protein (component B) of the SDIMO of *Xanthobacter autotrophicus* PY2 with the homologous component derived from SDIMOs of other groups. Activity dropped to 5% when the coupling protein was substituted by IsoD from *Rhodococcus* sp. AD45, which has 64.5% of similar residues to the native protein, and all less-similar proteins did not result in detectable activity. Component B binds to the hydroxylase α-subunit and is responsible for a dramatic increase in enzyme activity (Froland et al., 1992), suggesting that, even if the hydroxylase α-subunits could complement each other, this in itself might not result in an active enzyme, since effective interactions with other components are also required. Secondly, both strains exhibited clear phenotypes, suggesting that complementation, if it is possible, is not

efficient. Thirdly, proteomic analysis of strain ΔPrMO (Section 6.6) demonstrated that in addition to the α-subunit, the β-subunit is also not present in cells.

6.11.4 Oxidation of methane and propane

The data presented in Sections 6.5.2 and 6.10 show that *M. silvestris* consumes methane and propane at surprisingly similar rates in response to a mixture of these substrates, and the data summarised in Section 6.5.7 demonstrate that the PrMO is not necessary for the ability to oxidise propane. These data also demonstrate, however, that cells lacking the PrMO are disadvantaged in comparison to the wild-type during growth on methane/propane mixtures, and furthermore that at higher propane concentrations, this effect is increased. These data could be explained by the hypothesis that propane oxidation by the sMMO results in a toxic product, and that expression of the PrMO is necessary for the induction of enzymes to degrade it. Possibly, during growth of strain ΔPrMO on a high percentage of propane, these enzymes are not induced and the product accumulates to dangerous levels, whereas at 2.5%, constitutively-expressed enzymes are sufficient to remove the less rapid flux of this toxic intermediate. This hypothesis implies that the products of propane oxidation by the sMMO and the PrMO are different. Strain ΔMmoX, on the other hand, was unable to grow on methane at either of the concentrations tested, suggesting that the PrMO is unable to oxidise methane, a hypothesis confirmed by the failure of strain ΔMmoX to consume methane during growth on propane. Interestingly, this strain was unable to grow on 2.5% propane, suggesting either that the sMMO is primarily responsible for oxidation of propane at this concentration, or that, at this concentration, oxidation of propane by the sMMO is required for induction of the PrMO.

The suggestion that the sMMO has a high affinity for propane and the PrMO a low affinity does not appear to be supported by the oxygen electrode data presented in Section 6.8.2, lending weight to the hypothesis that additional factors are relevant. Using an oxygen electrode, the apparent K_m of propane-grown cells for propane (19 μM) was approximately half that of methane-grown cells for methane determined in Chapter 3. This value is comparable to reported values for methane determined by this method in other organisms (Harrison, 1973; Ferenci et al., 1975; Linton and Buckee, 1977), (although considerably higher than values determined using

alternative methods (Joergensen, 1985; Green and Dalton, 1986)). Very few kinetic data exist for propane monooxygenase, but working with whole cells of *Rhodococcus* sp. RR1 and *Mycobacterium vaccae* JOB5, Sharp et al. (2010) determined the apparent K_m for propane to be approximately 136 μM and 18 μM respectively.

6.11.5 Cometabolism by the sMMO and PrMO

Oxygen electrode data indicated wide substrate specificity for the sMMO, in keeping with previously published data. Interestingly, the PrMO also appeared capable of oxidising alternative substrates, including an increased activity with alkenes compared with the sMMO.

6.12 Conclusions

6.12.1 Discrimination between alkanes in SDIMO-containing organisms

Thauera butanivorans expresses a group III SDIMO which it uses to oxidise butane, and which is capable of oxidation of methane with a higher turnover rate than any of alkanes C1 – C5 (Cooley et al., 2009b). However, the soluble butane monooxygenase has low affinity (K_m > 1 mM) for methane and was found to be 1800-fold more specific for butane, such that during growth on a typical natural gas composition mixture comprising 96.5% methane, 2% ethane, 1% propane and 0.5% butane, less than 2% of the flux through the enzyme was methane (Cooley et al., 2009a). Green and Dalton (1986) found the sMMO of *Methylococcus capsulatus* (Bath) to be more efficient with methane as substrate, with V_{max} : K_m ratio sevenfold higher than with propane. Growth of *Methylococcus capsulatus* on the alkane mixture present in natural gas would result in a similarly low flux of non-metabolisable substrates. These strategies are necessary for both these organisms to prevent the accumulation of toxic intermediates and to avoid the inhibition of enzyme activity by competing substrates which cannot be used; *M. silvestris* has perhaps evolved an sMMO which treats methane and propane indiscriminately since it is not subject to these limitations.

6.12.2 Suggestions for future work

Time constraints prevented full analysis of the capabilities of strains ΔPrMO and ΔMmoX. For example, repeating the oxygen electrode experiments with these strains would yield useful data. This would require growth of these strains in fermenter culture in order to generate sufficient good quality biomass. The interesting co-metabolic potential of both SDIMOs should be investigated in more detail by GC analysis of substrate depletion and product formation. This would enable the addition of reductant-supplying substrates which would enhance the oxidative capability of cell suspensions. Full analysis of the kinetic parameters of the two SDIMOs is now required by purification and biochemical characterisation. This will be aided by the existence of the mutant strains, both in enabling the design of activity assays for the two enzymes, and, potentially, as sources of the respective enzymes.

Table 6.8. Primer sequences used in this chapter. The second column refers to the inter-gene PCR locations identified in Figure 6.7.

Primer name	Figure 6.7 ref.	Sequence 5' – 3'
51Ra1		TCGTCGTCGCATAGCACTTG
51Ra2		ATCGTGGAATGGCGGAACTC
51Ra3		TCTTCCTGCATCGGAAAGTACG
46Ra1		CCCACGCCTTCATAATGACG
5051f	A	TCAAGGCGCCCATCAAAGTG
5051r	A	CAGCGGCTTGCTCGTATCTG
4950f	B	CCCGGCGACAAACTAAGAATC
4950r	B	ACGGTGACGTCCTCGTAATG
4749f	C	CCTCTTCCGCGCTGATATCC
4749r	C	CTTCGGCATCTTCGACTCCC
4647f	D	TCCGCAATGCGGTTTCCTC
4647r	D	GGCGCCCATTCATTCAACTG
4546f	E	TTACGCAGCCTCGACAAACAG
4546r	E	GAGCGGGTTTGGCATTGATAG
4445f	F	CGCGGGATTTCCGTCTTTG
4445r	F	GCCGCAGCTCGTATTGAAC
4344f	G	AGCGAAGGCTCGTGATCAAC
4344r	G	GAAGGCCGCACCATAGAAG
4243f	H	TCGTGGAGGTCGTTTGATGG
4243r	H	ACACGAATATCGCCGCGGAG
4142f	I	GAGATTTGGCCGCTGTTTGG
4142r	I	GAGCCGACGATCACGACTAC
4041f	J	TGCGAGAATCCGACGTTGAC
4041r	J	GTTGCCGCTGCTTTAGATCC
4041rb	J*	GCAACGCGACTATCTGTTGC
PrPf		ACTCAATTGTCCGTTCCGTAACGCCTCTC
PrPr		CGGCCGGCTGAGCTCCCGCTACGC
1651f		TCCGCCATTCCACGATTCAG
1651r		TTTCCAGCGGCAGCATGTAG
1649f		AGGATCATCTCGGCGCCTAC
1649r		CTTGTTGACGGGCAAGGACC
1641f		AGCTGGGCTACAAGGAGGTG
1641r		CCATGGTGGTTCCGCGATAC

Chapter 7

Metabolism of propane

7.1 Introduction

7.1.1 The initial oxidation of propane

Monooxygenase-mediated oxidation of propane is possible in two ways; formation of 1-propanol by oxidation of the terminal carbon atom, or formation of 2-propanol by oxidation of the sub-terminal carbon. In addition, non-specific oxidation would result in a mixture of 1- and 2-propanol (Ashraf et al., 1994). Previous investigations of short-chain *n*-alkane oxidation in other organisms have identified both terminal and sub-terminal oxidation products. For example, oxidation of butane by *Thauera butanivorans* results mostly in 1-butanol (Arp, 1999), although a small amount of 2-butanol may also be produced (Vangnai and Arp, 2001), whereas sub-terminal propane oxidation was found to predominate in *Gordonia* TY5 (Kotani et al., 2003). *Rhodococcus rhodochrous* was found to oxidise propane to a mixture of 1-propanol and 2-propanol (Ashraf and Murrell, 1992). The presence of the sMMO in *M. silvestris* complicates the situation. As shown in Chapter 6, this enzyme is expressed during growth on propane, and is capable of propane oxidation. The product distribution following the oxidation of *n*-alkanes by the sMMO has been investigated extensively (Colby et al., 1977; Patel et al., 1982; Burrows et al., 1984; Green and Dalton, 1989; Froland et al., 1992), demonstrating that a mixture of primary and secondary alcohols results in most cases, with 2-propanol usually being the major product of propane oxidation, but protein B was shown to play an important part in the regioselectivity of the enzyme (Froland et al., 1992). Therefore it was difficult or impossible to predict the product(s) of propane oxidation in *M. silvestris.*

7.1.2 Alcohol dehydrogenase

Among short-chain alkane-utilizing bacteria, both $NAD(P)^+$-dependent and -independent alcohol dehydrogenases have been shown to oxidise the products of the initial alkane oxidation. Methanol dehydrogenase (MDH) is a pyrroloquinoline quinone (PQQ) containing enzyme (Anthony and Williams, 2003) which does not require nicotinamide cofactors for activity. Similarly, *Thauera butanivorans* expresses two PQQ-dependent alcohol dehydrogenases, BDH and BOH, during growth on butane, with maximal activity towards 1-butanol and 2-butanol respectively (Vangnai and Arp, 2001; Vangnai et al., 2002). *Gordonia* TY5 depends

on an NAD^+-dependent 2-propanol dehydrogenase for growth on propane (Kotani et al., 2003), as does *Mycobacterium vaccae* JOB5 (Coleman and Perry, 1985), whereas *Rhodococcus rhodochrous*, which oxidizes propane to a mixture of 1- and 2-propanol, expresses two NAD^+-dependent enzymes, with corresponding activities, both of which are required for growth on this substrate (Ashraf and Murrell, 1992).

7.1.3 Terminal oxidation and metabolism via 1-propanol

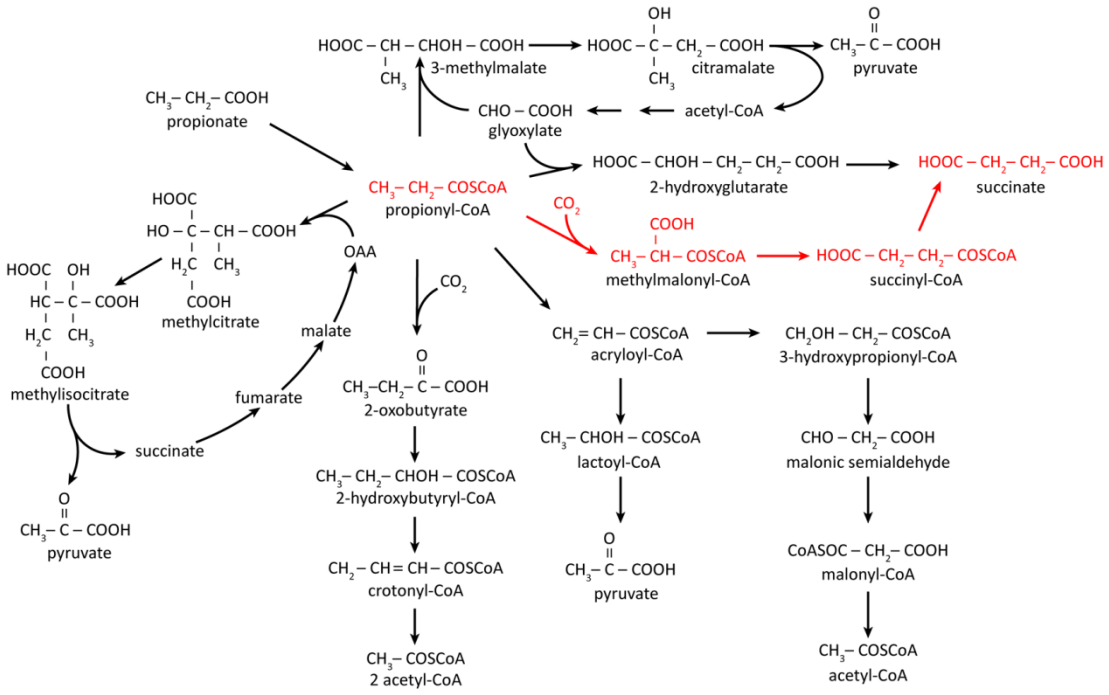

Figure 7.1. Pathways of propionate metabolism. The methylmalonyl-CoA pathway is shown in red. The inter-conversion of acryloyl-CoA and lactoyl-CoA, catalysed by lactoyl-CoA dehydratase in *Clostridium propionicum,* is extremely oxygen-sensitive (Hetzel et al., 2003), and this reaction is unlikely to operate in *M. silvestris.* Redrawn from Textor et al. (1997).

The expectation is that terminal propane oxidation (which results in 1-propanol), proceeds via propanal and propionate following two dehydrogenation reactions. The metabolism of propionate (summarised by Textor et al. (1997), see Figure 7.1) has several variations (Wegener et al., 1968), of which the methylcitrate and methylmalonyl-CoA pathways are well characterised in heterotrophic bacteria.

7.1.4 Subterminal oxidation and metabolism via 2-propanol

The dehydrogenation of 2-propanol would yield acetone, or 2-propanol could conceivably be subject to attack by an oxygenase resulting in acetol. Acetone can be used as growth substrate by a variety of aerobic and anaerobic bacteria (Taylor et al., 1980; Platen and Schink, 1987), and three aerobic mechanisms of the initial reaction have been described; carboxylation to acetoacetate, as for example in *Xanthobacter* strain PY2 (Sluis and Ensign, 1997), insertion of an oxygen atom by a Baeyer-Villiger monooxygenase (Kotani et al., 2007), or terminal hydroxylation forming acetol (Lukins and Foster, 1963; Koop and Casazza, 1985). These reactions and the subsequent steps required for assimilation into central metabolism are shown in Figure 7.2.

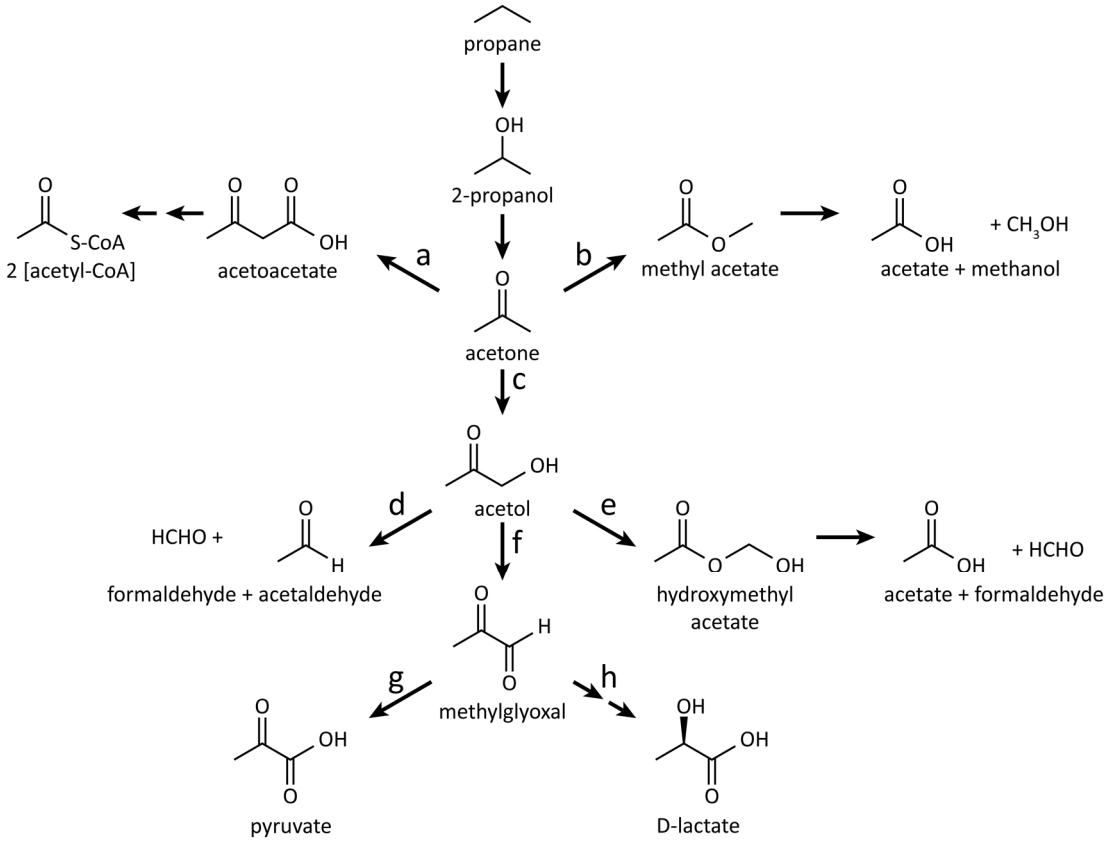

Figure 7.2. Sub-terminal oxidation of propane and metabolism via acetone. The enzymes identified are a) acetone carboxylase, b) Baeyer-Villiger acetone monooxygenase, c) acetone monooxygenase, d) acetol cleavage enzyme, e) acetol monooxygenase (which is followed by spontaneous cleavage of the resultant hydroxymethyl acetate), f) acetol dehydrogenase, g) methylglyoxal dehydrogenase, h) glyoxylase.

Metabolism of acetol is likewise possible in various ways, including cleavage to acetaldehyde and formaldehyde (Vestal and Perry, 1969), monooxygenase-catalysed oxidation to acetate and formaldehyde (Hartmans and de Bont, 1986), or dehydrogenation (Taylor et al., 1980) resulting in methylglyoxal. Subsequent dehydrogenation of methylglyoxal may result in pyruvate, or methylglyoxal may be metabolised via the glutathione-dependent glyoxylase system (Cooper, 1984).

7.1.5 Aims

It appeared unlikely, given the relatively low-intensity research into propane-utilizing organisms in the post-genomic era, that it would be possible to predict with any degree of accuracy the product(s) of propane oxidation by *M. silvestris.* In addition, the metabolic pathways for incorporation of terminal and, particularly, sub-terminal products of propane oxidation are diverse and have received relatively little study. The aims of this chapter therefore were to determine the products and pathways of propane oxidation in *M. silvestris.*

7.2 Identification of genes potentially involved in propane metabolism

To investigate the potential for expression of enzymes shown to be required for propane oxidation in other organisms, the *M. silvestris* genome was searched for genes homologous to known examples.

7.2.1 Alcohol dehydrogenase

Beside *mxaF*, the gene encoding methanol dehydrogenase (MDH), the pyrroloquinoline quinone (PQQ)-containing quinoprotein alcohol dehydrogenase (ADH) primarily responsible for methanol oxidation in methylotrophs (Anthony, 2004), the *M. silvestris* genome contains at least six additional genes predicted to encode PQQ-containing alcohol dehydrogenases. Of these, two (Msil1587 and Msil2260) are similar to the *xoxF* form recently shown also to be involved in one-carbon metabolism (Schmidt et al., 2010) (73% and 62% respectively amino acid identity to *xoxF* from *Methylobacterium extorquens* (YP_002963794.1)). No genes were identified with a high level of similarity to those encoding characterised quinoprotein ADHs involved in short chain alkane metabolism, for example the 1-

and 2-butanol dehydrogenases from *Thauera butanivorans* (Vangnai et al., 2002) (maximum 37% identity, Msil3387 and *T. butanivorans* BOH). Similarly, the *M. silvestris* genome contains eight genes predicted to encode NAD(P) dependent ADHs. Based on similarity and genome location relative to other genes suspected of involvement in propane metabolism, no obvious candidates for short chain alkane metabolism stood out, although Msil1827 and Msil2342 have 57% and 73% amino acid identity with ADH2 and ADH3 from *Gordonia* TY5 respectively. Although ADH3 from *Gordonia* has a primary structure homologous with aldehyde dehydrogenase, it was found to have activity with 2-propanol and not with any aldehyde tested (Kotani et al., 2003). These authors concluded that *Gordonia* TY5 contains three secondary ADHs involved in propane metabolism, although it was shown that disruption of a single gene (*adh1*) was sufficient to prevent growth on propane.

7.2.2 Propionate metabolism

M. silvestris contains genes which may encode enzymes catalysing the conversion of propionyl-CoA to succinyl-CoA via the methylmalonyl-CoA pathway, as shown in Table 7.1. However, no homologues of the *prp* operon genes encoding the methylisocitrate pathway of propionate catabolism in *S. typhimurium* were found, except low similarity hits to those of the analogous glyoxylate bypass.

Table 7.1. Similarities of predicted *M. silvestris* amino acid (query) sequences with those of characterised methylmalonyl-CoA pathway enzymes from *Rhodobacter sphaeroides* 2.4.1 or *Methylobacterium extorquens* AM1. The accession number and length (amino acids) refers to the target sequences.

Locus tag Msil	Annotation	Organism	Accession number	Length	% id
2934	Methylmalonyl-CoA epimerase	*R. sphaeroides*	YP_353891.1	134	76
3784	Methylmalonyl-CoA mutase α-subunit	*M. extorquens*	YP_002966130.1	721	72
3785	Methylmalonyl-CoA mutase β-subunit	*M. extorquens*	YP_002963450.1	605	45
3786	Propionyl-CoA carboxylase β-subunit	*R. sphaeroides*	YP_352242.1	510	72
3787	Propionyl-CoA carboxylase α-subunit	*R. sphaeroides*	YP_352246.1	668	60

7.2.3 Acetone metabolism

The amino acid sequence of acetone carboxylase from *Xanthobacter* sp. PY2 was used as query sequence for a BLAST search of the *M. silvestris* genome. No sequences with a significant level of homology to either the α-, β- or γ- subunit were found. Similarly, the sequences of acetone monooxygenase and methyl acetate hydrolase from *Gordonia* TY5 did not identify full-length homologous sequences. Oxidation of acetone to acetol was found to be catalysed by a cytochrome p450 in rabbit (Koop and Casazza, 1985), and the *M. silvestris* genome may encode at least two of these enzymes (Msil0731 and Msil1926).

7.2.4 Genetic potential for terminal or sub-terminal propane oxidation

It was therefore not possible to determine, on the basis of the identification of genes likely to be involved in propane metabolism, if this proceeds by the terminal or sub-terminal pathway, since the *M. silvestris* genome may encode enzymes capable of metabolising both 1- and 2-propanol.

7.3 Direct measurement of the products of propane oxidation

Working with *Thauera butanivorans*, Dan Arp (1999) determined the product of butane oxidation (1-butanol or 2-butanol) by inhibition of the further oxidation of the alcohol using an excess of 1-propanol, which resulted in the accumulation of 1-butanol when cells were incubated with butane. The same approach was later adopted by Kotani et al. (2006) to identify the products of propane oxidation in *Mycobacterium* sp. TY-6 and *Pseudonocardia* sp. TY-7. This method was attempted with *M. silvestris.* As proof of principle, cell suspensions (approximately 1 mg dw) of propane- and methane-grown cultures were incubated in a 1 ml volume in 10 ml vials with approximately 1 μmol (1 mM concentration) 1-propanol, and its consumption and build-up of products monitored by gas chromatography. Cells from both growth conditions reduced 1-propanol concentrations to below the limit of detection within four hours, (see Figure 7.3a), but propanal was not detectable. When butanal (5 mM) was included in vials, propanal accumulated in a nearly stoichiometric amount compared to the decrease of 1-propanol, demonstrating that 1-propanol was converted to propanal, and that oxidation of propanal was effectively inhibited by butanal (see Figure 7.3b).

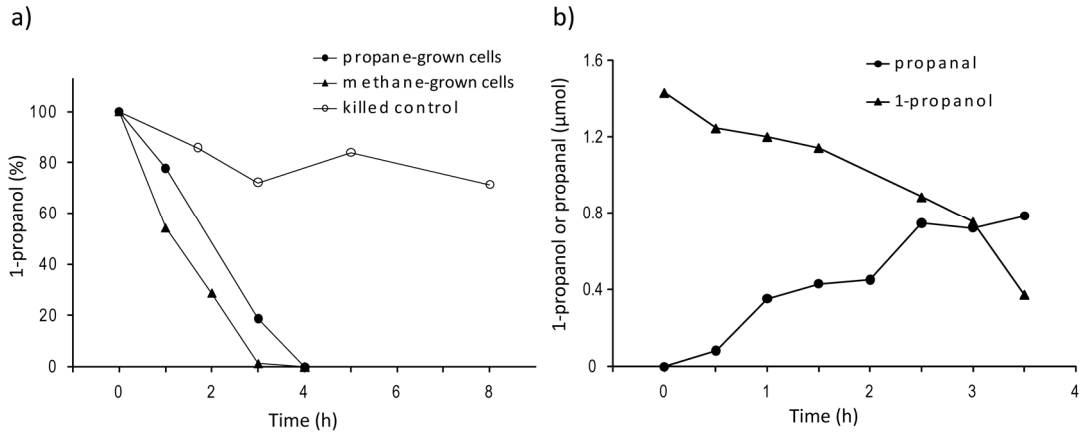

Figure 7.3. a) Consumption of 1-propanol in vials containing methane- or propane-grown cells incubated with 1 mM 1-propanol. When the experiment was repeated (b) using propane-grown cells in the presence of butanal (5 mM), propanal accumulated at a similar rate to the consumption of 1-propanol.

The rate of propane consumption by whole cells was assayed following the method of Arp (1999). Cells growing on propane (exponential phase, specific growth rate approximately 0.01 h^{-1}) were removed from a fermenter, concentrated by centrifugation (6,000 × g, 15 min, 10° C) re-suspended in buffer, and added to air-saturated buffer in a 1 ml gas-tight glass syringe without a needle fitted. Addition of liquids was made by injection through the resultant small opening, controlling the volume with the plunger, without introduction of any gas phase. Mixing was facilitated by the presence of a glass bead in the syringe. Propane was introduced as propane-saturated water. A final volume of 1 ml contained approximately 5 mg (dw) cells, 750 µl air-saturated buffer and 0.3 µmol propane. The syringe was incubated at room temperature and samples (0.5 µl) removed and analysed by GC every 15 minutes. However, propane was consumed at an unexpectedly slow rate, as shown in Figure 7.4, which shows representative data from one of three replicates. Assuming a growth rate in the fermenter of 0.01 h^{-1}, and the conversion factor for propane into biomass determined in the previous chapter, during growth this mass of cells would have been consuming propane at approximately 3 µmol h^{-1}. Therefore cells in the assay were consuming propane at considerably less than 1/10 of their consumption rate prior to harvesting. The experiment was repeated, attempting to harvest the cells in the presence of substrate by flushing bottles and tubes with propane and using propane-saturated buffer for re-suspension of the cells, but the rate of propane consumption was similar. This rate of propane consumption was too slow to generate

intermediates in measureable quantities in inhibition experiments, so this approach was abandoned.

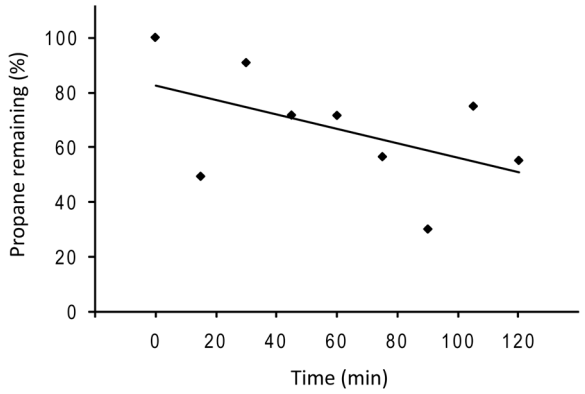

Figure 7.4. Propane consumption by cells incubated with substrate and air-saturated buffer.

7.4 Growth on possible products of propane metabolism

Possible products of propane oxidation were tested for their ability to support growth, since the ability to grow on these intermediates would demonstrate the existence of the required catabolic enzymes in *M. silvestris*.

7.4.1 Growth on 1-propanol and 2-propanol

The ability to grow on these products of terminal and sub-terminal propane oxidation was found to depend on the growth condition of the inoculum used for cultures. Using inoculum from cells grown on methane, *M. silvestris* grew well on 2-propanol, but not on 1-propanol at any of the concentrations tested (0.01 – 0.1% v/v), see Figure 7.5. Furthermore, when growth on 2-propanol was repeated, together with growth on 2-propanol in the presence of 1-propanol, 1-propanol inhibited growth on 2-propanol.

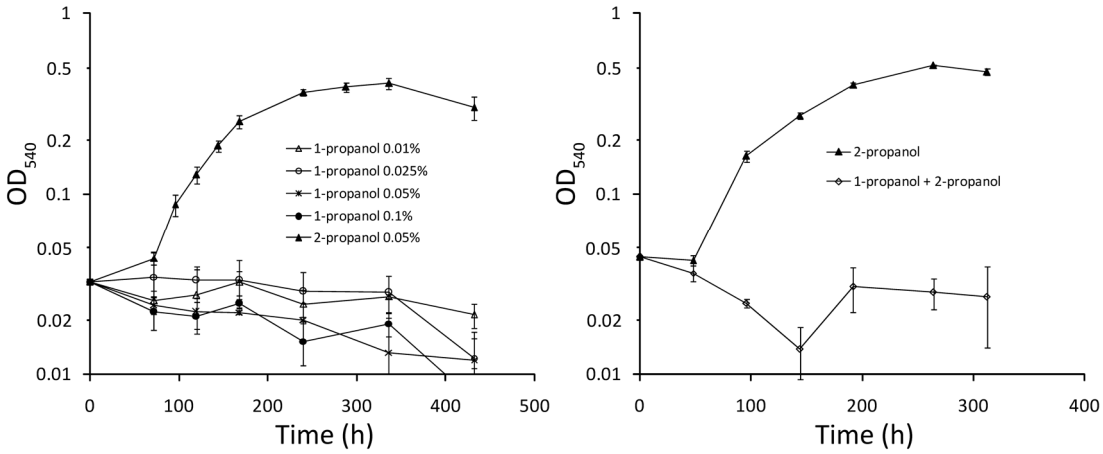

Figure 7.5. Left: growth of *M. silvestris* on 1-propanol or 2-propanol at the concentrations shown (v/v). Right: growth on 2-propanol (0.05% v/v) alone or in the presence of 1-propanol (0.05% v/v). Inoculum for all cultures was grown on methane. Data points are the mean of duplicate (1-propanol) or triplicate vials (2-propanol and 1-propanol with 2-propanol), and error bars show the standard deviation.

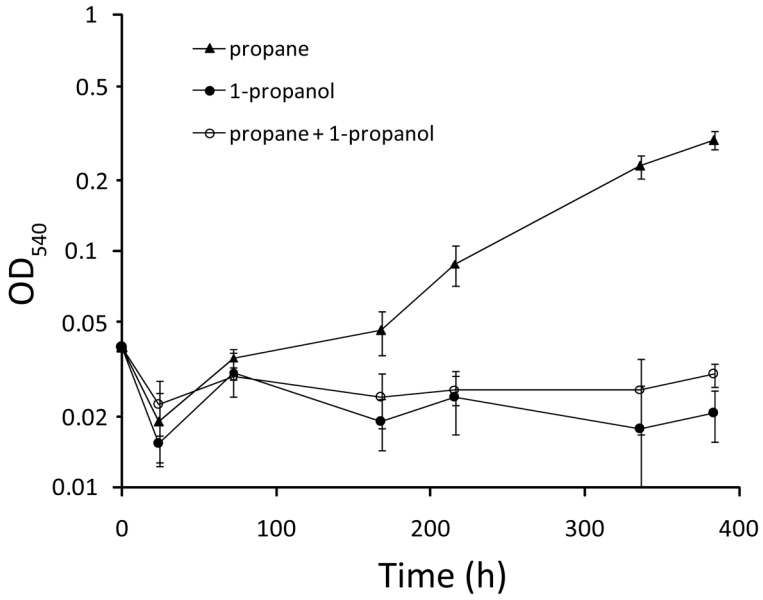

Figure 7.6. 1-propanol (0.05% v/v) completely inhibited growth on propane (30% v/v) when the inoculum was methanol-grown cells, and cultures were unable to grow on 1-propanol alone. Data points are the mean of triplicate vials, and error bars show the standard deviation.

Similarly, growth on propane was completely inhibited by 1-propanol when methanol-grown cells were used as inoculum, see Figure 7.6. However, when inoculum was grown on succinate, growth on succinate in the presence of 1-propanol was possible, although cultures were inhibited in comparison to growth on succinate alone, see Figure 7.7. No inhibition occurred in the presence of 2-propanol and cultures benefited from its presence in comparison to succinate alone.

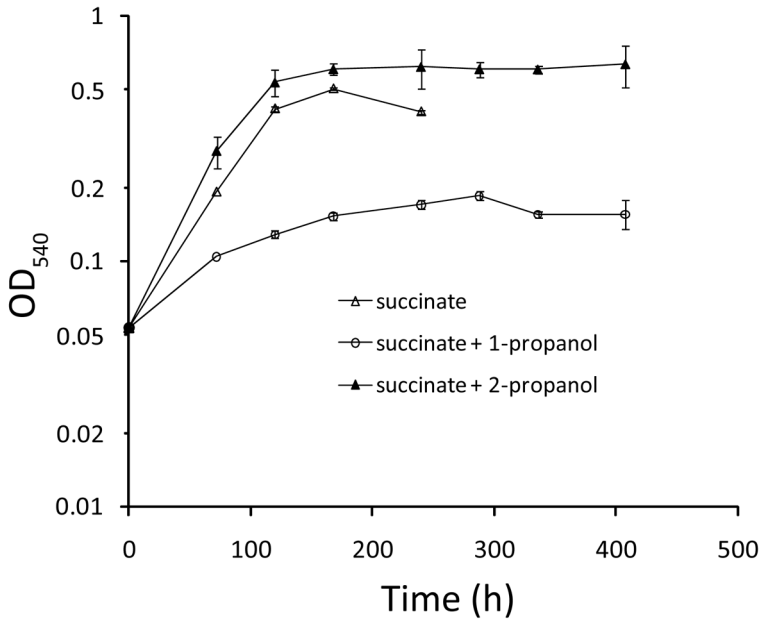

Figure 7.7. Cultures using succinate-grown inoculum were inhibited by the presence of 1-propanol (0.05% v/v) during growth on succinate (3 mM) in comparison to growth on succinate (3 mM) alone or succinate (3 mM) plus 2-propanol (0.05% v/v). Data points are the mean of duplicate vials, and error bars show the standard deviation

Finally, when the inoculum was from cells grown on propane, 1-propanol was less inhibitory during growth on succinate and growth on 1-propanol alone was also possible, although to a lower density and at a lower growth rate than on 2-propanol, see Figure 7.8. These data suggest that 1-propanol (or a product of its metabolism) is toxic to cells, and that the ability to detoxify this compound is not present in methane or methanol-grown cells, but is present to some extent in succinate grown cells and to a greater extent in propane-grown cells. These cells also have the ability to use 1-propanol as carbon and energy source, suggesting that the enzymes for the metabolism of 1-propanol are induced under these growth conditions.

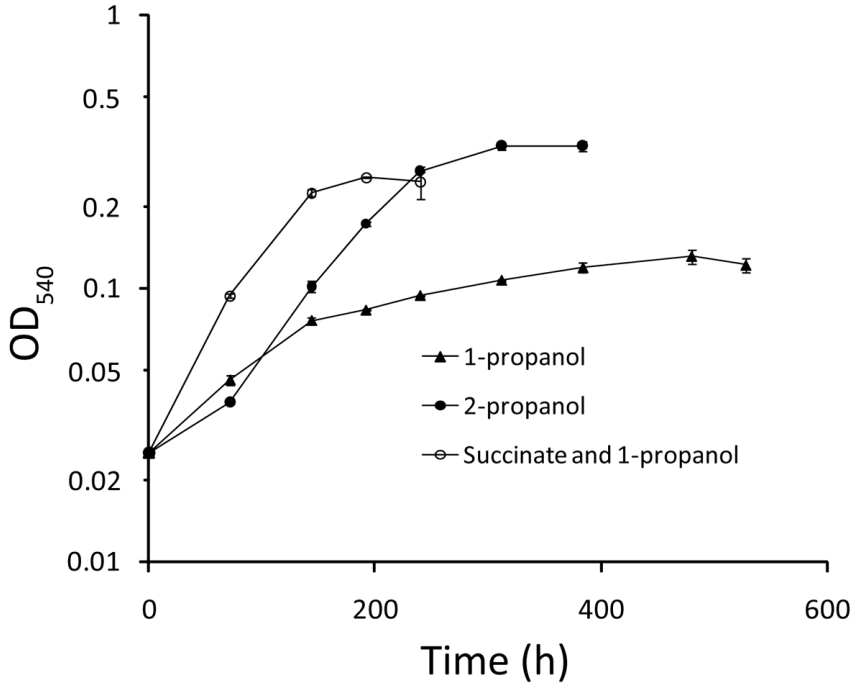

Figure 7.8. 1-propanol (0.05% v/v) was able to support growth when propane-grown cells were used as inoculum, and growth on succinate (5 mM) was not greatly inhibited by 1-propanol (0.05% v/v). Vials with 2-propanol (0.1% v/v) were included for comparison. Data points are the mean of duplicate vials, and error bars show the standard deviation.

7.4.2 Growth on 1,2-propanediol

As noted in Chapter 3, *M. silvestris* grew well on 1,2-propanediol.

7.4.3 Growth on terminal oxidation intermediates propanal and propionate

Similarly to 1-propanol, propanal (3 mM) both did not support growth and completely inhibited growth on 2-propanol when using methanol-grown inoculum (data not shown). Alternative sources of inoculum were not tested with this substrate. Propionate (5 mM) was used as growth substrate, and there was no difference between cultures set up with propane- or succinate-grown inoculum, see Figure 7.9.

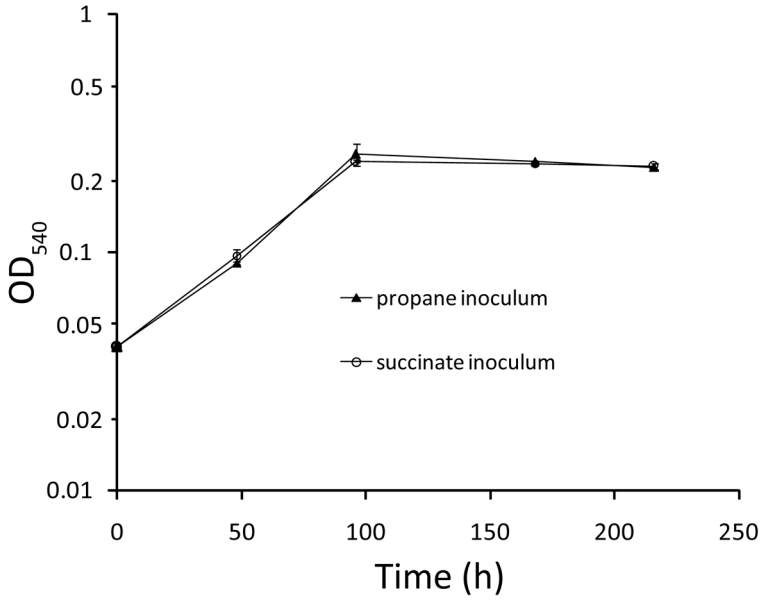

Figure 7.9. Growth on propionate (5 mM) was unaffected by the source of inoculum. Data points are the mean of duplicate vials and error bars show the standard deviation.

7.4.4 Growth on sub-terminal oxidation intermediates

As noted in Chapter 3, *M. silvestris* grew well on acetone and acetol in addition to 2-propanol.

7.5 SDS-PAGE

Soluble extract was prepared from cells grown on 2-propanol and acetone and run on 10% and 15% SDS-PAGE gels together with soluble extract from succinate-, propane- and methane-grown cells and the membrane fraction from succinate- and propane-grown cells, see Figure 7.10. Inspection of these gels suggested that the sMMO subunits were not expressed at a high level in 2-propanol- or acetone-grown cells, but that there was expression of the PrMO subunits during these growth conditions. Attempts were also made to identify bands (other than the SDIMO subunits) differing in expression level between propane-, 2-propanol-, acetone- and succinate-grown cells. Candidate bands were cut from the gels or from similar gels loaded with an increased amount of protein (Figure 7.11, Figure 7.12 and Figure 7.13) and analysed by mass spectrometry by the University of Warwick Proteomics and Mass Spectrometry Facility, and as discussed before (Section 3.12), polypeptide abundance was assumed to correlate with the number of peptides detected. Data are

reported in Table 7.2 and Table 6.2 (Chapter 6) and show that both subunits of the PrMO hydroxylase were found in lanes containing extract from both 2-propanol and acetone. No peptides from sMMO subunits were found in these lanes, although they were present in the lanes containing extract from propane-grown cells. Also detected in lanes loaded with extract from propane-, 2-propanol and acetone-grown cells (but not succinate- or methane-grown) was the product of Msil1641, the final gene in the PrMO gene cluster, annotated as gluconate dehydrogenase. Unfortunately, a band of similar size visible in the lane loaded with the membrane fraction from propane-grown cells (Figure 7.11) was not submitted for analysis. Despite analysis of all major bands present in lanes relating to propane-, 2-propanol- or acetone- but not succinate-grown cells, no obvious candidates for metabolism of the products of propane oxidation were found. A zinc-containing NAD(P)-dependent alcohol dehydrogenase was detected in the acetone growth condition, but no quinoprotein alcohol dehydrogenases (other than MDH) were detected in any lane. Aldehyde dehydrogenases were found in all growth conditions, apparently in less abundance in methane-grown cells. The data presented here and in Chapter 6 indicate that the sMMO is induced by both methane and propane but not by 2-propanol or acetone, whereas the PrMO is induced by these two potential products of sub-terminal propane oxidation, in addition to propane, but not by methane. The expression of Msil1641, apparently at a comparatively high level, under conditions which also led to expression of the PrMO, was noted.

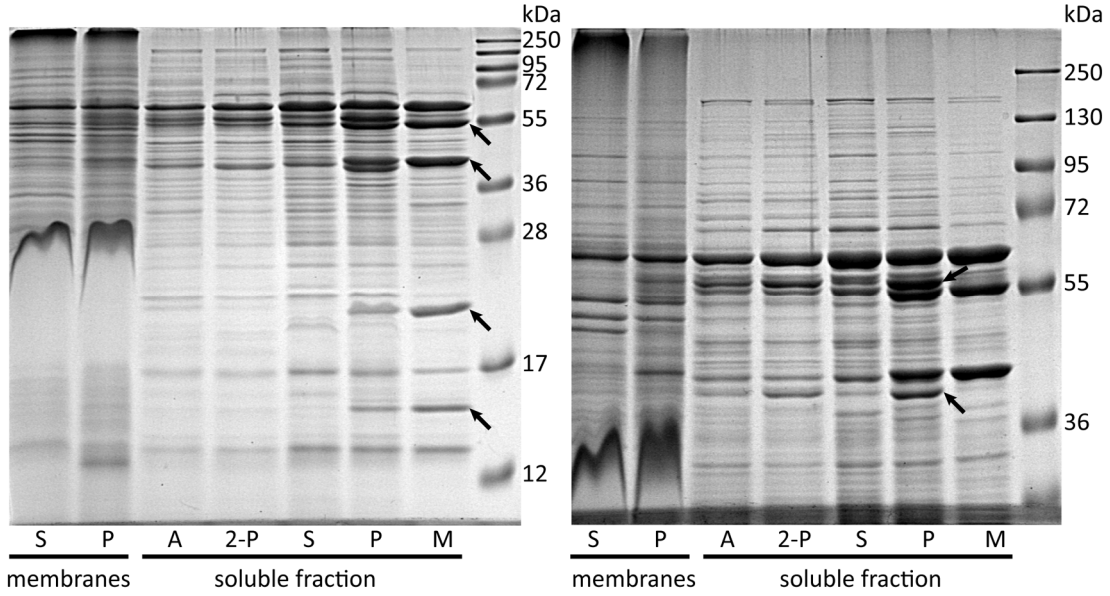

Figure 7.10. 15% (left) and 10% gels loaded with soluble fraction (16 µg) per lane, from cells grown on acetone (A), 2-propanol (2-P), succinate (S), propane (P) or methane (M), together with the membrane fraction from cells grown on succinate or propane. The bands identified as constituents of the sMMO (Chapter 6) are shown arrowed in the left-hand gel and the two subunits of the PrMO hydroxylase are indicated in the right-hand gel.

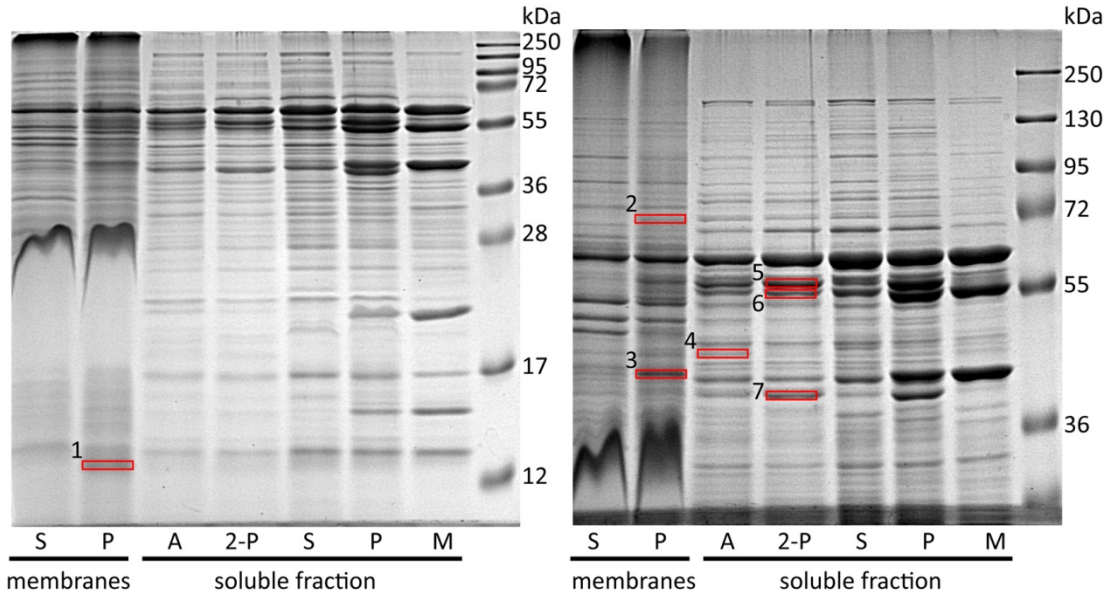

Figure 7.11. The bands shown were cut from the gels shown in Figure 7.10 for mass spectrometric analysis. Band identifying numbers refer to Table 7.2, and lane identifying letters are as Figure 7.10.

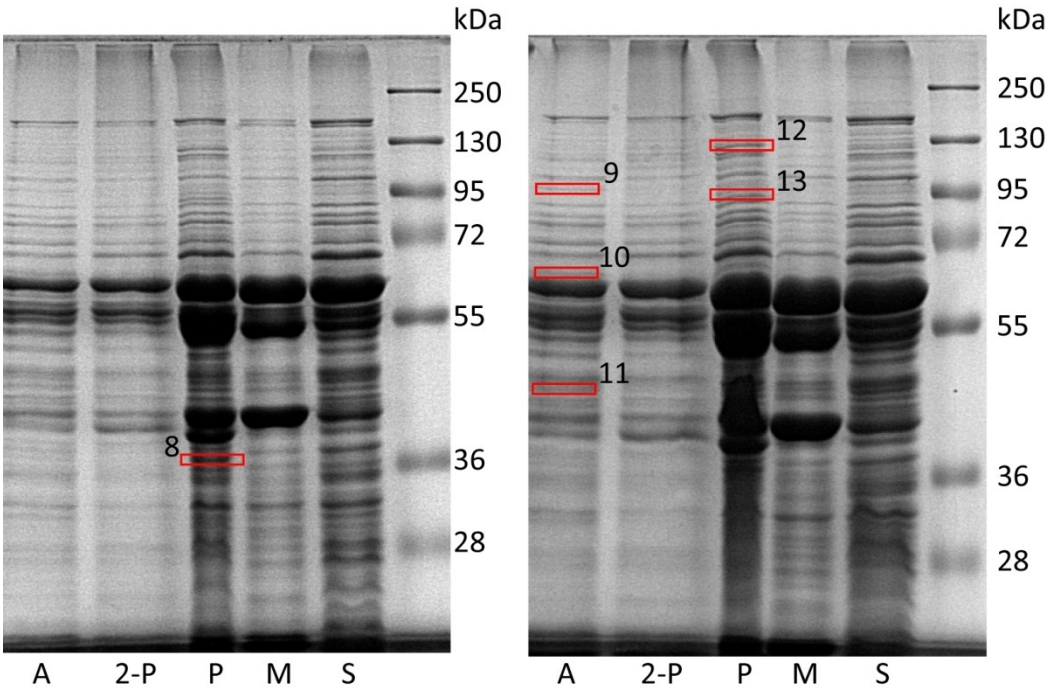

Figure 7.12. Ten percent SDS-PAGE gels were loaded with 38 µg to 64 µg protein (soluble fraction) per lane, from cells grown on acetone (A), 2-propanol (2-P), propane (P), methane, (M), or succinate (S). Band identifying numbers refer to Table 7.2.

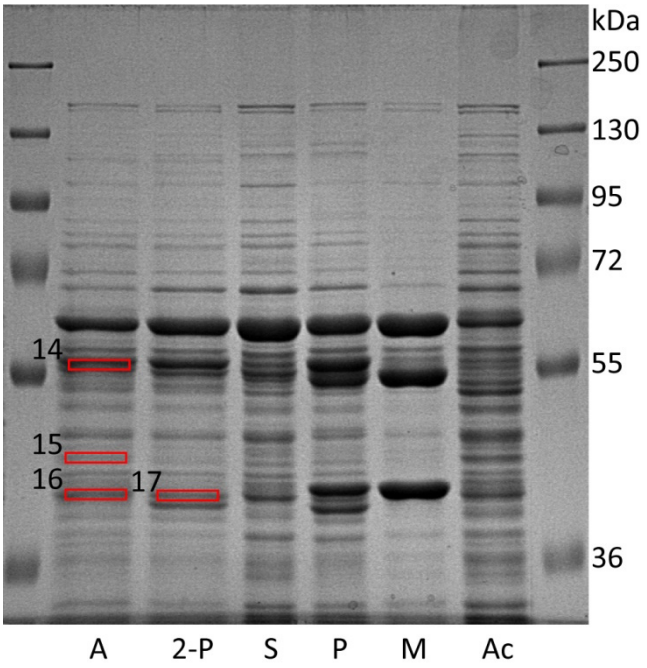

Figure 7.13. A ten percent SDS-PAGE gel was loaded with 16 µg protein (soluble fraction) per lane, from cells grown on acetone (A), 2-propanol (2-P), succinate (S), propane (P), or methane, (M), or acetate (Ac). Band identifying numbers refer to Table 7.2.

Table 7.2. Polypeptide identifications relating to the bands cut from gels shown in Figure 7.11 to Figure 7.13. The most abundant four polypeptides (on the basis of the number of peptides detected) identified in each band are shown. The number of peptides detected and used to identify each polypeptide is shown. The total number of peptides detected from all polypeptides identified in each band is shown for comparison. MM: theoretical molecular mass.

Band	Growth condition	Locus tag Msil	Annotation	Peptides	Total peptides	MM kDa
1	Propane	2345	Phasin	8	22	12.7
		0749	Uncharacterised	8		12.2
		0474	MDH β-subunit	2		10.9
		1861	Nitrogen regulatory protein	2		12.0
2	Propane	1268	mmoR transcriptional regulator	19	39	71.9
		2809	Uncharacterised	6		88.1
		0780	Metalloprotease	5		70.2
		3786	Carbamoyl phosphate synthase	4		71.9
3	Propane	1263	sMMO β-subunit	17	69	44.9
		2007	Urea transporter	12		43.5
		0631	Patatin-like protein	11		43.7
		1810	Uncharacterised	5		40.5
4	Acetone	2891	Methionine adenosyltransferase	13	37	42.4
		3002	Alcohol DH Zn binding	7		35.4
		2283	Phosphoglycerate kinase	6		43.2
		0675	Ribosomal protein	5		64.1
5	2-propanol	1651	PrMO α-subunit	29	86	64.2
		1641	Gluconate dehdrogenase	16		56.7
		1647	Chaperonin (PrMO cluster)	12		57.3
		1375	PEP carboxykinase	8		58.2
6	2-propanol	2342	Aldehyde DH	19	57	55.6
		1651	PrMO α-subunit	12		64.2
		3881	Aldehyde DH	10		53.3
		2810	Phosphoglucomutase	5		54.0
7	2-propanol	1649	PrMO β-subunit	16	31	40.2
		2400	Formylmethanofuran DH	4		39.2
		1194	Fructose bisphosphate aldolase	3		39.1
		2991	RNA polymerase α-subunit	3		37.1
8	Propane	2246	ABC transporter	8	29	37.4
		3011	Ketol acid isomerase	6		36.6
		0499	Cysteine synthase	5		35.9
		1693	Translation elongation factor	3		32.0
9	Acetone	3523	Alanyl tRNA synthetase	25	38	96.4
		1360	Pyruvate carboxylase	7		126.1
		2733	Coagulation factor-like protein	4		87.6
		0716	Pyruvate phosphate dikinase	2		96.1
10	Acetone	3157	Isocitrate lyase	12	42	59.8
		0471	MDH α-subunit	10		68.5
		3234	Dihydroxy acid dehydratase	6		65.2
		2999	Thiamine biosynthesis protein	6		67.1
11	Acetone	2891	Methionine adenosyltransferase	13	53	42.4
		2283	Phosphoglycerate kinase	8		43.2
		1716	Succinyl CoA synthetase	6		42.9
		2110	Glycine hydroxymethyltransferase	5		46.0

Table 7.2 (contd.)

Band	Growth condition	Locus tag Msil	Annotation	Peptides	Total peptides	MM kDa
12	Propane	1360	Pyruvate carboxylase	27	55	126.1
		0672	Carbamoyl P synthase	18		118.5
		2860	Isoleucyl tRNA synthetase	3		119.7
		1263	sMMO β-subunit	3		44.9
13	Propane	3131	Uncharacterised	24	41	88.1
		0716	Pyruvate phosphate dikinase	6		96.1
		2733	Coagulation factor-like protein	4		87.6
		1838	Phenylalanyl tRNA synthetase	3		85.5
14	Acetone	2342	Aldehyde dehydrogenase	12	46	55.6
		1651	PrMO α-subunit	11		64.2
		1375	PEP carboxykinase	9		58.2
		1641	Gluconate dehydrogenase	6		56.7
15	Acetone	2891	Methionine adenosyltransferase	15	29	42.4
		2283	Phosphoglycerate kinase	5		43.2
		1716	Succinyl CoA synthetase	4		42.9
		3002	Alcohol DH Zn binding	3		35.4
16	Acetone	1649	PrMO β-subunit	11	29	40.2
		2996	Acetyl CoA acetyltransferase	10		40.2
		0471	MDH α-subunit	2		68.5
		0832	Aminotransferase	2		41.8
17	2-propanol	1649	PrMO β-subunit	12	31	40.2
		2996	Acetyl CoA acetyltransferase	11		40.2
		1354	Uncharacterised	3		43.2
		0832	Aminotransferase	3		41.8

7.6 Measurement of intermediates in cell cultures

M. silvestris was grown on propane (1:5 propane:air ratio) in a fermenter, and metabolites present in the culture medium quantified by gas chromatography (GC), using direct injection of culture supernatant, as described in Materials and Methods. Concentrations of 2-propanol and acetone were monitored between days 63 and 105, reaching 15 and 9 mM respectively at day 91. The propane supply was interrupted between days 92 and 96, resulting in the decrease of 2-propanol and acetone concentrations to near zero, whereas culture density increased by approximately two OD units. Following the resumption of the propane supply on day 96, accumulation of 2-propanol and acetone was observed once again, see Figure 7.14. These data demonstrate that 2-propanol and acetone result (directly or indirectly) from propane oxidation and that cells growing on propane in the presence of these intermediates can metabolise them without an appreciable lag phase in the absence of propane.

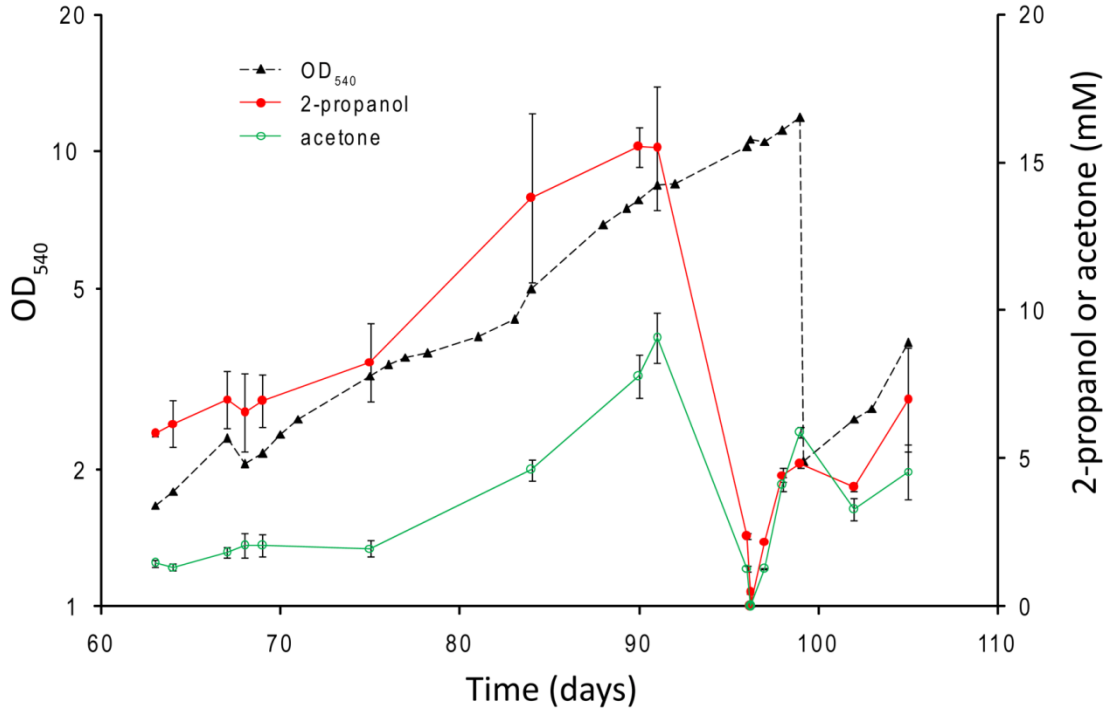

Figure 7.14. Growth of *M. silvestris* on propane in 2 l fermenter culture, and accumulation of 2-propanol and acetone. The propane supply was shut off on day 92 and resumed on day 96, during which period 2-propanol and acetone concentrations declined. Cells were removed from the fermenter and replaced with fresh medium on day 99. 2-propanol and acetone concentrations are the mean of triplicate measurements and error bars show the standard deviation.

This experiment was repeated using cells grown on 4% (v/v) propane in triplicate 120 ml serum vials containing 25 ml medium. Solvent extraction of metabolites, as described in Materials and Methods, enabled more sensitive measurement of 1-propanol, 2-propanol, acetone and acetol. Under these conditions 2-propanol accumulated to approximately 0.5 mM at 210 h before declining to below the limit of detection by 300 h, see Figure 7.15. No other intermediates were detected.

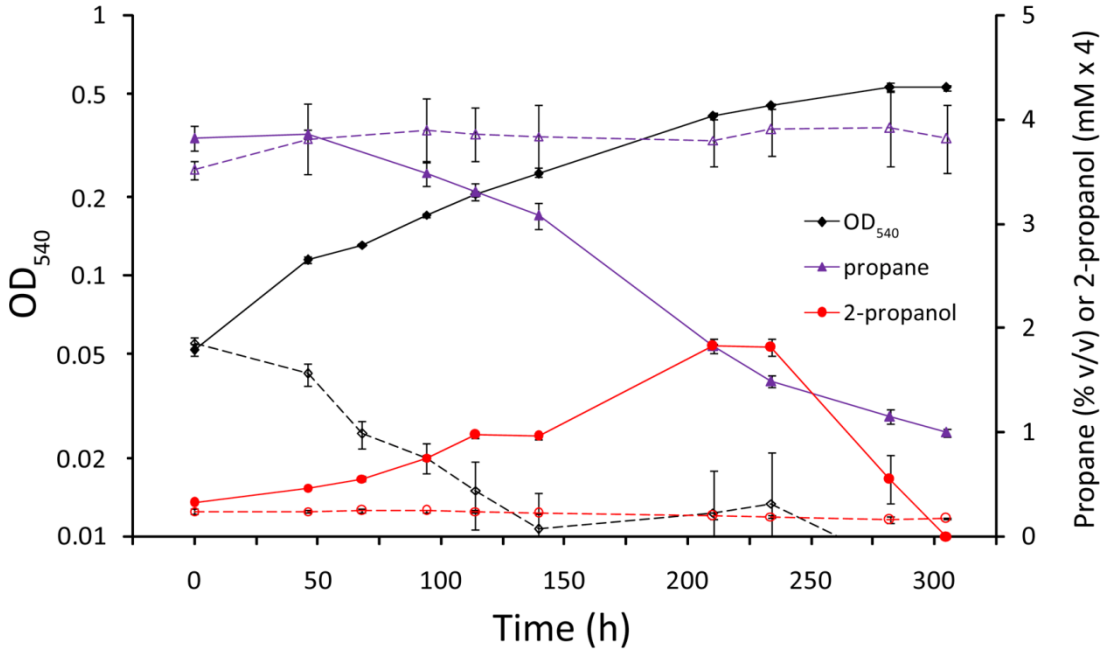

Figure 7.15. 2-propanol was detected in the culture medium of vials growing on 4% (v/v) propane, reaching 0.5 mM after 210 hours. Culture density (OD_{540}) is shown in black, propane concentration in purple and 2-propanol in red with solid lines and filled symbols. Control vials, containing cells killed by autoclaving, are shown as dotted lines and open symbols. The 2-propanol concentration is shown as × 4 on the y-axis. Data points are the mean of measurements from triplicate vials, and error bars show the standard deviation.

The molar ratio (2-propanol present in the medium) : (propane consumed) was calculated, (including 2-propanol removed during sampling since one millilitre aliquots were removed at each sampling point to measure the culture density), for each time point from 94 h to the end of the experiment. These data are plotted against time in Figure 7.16, and show approximately 25% at 94 h, declining as the 2-propanol was consumed by the culture. This figure (25%) therefore represents the minimum proportion of propane which is converted into 2-propanol (as opposed to other products) under these conditions, since no allowance has been made for consumption of 2-propanol by the cultures.

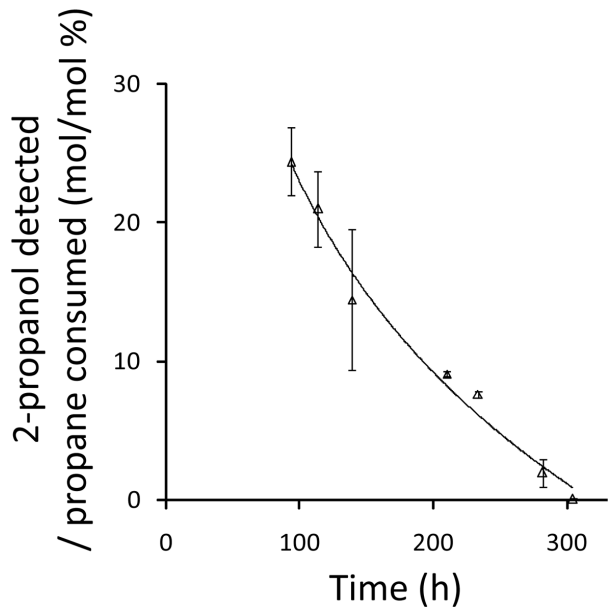

Figure 7.16. For the cultures growing on propane (4% v/v) shown in Figure 7.15, the molar amount of 2-propanol present at each time point (and including the amounts previously removed during sampling) is expressed as a percentage of the propane consumed. Each data point represents the mean of triplicate vials and error bars show the standard deviation.

7.7 Oxygen uptake of whole cells grown on methane, propane or succinate

A Clark oxygen electrode was used to assess the substrate-induced oxygen uptake of whole cells of *M. silvestris.* Cells grown in the fermenter on methane, propane or succinate were used as described in Materials and Methods, and tested with potential intermediates of propane oxidation (at 5 mM final concentration), and substrate-induced oxygen uptake rates recorded. As shown in Figure 7.17, whereas the rate in response to 1-propanol was similar between methane- and propane-grown cells, propane-grown cells showed double the response to 2-propanol, and approximately four and seven fold activity in response to acetone and acetol respectively. The response of succinate-grown cells to these substrates was similar to that of methane, suggesting that enzymes for the metabolism of these compounds are upregulated during growth on propane.

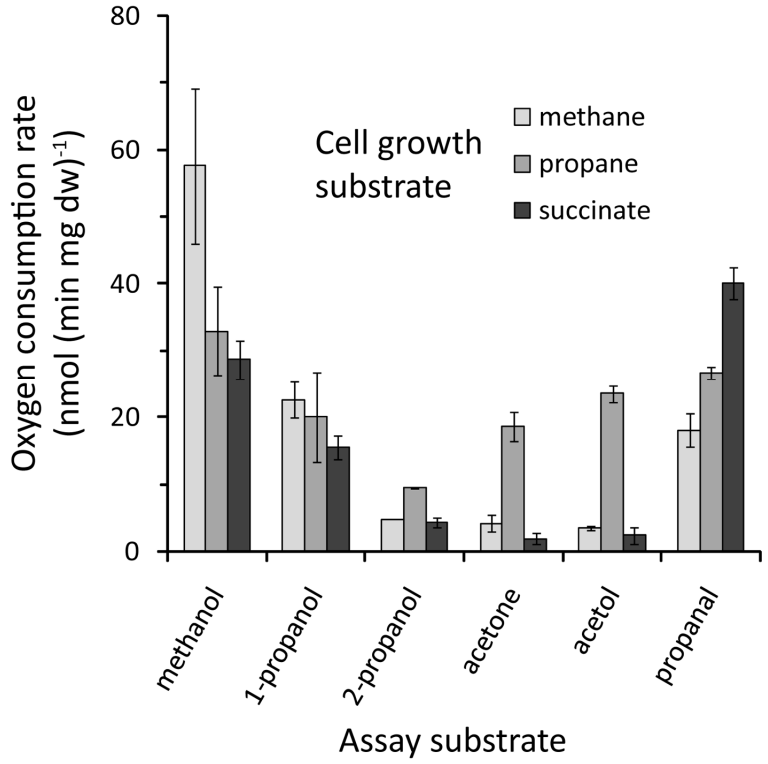

Figure 7.17. *M. silvestris* cells grown on methane, propane or succinate were used in a Clark oxygen electrode and oxygen uptake recorded, in response to the substrates shown. Substrates were used at a final concentration of 5 mM. Values are the mean of at least three measurements, and error bars show the standard deviation.

Since it was thought likely that propanal might be toxic to cells, the assay was repeated at a lower substrate concentration (82 μM). Under these conditions propanal-induced oxygen consumption was five fold higher in both propane- and succinate- compared with methane-grown cells (23.8 ± 6.3, 23.5 ± 1, 4.8 ± 0.4 nmol (min mg dw)$^{-1}$ (mean of three replicates ± standard deviation) respectively).

7.7.1 Stoichiometry of substrate-induced oxygen consumption

The stoichiometry of oxygen utilisation in cells from the different growth conditions was investigated by the addition of between 100 – 250 nmol of methanol, 1-propanol or propanal. As shown in Figure 7.18, methanol induced a similar amount of oxygen consumption in all cell types. However, propane-grown cells used approximately three and five times as much oxygen, when stimulated with 1-propanol and propanal respectively, as methane- or succinate-grown cells.

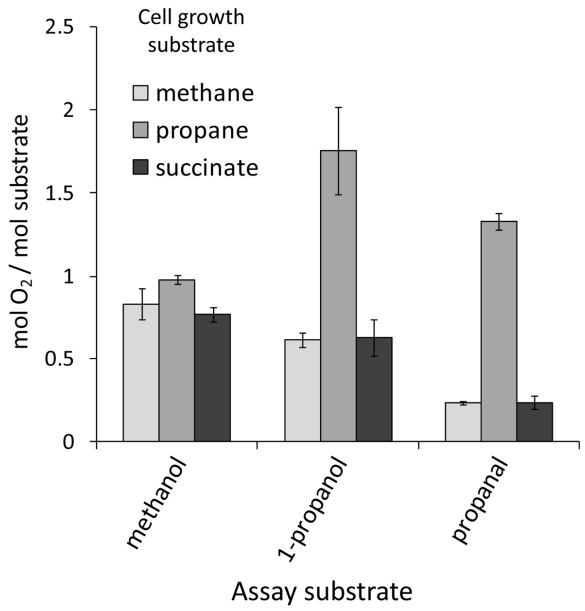

Figure 7.18. Stoichiometry of oxygen uptake as a fraction of substrate added. The data are the mean of triplicate measurements and error bars show the standard deviation.

The approximately equi-molar consumption of methanol and oxygen is consistent with the oxidation of most of the methanol to formate. The oxygen required for the oxidation of 1-propanol and propanal was nearly identical for cells grown on methane and succinate, but the greatly increased requirement for oxygen, in response to these compounds, by propane-grown cells demonstrated that oxidation of 1-propanol and propanal proceeded further in these cells, presumably due to induction of enzymes able to further metabolise the products of the initial oxidation.

7.7.2 1,2-propanediol-related activity

Propane-grown cells had no detectable activity with 1,2-propanediol (0.83 mM final concentration), nor did 1,2-propanediol-grown cells have detectable activity with propane (25 μM), 2-propanol or acetone (0.83 mM). These data suggest that different enzymes or mechanisms are responsible for growth on 1,2-propanediol compared to propane.

7.8 Alcohol dehydrogenase assay

Alcohol dehydrogenase (ADH) was assayed in *M. silvestris* soluble cell extract. Quinoprotein (methanol dehydrogenase (MDH) – like) ADH was assayed by

spectrophotometric measurement of dichlorophenolindophenol (DCPIP) reduction coupled to phenazine methosulfate (PMS) as artificial electron acceptor. As shown in Table 7.3, methane-grown extract had 14-fold higher activity with 1-propanol compared to 2-propanol, whereas propane-grown extract had 6-fold higher 2-propanol activity compared to methane-grown extract, and activity with 1-propanol and 2-propanol was similar. As is the case for MDH (Duine et al., 1979), 1- and 2-propanol activity was dependent on the presence of ammonium in the assay reaction, and no activity was detected in its absence.

Table 7.3. Quinoprotein ADH activity (mean of triplicate measurements ± standard deviation), assayed as DCPIP reduction (nmol (min mg)$^{-1}$) in soluble extract from methane- or propane-grown cells.

Growth substrate	Assay substrate	
	2-propanol	1-propanol
methane	63 ± 15	871 ± 13
propane	381 ± 30	363 ± 7

Nicotinamide nucleotide coenzyme-dependent ADH activity was measured by following the reduction of NAD^+ or $NADP^+$. Activity with the alcohols tested was low (Table 7.4) and there was no increased activity in propane-grown extract with potential intermediates of propane oxidation.

Table 7.4. NAD(P)$^+$- dependent ADH activity measured as coenzyme reduction (nmol (min mg)$^{-1}$) in soluble extract from methane- or propane-grown cells.

Assay substrate	Growth substrate / coenzyme			
	Methane		Propane	
	NAD^+	$NADP^+$	NAD^+	$NADP^+$
Ethanol	3.7	1.3	1.3	0
1-propanol	4.6	8.2	0.6	3.3
2-propanol	4.7	0	1.5	0
Acetol	25	11	0	7
glycerol	0	0	2	0

These data suggest that pyrroloquinoline quinone (PQQ)-containing enzymes are responsible for the oxidation of both 1-propanol and 2-propanol. MDH may be responsible for the oxidation of 1-propanol, and this enzyme has a known wide substrate specificity (Anthony, 2000), but the pronounced difference between the relative activities with the propanol isomers in methane- and propane-grown cells suggests that the enzyme responsible for 1-propanol oxidation in methane-grown

cells is different to the enzyme responsible for 2-propanol oxidation in propane-grown cells.

7.9 Non-denaturing PAGE

In order to identify or distinguish the enzymes responsible for 1- and 2-propanol oxidation, non-denaturing gels were stained for ADH activity. This method was successfully used by Vangnai and Arp (2001) to identify the ADHs responsible for butanol oxidation in *Thauera butanivorans.* Gels were stained by incubation in buffer containing PMS and nitroblue tetrazolium (NBT) with an alcohol substrate, with and without NAD^+. Figure 7.19 shows staining of gels loaded with extract from cells grown on 2-propanol, propane, succinate or methane, incubated with 1- or 2-propanol (1 or 2 mM), both with and without NAD^+, as described in Materials and Methods. A band was visible only in lanes containing extract from propane or 2-propanol-grown cells, suggesting that proteins capable of PMS-mediated reduction of NBT were present in propane or 2-propanol-grown cells but not in the other growth conditions. Lanes loaded with acetate-grown extract also did not contain the band present in the 2-propanol and propane lanes (data not shown). The prominent high molecular mass band is possibly related to MDH activity, shown to be present in all growth conditions. An NAD^+-dependent band which only appeared in the methane growth condition incubated with 2-propanol was not investigated further. Methanol-incubated gels also resulted in the appearance of similar bands in lanes loaded with extract from propane- or 2-propanol-grown cells, and it was subsequently noticed that these bands appeared (to a lesser density) when incubated without substrate. It was found that chemicals contained a significant quantity of alcohol. For example a 5 mg ml^{-1} stock solution of NBT contained more than 5 mM methanol. Despite purification by ether extraction, it was impossible to eliminate appearance of bands without substrate. No bands appeared in the absence of PMS, and since significant transient activity has frequently been reported for MDH without substrate in enzyme assays (Anthony and Zatman, 1964), it was thought that the same cause might also be responsible for this observation. Therefore it was not possible to associate the band which appeared only in lanes containing extract from propane- or 2-propanol-grown cells with a particular alcohol substrate. However,

since the band only occurred in lanes containing extract from these growth conditions, the band shown in Figure 7.20 was cut from the gel and submitted for mass spectrometric analysis by the University of Warwick Proteomics and Mass Spectrometry Service. This gel also included a lane loaded with extract from cells grown on acetone, demonstrating that the protein of interest was also expressed under these growth conditions.

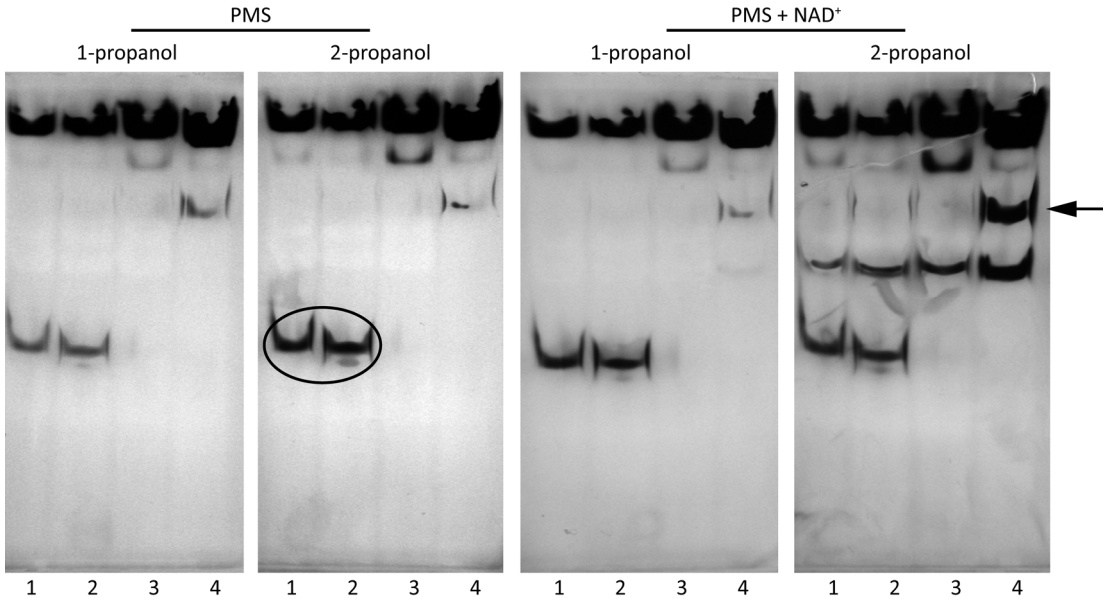

Figure 7.19. Non-denaturing gels were stained by incubation with 1-propanol or 2-propanol in the presence of PMS and NBT, either without (left) or with NAD^+ (right) (as shown above). Lanes were loaded with soluble extract (30 µg) from cells grown on 2-propanol (lane 1), propane (lane 2), succinate (lane 3), or methane (lane 4). Bands, independent of NAD^+, appeared in lanes containing extract from cells grown on 2-propanol or propane only (ringed in the 2-propanol/PMS gel). An NAD^+-dependent band visible in the methane-grown condition (arrowed) was not investigated further.

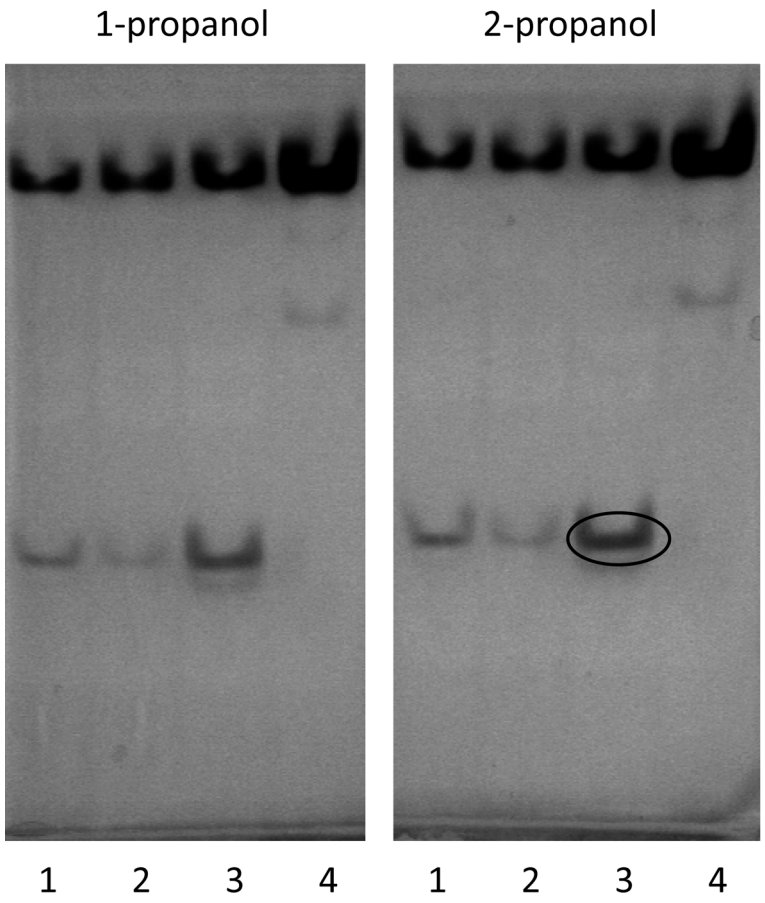

Figure 7.20. The band shown was cut from the gel and submitted for analysis by mass-spectrometry. Lanes were loaded with extract from cells grown on acetone (lane 1), 2-propanol (lane 2), propane (lane 3), or methane (lane 4).

Polypeptides identified from the gel-cut band are shown in Table 7.5. On the basis of the number of peptides, the most abundant polypeptide in the gel band corresponded with Msil1641, the final gene of the propane monooxygenase cluster. The adjacent gene, Msil1642 was also present in high abundance, together with the two subunits of the PrMO hydroxylase. These data suggested that the genes downstream of the monooxygenase structural genes might also be involved in propane metabolism. However, no polypeptide annotated as PQQ-dependent alcohol dehydrogenase was detected, despite evidence for its existence in enzyme assays.

Table 7.5. Polypeptides identified in the band cut from the gel shown in Figure 7.20. The number of peptides and corresponding percentage coverage used for identification of each polypeptide is shown. Polypeptides encoded by the propane monooxygenase gene cluster are shown shaded.

Locus tag	Peptides	Sequence coverage (%)	Annotation
0162	4	10.4	Hydro-lyase, Fe-S type
0178	4	10.9	Cysteine synthase
0202	4	15.1	Oxidoreductase, zinc-binding
0582	5	16.4	Translation elongation factor
0795	3	6.6	Chaperonin GroEL
0963	4	5.1	Phosphoribosylformylglycinamidine cyclo-ligase
1025	2	9.5	Inorganic disphosphatase
1160	2	8.8	Methyltransferase
1226	7	9	Acetate - CoA ligase
1262	2	4.4	sMMO alpha subunit
1611	3	20.6	Uncharacterised
1641	13	28.9	Gluconate dehydrogenase
1642	7	35.2	Uncharacterised
1649	5	15.4	Hydroxylase small subunit
1651	9	14.1	Hydroxylase large subunit
1808	7	22.1	Uncharacterised
2145	2	8.1	Methylthioadenosine phosphorylase
2390	3	22.9	Formaldehyde activating enzyme

7.10 Metabolism of the products of propane oxidation

Since the data indicated an increased ability to metabolise both 1-propanol and 2-propanol in propane-grown cells, the possible pathways involved were investigated. Initially, some data were provided by analysis of the phenotypes of the deletion strains discussed in previous chapters.

7.11 Growth of strain ΔPrMO and strain ΔMmoX on sub-terminal intermediates

Strain ΔPrMO, with a deletion of the PrMO α-subunit (Chapter 6), was tested for growth on the sub-terminal products of propane oxidation. There was little difference between the wild-type and strain ΔPrMO during growth on acetone or acetol, see Figure 7.21. However, in two independent experiments, strain ΔPrMO grew at half the rate of the wild-type on 2-propanol, and exhibited a much increased lag phase, see Figure 7.22 and Table 7.6.

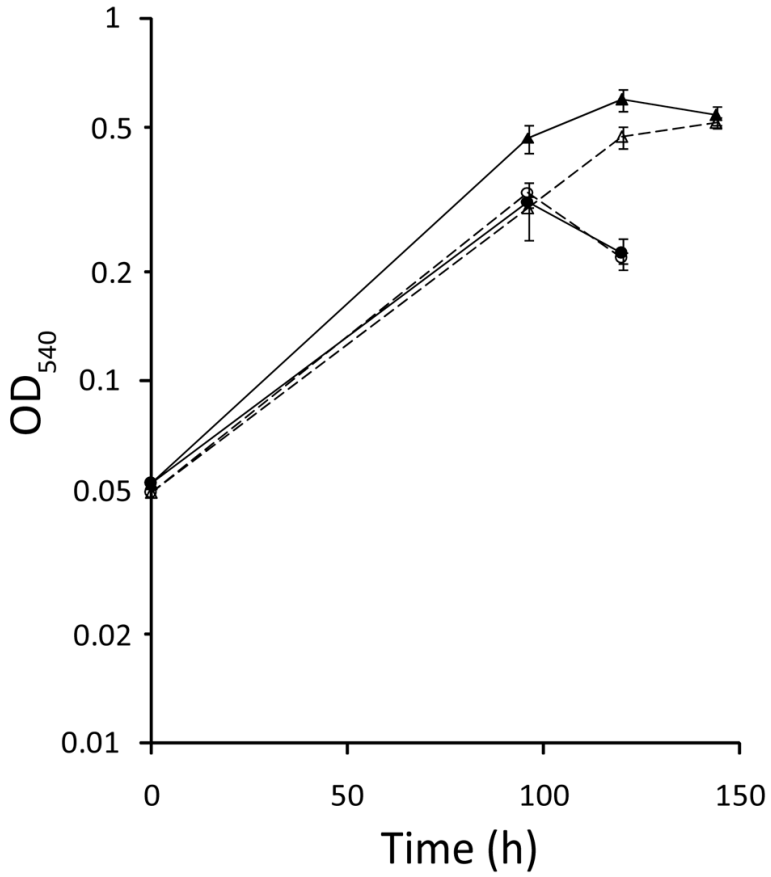

Figure 7.21. Growth of *M. silvestris* wild-type (solid lines and filled symbols) and strain ΔPrMO (dashed lines and open symbols) on acetone (triangles) or acetol (circles) (both 0.05% v/v). Error bars show the standard deviation of triplicate vials.

Table 7.6. Growth of *M. silvestris* wild-type and strain ΔPrMO on 2-propanol. Data are the mean of five or six replicates ± standard deviation.

Strain	Specific growth rate (h^{-1})	Lag time (h)
Wild-type	0.018 ± 0.002	55 ± 10
ΔPrMO	0.009 ± 0.001	167 ± 23

Strain ΔMmoX was able to grow on 2-propanol and acetone similarly to the wild-type (data not shown).

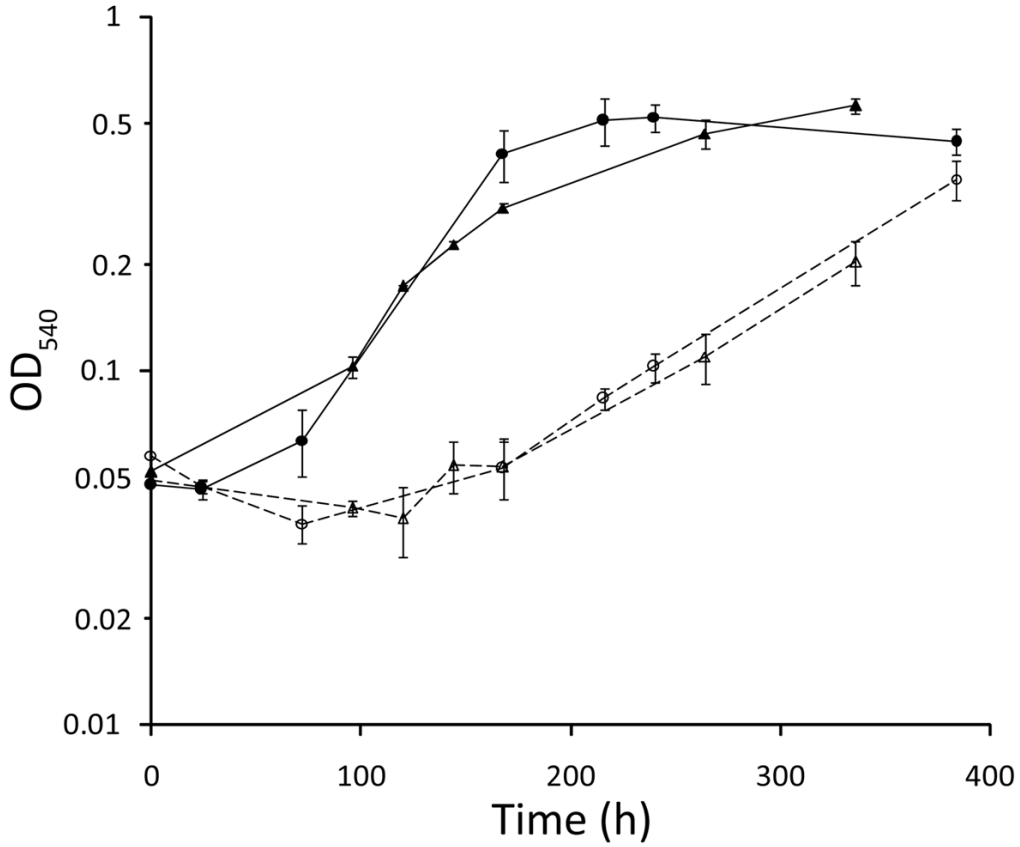

Figure 7.22. The growth of strain ΔPrMO (dashed lines and open symbols) on 2-propanol (0.05% v/v) was compared with the wild-type (solid lines and filled symbols) in two independent experiments (triangles or circles). Error bars show the standard deviation of triplicate vials (except wild-type, first experiment; duplicate vials).

7.12 Growth of strain ΔICL on propane, propionate, 2-propanol and acetone

The phenotype of strains ΔICL and ΔSGAT provided evidence as to the eventual products of propane metabolism. Strain ΔICL was able to grow on propane and 2-propanol at a similar rate to the wild type, although with an increased lag phase, as shown in Figure 7.23 and Table 7.7. Strain ΔICL was also able to grow on acetone (data not shown). Growth on propionate was somewhat reduced, but growth rate and density were more than 50% of the wild type. Since this strain was unable to grow on one-carbon compounds and growth on acetate or ethanol was severely restricted in comparison to the wild-type, (see Chapter 5, Section 5.6.2,) these data suggest that the products of propane metabolism were not one- or two carbon compounds. Expression of MDH was shown to be affected in strain ΔICL (see Chapter 5, Section 5.9), which might account for the increased lag phase exhibited by this strain during growth on propane or 2-propanol.

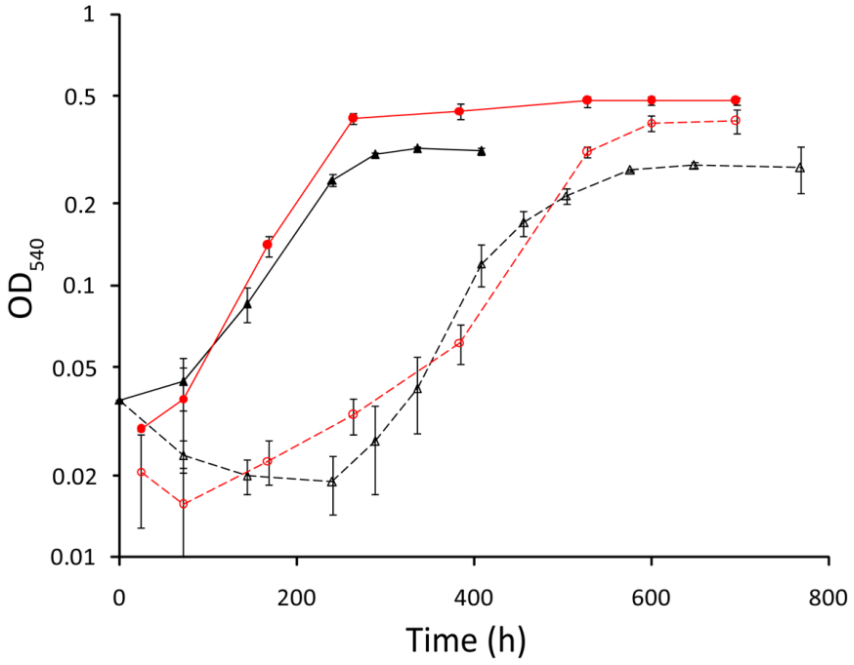

Figure 7.23. Growth of *M. silvestris* wild-type (solid lines and filled symbols) and strain ΔICL (dashed lines and open symbols) on propane (in black, triangles) (20% v/v) or 2-propanol (in red, circles) (0.1% v/v). Error bars show the standard deviation of triplicate vials.

Table 7.7. Growth of *M. silvestris* wild-type and strain ΔICL on propane and possible products of propane metabolism. Figures are the mean of at least three replicates ± standard deviation. Substrate concentrations: 5 mM, except propane: 20% (v/v), 2-propanol: 0.1% (v/v). Figures showing growth on succinate are included for comparison.

Growth substrate	Specific growth rate (h^{-1})		Lag time (h)		Increase in biomass (OD)	
	BL2	ΔICL	BL2	ΔICL	BL2	ΔICL
Propane	0.010 ± 0.001	0.013 ± 0.003	60 ± 23	321 ± 23	0.34 ± 0.11	0.27 ± 0.01
2-propanol	0.012 ± 0.001	0.011 ± 0.001	75 ± 22	329 ± 18	0.44 ± 0.02	0.37 ± 0.04
Propionate	0.024 ± 0.002	0.015 ± 0.002	108 ± 13	269 ± 25	0.19 ± 0.01	0.12 ± 0.03
Succinate	0.025 ± 0.001	0.027 ± 0.001	0 ± 1	0 ± 2	0.48 ± 0.06	0.42 ± 0.04

7.13 Growth of strain ΔSGAT on propane

Strain ΔSGAT was able to grow on propane with specific growth rate of 0.011 ± 0.001 h^{-1} (mean of three replicates ± standard deviation) (Figure 7.24) with a lag time of 59 ± 15 h, growth which is comparable to the wild-type, further confirming that propane is not metabolised via formaldehyde or other one-carbon compounds in *M. silvestris*.

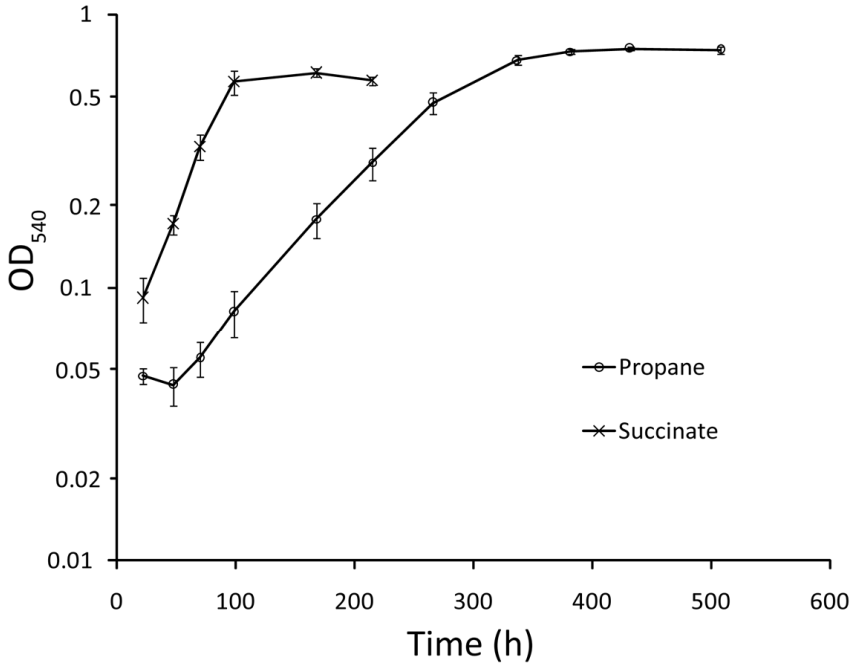

Figure 7.24. Growth of strain ΔSGAT on propane (20% v/v) or succinate (5 mM). Error bars show the standard deviation of measurements from triplicate vials.

7.14 Identification of polypeptides of the methylmalonyl-CoA pathway enzymes

Soluble extracts from cells grown on propane or succinate were supplied to the Biological Mass Spectrometry and Proteomics group at the University of Warwick, as mentioned in Section 2.11.3, and analysed by Nisha Patel using a development of a quantitative label-free mass-spectrometry method previously published by Vibhuti Patel et al. (2009) (manuscript in preparation). Apart from the polypeptides of the PrMO and sMMO and products of adjacent genes already identified by SDS-PAGE in Chapter 6, Section 7.5 and Section 7.9, notable findings were the presence of significant amounts of the components of the methylmalonyl-CoA pathway enzymes propionyl-CoA carboxylase and methylmalonyl-CoA mutase in extract from propane-grown cells. The amount of each polypeptide identified is shown in Table 7.8 as percentage of the total soluble fraction, and in propane-grown cells these two enzymes accounted for 1.2% of total soluble protein.

Table 7.8. Methylmalonyl-CoA pathway polypeptides detected in soluble extract from cells grown on succinate or propane.

Locus tag Msil	Gene product	Polypeptide abundance as proportion (%) of total soluble protein from cells grown on	
		Succinate	Propane
3784	Methylmalonyl-CoA mutase α-subunit	Not detected	0.242
3785	Methylmalonyl-CoA mutase β-subunit	Not detected	0.118
3786	Propionyl-CoA carboxylase β-subunit	0.070	0.665
3787	Propionyl-CoA carboxylase α-subunit	Not detected	0.158

7.15 Enzyme activities – terminal pathway

Incorporation of 1-propanol, the product of terminal propane oxidation, into biomass by the hypothesised pathway requires oxidation via propanal to propionate, followed by activation to form propionyl-CoA. The activities of the enzymes responsible were assayed.

7.15.1 Aldehyde dehydrogenase

NAD(P)-dependent aldehyde dehydrogenase was assayed in cell-free extract from cells grown on methane, propane or succinate. The pH optimum was found to be 9.25, and NAD^+ as cofactor was approximately 34% more effective than $NADP^+$ (standard deviation 2.6%, n = 3). Coenzyme A (0.3 mM final concentration) did not enhance activity. Propanal-associated activity was approximately 25 nmol $(min\ mg)^{-1}$ in extract from both propane- and succinate-grown cells (Figure 7.25), approximately four-fold higher than in methane-grown cell extract. To sustain a growth rate of 0.01 h^{-1} would require propane consumption of 1.11 μmol $(h\ mg)^{-1}$ assuming 50% conversion of substrate carbon into biomass (Chapter 6), equivalent to 18.5 nmol $(min\ mg)^{-1}$, assuming cell biomass is 50% protein, demonstrating that this level of activity is sufficient to metabolise all the propane consumed.

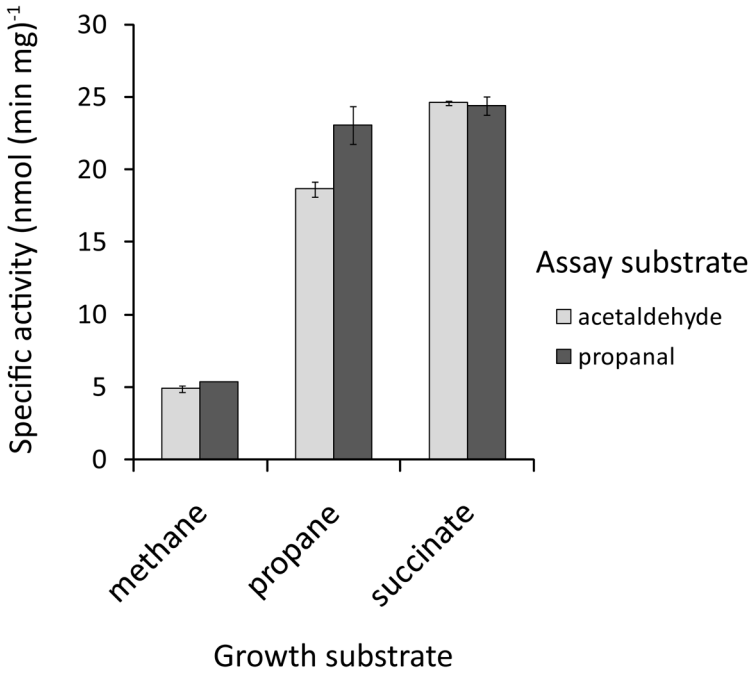

Figure 7.25. NAD^+-dependent aldehyde dehydrogenase activity in cell-free extract from *M. silvestris* grown on methane, propane or succinate. Activity is shown as formation of NADH. Error bars show the standard deviation of triplicate measurements.

7.15.2 Acyl-CoA synthetase

Acyl-CoA synthetase activity in cell-free extract from cells grown on acetate, propane or succinate was assayed using a discontinuous hydroxamate assay by measuring the formation of acetylhydroxamate against blanks without coenzyme A. Activity was high in extract from each growth condition, (see Figure 7.26), and propionate-dependent activity was not up-regulated in extracts from propane- compared to succinate-grown cells. Measurement of this enzyme activity was also attempted using a continuous coupled assay, by using pyruvate kinase to detect the formation of ADP and monitoring the lactate dehydrogenase-catalysed oxidation of NADH. However, high endogenous rates in the absence of substrate (largely dependent on the presence of coenzyme A), using both cell-free extract and the soluble fraction, made measurements unreliable, and this method was not pursued.

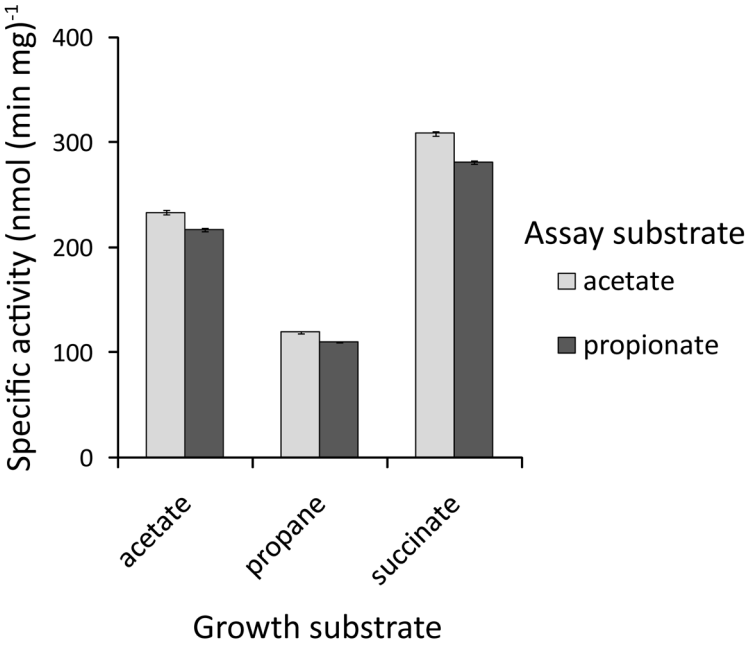

Figure 7.26. Acyl-CoA synthetase activity was measured as the formation of acetylhydroxamate. Error bars show the standard deviation of triplicate measurements.

7.15.3 Methylmalonyl CoA mutase

Considerable effort was expended developing a method to measure the formation of succinyl-CoA from methylmalonyl-CoA by detection of dimethylated derivatives of these compounds (following hydrolysis) by gas chromatography. Cell-free extract (100 μg) prepared from cells grown on succinate or propane was incubated with methylmalonyl-CoA (200 nmol) and the reaction stopped at 0, 10, 20 and 30 min. Dimethylmethyl malonate (formed from methylmalony-CoA which was present in excess) was detectable at a level indistinguishable from controls in all reactions. Dimethylsuccinate (approximately 3 nmol) was detectable in reactions containing cell-free extract from propane-grown cells at 10, 20 and 30 min and was not detectable at the zero timepoint nor in any of the reactions containing extract from succinate-grown cells. However, the amount detected did not increase between 10 and 30 min, suggesting that either the succinyl-CoA formed was consumed at a corresponding rate, or that its production was short lived, possibly due to inactivation of the enzyme, reported to be relatively unstable. Therefore it was impossible to calculate a rate from these data. Lack of time prevented further optimisation of this assay.

7.16 Reduction of ferricyanide by cell extracts – acetol dehydrogenase assay

The capacity of cell extract to reduce ferricyanide as artificial electron acceptor was assayed in extract from cells grown on propane and succinate, using the discontinuous assay described in Materials and Methods. No significant increase over background activity was detectable following the addition of methanol, ethanol, 2-propanol, 1,2-propanediol, acetone, or D-gluconate. High acetol dehydrogenase activity was present in extract from cells grown on propane. Significant activity was also detected with all aldehydes tested (acetaldehyde, propanal and methylglyoxal) in extract from both growth conditions. Figure 7.27 shows activity in response to propanal or acetol, using extract from cells grown on methane in addition to propane and succinate. Acetol dehydrogenase activity was 2.5-fold and 6-fold higher in extract from propane-grown compared to succinate- or methane-grown cells respectively, whereas propanal dehydrogenase activity was higher in succinate-grown cell extract.

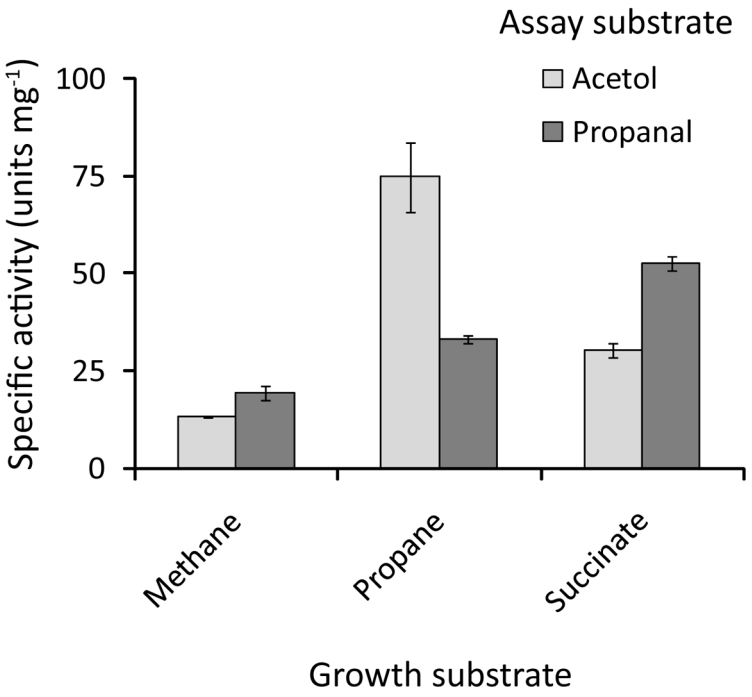

Figure 7.27. Acetol dehydrogenase activity was measured in cell-free extract from cells grown on methane, propane or succinate, by measuring the reduction of ferricyanide to ferrocyanide. One unit is defined as the reduction of 2 nmol ferricyanide min^{-1} under the assay conditions. Data are the mean of triplicate measurements and error bars indicate the standard deviation.

In order to determine the intracellular location of this activity, crude extract was separated into soluble and membrane fractions as described in Materials and Methods, and the assay repeated. Acetol dehydrogenase activity in the membrane fraction was 48% of the activity in the soluble fraction, suggesting that both soluble and membrane-bound enzymes are involved and/or that the enzyme became partially detached from the membranes during purification. These data are consistent with the hypothesis that the activity of at least two different enzymes contributed to the measured rates; one likely a non-specific aldehyde dehydrogenase perhaps with some activity towards acetol, and in addition a more acetol-specific enzyme which is induced during growth on propane and which may be a membrane-bound protein.

7.17 Msil1641

Msil1641 is the last predicted gene in the propane monooxygenase gene cluster. It was not possible to determine categorically if it was co-transcribed with the genes immediately upstream (Chapter 6), but neither was evidence found of independent transcription. Native gels (Section 7.9) suggested possible involvement in propane metabolism, as did the detection of the polypeptide only in cell extract from cells expressing the PrMO structural genes cells (Sections 6.4 and 7.5). Therefore, it was decided that this gene deserved further investigation.

7.17.1 Predicted function of Msil1641

Msil1641 is the last of five predicted genes of the PrMO gene cluster which do not have homologues associated with the sMMO. The PrMO gene cluster is shown in Figure 7.28.

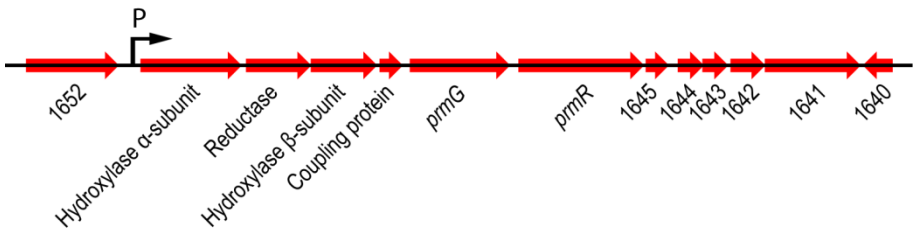

Figure 7.28. The location of ORFs Msil1645 – Msil1641, downstream of the PrMO structural genes.

NCBI BLAST was used to identify homologues to these putative genes, as shown in Table 7.9, and Msil1641 was examined in more detail. The product of this gene is annotated as gluconate dehydrogenase (GADH), but most of the high similarity sequences appear to have an inferred rather than experimentally determined function, and no close hits were identified from manually curated databases (for example SwissProt). The highest-similarity sequences found, for which experimental evidence of gene function exists, were from *Mycobacterium austroafricanum* (Lopes Ferreira et al., 2006), *Gluconobacter dioxyacetonicus* (Toyama et al., 2007) and *Erwinia cypripedii* (Yum et al., 1997) which have between 33% and 24% amino acid identity to the product of Msil1641. While the second two examples encode gluconate dehydrogenases, the substrate and product of the enzyme from *M. austroafricanum* are reported to be 2-methyl 1,2-propanediol and hydroxyisobutyraldehyde respectively.

Table 7.9. Top BLAST hits to the SWISS-PROT/TrEMBL database and protein annotations of translated sequences of the PrMO gene cluster downstream genes shown in Figure 7.28.

Locus tag Msil	Annotation	Organism	aa	% id
1645	Siderephore biosynthesis-like protein	*Beijerinckia indica*	117	70
1644	Cytochrome C	*Beijerinckia indica*	133	64
1643	Glyoxylase-like protein	*Beijerinckia indica*	131	77
1642	Uncharacterised	*Beijerinckia indica*	182	67
1641	Gluconate 2-dehydrogenase	*Beijerinckia indica*	522	82

A search of the conserved domain database (CDD) identified the Msil1641 gene product as belonging to the family of glucose methanol choline (GMC) oxidoreductases. The GMC family comprises a group of homologous flavoenzymes catalysing a diverse range of reactions (Cavener, 1992). The amino acid sequences of Msil1641 and the enzymes from *M. austroafricanum* and *G. dioxyacetonicus* were aligned with some of the representative members of this group identified by Kiess et al. (1998), and the alignment is shown in Figure 7.30. The sequences are homologous and contain an FAD binding domain, including the well-characterised N-terminal ADP-binding GXGXXG motif (Wierenga et al., 1986).

FAD-containing GADH is a membrane-bound three component enzyme (Adachi et al., 2007) which in *G. dioxyacetonicus* catalyses the oxidation of D-gluconate to 2-keto-D-gluconate. Examples from many organisms are co-transcribed in gene-

clusters encoding large and small subunits and a cytochrome c that links to the electron transport chain (Pajaniappan et al., 2008), prompting investigation of the genes adjacent to Msil1641. Msil1642 encodes a predicted small polypeptide with no homology to proteins of known function. However, examination of the amino acid sequence revealed a probable twin-arginine translocation (TAT) signal sequence, as shown in Figure 7.29. The TAT system transports folded enzymes across the plasma membrane (Lee et al., 2006) and the *M. silvestris* genome contains genes predicted to encode the TatABC polypeptides required (data not shown).

Figure 7.29. The N-terminal region of the translation of Msil1642, showing a probable TAT signal sequence (Palmer et al., 2005). The twin-arginine motif is shown in a rectangle, and spans a positively charged N-terminal region (green) followed by a hydrophobic region of approximately 20 amino acids (pink). A possible cleavage site is indicated with an arrow.

The online bioinformatics tool Pred-TAT (Bagos et al., 2010) was used to identify TAT signal sequences in the small subunits of characterised GADH enzymes from *Campylobacter jejuni* (accession number YP_002343851.1) (Pajaniappan et al., 2008) *Erwinia cypripedii* (AAC45883.1) (Yum et al., 1997), *Gluconobacter dioxyacetonicus* (BAF52626.1) (Toyama et al., 2007) and *Pseudomonas aeruginosa* (NP_250954.1) (Matsushita et al., 1979). High probability sites were predicted in all cases, although these polypeptides did not show particularly high similarity to each other (identity between 32 and 51% over approximately 220 amino acids, data not shown), and did not display a significant level of homology with Msil1642 (highest similarity to the sequence from *E. cypripedii,* 22% identical, 41% similar residues, E-value 0.19). Since Msil1644 is predicted to encode a class I cytochrome c (40% identity to the well-characterised cytochrome c2 from *Rhodopila globiformis*), the *M. silvestris* cluster encodes elements similar in some respects to the characterised GADH enzymes. It was tempting to hypothesise that these genes encode a membrane-bound FAD-containing dehydrogenase, with involvement in propane metabolism. The presence of Msil1643, predicted to encode glyoxylase I, is consistent with metabolism of methylglyoxal (Cooper, 1984), a possible product of acetol dehydrogenase.

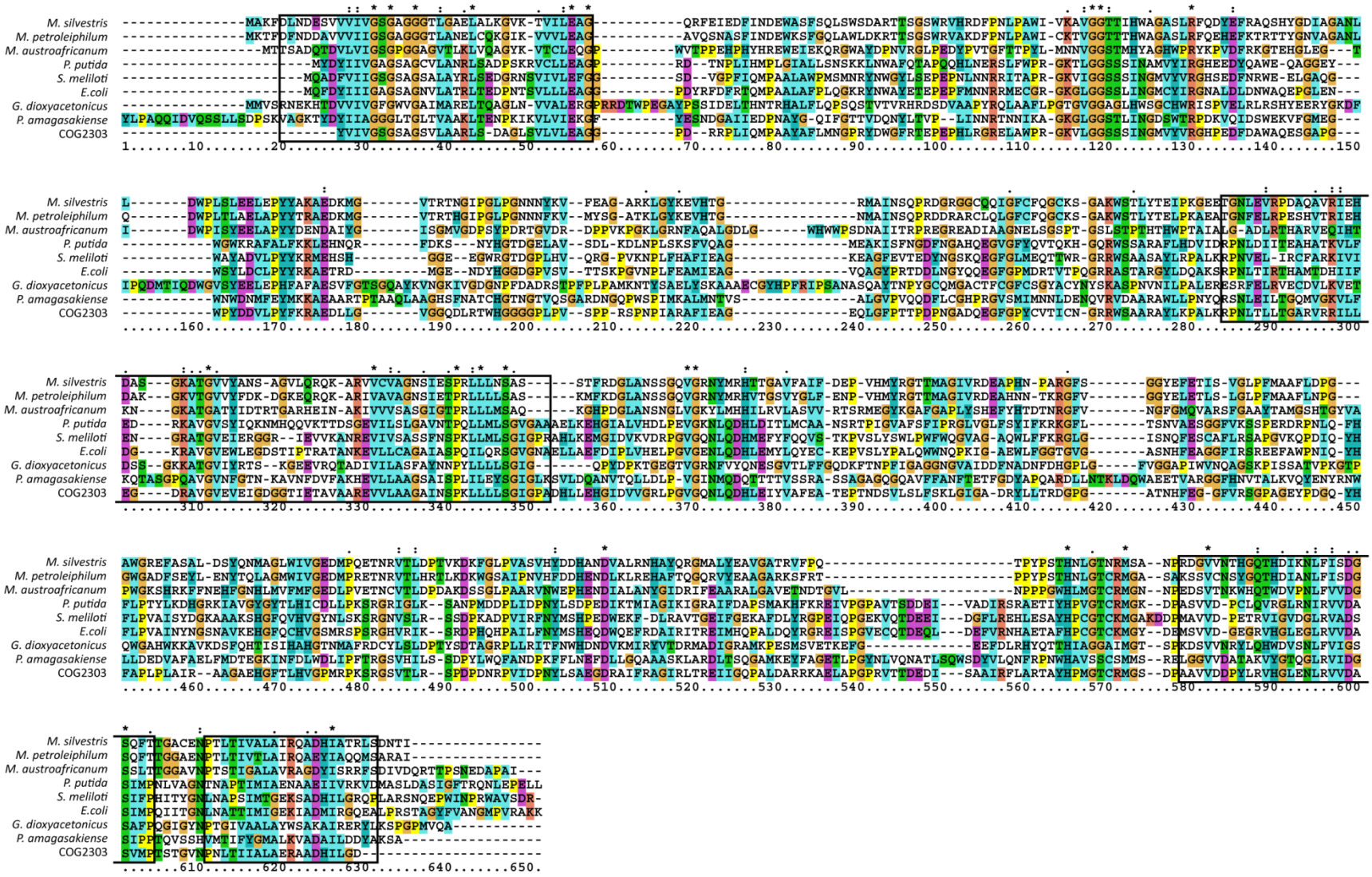
M. silvestris
M. petroleiphilum
M. austroafricanum
P. putida
S. meliloti
E.coli
G. dioxyacetonicus
P. amagasakiense
COG2303

Figure 7.30. ClustalX was used to align the gene product of Msil1641 (522 aa) with gluconate dehydrogenase from *Methylibium petroleiphilum* (YP001020142.1), 2-methyl 1,2-propanediol dehydrogenase from *Mycobacterium austroafricanum* (AAZ78237.1), alcohol dehydrogenase from *Pseudomonas putida* (CAB51051.1), choline dehydrogenases from *Sinorhizobium meliloti* (AAC13369.1) and *E. coli* (CAA37093.1), gluconate dehydrogenase from *Gluconobacter dioxyacetonicus* (AB292729), glucose oxidase from *Penicillium amagasakiense* (P81156.1) and the consensus Conserved Domains Database sequence COG2303. The FAD-binding domain is shown as four regions surrounded by rectangles (Kiess et al., 1998). Residues 117-139 form the flavin attachment loop. The substrate binding region covers residues 366-571. Active site residues 567 (which accepts protons from the substrate) and 611 are conserved throughout GMC enzymes. Asterisks denote identical residues, two dots highly conserved and one dot conserved residues.

7.17.2 Deletion of Msil1641

To determine the involvement (if any) of the gene product of Msil1641 in propane metabolism, strain Δ1641 was constructed as described in Chapter 4. As confirmed by sequencing, this strain has a deletion of 1,650 bp, from 77 bp upstream of the start codon of Msil1641 to 4 bp upstream of the end of the coding sequence, and the insertion of 100 bp containing a single *loxP* sequence. Since the downstream gene, Msil1640, is predicted to be transcribed in the reverse direction, polar effects of the deletion were unlikely.

7.17.3 Growth phenotype of strain Δ1641

There was no difference between the growth of *M. silvestris* wild-type and strain Δ1641 on methane, methanol or D-gluconate, see Figure 7.31 and Table 7.10. However, this strain grew more slowly and to a lower final density on propane, and was unable to grow on 2-propanol, (Figure 7.32) or acetone (Figure 7.35). These data suggest that the gene-product of Msil1641 may be involved in propane metabolism via the sub-terminal pathway.

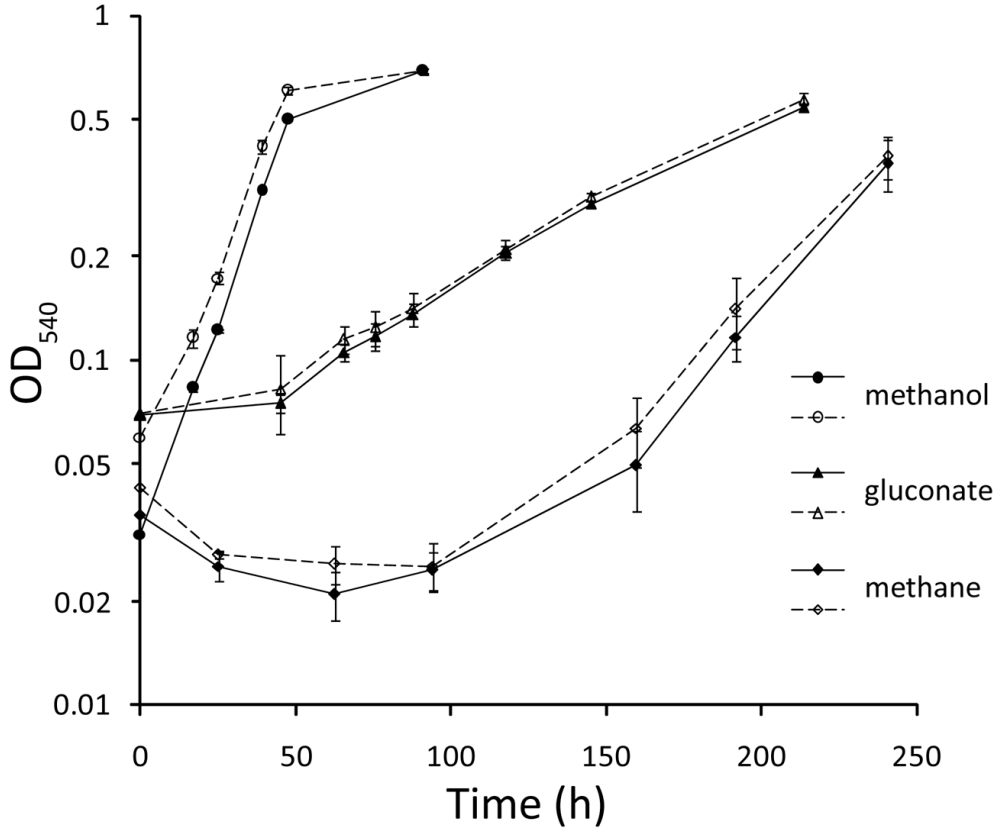

Figure 7.31. Growth of *M. silvestris* wild-type (solid lines and filled symbols) and strain Δ1641 (dashed lines and open symbols) on methanol (0.1% v/v) (circles), D-gluconate (5 mM) (triangles), and methane (20% v/v) (diamonds). Error bars show the standard deviation of triplicate vials.

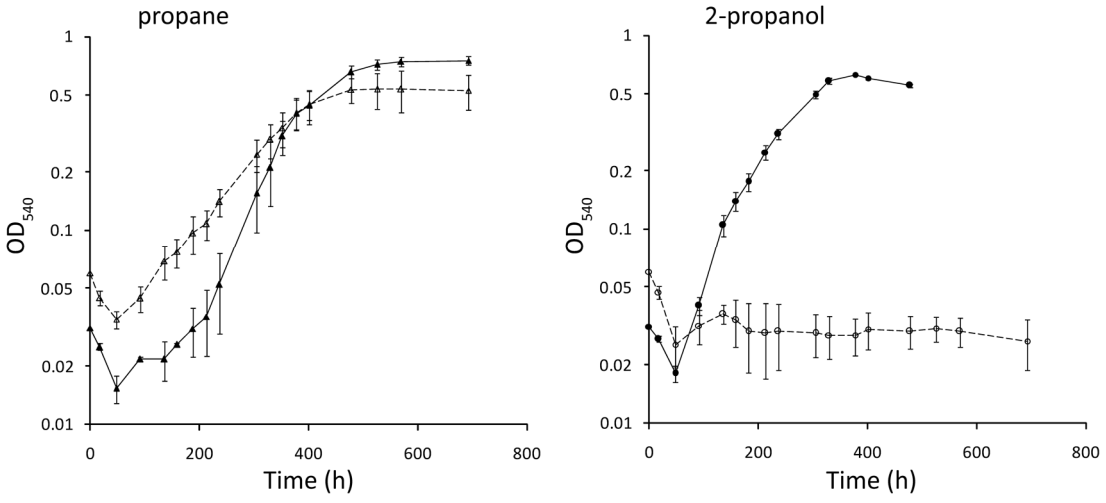

Figure 7.32. Growth of *M. silvestris* wild-type (solid lines and filled symbols) and strain Δ1641 (dashed lines and open symbols) on propane (20% v/v) (left) or 2-propanol (0.05% v/v) (right). (Inoculum was grown on methanol.) Error bars show the standard deviation of triplicate vials.

Table 7.10. Growth of the wild-type and strain Δ1641. Data are the mean of triplicate measurements ± standard deviation. Substrate concentrations 0.05% v/v, except methanol: 0.1% v/v, D-gluconate: 5 mM and propane: 20% v/v.

	Specific growth rate (h^{-1})		Lag time (h)		Biomass increase (OD)	
Substrate	BL2	Δ1641	BL2	Δ1641	BL2	Δ1641
Methanol	0.060 ± 0.001	0.059 ± 0.002	1 ± 0	6 ± 1	0.66 ± 0.02	0.63 ± 0.01
Propane	0.016 ± 0.001	0.009 ± 0.000	206 ± 27	144 ± 16	0.72 ± 0.04	0.51 ± 0.09
2-propanol	0.020 ± 0.002	0.000 ± 0.000	76 ± 4	-	0.60 ± 0.01	0.00 ± 0.00
D-gluconate	0.013 ± 0.001	0.013 ± 0.002	36 ± 4	29 ± 17	0.47 ± 0.01	0.50 ± 0.02
Methane	0.025 ± 0.001	0.022 ± 0.001	146 ± 10	141 ± 12	0.34 ± 0.06	0.35 ± 0.06
Acetone	0.037 ± 0.001	0.000 ± 0.000	35 ± 4	-	0.48 ± 0.02	0.00 ± 0.00
Acetol	0.028 ± 0.004	0.032 ± 0.000	3 ± 10	28 ± 2	0.16 ± 0.01	0.45 ± 0.01

7.17.4 Detection of the products of propane oxidation during growth of strain Δ1641

Since it had been noted that *M. silvestris* growing on propane accumulates 2-propanol and sometimes acetone in the culture medium (Section 7.6), and strain Δ1641 appeared unable to metabolise these intermediates, both wild-type and strain Δ1641 were grown in 25 ml medium in 120 ml serum vials and supplied with propane (20% v/v). Inoculum was from propane-grown cultures. 1-propanol, 2-propanol, acetone and acetol were measured in the culture supernatant as shown in Figure 7.33. As before, growth of strain Δ1641 was slower than that of the wild type (specific growth rates 0.0075 ± 0.0002 h^{-1}, and 0.0174 ± 0.0003 h^{-1} (mean ± standard deviation of three vials) respectively). 1-propanol was not detected in any vial at any time. 2-propanol and acetone were detected in the cultures at the start due to the transfer of small amounts of these oxidation products with the inoculum. 2-propanol accumulated in the medium of wild-type and strain Δ1641 vials from the start, and acetone after approximately 150 h. Acetol was detected in vials containing strain Δ1641 at 92 h and reached approximately 2 mM by the end of the experiment, but was not detected at any time in wild-type cultures.

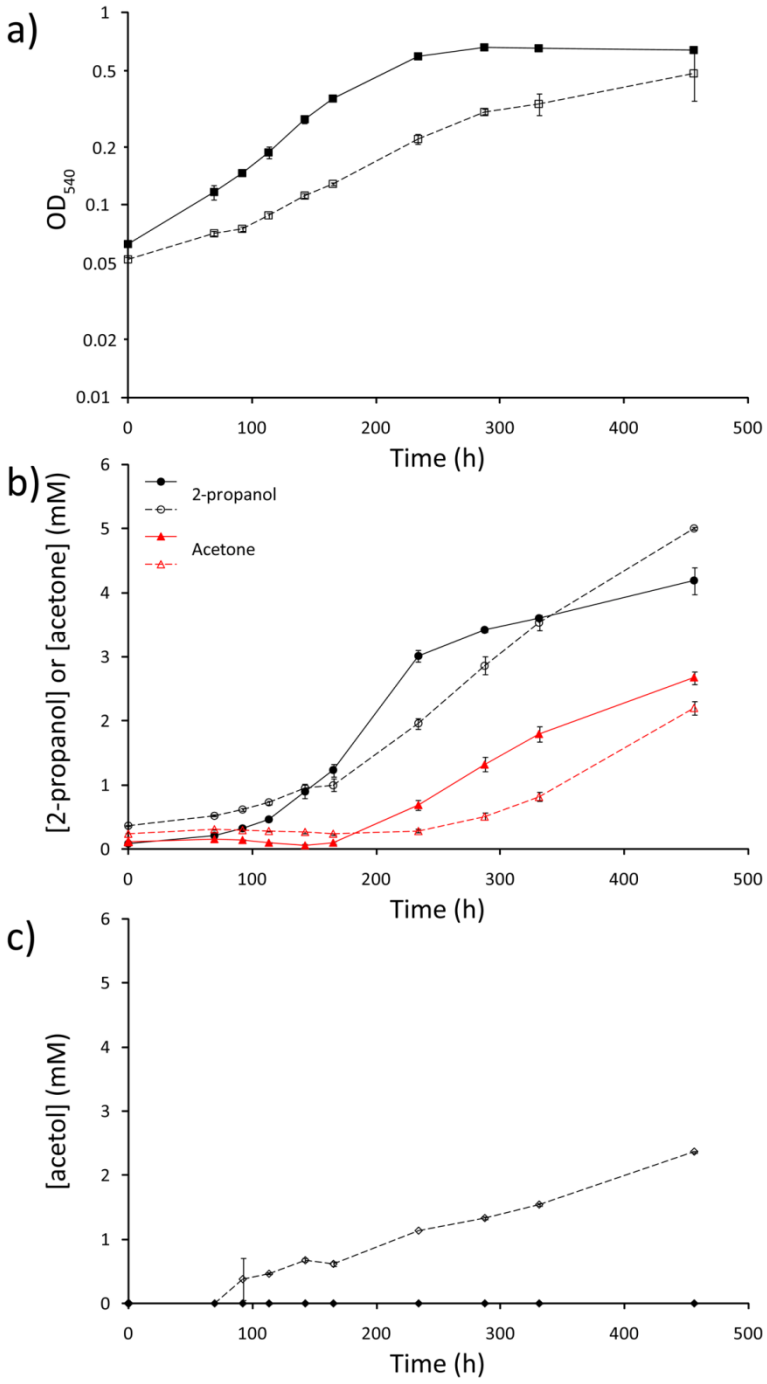

Figure 7.33. *M. silvestris* wild-type (solid lines and filled symbols) and strain Δ1641 (dashed lines and open symbols) were grown on propane (20% v/v) in 25 ml medium in 120 ml serum vials, and 2-propanol, acetone and acetol quantified in the culture medium. The growth of the cultures is shown at a) and the concentrations of 2-propanol (black) and acetone (red) (b) or acetol (c) below. Error bars (present for every data point) show the standard deviation of triplicate vials. Acetol was not detected in wild type cultures at any time during the experiment.

Data shown in Figure 7.33, during the growth phase of the cultures, were used to calculate the total of the metabolites released (2-propanol, acetone and acetol) in

each vial at each time point. This was plotted as a function of the increase of biomass in the vials (calculated from the OD, assuming OD_{540} = 1.0 represents 0.25 mg dw), and is shown in Figure 7.34. The wild type strain accumulated these products of sub-terminal oxidation at a linear rate of approximately 14 µmol (mg of biomass produced)$^{-1}$ during the exponential phase of growth up to 165 h, after which time the rate of accumulation increased. This strain continued to produce 2-propanol and acetone during stationary phase, as can be seen from Figure 7.33. At this point propane is still available to the cells, which are presumably limited by some other factor.

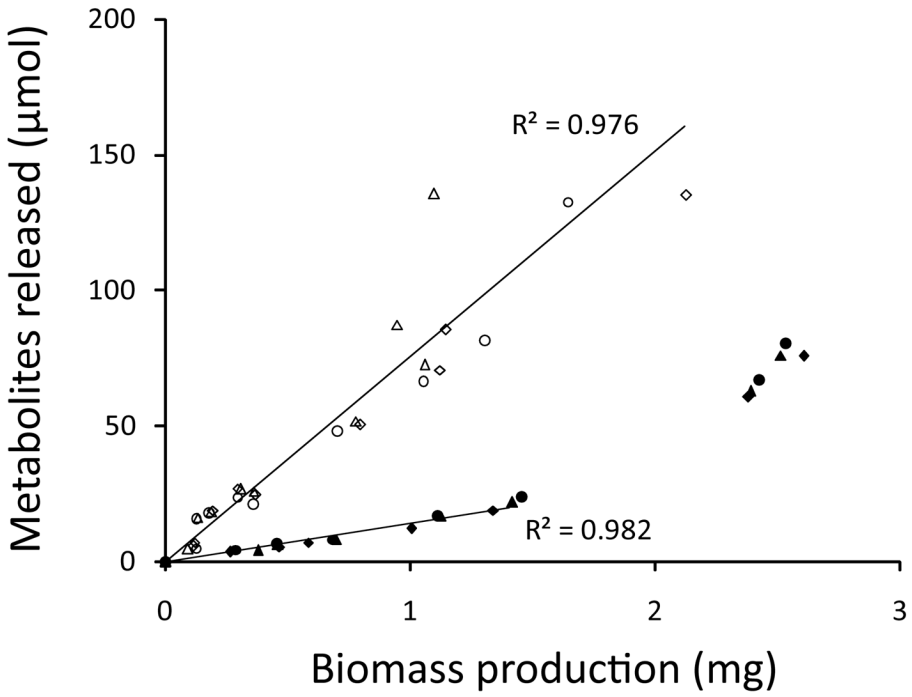

Figure 7.34. Data from Figure 7.33 were used to plot the total of metabolites (2-propanol, acetone and acetol) detected in each vial against the production of biomass. Vials (each strain in triplicate) are depicted as diamonds, triangles or circles, the wild-type strain with filled symbols and strain Δ1641 with open symbols. Only data up to the maximum culture density reached during the experiment for each strain are included, and the wild-type trendline is fitted to the exponential phase of growth up to 165.5 h only.

Strain Δ1641, however, accumulated these metabolites at approximately 5 times the wild-type exponential-phase rate (75 µmol (mg of biomass produced)$^{-1}$) throughout. These data are consistent with the hypothesis that the wild-type uses 2-propanol and acetone as carbon and/or energy sources during growth on propane, and that strain Δ1641 is unable to do so.

7.17.5 Growth of *M. silvestris* wild-type and strain Δ1641 on acetol

It was noticed that the wild-type strain did not grow to a high density on acetol (0.05% v/v) (Figure 7.21), reaching a final density of only approximately 0.3, despite rapid initial growth. In addition, at stationary phase culture density declined rapidly, suggesting cell lysis. The pH of the medium was measured at stationary phase and found to be approximately 4.0 – 4.5 (nitrate as nitrogen source), in comparison with vials supplied with acetone, which did not appreciably alter from the initial value of pH 5.5. Strain Δ1641 was grown alongside the wild-type on acetol (0.05% v/v), as illustrated in Figure 7.35.

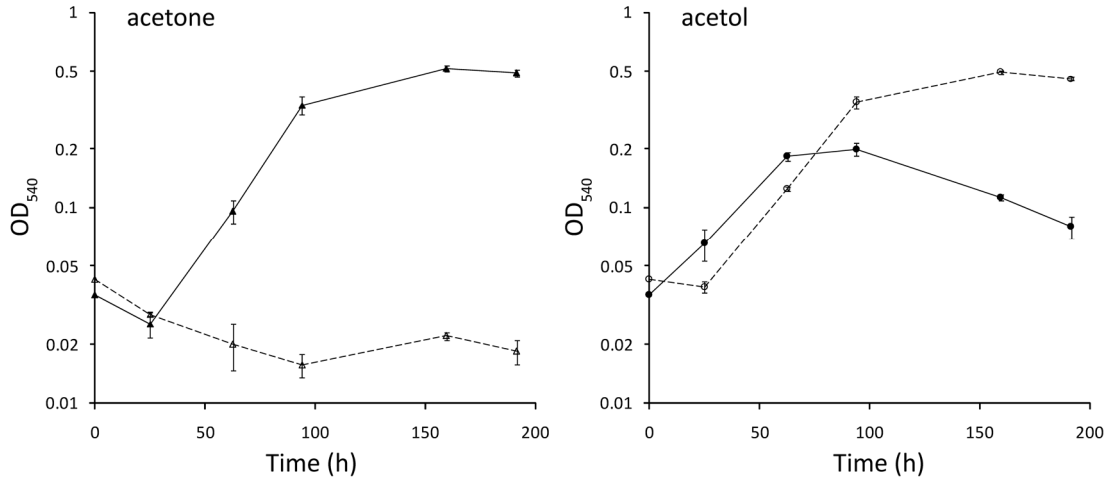

Figure 7.35. Growth of *M. silvestris* wild-type (solid lines and filled symbols) and strain Δ1641 (dashed lines and open symbols) on acetone (0.05% v/v) (left) or acetol (0.05% v/v) (right). Error bars show the standard deviation of triplicate vials.

Unexpectedly, strain Δ1641 was able to grow on acetol, and indeed grew to a higher cell density than the wild-type, reaching more than double the maximum density (Table 7.10). Cells from one of the vials of strain Δ1641 growing on acetol shown in Figure 7.35 were diluted $1/10^6$ and 100 µl of the diluted suspension spread on DAMS plates and incubated in a methanol-rich atmosphere. After two weeks colonies appeared (at the rate of 3.8×10^8 cfu ml^{-1} of the original culture), 10 of which were used for colony-PCR using primers 1641Tf/1641Tr, on either side of the area of gene-deletion. In every case (10/10), the PCR amplicon size indicated the deletion genotype (data not shown). An additional colony was transferred into liquid culture and grown on methanol (0.1% v/v). At stationary phase this culture was used as inoculum in a repeat test for growth of strain Δ1641 on acetone or acetol, and the

previously observed phenotype was repeated, see Figure 7.36. As before, during the experiment the pH of all vials remained at the initial value of pH 5.5.

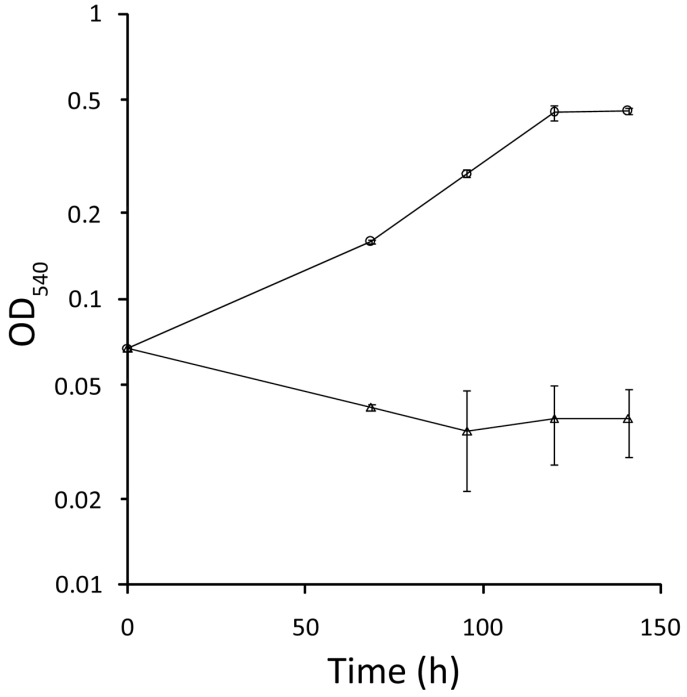

Figure 7.36. A repeat experiment to test the growth of strain Δ1641 on acetone (0.05% v/v) (triangles) or acetol (0.05% v/v) (circles) using, as inoculum, cells derived from a single colony following plating of dilutions of an acetol-grown culture. Error bars show the standard deviation of triplicate vials.

These data suggest that the acetol-metabolising enzymes expressed during growth on propane and on acetol may be different, since, during growth on propane, metabolism of acetol seems prevented or reduced in strain Δ1641, whereas this strain was able to grow on acetol when supplied as substrate. The difference in the production of acid during growth on this substrate indicates a difference in the metabolism of this compound by these two strains.

7.18 Discussion

7.18.1 The products of propane oxidation in *M. silvestris*

One of the aims of the work described in this chapter was to identify the product(s) of propane oxidation. Unfortunately, however, it was not possible to directly detect these products in cell suspensions of propane-grown cells using inhibitors of further

metabolism, as described in Section 7.3. Cells, once removed from the growth environment, had a low propane oxidation capacity, as previously noted during oxygen electrode experiments (Chapter 6), and products were not detected. Therefore, alternative methods were used to gather evidence which supported both terminal and sub-terminal oxidation pathways.

7.18.1.1 Evidence supporting terminal oxidation of propane

Only cultures already expressing propane-metabolising enzymes, set up using propane-grown inoculum, were not inhibited by the presence of 1-propanol, and were also able to grow on this substrate, in contrast to the severe inhibition of growth when using inoculum grown on other substrates (see Section 7.4.1). Inhibition might be caused by rapid intracellular accumulation of a product of 1-propanol oxidation, possibly propionate. Exogenous supply of propionate, which at the growth pH (pH 5.5) would be mostly de-protonated (pKa of propionic acid = 4.86) resulting in relatively slow diffusion into the cell, would possibly allow time for the induction of enzymes required for its metabolism. (The inhibitory effect of propionate in *Thauera butanivorans* was mentioned in Chapter 1, Section 1.17.) In any event, these data suggest that propane-grown cells express enzymes capable of 1-propanol metabolism or detoxification, which are absent from cells grown on other substrates.

Experiments using the oxygen electrode revealed a striking difference in the stoichiometry of oxygen uptake between cells grown on propane and other substrates in response to 1-propanol and propanal. Propane grown cells consumed three times as much oxygen as succinate-grown cells when 1-propanol was added (Section 7.7.1), demonstrating that the oxidation of these substrates proceeds further in propane-grown cells.

Quantitative proteomics data supplied by the Biological Mass Spectrometry and Proteomics group at the University of Warwick identified significant amounts of the methylmalonyl-CoA pathway enzyme polypeptides in soluble extract from propane- but not succinate-grown cells.

Strain Δ1641, which was unable to grow on 2-propanol or acetone, was able to grow on propane at a somewhat reduced rate, demonstrating that this strain is able to grow on propane although unable to metabolise the products of sub-terminal oxidation.

7.18.1.2 Evidence supporting sub-terminal oxidation of propane

The accumulation of 2-propanol and acetone in the culture medium provides convincing evidence that propane is also oxidised at the sub-terminal carbon atom. Several examples have appeared in the literature of organisms excreting acetone during growth on, or when incubated with propane, for example species of mycobacteria, *Brevibacterium, Nocardia, Pseudomonas* and *Arthrobacter* (Lukins and Foster, 1963; Hou et al., 1983b; Stephens and Dalton, 1986). However, in some cases acetone was excreted without the ability for further oxidation or incorporation into cellular material (Stephens and Dalton, 1986), suggesting that sometimes 2-propanol is an unused by-product of propane oxidation. Several lines of evidence suggest that sub-terminal oxidation is productive in *M. silvestris*. Both 2-propanol and acetone were good substrates for growth, and although these intermediates accumulated during growth on propane, they were also consumed when the propane supply was interrupted or exhausted (Figure 7.14 and Figure 7.15). Extract from propane-grown cells contained six-fold higher PMS-linked 2-propanol dehydrogenase activity in comparison to extract from methane-grown cells (Table 7.3), and in oxygen electrode experiments propane-grown cells had increased ability to oxidise sub-terminal intermediates, particularly acetone and acetol (Figure 7.17). Additionally, both 2-propanol and acetone, as growth substrates, induced expression of the PrMO (Section 7.5). Finally, strain Δ1641, which was unable to grow on 2-propanol or acetone, both grew more slowly on propane compared to the wild-type (Figure 7.33), and also accumulated sub-terminal intermediates at a higher rate (Figure 7.34) in comparison to the formation of biomass.

7.18.2 1,2-propanediol as an intermediate in propane oxidation

In some bacteria and other organisms it has been shown or suggested that 1,2-propanediol may be an intermediate of propane or acetone oxidation, and the production of acetol from 1,2-propanediol has been demonstrated (Walti, 1934; Rudney, 1954; Lukins and Foster, 1963; Hou et al., 1983a). It could also be hypothesised that 1- or 2-propanol could be subject to monooxygenase-mediated oxidation to 1,2-propanediol, which could be oxidised by a primary alcohol dehydrogenase forming lactate, a reaction shown to be catalysed by MDH (Bolbot and Anthony, 1980a). The lack of activity of propane-grown cells with 1,2-

propanediol in the oxygen electrode (Section 7.7.2) argues against involvement of this compound, and the accumulation of acetone in the culture medium suggests the conversion of 2-propanol into acetone.

7.18.3 The enzymes of propane metabolism

The monooxygenases responsible for propane oxidation have been discussed in Chapter 6. Enzymes of terminal and sub-terminal pathways were assayed to determine if cells contained the capacity for operation of these metabolic pathways.

7.18.3.1 Alcohol dehydrogenase

The evidence suggests that propane is oxidised to both 1-propanol and 2-propanol, which must then be dehydrogenated to propanal and acetone respectively. Only very low levels of NAD(P)-dependent alcohol dehydrogenase could be detected in extract from propane-grown cells, but high levels of PMS-linked dehydrogenase activity (Table 7.3 and Table 7.4). Methanol dehydrogenase (MDH) was expressed at high levels in all growth conditions, as shown by SDS-PAGE gels and enzyme assays (Chapter 6, Figure 6.13 and Chapter 5, Section 5.9.2). MDH has a well-characterised wide substrate specificity for primary alcohols (Anthony, 1982), and may be responsible for 1-propanol dehydrogenase activity in propane-grown cell extract. Some MDH enzymes have been shown to have secondary alcohol activity (Goldberg, 1976; Sahm et al., 1976), but, in *M. silvestris,* 2-propanol activity was greatly up-regulated compared to 1-propanol activity in propane-grown cell extract. This implies that a different alcohol dehydrogenase is induced during growth on propane with activity towards secondary alcohols. The 2-propanol activity detected in the soluble fraction from this extract was relatively high (381 nmol (min mg)$^{-1}$) but no prominent bands unique to lanes loaded with extract from propane-grown cells were identified in SDS-PAGE gels (Table 7.2) containing putative alcohol dehydrogenase polypeptides. It seems surprising that a secondary alcohol dehydrogenase with activity comparable to MDH is expressed in propane-grown cells but is not evident in SDS-PAGE gels. An alternative might be that the MDH activity detected in all growth conditions is modified in propane-grown cells to include secondary alcohols. In the time available it was not possible to identify the enzyme responsible for the secondary alcohol activity in propane-grown cells.

7.18.3.2 Terminal pathway enzymes

NAD^+-dependent aldehyde dehydrogenase activity was present in extract from cells grown on propane or succinate at a level four times that of methane-grown cell extract (Section 7.15.1). This activity is sufficient to support the observed growth rate on propane. Similarly, a relatively high level of acyl-CoA synthetase was found in extract of cells grown on acetate, propane and succinate, but the acetyl-CoA and propionyl-CoA activities were similar in extracts from all growth conditions, suggesting that a relatively non-specific enzyme may be responsible (Section 7.15.2). In the time available it was not possible to assay propionyl-CoA carboxylase, and quantitative data regarding methylmalonyl-CoA mutase were not obtained. However, succinyl-CoA appeared to be formed from methylmalonyl-CoA in propane-grown cell extract only (Section 7.15.3), suggesting that methymalonyl-CoA mutase may be induced during growth on propane. It was not possible to optimise this assay due to constraints of time.

7.18.3.3 Sub-terminal pathway enzymes

Conversion of acetone into acetol would require oxidation of the terminal methyl group by a monooxygenase. Polypeptides likely to catalyse this reaction specifically were not identified on SDS-PAGE gels. This enzyme was not assayed in cell extract, and activity has not always been detected in past studies (Taylor et al., 1980)(Woods and Murrell, 1989). However, both acetone- and acetol-stimulated oxygen uptake was greatly increased in propane-grown cells as measured in the oxygen electrode (Section 7.7). Ferricyanide-linked acetol dehydrogenase activity was upregulated in extract from propane-grown cells compared to extract from cells grown on succinate or methane (Section 7.16).

7.18.4 The phenotype of strain ΔICL and strain ΔSGAT

There was no difference between the growth of strain ΔSGAT and the wild-type on propane (Section 7.13), demonstrating that the products of propane metabolism are not one-carbon compounds in *M. silvestris,* since strain ΔSGAT was unable to grow on one-carbon compounds (Chapter 5). Similarly, strain ΔICL was able to grow on propane at a similar rate and to a similar final density as the wild-type, implying that propane is not metabolised to two-carbon compounds, for example acetate or acetyl-

CoA, since, as shown in Chapter 5, this strain has a pronounced phenotype during growth on two-carbon compounds. Therefore these data allow the elimination of several of the potential pathways shown in Figure 7.1 and Figure 7.2, since many of these result in one- or two-carbon compounds, or require the conversion of acetyl-CoA to glyoxylate, necessitating, in *M. silvestris,* the reaction catalysed by isocitrate lyase. The methylmalonyl-CoA pathway appears to be the only feasible option for metabolism of terminal oxidation products without generating 1- or 2-carbon compounds, since *M. silvestris* does not have homologues of the methylcitrate pathway genes as mentioned in Section 7.2.2. Applying the same argument to metabolism of sub-terminal products of propane oxidation via acetone (Figure 7.2) restricts the possibilities for the breakdown of acetone to reactions resulting in acetol and methylglyoxal. These data are in contrast to the situation in *Mycobacterium* JOB5, where isocitrate lyase was shown to be induced during propane metabolism (Vestal and Perry, 1969).

7.18.5 Growth of strain ΔPrMO on sub-terminal intermediates

Interestingly, the growth rate of strain ΔPrMO on 2-propanol was halved compared to the wild-type (Section 7.11), although growth on acetone and acetol was unaffected. This implies either a polar effect of the gene deletion exerting an influence on genes responsible for 2-propanol metabolism, or involvement of the PrMO itself in 2-propanol oxidation, or regulatory changes due to the deletion of the PrMO α-subunit. Evidence has been presented (Section 7.17) that down-stream genes are involved in metabolism of products of sub-terminal propane oxidation; however it is not clear how these might be directly involved in 2-propanol oxidation nor how disruption would affect 2-propanol but not acetone metabolism. A similar effect was observed for *Gordonia* TY5 (Kotani et al., 2003), where disruption of the hydroxylase subunit of the PrMO reduced growth on 2-propanol. The authors demonstrated that transcription of the downstream *adh1* gene, encoding alcohol dehydrogenase, was prevented, although this gene is in a cluster thought to be transcribed independently from the PrMO gene cluster. Recently Furuya et al. (2011) noted that deletion of *mimA*, encoding the PrMO α-subunit in *Mycobacterium smegmatis,* prevented growth on both 2-propanol and acetone, (but not acetol), in addition to propane. Growth on acetone was largely, and on 2-propanol partially,

restored by complementation with the *mimA* gene from the closely related *M. goodii.* The authors concluded that the PrMO was involved in the conversion of acetone into acetol. In *M. silvestris,* both strain ΔPrMO and strain ΔMmoX were able to grow on acetone. A double mutant with a deletion of both these genes was not constructed, and so it is not possible to categorically state that the PrMO and the sMMO are not interchangeably responsible for the oxidation of acetone, although the facts that the sMMO was not expressed during growth of the wild-type on acetone (Chapter 6, Section 6.6), and that strain ΔPrMO grew on acetone similarly to the wild-type (Section 7.11), strongly suggest that this is not the case. Therefore the data suggest that the inhibition of growth on 2-propanol in strain ΔPrMO is more likely due to regulatory effects in *M. silvestris*, the mechanisms of which are unknown.

7.18.6 The role of Msil1641

Deletion of Msil1641, the final gene of the PrMO gene cluster, annotated as encoding gluconate dehydrogenase, abolished growth on 2-propanol and acetone and decreased the specific growth rate on propane to a little over half the wild-type figure (Section 7.17.3). Together with the detection of acetol in the medium of strain Δ1641 during growth on propane, these data suggest that this gene-product is involved in sub-terminal oxidation of propane, possibly in the conversion of acetol into methylglyoxal. Methylglyoxal is produced in many organisms, both as a by-product of glycolysis and during the catabolism of amino acids (Cooper, 1984) and pathways for its transformation to pyruvate or lactate are usually present. The presence of Msil1643, annotated as glyoxylase I, in the same cluster of genes, may be significant. Enzyme assay data (Section 7.16) suggest that there may be more than one enzyme with acetol dehydrogenase activity, possibly with different intracellular locations, as does the ability of strain Δ1641 to grow on acetol (Section 7.17.3). This hypothesis is reinforced by the observation that whereas the wild-type strain acidifies the culture medium during growth on acetol, growth of strain Δ1641 under the same conditions does not have this effect.

7.18.7 The sub-terminal oxidation pathway

At low propane concentrations (4% v/v) 2-propanol was detected in the culture medium and at higher concentrations (20% v/v) acetone was also detected.

Furthermore, although acetol was not detected with the wild-type, this intermediate was formed during growth of strain Δ1641 on propane. These data are consistent with sub-terminal oxidation of propane, resulting in 2-propanol, which proceeds via acetone and acetol, which is metabolised by the gene-product of Msil1641, probably resulting in methylglyoxal which is assimilated into central metabolism via pyruvate or lactate. The range of substrates capable of supporting growth and enzyme assay and oxygen electrode data support this hypothesis.

7.18.8 Regulation of propane and methane oxidation

Previous studies did not identify substrates other than methane which induced expression of the sMMO (Dedysh et al., 2005a; Theisen et al., 2005), (and sMMO expression was found to be repressed by the presence of acetate in addition to methane). In this work, transcription of the sMMO genes did not occur during growth on methanol (Chapter 6, Section 6.2.6), but these genes were shown to be both transcribed and expressed during growth on methane and on propane (Chapter 6, Section 6.4). Since methane is metabolised via methanol, and one-carbon compounds were shown not to be products of propane metabolism, the most conservative interpretation of these data is that the methane molecule provides the signal for sMMO gene expression, and that the propane molecule is also effective in this role. However, 2-propanol and acetone, while inducing expression of the PrMO, did not induce sMMO expression, suggesting that an intermediate of propane metabolism regulates expression of the PrMO. The alternative explanation, that transcription of the sMMO is constitutive in the absence of a repressor, is not supported since sMMO expression is not prevented by the presence of 2-propanol or acetone during growth on propane, but does not occur during growth on these intermediates alone. Therefore the data suggest that expression of the sMMO requires both induction by methane (or propane) and the absence of repression by some (but not all) multi carbon compounds. Repression of methane oxidation in the presence of other 3-carbon compounds was not investigated.

7.18.9 Conclusions

The data presented in this chapter suggest that *M. silvestris* oxidises propane at both terminal and sub-terminal carbons, producing 1-propanol and 2-propanol, and that both these products are assimilated. Although at least 25% of propane was oxidised to 2-propanol it was not possible to further quantify the relative contribution of each pathway. Flux analysis using techniques such as ^{13}C metabolomics might provide valuable data (Peyraud et al., 2009), and should be considered for the future. The terminal pathway probably proceeds via methylmalonyl-CoA, resulting in succinate. Sub-terminal oxidation proceeds via acetone and acetol which is likely converted to methylglyoxal perhaps by a membrane-bound FAD-containing enzyme with novel substrate specificity. Methylglyoxal may be converted to pyruvate or lactate via established mechanisms. The activity of a PMS-linked secondary alcohol dehydrogenase was detected in propane-grown cells, although the genes responsible for encoding this enzyme and also an acetone oxygenase were not located. Suggestions for future work include further investigation of the enzyme activities present in the mutant strains already constructed. In addition, the phenotype of a mutant with a deletion of MDH would shed light on the role of this enzyme in propane metabolism, and might help towards identification of the secondary alcohol dehydrogenase. The possibility of a gluconate-dehydrogenase-like enzyme with activity towards acetol requires further investigation. Research into the mechanisms of methane and propane regulation might reveal findings that could also assist in understanding the regulation of methane oxidation in other methanotrophs.

Chapter 8

Summary and future prospects

8.1 Physiology and growth

Chapter 3 described attempts to predict and optimise the conditions for the successful growth of *M. silvestris*. Salt concentration was not found to be as critical as previously assumed, and the tendency of cultures to vary the medium pH was frequently found to be the cause of limited growth. An improved trace elements solution was developed, and a better understanding of the optimal growth conditions was gained. These preliminary investigations were essential for the successful development of genetic methods, which were important tools in this study. The realisation that, under oxygen limitation, cells can be grown without accumulating large amounts of polysaccharide was essential for the generation of high quality biomass for biochemical and proteomic analysis. The ability to grow on propane in addition to methane (which is unique among known life forms), highlighted an interesting and potentially useful metabolic potential.

8.2 Development of a genetic system

Chapter 4 detailed the development of the genetic methods which were to form the basis of analysis of metabolic pathways and of the roles of key enzymes. A method of targeted mutagenesis, using methods unusual among methanotrophs, was developed which, by relying on electroporation with linear DNA fragments, resulted in gene replacement with a minimum of colony transfers on plates. This method was shown to be simple and effective, and several mutant strains were constructed. A second method was developed, although not tested, which should allow the replacement of components of the sMMO with heterologous genes, or with engineered or mutated versions, using the SacB counter-selectable marker.

8.3 The role of the glyoxylate bypass enzymes

Chapter 5 described the role of enzymes of the glyoxylate pathway. Analysis of mutant strains demonstrated that isocitrate lyase is essential for one-carbon metabolism, despite the measured low-activity of this enzyme in wild-type methane-grown cells, and that both isocitrate lyase and malate synthase are required for two-carbon metabolism. Interestingly, methanol dehydrogenase (MDH) regulation was found to be influenced by flux through isocitrate lyase, since deletion of isocitrate lyase abolished or repressed MDH expression. One-carbon growth was unexpectedly

found to be affected by deletion of malate synthase. During operation of the serine cycle no flux would be expected through malate synthase, since glyoxylate is substrate for serine cycle enzyme serine-glyoxylate aminotransferase, and removal of this intermediate would prevent operation of the cycle. Deletion of serine-glyoxylate aminotransferase also affected growth on ethanol, but not on acetate. One possible explanation for these data is that deletion of these enzymes, which form a metabolic branch point, also affected expression of MDH.

8.4 Oxidation of methane and propane

Chapter 6 described the identification of the transcriptional start site of the propane monooxygenase (PrMO) gene cluster, under the control of a putative σ^{54} promoter. This cluster is likely to be co- transcribed as an operon, but intergene PCR was not entirely successful in demonstrating this, highlighting the importance of controls which are not always included in this approach. Using the wild-type strain and also strains with a deletion of either the soluble methane monooxygenase (sMMO) or the PrMO, the ability of each enzyme to oxidise methane and propane was investigated. It was shown that the PrMO is not able to oxidise methane significantly, and is neither expressed nor transcribed during growth on methane. In contrast, the sMMO, expressed during growth on propane, is able to oxidise propane and there was a relatively minor difference between the phenotypes of the wild-type and strain ΔPrMO during growth on a mixture of 2.5% (v/v) methane and propane. However, propane was assimilated less efficiently, such that although growth of strain ΔPrMO was possible on 2.5% (v/v) propane, the efficiency of its assimilation into biomass was approximately half that of the wild type. Propane also had an inhibitory or toxic effect on the strain lacking the PrMO, and growth on 20% (v/v) propane was prevented. The ability of the wild-type to oxidise a range of non-growth substrates was examined using an oxygen electrode and cells grown on methane or propane. A wide range of aliphatic and aromatic compounds were oxidised, and comparison of the relative rates between cells grown on the two substrates suggested that the PrMO was also able to oxidise many of these compounds, including alkenes and aromatics such as benzene and phenol.

8.5 Metabolism of propane

In Chapter 7, attempts to unravel the metabolism of propane were described. Propane was shown to be oxidised to a mixture of 1-propanol and 2-propanol. The data presented show that 1-propanol was assimilated via pathways comparatively well characterised in heterotrophic organisms, and that 2-propanol was oxidised to acetone and acetol. Interestingly, deletion of the PrMO affected growth on 2-propanol, but not on acetone, suggesting that the inhibition of growth of this strain on this substrate is due to a regulatory effect. An enzyme, encoded at locus Msil1641 and annotated as gluconate dehydrogenase, was shown to be essential for 2-propanol and acetone metabolism. The data suggested that acetol was the substrate of this enzyme, which was possibly membrane-associated, exported via the twin-arginine translocation pathway and catalysed reactions in the periplasm. It was noted that while only the sMMO is expressed at high level during growth on methane, growth on propane induces expression of both the sMMO and the PrMO, and the PrMO is also expressed during growth on 2-propanol and acetone, suggesting that two substantially different mechanisms regulate expression of these enzymes.

8.6 Prospects for future research

The data presented here highlight numerous avenues for productive research in the future. Alternative pathways of acetate assimilation and glyoxylate regeneration (the ethylmalonyl-CoA (EMC) pathway) have been the subject of intense research recently (Erb et al., 2009) and may have interesting biotechnological applications (Alber, 2011). The finding that *M. silvestris* uses the glyoxylate pathway for two-carbon assimilation and a variant of the serine cycle that depends on isocitrate lyase, is significant because this is comparatively uncommon among methylotrophs (Anthony, 1982). Coordinated regulation of glyoxylate bypass enzymes is necessary in these organisms as mentioned in Chapter 1, but it is not known if these regulatory mechanisms have features in common with EMC pathway-possessing organisms. The genetic tractability of *M. silvestris* suggests that this may be a suitable organism to investigate these issues. The unexpected changes in MDH expression noted during disruption of glyoxylate bypass enzymes also deserve further investigation. Comparatively little research has been published on the regulation of MDH in other methylotrophs, although regulatory proteins have been identified, possibly

responsive to formaldehyde, as outlined in Chapter 1. Since differences in MDH expression between *M. silvestris* strains were noted during growth on succinate, a different mechanism may be involved here. A better understanding of these topics may be important for a fuller understanding of the regulation of one-carbon metabolism both in *M. silvestris*, and also in other methylotrophs.
The identification and initial characterisation of a second soluble diiron monooxygenase (SDIMO) enzyme in *M. silvestris* is interesting. It is the first example of an additional enzyme from a different group of this family in a methanotroph. Enzymes of this type have potential applications in biotechnology and bioremediation (van Beilen and Funhoff, 2005) and are being sought for these reasons (Holmes and Coleman, 2008), and the PrMO may have interesting characteristics and catalytic potential. Further characterisation of the *M. silvestris* SDIMOs is required, including purification and kinetic analysis and this would be facilitated by the mutant strains already developed. Investigation of the regulatory mechanisms would identify the conditions under which they are expressed *in vivo* and suggest effective mechanisms to engineer strains for particular applications, for example constitutive expression of the sMMO or PrMO, for applications in bioremediation or biocatalysis. The genetic systems developed here would enable the substitution of elements, from individual amino acid residues to entire enzyme subunits, of the sMMO or PrMO, for development of enzymes with novel characteristics, and the construction of a strain with a counter-selectable element should facilitate this. The ability to use alternative substrates for growth, the lack of the particulate methane monooxygenase and the potential to engineer control of gene expression highlights the suitability of *M. silvestris* for this application, as an alternative to the use of less tractable hosts (Smith et al., 2002).
Quantification of the product distribution of propane oxidation is required and would be possible using an approach such as ^{13}C metabolic flux analysis (Zamboni and Sauer, 2009), which would also help to confirm the metabolic pathways involved. There is also scope for additional analysis using traditional biochemical tools including enzyme assays, and identification and characterisation of an acetone-oxidising enzyme is essential. Additional mutant strains might be required to demonstrate the role of specific enzymes, including, for example, the role of MDH during growth on propane. Finally, the gene product of Msil1641 requires characterisation. If this enzyme is responsible for oxidation of acetol, this would be

the first reported example of this compound as substrate for an enzyme of this type. Examples of this enzyme family, for example D-gluconate dehydrogenase from *Gluconobacter dioxyacetonicus* have been purified and characterised, (most have a narrow substrate specificity), suggesting a possible approach for this task (Shinagawa et al., 1984). These enzymes are also of biotechnological interest due to their biocatalytic potential (Stottmeister et al., 2005).

In summary, *M. silvestris* displays many interesting and unique characteristics. The work described here builds on that of previous researchers in attempting to understand the metabolic versatility of this extraordinary organism and, in common with much scientific research, has identified at least as many questions as it has answered.

References

Acha, V., Alba, J., and Thalasso, F. (2002) The absolute requirement for carbon dioxide for aerobic methane oxidation by a methanotrophic-heterotrophic soil community of bacteria. *Biotechnol Lett* **24**: 675-679.

Adachi, O., Ano, Y., Toyama, H., and Matsushita, K. (2007) Biooxidation with PQQ- and FAD-dependent dehydrogenases. In *Modern Biooxidation: Enzymes, Reactions and Applications*. Schmid, R.D., and Urlacher, V.B. (eds). Weinheim: Wiley-VCH, pp. 1-41.

Alber, B. (2011) Biotechnological potential of the ethylmalonyl-CoA pathway. *Appl Microbiol Biotechnol* **89**: 17-25.

Ali, H. (2006) Development of genetic tools in methanotrophs and the molecular regulation of methane monooxygenase. *PhD Thesis*. UK: University of Warwick.

Ali, H., and Murrell, J.C. (2009) Development and validation of promoter-probe vectors for the study of methane monooxygenase gene expression in *Methylococcus capsulatus* Bath. *Microbiology* **155**: 761-771.

Anisimov, O.A. (2007) Potential feedback of thawing permafrost to the global climate system through methane emission. *Environ Res Lett* **2**: 045016.

Anstrom, D.M., and Remington, S.J. (2006) The product complex of *M. tuberculosis* malate synthase revisited. *Protein Sci* **15**: 2002-2007.

Anstrom, D.M., Kallio, K., and Remington, S.J. (2003) Structure of the *Escherichia coli* malate synthase G:pyruvate:acetyl-coenzyme A abortive ternary complex at 1.95 Å resolution. *Protein Sci* **12**: 1822-1832.

Anthony, C. (1975) The microbial metabolism of C_1 compounds. The cytochromes of *Pseudomonas* AM1. *Biochem J* **146**: 289-298.

Anthony, C. (1982) *Biochemistry of methylotrophs*. London: Academic Press.

Anthony, C. (1992) The c-type cytochromes of methylotrophic bacteria. *Biochim Biophys Acta* **1099**: 1-15.

Anthony, C. (2000) Methanol dehydrogenase; a PQQ-containing quinoprotein dehydrogenase. *Subcell Biochem* **35**: 73-117.

Anthony, C. (2004) The quinoprotein dehydrogenases for methanol and glucose. *Arch Biochem Biophys* **428**: 2-9.

Anthony, C. (2011) How half a century of research was required to understand bacterial growth on C_1 and C_2 compounds; the story of the serine cycle and the ethylmalonyl-CoA pathway. *Sci Prog* **94**: 109-137.

Anthony, C., and Zatman, L.J. (1964) The microbial oxidation of methanol. 2. The methanol-oxidizing enzyme of *Pseudomonas* sp. M 27. *Biochem J* **92**: 614-621.

Anthony, C., and Williams, P. (2003) The structure and mechanism of methanol dehydrogenase. *Biochim Biophys Acta* **1647**: 18-23.

Arp, D.J. (1999) Butane metabolism by butane-grown *Pseudomonas butanovora*. *Microbiology* **145**: 1173-1180.

Ashraf, W., and Murrell, J.C. (1992) Genetic, biochemical and immunological evidence for the involvement of two alcohol dehydrogenases in the metabolism of propane by *Rhodococcus rhodochrous* PNKb1. *Arch Microbiol* **157**: 488-492.

Ashraf, W., Mihdhir, A., and Murrell, J.C. (1994) Bacterial oxidation of propane. *FEMS Microbiol Lett* **122**: 1-6.

Attwood, M.M. (1990) Formaldehyde dehydrogenases from methylotrophs. *Methods Enzymol* **188**: 314-327.

Attwood, M.M., and Harder, W. (1974) The oxidation and assimilation of C_2 compounds by *Hyphomicrobium* sp. *J Gen Microbiol* **84**: 350-356.

Ayres, E.K., Thomson, V.J., Merino, G., Balderes, D., and Figurski, D.H. (1993) Precise deletions in large bacterial genomes by vector-mediated excision (VEX) : The *trfA* gene of promiscuous plasmid RK2 is essential for replication in several Gram-negative hosts. *J Mol Biol* **230**: 174-185.

Baani, M., and Liesack, W. (2008) Two isozymes of particulate methane monooxygenase with different methane oxidation kinetics are found in *Methylocystis* sp. strain SC2. *Proc Natl Acad Sci USA* **105**: 10203-10208.

Bagos, P.G., Nikolaou, E.P., Liakopoulos, T.D., and Tsirigos, K.D. (2010) Combined prediction of Tat and Sec signal peptides with hidden Markov models. *Bioinformatics* **26**: 2811-2817.

Balasubramanian, R., Smith, S.M., Rawat, S., Yatsunyk, L.A., Stemmler, T.L., and Rosenzweig, A.C. (2010) Oxidation of methane by a biological dicopper centre. *Nature* **465**: 115-119.

Barrios, H., Valderrama, B., and Morett, E. (1999) Compilation and analysis of σ^{54}-dependent promoter sequences. *Nucleic Acids Res* **27**: 4305-4313.

Barta, T.M., and Hanson, R.S. (1993) Genetics of methane and methanol oxidation in Gram-negative methylotrophic bacteria. *Antonie Van Leeuwenhoek* **64**: 109-120.

Becking, J. (2006) The Genus *Beijerinckia*. In *The Prokaryotes*. Dworkin, M., Falkow, S., Rosenberg, E., Schleifer, K.-H., and Stackebrandt, E. (eds). New York: Springer, pp. 151-162.

Bellion, E., and Hersh, L.B. (1972) Methylamine metabolism in a *Pseudomonas* species. *Arch Biochem Biophys* **153**: 368-374.

Bellion, E., and Woodson, J. (1975) Two distinct isocitrate lyases from a *Pseudomonas* species. *J Bacteriol* **122**: 557-564.

Bellion, E., and Spain, J.C. (1976) The distribution of the isocitrate lyase serine pathway amongst one-carbon utilizing organisms. *Can J Microbiol* **22**: 404-408.

Bellion, E., and Yu, S.K. (1978) Catabolite repression of isocitrate lyase in methylamine-grown *Pseudomonas* MA: Effect of carbon and nitrogen sources. *Biochim Biophys Acta* **541**: 425-434.

Belova, S.E., Baani, M., Suzina, N.E., Bodelier, P.L.E., Liesack, W., and Dedysh, S.N. (2011) Acetate utilization as a survival strategy of peat-inhabiting *Methylocystis* spp. *Environ Microbiol Rep* **3**: 36-46.

Best, D.J., and Higgins, I.J. (1981) Methane-oxidizing activity and membrane morphology in a methanol-grown obligate methanotroph, *Methylosinus trichosporium* OB3b. *J Gen Microbiol* **125**: 73-84.

Birch, A., Leiser, A., and Robinson, J.A. (1993) Cloning, sequencing, and expression of the gene encoding methylmalonyl-coenzyme A mutase from *Streptomyces cinnamonensis*. *J Bacteriol* **175**: 3511-3519.

Bloor, A.E., and Cranenburgh, R.M. (2006) An efficient method of selectable marker gene excision by Xer recombination for gene replacement in bacterial chromosomes. *Appl Environ Microbiol* **72**: 2520-2525.

Bobik, T. (2006) Polyhedral organelles compartmenting bacterial metabolic processes. *Appl Microbiol Biotechnol* **70**: 517-525.

Boissard, C., Bonsang, B., Kanakidou, M., and Lambert, G. (1996) TROPOZ II: Global distributions and budgets of methane and light hydrocarbons. *J Atmos Chem* **25**: 115-148.

Bolbot, J.A., and Anthony, C. (1980a) The metabolism of 1,2-propanediol by the facultative methylotroph *Pseudomonas* AM1. *J Gen Microbiol* **120**: 245-254.

Bolbot, J.A., and Anthony, C. (1980b) The metabolism of pyruvate by the facultative methylotroph *Pseudomonas* AM1. *J Gen Microbiol* **120**: 233-244.

Borodina, E., McDonald, I.R., and Murrell, J.C. (2004) Chloromethane-dependent expression of the *cmu* gene cluster of *Hyphomicrobium chloromethanicum*. *Appl Environ Microbiol* **70**: 4177-4186.

Bothe, H., Møller Jensen, K.M.J., Mergel, A.M., Larsen, J.L., Jørgensen, C.J., Bothe, H., and Jørgensen, L.J. (2002) Heterotrophic bacteria growing in association with *Methylococcus capsulatus* (Bath) in a single cell protein production process. *Appl Microbiol Biotechnol* **59**: 33-39.

Bousquet, P., Ciais, P., Miller, J.B., Dlugokencky, E.J., Hauglustaine, D.A., Prigent, C. et al. (2006) Contribution of anthropogenic and natural sources to atmospheric methane variability. *Nature* **443**: 439-443.

Brisbane, P.G., and Ladd, J.N. (1965) The role of microorganisms in petroleum exploration. *Annu Rev Microbiol* **19**: 351-364.

Britton, K.L., Abeysinghe, I.S.B., Baker, P.J., Barynin, V., Diehl, P., Langridge, S.J. et al. (2001) The structure and domain organization of *Escherichia coli* isocitrate lyase. *Acta Cryst* **D57**: 1209-1218.

Brusseau, G.A., Tsien, H.-C., Hanson, R.S., and Wackett, L.P. (1990) Optimization of trichloroethylene oxidation by methanotrophs and the use of a colorimetric assay to detect soluble methane monooxygenase activity. *Biodegradation* **1**: 19-29.

Burrows, K.J., Cornish, A., Scott, D., and Higgins, I.J. (1984) Substrate specificities of the soluble and particulate methane mono-oxygenases of *Methylosinus trichosporium* OB3b. *J Gen Microbiol* **130**: 3327-3333.

Bushnell, L.D., and Haas, H.F. (1941) The utilization of certain hydrocarbons by microorganisms. *J Bacteriol* **41**: 653-673.

Cardy, D.L.N., Laidler, V., Salmond, G.P.C., and Murrell, J.C. (1991a) Molecular analysis of the methane monooxygenase (MMO) gene cluster of *Methylosinus trichosporium* OB3b. *Mol Microbiol* **5**: 335-342.

Cardy, D.L.N., Laidler, V., Salmond, G.P.C., and Murrell, J.C. (1991b) The methane monooxygenase gene cluster of *Methylosinus trichosporium*: cloning and sequencing of the *mmo*C gene. *Arch Microbiol* **156**: 477-483.

Carnoy, C., and Roten, C.-A. (2009) The *dif*/Xer recombination systems in proteobacteria. *PLoS ONE* **4**: e6531. doi:6510.1371/journal.pone.0006531.

Cavener, D.R. (1992) GMC oxidoreductases : A newly defined family of homologous proteins with diverse catalytic activities. *J Mol Biol* **223**: 811-814.

Champreda, V., Choi, Y.J., Zhou, N.Y., and Leak, D.J. (2006) Alteration of the stereo- and regioselectivity of alkene monooxygenase based on coupling protein interactions. *Appl Microbiol Biotechnol* **71**: 840-847.

Chen, Y., and Murrell, J.C. (2010) When metagenomics meets stable-isotope probing: progress and perspectives. *Trends Microbiol* **18**: 157-163.

Chen, Y., Dumont, M.G., Cebron, A., and Murrell, J.C. (2007) Identification of active methanotrophs in a landfill cover soil through detection of expression of 16S rRNA and functional genes. *Environ Microbiol* **9**: 2855-2869.

Chen, Y., Crombie, A., Rahman, M.T., Dedysh, S.N., Liesack, W., Stott, M.B. et al. (2010) Complete genome sequence of the aerobic facultative methanotroph *Methylocella silvestris* BL2. *J Bacteriol* **192**: 3840-3841.

Chistoserdova, L., Chen, S.-W., Lapidus, A., and Lidstrom, M.E. (2003) Methylotrophy in *Methylobacterium extorquens* AM1 from a genomic point of view. *J Bacteriol* **185**: 2980-2987.

Chistoserdova, L.V., and Lidstrom, M.E. (1994) Genetics of the serine cycle in *Methylobacterium extorquens* AM1: identification of *sgaA* and *mtdA* and sequences of *sgaA*, *hprA*, and *mtdA*. *J Bacteriol* **176**: 1957-1968.

Claassen, P.A.M., and Zehnder, A.J.B. (1986) Isocitrate lyase activity in *Thiobacillus versutus* grown anaerobically on acetate and nitrate. *J Gen Microbiol* **132**: 3179-3185.

Clarkson, T.S., Martin, R.J., and Rudolph, J. (1997) Ethane and propane in the southern marine troposphere. *Atmos Environ* **31**: 3763-3771.

Colby, J., Stirling, D.I., and Dalton, H. (1977) The soluble methane mono-oxygenase of *Methylococcus capsulatus* (Bath). Its ability to oxygenate *n*-alkanes, *n*-alkenes, ethers, and alicyclic, aromatic and heterocyclic compounds. *Biochem J* **165**: 395-402.

Coleman, J.P., and Perry, J.J. (1985) Purification and characterization of the secondary alcohol dehydrogenase from propane-utilizing *Mycobacterium vaccae* strain JOB-5. *J Gen Microbiol* **131**: 2901-2907.

Coleman, N.V., Bui, N.B., and Holmes, A.J. (2006) Soluble di-iron monooxygenase gene diversity in soils, sediments and ethene enrichments. *Environ Microbiol* **8**: 1228-1239.

Coleman, N.V., Le, N.B., Ly, M.A., Ogawa, H.E., McCarl, V., Wilson, N.L., and Holmes, A.J. (2011a) Hydrocarbon monooxygenase in *Mycobacterium*: recombinant expression of a member of the ammonia monooxygenase superfamily. *ISME J*.

Coleman, N.V., Yau, S., Wilson, N.L., Nolan, L.M., Migocki, M.D., Ly, M.-a. et al. (2011b) Untangling the multiple monooxygenases of *Mycobacterium chubuense* strain NBB4, a versatile hydrocarbon degrader. *Environ Microbiol Rep* **3**: 297-307.

Conrad, R. (1996) Soil microorganisms as controllers of atmospheric trace gases (H_2, CO, CH_4, OCS, N_2O, and NO). *Microbiol Rev* **60**: 609-640.

Cooley, R.B., Bottomley, P.J., and Arp, D.J. (2009a) Growth of a non-methanotroph on natural gas: ignoring the obvious to focus on the obscure. *Environ Microbiol Rep* **1**: 408-413.

Cooley, R.B., Dubbels, B.L., Sayavedra-Soto, L.A., Bottomley, P.J., and Arp, D.J. (2009b) Kinetic characterization of the soluble butane monooxygenase from *Thauera butanivorans*, formerly *Pseudomonas butanovora*. *Microbiology* **155**: 2086-2096.

Coon, M.J. (2005) Omega oxygenases: Nonheme-iron enzymes and P450 cytochromes. *Biochem Biophys Res Commun* **338**: 378-385.

Cooper, R.A. (1984) Metabolism of methylglyoxal in microorganisms. *Annu Rev Microbiol* **38**: 49-68.

Corkey, B.E., Brandt, M., Williams, R.J., and Williamson, J.R. (1981) Assay of short-chain acyl coenzyme a intermediates in tissue extracts by high-pressure liquid chromatography. *Anal Biochem* **118**: 30-41.

Cornah, J.E., Germain, V., Ward, J.L., Beale, M.H., and Smith, S.M. (2004) Lipid utilization, gluconeogenesis, and seedling growth in *Arabidopsis* mutants lacking the glyoxylate cycle enzyme malate synthase. *J Biol Chem* **279**: 42916-42923.

Cox, R.B., and Quayle, J.R. (1976) Synthesis and hydrolysis of malyl-coenzyme A by *Pseudomonas* AM1: an apparent malate synthase activity. *J Gen Microbiol* **95**: 121-133.

Cozzone, A.J. (1998) Regulation of acetate metabolism by protein phosphorylation in enteric bacteria. *Annu Rev Microbiol* **52**: 127-164.

Crowther, G.J., Kosaly, G., and Lidstrom, M.E. (2008) Formate as the main branch point for methylotrophic metabolism in *Methylobacterium extorquens* AM1. *J Bacteriol* **190**: 5057-5062.

Csaki, R., Bodrossy, L., Klem, J., Murrell, J.C., and Kovacs, K.L. (2003) Genes involved in the copper-dependent regulation of soluble methane monooxygenase of *Methylococcus capsulatus* (Bath): cloning, sequencing and mutational analysis. *Microbiology* **149**: 1785-1795.

da Silva Cruz, A.H., Brock, M., Zambuzzi-Carvalho, P.F., Santos-Silva, L.K., Troian, R.F., Góes, A.M. et al. (2011) Phosphorylation is the major mechanism regulating isocitrate lyase activity in Paracoccidioides brasiliensis yeast cells. *FEBS J* **278**: 2318-2332.

Dalton, H. (2005) The Leeuwenhoek Lecture 2000 the natural and unnatural history of methane-oxidizing bacteria. *Philos T Roy Soc B* **360**: 1207-1222.

Datta, N., Hedges, R.W., Shaw, E.J., Sykes, R.B., and Richmond, M.H. (1971) Properties of an R factor from *Pseudomonas aeruginosa*. *J Bacteriol* **108**: 1244-1249.

Davison, J. (2005) Risk mitigation of genetically modified bacteria and plants designed for bioremediation. *J Ind Microbiol Biotechnol* **32**: 639-650.

Day, D., and Anthony, C. (1990) Methanol dehydrogenase from *Methylobacterium extorquens* AM1. *Methods Enzymol* **188**: 210-216.

de Hemptinne, J.-C., Delepine, H., Jose, C., and Jose, J. (1998) Aqueous solubility of hydrocarbon mixtures. *Rev I Fr Petrol* **53**: 409-419.

Dedysh, S.N. (2002) Methanotrophic bacteria of acid sphagnum bogs. *Mikrobiologiia* **71**: 741-754.

Dedysh, S.N., and Dunfield, P.F. (2011) Facultative and obligate methanotrophs how to identify and differentiate them. In *Methods in Enzymology: Methods in Methane Metabolism, Vol 495, Pt B*. Rosenzweig, A.C., and Ragsdale, S.W. (eds). San Diego: Elsevier Academic Press Inc, pp. 32-61.

Dedysh, S.N., Derakshani, M., and Liesack, W. (2001) Detection and enumeration of methanotrophs in acidic sphagnum peat by 16S rRNA fluorescence in situ hybridization, including the use of newly developed oligonucleotide probes for *Methylocella palustris*. *Appl Environ Microbiol* **67**: 4850-4857.

Dedysh, S.N., Knief, C., and Dunfield, P.F. (2005a) *Methylocella* species are facultatively methanotrophic. *J Bacteriol* **187**: 4665-4670.

Dedysh, S.N., Panikov, N.S., Liesack, W., Grosskopf, R., Zhou, J., and Tiedje, J.M. (1998) Isolation of acidophilic methane-oxidizing bacteria from northern peat wetlands. *Science* **282**: 281-284.

Dedysh, S.N., Smirnova, K.V., Khmelenina, V.N., Suzina, N.E., Liesack, W., and Trotsenko, Y.A. (2005b) Methylotrophic autotrophy in *Beijerinckia mobilis*. *J Bacteriol* **187**: 3884-3888.

Dedysh, S.N., Khmelenina, V.N., Suzina, N.E., Trotsenko, Y.A., Semrau, J.D., Liesack, W., and Tiedje, J.M. (2002) *Methylocapsa acidiphila* gen. nov., sp. nov., a novel methane-oxidizing and dinitrogen-fixing acidophilic bacterium from *Sphagnum* bog. *Int J Syst Evol Microbiol* **52**: 251-261.

Dedysh, S.N., Liesack, W., Khmelenina, V.N., Suzina, N.E., Trotsenko, Y.A., Semrau, J.D. et al. (2000) *Methylocella palustris* gen. nov., sp. nov., a new methane-oxidizing acidophilic bacterium from peat bogs, representing a novel subtype of serine-pathway methanotrophs. *Int J Syst Evol Microbiol* **50 Pt 3**: 955-969.

Dedysh, S.N., Berestovskaya, Y.Y., Vasylieva, L.V., Belova, S.E., Khmelenina, V.N., Suzina, N.E. et al. (2004) *Methylocella tundrae* sp. nov., a novel methanotrophic bacterium from acidic tundra peatlands. *Int J Syst Evol Microbiol* **54**: 151-156.

Dennis, J.J., and Zylstra, G.J. (1998) Plasposons: modular self-cloning minitransposon derivatives for rapid genetic analysis of Gram-negative bacterial genomes. *Appl Environ Microbiol* **64**: 2710-2715.

Devai, I., and Delaune, R.D. (1996) Light hydrocarbon production in freshwater marsh soil as influenced by soil redox conditions. *Water, Air, Soil Pollut* **88**: 39-46.

Díaz-Pérez, A.L., Román-Doval, C., Díaz-Pérez, C., Cervantes, C., Sosa-Aguirre, C.R., López-Meza, J.E., and Campos-García, J. (2007) Identification of the *aceA* gene encoding isocitrate lyase required for the growth of *Pseudomonas aeruginosa* on acetate, acyclic terpenes and leucine. *FEMS Microbiol Lett* **269**: 309-316.

Dixon, G.H., and Kornberg, H.L. (1959) Assay methods for key enzymes of the glyoxylate cycle. *Biochem J* **72**: 3P.

Dlugokencky, E.J., Nisbet, E.G., Fisher, R., and Lowry, D. (2011) Global atmospheric methane: budget, changes and dangers. *Philos T R Roy Soc A* **369**: 2058-2072.

Doughty, D.M., Sayavedra-Soto, L.A., Arp, D.J., and Bottomley, P.J. (2006) Product repression of alkane monooxygenase expression in *Pseudomonas butanovora*. *J Bacteriol* **188**: 2586-2592.

Doughty, D.M., Halsey, K.H., Vieville, C.J., Sayavedra-Soto, L.A., Arp, D.J., and Bottomley, P.J. (2007) Propionate inactivation of butane monooxygenase activity in *Pseudomonas butanovora*: biochemical and physiological implications. *Microbiology* **153**: 3722-3729.

Driskell, L.O., Yu, X.-j., Zhang, L., Liu, Y., Popov, V.L., Walker, D.H. et al. (2009) Directed mutagenesis of the *Rickettsia prowazekii pld* gene encoding phospholipase D. *Infect Immun* **77**: 3244-3248.

Dubbels, B.L., Sayavedra-Soto, L.A., and Arp, D.J. (2007) Butane monooxygenase of *Pseudomonas butanovora*: purification and biochemical characterization of a terminal-alkane hydroxylating diiron monooxygenase. *Microbiology* **153**: 1808-1816.

Duine, J.A., Frank, J., and De Ruiter, L.G. (1979) Isolation of a methanol dehydrogenase with a functional coupling to cytochrome c. *J Gen Microbiol* **115**: 523-526.

Dunfield, P.F., Khmelenina, V.N., Suzina, N.E., Trotsenko, Y.A., and Dedysh, S.N. (2003) *Methylocella silvestris* sp. nov., a novel methanotroph isolated from an acidic forest cambisol. *Int J Syst Evol Microbiol* **53**: 1231-1239.

Dunfield, P.F., Belova, S.E., Vorob'ev, A.V., Cornish, S.L., and Dedysh, S.N. (2010) *Methylocapsa aurea* sp. nov., a facultative methanotroph possessing a particulate methane monooxygenase, and emended description of the genus *Methylocapsa*. *Int J Syst Evol Microbiol* **60**: 2659-2664.

Dunstan, P.M., and Anthony, C. (1973) Microbial metabolism of C_1 and C_2 compounds. The role of acetate during growth of *Pseudomonas* AM1 on C_1 compounds, ethanol and beta-hydroxybutyrate. *Biochem J* **132**: 797-801.

Dunstan, P.M., Anthony, C., and Drabble, W.T. (1972a) Microbial metabolism of C_1 and C_2 compounds. The role of glyoxylate, glycollate and acetate in the growth of *Pseudomonas* AM1 on ethanol and on C_1 compounds. *Biochem J* **128**: 107-115.

Dunstan, P.M., Anthony, C., and Drabble, W.T. (1972b) Microbial metabolism of C_1 and C_2 compounds. The involvement of glycollate in the metabolism of ethanol and of acetate by *Pseudomonas* AM1. *Biochem J* **128**: 99-106.

Eccleston, M., and Kelly, D.P. (1973) Assimilation and toxicity of some exogenous C_1 compounds, alcohols, sugars and acetate in the methane-oxidizing bacterium *Methylococcus capsulatus*. *J Gen Microbiol* **75**: 211-221.

Eikmanns, B.J., Rittmann, D., and Sahm, H. (1995) Cloning, sequence analysis, expression, and inactivation of the *Corynebacterium glutamicum icd* gene encoding isocitrate dehydrogenase and biochemical characterization of the enzyme. *J Bacteriol* **177**: 774-782.

El Karoui, M., Amundsen, S.K., Dabert, P., and Gruss, A. (1999) Gene replacement with linear DNA in electroporated wild-type *Escherichia coli*. *Nucleic Acids Res* **27**: 1296-1299.

Elango, N.A., Radhakrishnan, R., Froland, W.A., Wallar, B.J., Earhart, C.A., Lipscomb, J.D., and Ohlendorf, D.H. (1997) Crystal structure of the hydroxylase component of methane monooxygenase from *Methylosinus trichosporium* OB3b. *Protein Sci* **6**: 556-568.

Elliott, S.J., Zhu, M., Tso, L., Nguyen, H.H.T., Yip, J.H.K., and Chan, S.I. (1997) Regio- and stereoselectivity of particulate methane monooxygenase from *Methylococcus capsulatus* (Bath). *J Am Chem Soc* **119**: 9949-9955.

Erb, T.J., Fuchs, G., and Alber, B.E. (2009) (2*S*)-Methylsuccinyl-CoA dehydrogenase closes the ethylmalonyl-CoA pathway for acetyl-CoA assimilation. *Mol Microbiol* **73**: 992-1008.

Erb, T.J., Retey, J., Fuchs, G., and Alber, B.E. (2008) Ethylmalonyl-CoA mutase from *Rhodobacter sphaeroides* defines a new subclade of Coenzyme B12-dependent acyl-CoA mutases. *J Biol Chem* **283**: 32283-32293.

Erb, T.J., Frerichs-Revermann, L., Fuchs, G., and Alber, B.E. (2010) The apparent malate synthase activity of *Rhodobacter sphaeroides* is due to two paralogous enzymes, (3S)-malyl-coenzyme A (CoA)/β-methylmalyl-CoA lyase and (3S)- malyl-CoA thioesterase. *J Bacteriol* **192**: 1249-1258.

Erb, T.J., Berg, I.A., Brecht, V., Muller, M., Fuchs, G., and Alber, B.E. (2007) Synthesis of C_5-dicarboxylic acids from C_2-units involving crotonyl-CoA carboxylase/reductase: The ethylmalonyl-CoA pathway. *Proc Natl Acad Sci U S A* **104**: 10631-10636.

Etiope, G., and Ciccioli, P. (2009) Earth's degassing: A missing ethane and propane source. *Science* **323**: 478.

Etiope, G., and Klusman, R.W. (2010) Microseepage in drylands: Flux and implications in the global atmospheric source/sink budget of methane. *Global Planet Change* **72**: 265-274.

Etiope, G., Lassey, K.R., Klusman, R.W., and Boschi, E. (2008) Reappraisal of the fossil methane budget and related emission from geologic sources. *Geophys Res Lett* **35**: L09307.

Ferenci, T., Strom, T., and Quayle, J.R. (1975) Oxidation of carbon monoxide and methane by *Pseudomonas methanica*. *J Gen Microbiol* **91**: 79-91.

Forney, F.W., and Markovetz, A.J. (1970) Subterminal oxidation of aliphatic hydrocarbons. *J Bacteriol* **102**: 281-282.

Foster, J. (1962) Hydrocarbons as substrates for microorganisms. *Antonie Van Leeuwenhoek* **28**: 241-274.

Fox, B.G., Froland, W.A., Dege, J.E., and Lipscomb, J.D. (1989) Methane monooxygenase from *Methylosinus trichosporium* OB3b. Purification and properties of a three-component system with high specific activity from a type II methanotroph. *J Biol Chem* **264**: 10023-10033.

Frascari, D., Pinelli, D., Nocentini, M., Zannoni, A., Fedi, S., Baleani, E. et al. (2006) Long-term aerobic cometabolism of a chlorinated solvent mixture by vinyl chloride-, methane- and propane-utilizing biomasses. *J Hazard Mater* **138**: 29-39.

Fredricks, K.M. (1967) Products of the oxidation of *n*-decane by *Pseudomonas aeruginosa* and *Mycobacterium rhodochrous*. *Antonie Van Leeuwenhoek* **33**: 41-48.

Froland, W.A., Andersson, K.K., Lee, S.K., Liu, Y., and Lipscomb, J.D. (1992) Methane monooxygenase component B and reductase alter the regioselectivity of the hydroxylase component-catalyzed reactions. A novel role for protein-protein interactions in an oxygenase mechanism. *J Biol Chem* **267**: 17588-17597.

Fuhs, G.W. (1961) Der mikrobielle Abbau von Kohlenwasserstoffen. *Arch Microbiol* **39**: 374-422.

Fukuda, H., Fujii, T., and Ogawa, T. (1984) Microbial production of C_3- and C_4-hydrocarbons under aerobic conditions. *Agric Biol Chem* **48**: 1679-1682.

Furuya, T., Hirose, S., Osanai, H., Semba, H., and Kino, K. (2011) Identification of the monooxygenase gene clusters responsible for the regioselective oxidation of phenol to hydroquinone in mycobacteria. *Appl Environ Microbiol* **77**: 1214-1220.

Gallagher, S.C., Cammack, R., and Dalton, H. (1997) Alkene monooxygenase from *Nocardia corallina* B-276 is a member of the class of dinuclear iron proteins capable of stereospecific epoxygenation reactions. *Eur J Biochem* **247**: 635-641.

Gerstmeir, R., Wendisch, V.F., Schnicke, S., Ruan, H., Farwick, M., Reinscheid, D., and Eikmanns, B.J. (2003) Acetate metabolism and its regulation in *Corynebacterium glutamicum*. *J Biotechnol* **104**: 99-122.

Ghosh, R., and Quayle, J.R. (1981) Purification and properties of the methanol dehydrogenase from *Methylophilus methylotrophus*. *Biochem J* **199**: 245-250.

Gilbert, B., McDonald, I.R., Finch, R., Stafford, G.P., Nielsen, A.K., and Murrell, J.C. (2000) Molecular analysis of the pmo (particulate methane monooxygenase) operons from two type II methanotrophs. *Appl Environ Microbiol* **66**: 966-975.

Goldberg, I. (1976) Purification and properties of a methanol-oxidizing enzyme in *Pseudomonas* C. *Eur J Biochem* **63**: 233-240.

Goodwin, P.M., and Anthony, C. (1998) The biochemistry, physiology and genetics of PQQ and PQQ-containing enzymes. In *Adv Microb Physiol*. Poole, R.K. (ed): Academic Press, pp. 1-80.

Görisch, H., and Rupp, M. (1989) Quinoprotein ethanol dehydrogenase from *Pseudomonas*. *Antonie Van Leeuwenhoek* **56**: 35-45.

Green, J., and Dalton, H. (1986) Steady-state kinetic analysis of soluble methane mono-oxygenase from *Methylococcus capsulatus* (Bath). *Biochem J* **236**: 155-162.

Green, J., and Dalton, H. (1989) Substrate specificity of soluble methane monooxygenase. Mechanistic implications. *J Biol Chem* **264**: 17698-17703.

Green, L.S., Karr, D.B., and Emerich, D.W. (1998) Isocitrate dehydrogenase and glyoxylate cycle enzyme activities in *Bradyrhizobium japonicum* under various growth conditions. *Arch Microbiol* **169**: 445-451.

Green, M.J., and Hill, H.A.O. (1984) [1] Chemistry of dioxygen. In *Methods Enzymol*. Lester, P. (ed): Academic Press, pp. 3-22.

Griffiths, R.I., Whiteley, A.S., O'Donnell, A.G., and Bailey, M.J. (2000) Rapid method for coextraction of DNA and RNA from natural environments for analysis of ribosomal DNA- and rRNA-based microbial community composition. *Appl Environ Microbiol* **66**: 5488-5491.

Guacucano, M., Levican, G., Holmes, D.S., and Jedlicki, E. (2000) An RT-PCR artifact in the characterization of bacterial operons. *Electronic Journal of Biotechnology [online]* **3**: 213-216 http://www.ejbiotechnology.info/content/vol213/issue213/full/215/215.pdf.

Haase, K., Wendlandt, K.D., Gräber, A., and Stottmeister, U. (2006) Cometabolic degradation of MTBE using methane-propane- and butane-utilizing enrichment cultures and *Rhodococcus* sp. BU3. *Eng Life Sci* **6**: 508-513.

Hakemian, A.S., and Rosenzweig, A.C. (2007) The biochemistry of methane oxidation. *Annu Rev Biochem* **76**: 223-241.

Hamamura, N., and Arp, D.J. (2000) Isolation and characterization of alkane-utilizing *Nocardioides* sp. strain CF8. *FEMS Microbiol Lett* **186**: 21-26.

Hansen, E.J., Latimer, J.L., Thomas, S.E., Helminen, M., Albritton, W.L., and Radolf, J.D. (1992) Use of electroporation to construct isogenic mutants of *Haemophilus ducreyi*. *J Bacteriol* **174**: 5442-5449.

Hansen, J., Sato, M., Ruedy, R., Lacis, A., and Oinas, V. (2000) Global warming in the twenty-first century: An alternative scenario. *Proc Natl Acad Sci U S A* **97**: 9875-9880.

Hansen, J., Sato, M., Kharecha, P., Russell, G., Lea, D.W., and Siddall, M. (2007) Climate change and trace gases. *Philos T R Roy Soc A* **365**: 1925-1954.

Hanson, R.S., and Hanson, T.E. (1996) Methanotrophic bacteria. *Microbiol Rev* **60**: 439-471.

Harley, C.B., and Reynolds, R.P. (1987) Analysis of *E. Coli* promoter sequences. *Nucl Acids Res* **15**: 2343-2361.

Harms, N., Reijnders, W.N.M., Koning, S., and van Spanning, R.J.M. (2001) Two-component system that regulates methanol and formaldehyde oxidation in *Paracoccus denitrificans*. *J Bacteriol* **183**: 664-670.

Harms, N., Reijnders, W.N., Anazawa, H., van der Palen, C.J., van Spanning, R.J., Oltmann, L.F., and Stouthamer, A.H. (1993) Identification of a two-component regulatory system controlling methanol dehydrogenase synthesis in *Paracoccus denitrificans*. *Mol Microbiol* **8**: 457-470.

Harrison, D.E.F. (1973) Studies on the affinity of methanol- and methane-utilizing bacteria for their carbon substrates. *J Appl Microbiol* **36**: 301-308.

Hartig, A., Simon, M.M., Schuster, T., Daugherty, J.R., Yoo, H.S., and Cooper, T.G. (1992) Differentially regulated malate synthase genes participate in carbon and nitrogen metabolism of *S. cerevisiae*. *Nucleic Acids Res* **20**: 5677-5686.

Hartmans, S., and de Bont, J.A.M. (1986) Acetol monooxygenase from *Mycobacterium* Py1 cleaves acetol into acetate and formaldehyde. *FEMS Microbiol Lett* **36**: 155-158.

Hausinger, R.P. (2007) New insights into acetone metabolism. *J Bacteriol* **189**: 671-673.

Heidelberg, J.F., Eisen, J.A., Nelson, W.C., Clayton, R.A., Gwinn, M.L., Dodson, R.J. et al. (2000) DNA sequence of both chromosomes of the cholera pathogen *Vibrio cholerae*. *Nature* **406**: 477-483.

Hetzel, M., Brock, M., Selmer, T., Pierik, A.J., Golding, B.T., and Buckel, W. (2003) Acryloyl-CoA reductase from *Clostridium propionicum*. *Eur J Biochem* **270**: 902-910.

Hines, M.E., Duddleston, K.N., and Kiene, R.P. (2001) Carbon flow to acetate and C_1 compounds in northern wetlands. *Geophys Res Lett* **28**: 4251-4254.

Hinrichs, K.U., Hayes, J.M., Bach, W., Spivack, A.J., Hmelo, L.R., Holm, N.G. et al. (2006) Biological formation of ethane and propane in the deep marine subsurface. *Proc Natl Acad Sci U S A* **103**: 14684-14689.

Hoang, T.T., Karkhoff-Schweizer, R.R., Kutchma, A.J., and Schweizer, H.P. (1998) A broad-host-range Flp-FRT recombination system for site-specific excision of chromosomally-located DNA sequences: application for isolation of unmarked *Pseudomonas aeruginosa* mutants. *Gene* **212**: 77-86.

Hollmann, F., Arends, I.W.C.E., Buehler, K., Schallmey, A., and Buhler, B. (2011) Enzyme-mediated oxidations for the chemist. *Green Chemistry* **13**: 226-265.

Holmes, A.J., and Coleman, N.V. (2008) Evolutionary ecology and multidisciplinary approaches to prospecting for monooxygenases as biocatalysts. *Antonie Van Leeuwenhoek* **94**: 75-84.

Honer Zu Bentrup, K., Miczak, A., Swenson, D.L., and Russell, D.G. (1999) Characterization of activity and expression of isocitrate lyase in *Mycobacterium avium* and *Mycobacterium tuberculosis*. *J Bacteriol* **181**: 7161-7167.

Horswill, A.R., and Escalante-Semerena, J.C. (2002) Characterization of the propionyl-CoA synthetase (PrpE) enzyme of *Salmonella enterica*: residue Lys592 is required for propionyl-AMP synthesis *Biochemistry* **41**: 2379-2387.

Hou, C.T., Patel, R.N., Laskin, A.I., Barnabe, N., and Barist, I. (1983a) Purification and properties of a NAD-linked 1,2-propanediol dehydrogenase from propane-grown *Pseudomonas fluorescens* NRRL B-1244. *Arch Biochem Biophys* **223**: 297-308.

Hou, C.T., Patel, R., Laskin, A.I., Barnabe, N., and Barist, I. (1983b) Production of methyl ketones from secondary alcohols by cell suspensions of C_2 to C_4 *n*-alkane-grown bacteria. *Appl Environ Microbiol* **46**: 178-184.

Hou, C.T., Patel, R., Laskin, A.I., Barnabe, N., and Barist, I. (1983c) Epoxidation of short-chain alkenes by resting-cell suspensions of propane-grown bacteria. *Appl Environ Microbiol* **46**: 171-177.

Hoyt, J.C., Lin, H.P.P., and Reeves, H.C. (1994) In vivo phosphorylation of isocitrate lyase in *Escherichia coli* and *Acinetobacter calcoaceticus*. *Curr Microbiol* **28**: 67-69.

Hurley, J.H., Dean, A.M., Sohl, J.L., Koshland, D.E., Jr., and Stroud, R.M. (1990) Regulation of an enzyme by phosphorylation at the active site. *Science* **249**: 1012-1016.

Hyder, S.L., Meyers, A., and Cayer, M.L. (1979) Membrane modulation in a methylotrophic bacterium *Methylococcus capsulatus* (Texas) as a function of growth substrate. *Tissue and Cell* **11**: 597-610.

Iguchi, H., Yurimoto, H., and Sakai, Y. (2010a) *Methylovulum miyakonense* gen. nov., sp. nov., a novel type I methanotroph from a forest soil in Japan. *Int J Syst Evol Microbiol*: ijs.0.019604-019600.

Iguchi, H., Yurimoto, H., and Sakai, Y. (2010b) Soluble and particulate methane monooxygenase gene clusters of the type I methanotroph *Methylovulum miyakonense* HT12. *FEMS Microbiol Lett* **312**: 71-76.

Im, J., and Semrau, J.D. (2011) Pollutant degradation by a *Methylocystis* strain SB2 grown on ethanol: bioremediation via facultative methanotrophy. *FEMS Microbiol Lett* **318**: 137-142.

Im, J., Lee, S.W., Yoon, S., DiSpirito, A.A., and Semrau, J.D. (2010) Characterization of a novel facultative *Methylocystis* species capable of growth on methane, acetate and ethanol. *Environ Microbiol Rep*: (in press) doi:10.1111/j.1758-2229.2010.00204.x.

Inoue, H., Nojima, H., and Okayama, H. (1990) High efficiency transformation of *Escherichia coli* with plasmids. *Gene* **96**: 23-28.

IPCC (2007) Summary for policymakers. In *Climate change 2007: The physical science basis – Contribution of Working Group I to the fourth assessment report of the Intergovernmental Panel on Climate Change* Solomon, S., Qin, D., Manning, M., Chen, Z., Marquis, M., Averyt, K.B. et al. (eds). Cambridge: Cambridge University Press.

Jasin, M., and Schimmel, P. (1984) Deletion of an essential gene in *Escherichia coli* by site-specific recombination with linear DNA fragments. *J Bacteriol* **159**: 783-786.

Joergensen, L. (1985) The methane mono-oxygenase reaction system studied *in vivo* by membrane-inlet mass spectrometry. *Biochem J* **225**: 441-448.

Johnson, E.L., and Hyman, M.R. (2006) Propane and n-butane oxidation by *Pseudomonas putida* GPo1. *Appl Environ Microbiol* **72**: 950-952.

Johnson, G.V., Evans, H.J., and Ching, T. (1966) Enzymes of the glyoxylate cycle in rhizobia and nodules of legumes. *Plant Physiol* **41**: 1330-1336.

Kalyuzhnaya, M.G., and Lidstrom, M.E. (2003) QscR, a LysR-type transcriptional regulator and CbbR homolog, is involved in regulation of the serine cycle genes in *Methylobacterium extorquens* AM1. *J Bacteriol* **185**: 1229-1235.

Kalyuzhnaya, M.G., and Lidstrom, M.E. (2005) QscR-mediated transcriptional activation of serine cycle genes in *Methylobacterium extorquens* AM1. *J Bacteriol* **187**: 7511-7517.

Kalyuzhnaya, M.G., Hristova, K.R., Lidstrom, M.E., and Chistoserdova, L. (2008) Characterization of a novel methanol dehydrogenase in representatives of *Burkholderiales*: implications for environmental detection of methylotrophy and evidence for convergent evolution. *J Bacteriol* **190**: 3817-3823.

Kane, S.R., Chakicherla, A.Y., Chain, P.S., Schmidt, R., Shin, M.W., Legler, T.C. et al. (2007) Whole-genome analysis of the methyl tert-butyl ether-degrading beta-proteobacterium *Methylibium petroleiphilum* PM1. *J Bacteriol* **189**: 1931-1945.

Kennedy, I.R., and Dilworth, M.J. (1963) Activation of isocitrate lyase and triosephosphate dehydrogenase in *Azotobacter vinelandii* extracts. *Biochim Biophys Acta* **67**: 226-239.

Keppler, F., Hamilton, J.T.G., Braß, M., and Rockmann, T. (2006) Methane emissions from terrestrial plants under aerobic conditions. *Nature* **439**: 187-191.

Keppler, F., Hamilton, J.T.G., McRoberts, W.C., Vigano, I., Braß, M., and Röckmann, T. (2008) Methoxyl groups of plant pectin as a precursor of atmospheric methane: evidence from deuterium labelling studies. *New Phytol* **178**: 808-814.

Khadem, A.F., Pol, A., Wieczorek, A., Mohammadi, S.S., Francoijs, K.-J., Stunnenberg, H.G. et al. (2011) Autotrophic methanotrophy in *Verrucomicrobia*: *Methylacidiphilum fumariolicum* SolV uses the Calvin-Benson-Bassham cycle for carbon dioxide fixation. *J Bacteriol* **193**: 4438-4446.

Khomyakova, M., Bukmez, O., Thomas, L.K., Erb, T.J., and Berg, I.A. (2011) A methylaspartate cycle in haloarchaea. *Science* **331**: 334-337.

Kiefer, P., Buchhaupt, M., Christen, P., Kaup, B., Schrader, J., and Vorholt, J.A. (2009) Metabolite profiling uncovers plasmid-induced cobalt limitation under methylotrophic growth conditions. *PLoS ONE* **4**: e7831.

Kiess, M., Hecht, H.-J., and Kalisz, H.M. (1998) Glucose oxidase from *Penicillium amagasakiense:* primary structure and comparison with other glucose-methanol-choline (GMC) oxidoreductases. *Eur J Biochem* **252**: 90-99.

Kim, C., and Wood, T.K. (1998) Electroporation of pink-pigmented methylotrophic bacteria. *Appl Biochem Biotechnol* **73**: 81-88.

Kinnaman, F.S., Valentine, D.L., and Tyler, S.C. (2007) Carbon and hydrogen isotope fractionation associated with the aerobic microbial oxidation of methane, ethane, propane and butane. *Geochim Cosmochim Acta* **71**: 271-283.

Klein, D.A., Davis, J.A., and Casida, L.E. (1968) Oxidation of *n*-alkanes to ketones by an *Arthrobacter* species. *Antonie Van Leeuwenhoek* **34**: 495-503.

Klusman, R.W. (2006) Detailed compositional analysis of gas seepage at the National Carbon Storage Test Site, Teapot Dome, Wyoming, USA. *Appl Geochem* **21**: 1498-1521.

Knief, C., Vanitchung, S., Harvey, N.W., Conrad, R., Dunfield, P.F., and Chidthaisong, A. (2005) Diversity of methanotrophic bacteria in tropical upland soils under different land uses. *Appl Environ Microbiol* **71**: 3826-3831.

Kolb, S., Knief, C., Dunfield, P.F., and Conrad, R. (2005) Abundance and activity of uncultured methanotrophic bacteria involved in the consumption of atmospheric methane in two forest soils. *Environ Microbiol* **7**: 1150-1161.

Koop, D.R., and Casazza, J.P. (1985) Identification of ethanol-inducible P-450 isozyme 3a as the acetone and acetol monooxygenase of rabbit microsomes. *J Biol Chem* **260**: 13607-13612.

Kornberg, H.L. (1966) The role and control of the glyoxylate cycle in *Escherichia coli*. *Biochem J* **99**: 1-11.

Kornberg, H.L., and Krebs, H.A. (1957) Synthesis of cell constituents from C_2-units by a modified tricarboxylic acid cycle. *Nature* **179**: 988-991.

Kornberg, H.L., and Lund, P. (1959) Influence of growth substrates on levels of glyoxylate cycle enzymes in *Pseudomonas ovalis* Chester. *Biochem J* **72**: 33P.

Kornberg, H.L., and Lascelles, J. (1960) The Formation of isocitratase by the Athiorhodaceae. *J Gen Microbiol* **23**: 511-517.

Korotkova, N., Chistoserdova, L., Kuksa, V., and Lidstrom, M.E. (2002) Glyoxylate regeneration pathway in the methylotroph *Methylobacterium extorquens* AM1. *J Bacteriol* **184**: 1750-1758.

Kotani, T., Yurimoto, H., Kato, N., and Sakai, Y. (2007) Novel acetone metabolism in a propane-utilizing bacterium, *Gordonia* sp. strain TY-5. *J Bacteriol* **189**: 886-893.

Kotani, T., Yamamoto, T., Yurimoto, H., Sakai, Y., and Kato, N. (2003) Propane monooxygenase and NAD^+-dependent secondary alcohol dehydrogenase in propane metabolism by *Gordonia* sp. strain TY-5. *J Bacteriol* **185**: 7120-7128.

Kotani, T., Kawashima, Y., Yurimoto, H., Kato, N., and Sakai, Y. (2006) Gene structure and regulation of alkane monooxygenases in propane-utilizing *Mycobacterium* sp. TY-6 and *Pseudonocardia* sp. TY-7. *J Biosci Bioeng* **102**: 184-192.

Kretzschmar, U., Khodaverdi, V., Jeoung, J.H., and Gorisch, H. (2008) Function and transcriptional regulation of the isocitrate lyase in *Pseudomonas aeruginosa*. *Arch Microbiol* **190**: 151-158.

Krum, J.G., and Ensign, S.A. (2001) Evidence that a linear megaplasmid encodes enzymes of aliphatic alkene and epoxide metabolism and coenzyme M (2-mercaptoethanesulfonate) biosynthesis in *Xanthobacter* Strain Py2. *J Bacteriol* **183**: 2172-2177.

Kunau, W.-H., Dommes, V., and Schulz, H. (1995) β-Oxidation of fatty acids in mitochondria, peroxisomes, and bacteria: A century of continued progress. *Prog Lipid Res* **34**: 267-342.

Kuramochi, H., Nakajima, D., Goto, S., and Kawamoto, K. (2006) Water solubility of solid solution of phenanthrene and anthracene mixture. *Polycyc Aromatic Compounds* **26**: 299-312.

Kurth, E.G., Doughty, D.M., Bottomley, P.J., Arp, D.J., and Sayavedra-Soto, L.A. (2008) Involvement of BmoR and BmoG in n-alkane metabolism in *Pseudomonas butanovora*. *Microbiology* **154**: 139-147.

Kvenvolden, K.A., and Rogers, B.W. (2005) Gaia's breath--global methane exhalations. *Mar Pet Geol* **22**: 579-590.

Lane, D.J. (1991) 16S/23S rRNA sequencing. In *Nucleic acid techniques in bacterial systematics*. Stackebrandt, E. (ed). Chichester: Wiley & Sons, pp. 115 - 175.

Large, P.J., and Quayle, J.R. (1963) Microbial growth on C_1 compounds. 5. Enzyme activities in extracts of *Pseudomonas* AM1. *Biochem J* **87**: 386-396.

Lau, E., Ahmad, A., Steudler, P.A., and Cavanaugh, C.M. (2007) Molecular characterization of methanotrophic communities in forest soils that consume atmospheric methane. *FEMS Microbiol Ecol* **60**: 490-500.

Lawrence, A.J., and Quayle, J.R. (1970) Alternative carbon assimilation pathways in methane-utilizing bacteria. *J Gen Microbiol* **63**: 371-374.

Le Mer, J., and Roger, P. (2001) Production, oxidation, emission and consumption of methane by soils: A review. *Eur J Soil Biol* **37**: 25-50.

Leahy, J.G., Batchelor, P.J., and Morcomb, S.M. (2003) Evolution of the soluble diiron monooxygenases. *FEMS Microbiol Rev* **27**: 449-479.

Leak, D., and Dalton, H. (1986) Growth yields of methanotrophs. *Appl Microbiol Biotechnol* **23**: 470-476.

Leal, N., Havemann, G., and Bobik, T. (2003) PduP is a coenzyme-A-acylating propionaldehyde dehydrogenase associated with the polyhedral bodies involved in B_{12}-dependent 1,2-propanediol degradation by *Salmonella enterica* serovar Typhimurium LT2. *Arch Microbiol* **180**: 353-361.

Lee, P.A., Tullman-Ercek, D., and Georgiou, G. (2006) The bacterial twin-arginine translocation pathway. *Annu Rev Microbiol* **60**: 373-395.

Lee, S.G., Goo, J.H., Kim, H.G., Oh, J.-I., Kim, Y.M., and Kim, S.W. (2004) Optimization of methanol biosynthesis from methane using *Methylosinus trichosporium* OB3b. *Biotechnol Lett* **26**: 947-950.

Lelieveld, J.O.S., Crutzen, P.J., and Dentener, F.J. (1998) Changing concentration, lifetime and climate forcing of atmospheric methane. *Tellus B* **50**: 128-150.

Li, S., and Wackett, L.P. (1992) Trichloroethylene oxidation by toluene dioxygenase. *Biochem Biophys Res Commun* **185**: 443-451.

Lieberman, R.L., and Rosenzweig, A.C. (2005) Crystal structure of a membrane-bound metalloenzyme that catalyses the biological oxidation of methane. *Nature* **434**: 177-182.

Linton, J.D., and Buckee, J.C. (1977) Interactions in a methane-utilizing mixed bacterial culture in a chemostat. *J Gen Microbiol* **101**: 219-225.

Linton, J.D., and Vokes, J. (1978) Growth of the methane utilising bacterium *Methylococcus* NCIB 11083 in mineral salts medium with methanol as the sole source of carbon. *FEMS Microbiol Lett* **4**: 125-128.

Lipmann, F., and Tuttle, L.C. (1945) A specific micromethod for the determination of acyl phosphates. *J Biol Chem* **159**: 21-28.

Lohman, J.R., Olson, A.C., and Remington, S.J. (2008) Atomic resolution structures of *Escherichia coli* and *Bacillus anthracis* malate synthase A: Comparison with isoform G and implications for structure-based drug discovery. *Protein Sci* **17**: 1935-1945.

Long, A.R., and Anthony, C. (1991) The periplasmic modifier protein for methanol dehydrogenase in the methylotrophs *Methylophilus methylotrophus* and *Paracoccus denitrificans*. *J Gen Microbiol* **137**: 2353-2360.

Lopes Ferreira, N., Labbe, D., Monot, F., Fayolle-Guichard, F., and Greer, C.W. (2006) Genes involved in the methyl tert-butyl ether (MTBE) metabolic pathway of *Mycobacterium austroafricanum* IFP 2012. *Microbiology* **152**: 1361-1374.

Lorah, M.M., and Voytek, M.A. (2004) Degradation of 1,1,2,2-tetrachloroethane and accumulation of vinyl chloride in wetland sediment microcosms and in situ porewater: biogeochemical controls and associations with microbial communities. *J Contam Hydrol* **70**: 117-145.

Lukins, H.B., and Foster, J.W. (1963) Methyl ketone metabolism in hydrocarbon-utilizing mycobacteria. *J Bacteriol* **85**: 1074-1087.

Mackay, D., and Shiu, W.Y. (1981) A critical review of Henry's law constants for chemicals of environmental interest. *J Phys Chem Ref Data* **10**: 1175-1199.

Madigan, M., and Martinko, J. (2006) *Brock Biology of Microorganisms*. Upper Saddle River: Pearson Prentice Hall.

Maeng, J., Sakai, Y., Tani, Y., and Kato, N. (1996) Isolation and characterization of a novel oxygenase that catalyzes the first step of n-alkane oxidation in *Acinetobacter* sp. strain M-1. *J Bacteriol* **178**: 3695-3700.

Mahendra, S., and Alvarez-Cohen, L. (2006) Kinetics of 1,4-dioxane biodegradation by monooxygenase-expressing bacteria. *Environ Sci Technol* **40**: 5435-5442.

Marison, I.W., and Attwood, M.M. (1982) A possible alternative mechanism for the oxidation of formaldehyde to formate. *J Gen Microbiol* **128**: 1441-1446.

Marrin, D.L., and Adriany, J.J. (1999) C_2 and C_3 hydrocarbon gases associated with highly reducing conditions in groundwater. *Biogeochemistry* **47**: 15-23.

Martin, H., and Murrell, J.C. (1995) Methane monooxygenase mutants of *Methylosinus trichosporium* constructed by marker-exchange mutagenesis. *FEMS Microbiol Lett* **127**: 243-248.

Martinson, G.O., Werner, F.A., Scherber, C., Conrad, R., Corre, M.D., Flessa, H. et al. (2010) Methane emissions from tank bromeliads in neotropical forests. *Nature Geosci* **3**: 766-769.

Marx, C.J., and Lidstrom, M.E. (2001a) Development of improved versatile broad-host-range vectors for use in methylotrophs and other Gram-negative bacteria. *Microbiology* **147**: 2065-2075.

Marx, C.J., and Lidstrom, M.E. (2001b) Development of improved versatile broad-host-range vectors for use in methylotrophs and other Gram-negative bacteria. *Microbiology* **147**: 2065-2075.

Marx, C.J., and Lidstrom, M.E. (2002) Broad-host-range *cre-lox* system for antibiotic marker recycling in gram-negative bacteria. *BioTechniques* **33**: 1062-1067.

Matsushita, K., Shinagawa, E., Adachi, O., and Ameyama, M. (1979) Membrane-bound D-gluconate dehydrogenase from *Pseudomonas aeruginosa*. *Journal of Biochemistry* **86**: 249-256.

Mattes, T.E., Alexander, A.K., and Coleman, N.V. (2010) Aerobic biodegradation of the chloroethenes: pathways, enzymes, ecology, and evolution. *FEMS Microbiol Rev* **34**: 445-475.

McDonald, I., Uchiyama, H., Kambe, S., Yagi, O., and Murrell, J. (1997) The soluble methane monooxygenase gene cluster of the trichloroethylene- degrading methanotroph *Methylocystis* sp. strain M. *Appl Environ Microbiol* **63**: 1898-1904.

McDonald, I.R., Hall, G.H., Pickup, R.W., and Colin Murrell, J. (1996) Methane oxidation potential and preliminary analysis of methanotrophs in blanket bog peat using molecular ecology techniques. *FEMS Microbiol Ecol* **21**: 197-211.

McGuinness, P.H., Bishop, G.A., McCaughan, G.W., Trowbridge, R., and Gowans, E.J. (1994) False detection of negative-strand hepatitis C virus RNA. *The Lancet* **343**: 551-552.

McNerney, T., and O'Connor, M.L. (1980) Regulation of enzymes associated with C_1 metabolism in three facultative methylotrophs. *Appl Environ Microbiol* **40**: 370-375.

Meister, M., Saum, S., Alber, B.E., and Fuchs, G. (2005) L-malyl-coenzyme A/β-methylmalyl-coenzyme A lyase is involved in acetate assimilation of the isocitrate lyase-negative bacterium *Rhodobacter capsulatus*. *J Bacteriol* **187**: 1415-1425.

Merkx, M., and Lippard, S.J. (2002) Why OrfY? *J Biol Chem* **277**: 5858-5865.

Miura, A., and Dalton, H. (1995) Purification and characterization of the alkene monooxygenase from *Nocardia corallina* B-276. *Biosci, Biotechnol, Biochem* **59**: 853-859.

Molina, I., Pellicer, M.T., Badia, J., Aguilar, J., and Baldoma, L. (1994) Molecular characterization of *Escherichia coli* malate synthase G. Differentiation with the malate synthase A isoenzyme. *Eur J Biochem* **224**: 541-548.

Morales, M., Nava, V., Velásquez, E., Razo-Flores, E., and Revah, S. (2009) Mineralization of methyl *tert* -butyl ether and other gasoline oxygenates by Pseudomonads using short *n*-alkanes as growth source. *Biodegradation* **20**: 271-280.

Morris, C.J., and Lidstrom, M.E. (1992) Cloning of a methanol-inducible *moxF* promoter and its analysis in *moxB* mutants of *Methylobacterium extorquens* AM1rif. *J Bacteriol* **174**: 4444-4449.

Morris, C.J., Kim, Y.M., Perkins, K.E., and Lidstrom, M.E. (1995) Identification and nucleotide sequences of *mxaA*, *mxaC*, *mxaK*, *mxaL*, and *mxaD* genes from *Methylobacterium extorquens* AM1. *J Bacteriol* **177**: 6825-6831.

Mörsky, S.K., Haapala, J.K., Rinnan, R., Tiiva, P., Saarnio, S., Silvola, J. et al. (2008) Long-term ozone effects on vegetation, microbial community and methane dynamics of boreal peatland microcosms in open-field conditions. *Global Change Biol* **14**: 1891-1903.

Mountfort, D.O. (1990) Oxidation of aromatic alcohols by purified methanol dehydrogenase from *Methylosinus trichosporium*. *J Bacteriol* **172**: 3690-3694.

Munoz-Elias, E.J., and McKinney, J.D. (2005) *Mycobacterium tuberculosis* isocitrate lyases 1 and 2 are jointly required for *in vivo* growth and virulence. *Nat Med* **11**: 638-644.

Murphy, K.C. (1998) Use of bacteriophage lambda recombination functions to promote gene replacement in *Escherichia coli*. *J Bacteriol* **180**: 2063-2071.

Murrell, J.C. (1992) Genetics and molecular biology of methanotrophs. *FEMS Microbiol Lett* **88**: 233-248.

Murrell, J.C. (2010) The aerobic methane oxidizing bacteria (methanotrophs). In *Handbook of Hydrocarbon and Lipid Microbiology*. Timmis, K.N. (ed): Springer Berlin Heidelberg, pp. 1953-1966.

Murrell, J.C., Gilbert, B., and McDonald, I.R. (2000a) Molecular biology and regulation of methane monooxygenase. *Arch Microbiol* **173**: 325-332.

Murrell, J.C., McDonald, I.R., and Gilbert, B. (2000b) Regulation of expression of methane monooxygenases by copper ions. *Trends Microbiol* **8**: 221-225.

Myronova, N., Kitmitto, A., Collins, R.F., Miyaji, A., and Dalton, H. (2006) Three-dimensional structure determination of a protein supercomplex that oxidizes methane to formaldehyde in *Methylococcus capsulatus* (Bath). *Biochemistry* **45**: 11905-11914.

Nakatsu, C.H., Hristova, K., Hanada, S., Meng, X.Y., Hanson, J.R., Scow, K.M., and Kamagata, Y. (2006) *Methylibium petroleiphilum* gen. nov., sp. nov., a novel methyl tert-butyl ether-degrading methylotroph of the *Betaproteobacteria*. *Int J Syst Evol Microbiol* **56**: 983-989.

Nava, V., Morales, M., and Revah, S. (2007) Cometabolism of methyl *tert*-butyl ether (MTBE) with alkanes. *Reviews in Environmental Science and Biotechnology* **6**: 339-352.

Newman, L.M., and Wackett, L.P. (1995) Purification and characterization of toluene 2-monooxygenase from *Burkholderia cepacia* G4. *Biochemistry* **34**: 14066-14076.

Nielsen, A.K., Gerdes, K., and Murrell, J.C. (1997) Copper-dependent reciprocal transcriptional regulation of methane monooxygenase genes in *Methylococcus capsulatus* and *Methylosinus trichosporium*. *Mol Microbiol* **25**: 399-409.

Nielsen, A.K., Gerdes, K., Degn, H., and Murrell, J.C. (1996) Regulation of bacterial methane oxidation: transcription of the soluble methane mono-oxygenase operon of *Methylococcus capsulatus* (Bath) is repressed by copper ions. *Microbiology* **142**: 1289-1296.

Nisbet, R.E., Fisher, R., Nimmo, R.H., Bendall, D.S., Crill, P.M., Gallego-Sala, A.V. et al. (2009) Emission of methane from plants. *Proc Biol Sci*.

Nordlund, I., Powlowski, J., and Shingler, V. (1990) Complete nucleotide sequence and polypeptide analysis of multicomponent phenol hydroxylase from *Pseudomonas* sp. strain CF600. *J Bacteriol* **172**: 6826-6833.

Nordlund, P., and Eklund, H. (1995) Di-iron--carboxylate proteins. *Curr Opin Struct Biol* **5**: 758-766.

Notomista, E., Lahm, A., Di Donato, A., and Tramontano, A. (2003) Evolution of bacterial and archaeal multicomponent monooxygenases. *J Mol Evol* **56**: 435-445.

Nunn, D.N., and Lidstrom, M.E. (1986a) Isolation and complementation analysis of 10 methanol oxidation mutant classes and identification of the methanol dehydrogenase structural gene of *Methylobacterium* sp. strain AM1. *J Bacteriol* **166**: 581-590.

Nunn, D.N., and Lidstrom, M.E. (1986b) Phenotypic characterization of 10 methanol oxidation mutant classes in *Methylobacterium* sp. strain AM1. *J Bacteriol* **166**: 591-597.

Nunn, D.N., Day, D., and Anthony, C. (1989) The second subunit of methanol dehydrogenase of *Methylobacterium extorquens* AM1. *Biochem J* **260**: 857-862.

Oakley, C.J., and Colin Murrell, J. (1988) *nifH* genes in the obligate methane oxidizing bacteria. *FEMS Microbiol Lett* **49**: 53-57.

Oh, S.H., and Chater, K.F. (1997) Denaturation of circular or linear DNA facilitates targeted integrative transformation of *Streptomyces coelicolor* A3(2): possible relevance to other organisms. *J Bacteriol* **179**: 122-127.

Okubo, Y., Yang, S., Chistoserdova, L., and Lidstrom, M.E. (2010) Alternative route for glyoxylate consumption during growth on two-carbon compounds by *Methylobacterium extorquens* AM1. *J Bacteriol* **192**: 1813-1823.

Oldenhuis, R., Vink, R.L., Janssen, D.B., and Witholt, B. (1989) Degradation of chlorinated aliphatic hydrocarbons by *Methylosinus trichosporium* OB3b expressing soluble methane monooxygenase. *Appl Environ Microbiol* **55**: 2819-2826.

Op den Camp, H.J.M., Islam, T., Stott, M.B., Harhangi, H.R., Hynes, A., Schouten, S. et al. (2009) Environmental, genomic and taxonomic perspectives on methanotrophic *Verrucomicrobia*. *Environ Microbiol Rep* **1**: 293-306.

Oremland, R.S., Miller, L.G., and Whiticar, M.J. (1987) Sources and flux of natural gases from Mono Lake, California. *Geochim Cosmochim Acta* **51**: 2915-2929.

Pajaniappan, M., Hall, J.E., Cawthraw, S.A., Newell, D.G., Gaynor, E.C., Fields, J.A. et al. (2008) A temperature-regulated *Campylobacter jejuni* gluconate dehydrogenase is involved in respiration-dependent energy conservation and chicken colonization. *Mol Microbiol* **68**: 474-491.

Palmer, T., Sargent, F., and Berks, B.C. (2005) Export of complex cofactor-containing proteins by the bacterial Tat pathway. *Trends Microbiol* **13**: 175-180.

Parkhill, J., Wren, B.W., Thomson, N.R., Titball, R.W., Holden, M.T.G., Prentice, M.B. et al. (2001) Genome sequence of *Yersinia pestis*, the causative agent of plague. *Nature* **413**: 523-527.

Patel, N.A., Thalassinos, K., Slade, S.E., Hughes, C., Connolly, J.B., Langridge, J. et al. (2011) A comparison of one- and two-dimensional liquid chromatography approaches in the label-free quantitative analysis of *Methylocella silvestris*. (Manuscript in preparation).

Patel, R.N., Hoare, S.L., Hoare, D.S., and Taylor, B.F. (1977) [^{14}C]acetate assimilation by a type I obligate methylotroph, *Methylococcus capsulatus*. *Appl Environ Microbiol* **34**: 607-610.

Patel, R.N., Hou, C.T., Laskin, A.I., and Felix, A. (1982) Microbial oxidation of hydrocarbons: properties of a soluble methane monooxygenase from a facultative methane-utilizing organism, *Methylobacterium* sp. strain CRL-26. *Appl Environ Microbiol* **44**: 1130-1137.

Patel, V.J., Thalassinos, K., Slade, S.E., Connolly, J.B., Crombie, A., Murrell, J.C., and Scrivens, J.H. (2009) A comparison of labeling and label-free mass spectrometry-based proteomics approaches. *J Proteome Res* **8**: 3752-3759.

Pellicer, M.T., Fernandez, C., Badia, J., Aguilar, J., Lin, E.C., and Baldom, L. (1999) Cross-induction of *glc* and *ace* operons of *Escherichia coli* attributable to pathway intersection. Characterization of the *glc* promoter. *J Biol Chem* **274**: 1745-1752.

Perry, J.J. (1980) Propane utilization by microorganisms. In *Adv Appl Microbiol*. Perlman, D. (ed): Academic Press, pp. 89-115.

Peyraud, R., Kiefer, P., Christen, P., Massou, S., Portais, J.-C., and Vorholt, J.A. (2009) Demonstration of the ethylmalonyl-CoA pathway by using ^{13}C metabolomics. *Proc Natl Acad Sci U S A* **106**: 4846-4851.

Pieja, A., Rostkowski, K., and Criddle, C. (2011) Distribution and selection of poly-3-hydroxybutyrate production capacity in methanotrophic proteobacteria. *Microb Ecol*: (in press) doi: 10.1007/s00248-00011-09873-00240.

Pikus, J.D., Studts, J.M., Achim, C., Kauffmann, K.E., Münck, E., Steffan, R.J. et al. (1996) Recombinant toluene-4-monooxygenase: catalytic and Mössbauer studies of the purified diiron and Rieske components of a four-protein complex. *Biochemistry* **35**: 9106-9119.

Plass-Dülmer, C., Koppmann, R., Ratte, M., and Rudolph, J. (1995) Light nonmethane hydrocarbons in seawater. *Global Biogeochem Cycles* **9**: 79-100.

Platen, H., and Schink, B. (1987) Methanogenic degradation of acetone by an enrichment culture. *Arch Microbiol* **149**: 136-141.

Pollard, D.J., and Woodley, J.M. (2007) Biocatalysis for pharmaceutical intermediates: the future is now. *Trends Biotechnol* **25**: 66-73.

Pomerantsev, A.P., Camp, A., and Leppla, S.H. (2009) A new minimal replicon of *Bacillus anthracis* plasmid pXO1. *J Bacteriol* **191**: 5134-5146.

Popov, V., Moskalev, E., Shevchenko, M., and Eprintsev, A. (2005) Comparative analysis of glyoxylate cycle key enzyme isocitrate lyase from organisms of different systematic groups. *J Evol Biochem Phys* **41**: 631-639.

Powlowski, J., and Shingler, V. (1994) Genetics and biochemistry of phenol degradation by *Pseudomonas* sp. CF600. *Biodegradation* **5**: 219-236.

Rahman, M.T., Crombie, A., Moussard, H., Chen, Y., and Murrell, J.C. (2011) Acetate repression of methane oxidation by supplemental *Methylocella silvestris* in a peat soil microcosm. *Appl Environ Microbiol* **77**: 4234-4236.

Ramirez-Trujillo, J.A., Encarnacion, S., Salazar, E., de los Santos, A.G., Dunn, M.F., Emerich, D.W. et al. (2007) Functional characterization of the *Sinorhizobium meliloti* acetate metabolism genes *aceA*, SMc00767, and *glcB*. *J Bacteriol* **189**: 5875-5884.

Rappsilber, J., Ryder, U., Lamond, A.I., and Mann, M. (2002) Large-scale proteomic analysis of the human spliceosome. *Genome Res* **12**: 1231-1245.

Reay, D.S., Smith, P., and van Amstel, A. (2010) Methane sources and the global methane budget. In *Methane and Climate Change*. Reay, D.S., Smith, P., and van Amstel, A. (eds). London: Earthscan.

Reeburgh, W.S. (2007) Global methane biogeochemistry. In *Treatise on Geochemistry*. Holland, H.D., and Turekian, K.K. (eds). Amsterdam: Elsevier, pp. 1-32.

Reinscheid, D.J., Eikmanns, B.J., and Sahm, H. (1994a) Malate synthase from *Corynebacterium glutamicum*: sequence analysis of the gene and biochemical characterization of the enzyme. *Microbiology* **140**: 3099-3108.

Reinscheid, D.J., Eikmanns, B.J., and Sahm, H. (1994b) Characterization of the isocitrate lyase gene from Corynebacterium glutamicum and biochemical analysis of the enzyme. *J Bacteriol* **176**: 3474-3483.

Rice, A.L., Butenhoff, C.L., Shearer, M.J., Teama, D., Rosenstiel, T.N., and Khalil, M.A.K. (2010) Emissions of anaerobically produced methane by trees. *Geophys Res Lett* **37**: L03807.

Rigby, M., Prinn, R.G., Fraser, P.J., Simmonds, P.G., Langenfelds, R.L., Huang, J. et al. (2008) Renewed growth of atmospheric methane. *Geophys Res Lett* **35**: L22805.

Roback, P., Beard, J., Baumann, D., Gille, C., Henry, K., Krohn, S. et al. (2007) A predicted operon map for *Mycobacterium tuberculosis*. *Nucleic Acids Res* **35**: 5085-5095.

Rojo, F. (2009) Degradation of alkanes by bacteria. *Environ Microbiol* **11**: 2477-2490.

Rosenzweig, A.C., Frederick, C.A., Lippard, S.J., and Nordlund, P. (1993) Crystal structure of a bacterial non-haem iron hydroxylase that catalyses the biological oxidation of methane. *Nature* **366**: 537-543.

Rosenzweig, A.C., Brandstetter, H., Whittington, D.A., Nordlund, P., Lippard, S.J., and Frederick, C.A. (1997) Crystal structures of the methane monooxygenase hydroxylase from *Methylococcus capsulatus* (Bath): Implications for substrate gating and component interactions. *Proteins* **29**: 141-152.

Rothstein, R.J. (1983) One-step gene disruption in yeast. *Methods Enzymol* **101**: 202-211.

Rudney, H. (1954) Propanediol phosphate as a possible intermediate in the metabolism of acetone. *J Biol Chem* **210**: 361-371.

Saeki, H., and Furuhashi, K. (1994) Cloning and characterization of a *Nocardia corallina* B-276 gene cluster encoding alkene monooxygenase. *J Ferment Bioeng* **78**: 399-406.

Saeki, H., Akira, M., Furuhashi, K., Averhoff, B., and Gottschalk, G. (1999) Degradation of trichloroethene by a linear-plasmid-encoded alkene monooxygenase in *Rhodococcus corallinus* (*Nocardia corallina*) B-276. *Microbiology* **145**: 1721-1730.

Sahm, H., Cox, R.B., and Quayle, J.R. (1976) Metabolism of methanol by *Rhodopseudomonas acidophila*. *J Gen Microbiol* **94**: 313-322.

Salem, A.R., Hacking, A.J., and Quayle, J.R. (1973a) Cleavage of malyl-Coenzyme A into acetyl-Coenzyme A and glyoxylate by *Pseudomonas* AM1 and other C_1-unit-utilizing bacteria. *Biochem J* **136**: 89-96.

Salem, A.R., Wagner, C., Hacking, A.J., and Quayle, J.R. (1973b) The metabolism of lactate and pyruvate by *Pseudomonas* AM1. *J Gen Microbiol* **76**: 375-388.

Sales, C.M., Mahendra, S., Grostern, A., Parales, R.E., Goodwin, L.A., Woyke, T. et al. (2011) Genome sequence of the 1,4-dioxane-degrading *Pseudonocardia dioxanivorans* strain CB1190. *J Bacteriol* **193**: 4549-4550.

Sambrook, J., and Russell, D.W. (2001) *Molecular cloning: A laboratory manual*. New York: Cold Spring Harbor Laboratory Press

Sander, R. (1999). Compilation of Henry's Law constants for inorganic and organic species of potential importance in environmental chemistry (Version 3). URL http://www.henrys-law.org

Sarraute, S., Delepine, H., Costa Gomes, M.F., and Majer, V. (2004) Aqueous solubility, Henry's law constants and air/water partition coefficients of *n*-octane and two halogenated octanes. *Chemosphere* **57**: 1543-1551.

Sauer, U., and Eikmanns, B.J. (2005) The PEP–pyruvate–oxaloacetate node as the switch point for carbon flux distribution in bacteria. *FEMS Microbiol Rev* **29**: 765-794.

Sayavedra-Soto, L.A., Doughty, D.M., Kurth, E.G., Bottomley, P.J., and Arp, D.J. (2005) Product and product-independent induction of butane oxidation in *Pseudomonas butanovora*. *FEMS Microbiol Lett* **250**: 111-116.

Sayavedra-Soto, L.A., Hamamura, N., Liu, C.-W., Kimbrel, J.A., Chang, J.H., and Arp, D.J. (2011) The membrane-associated monooxygenase in the butane-oxidizing Gram-positive bacterium *Nocardioides* sp. strain CF8 is a novel member of the AMO/PMO family. *Environ Microbiol Rep* **3**: 390-396.

Sazinsky, M.H., and Lippard, S.J. (2006) Correlating structure with function in bacterial multicomponent monooxygenases and related diiron proteins. *Acc Chem Res* **39**: 558-566.

Sazinsky, M.H., Bard, J., Di Donato, A., and Lippard, S.J. (2004) Crystal Structure of the Toluene/*o*-Xylene Monooxygenase Hydroxylase from *Pseudomonas stutzeri* OX1. *J Biol Chem* **279**: 30600-30610.

Schäfer, A., Tauch, A., Jäger, W., Kalinowski, J., Thierbach, G., and Pühler, A. (1994) Small mobilizable multi-purpose cloning vectors derived from the *Escherichia coli* plasmids pK18 and pK19: selection of defined deletions in the chromosome of *Corynebacterium glutamicum*. *Gene* **145**: 69-73.

Schmidt, R., Battaglia, V., Scow, K., Kane, S., and Hristova, K.R. (2008) Involvement of a novel enzyme, MdpA, in methyl tert-butyl ether degradation in *Methylibium petroleiphilum* PM1. *Appl Environ Microbiol* **74**: 6631-6638.

Schmidt, S., Christen, P., Kiefer, P., and Vorholt, J.A. (2010) Functional investigation of methanol dehydrogenase-like protein XoxF in *Methylobacterium extorquens* AM1. *Microbiology* **156**: 2575-2586.

Schneider, G. (1999) How many potentially secreted proteins are contained in a bacterial genome? *Gene* **237**: 113-121.

Schoell, M. (1988) Multiple origins of methane in the Earth. *Chemical Geology* **71**: 1-10.

Selbitschka, W., Niemann, S., and Pühler, A. (1993) Construction of gene replacement vectors for Gram - bacteria using a genetically modified *sacRB* gene as a positve selection marker. *Appl Microbiol Biotechnol* **38**: 615-618.

Semrau, J.D., DiSpirito, A.A., and Yoon, S. (2010) Methanotrophs and copper. *FEMS Microbiol Rev* **34**: 496-531.

Semrau, J.D., DiSpirito, A.A., and Vuilleumier, S. (2011) Facultative methanotrophy: false leads, true results, and suggestions for future research. *FEMS Microbiol Lett*: (In press) doi: 10.1111/j.1574-6968.2011.02315.x.

Shah, V.K., Ugalde, R.A., Imperial, J., and Brill, W.J. (1984) Molybdenum in nitrogenase. *Annu Rev Biochem* **53**: 231-257.

Sharma, V., Sharma, S., zu Bentrup, K.H., McKinney, J.D., Russell, D.G., Jacobs, W.R., and Sacchettini, J.C. (2000) Structure of isocitrate lyase, a persistence factor of *Mycobacterium tuberculosis*. *Nat Struct Mol Biol* **7**: 663-668.

Sharp, J.O., Sales, C.M., and Alvarez-Cohen, L. (2010) Functional characterization of propane-enhanced *N*-nitrosodimethylamine degradation by two actinomycetales. *Biotechnol Bioeng* **107**: 924-932.

Shennan, J.L. (2006) Utilisation of C_2–C_4 gaseous hydrocarbons and isoprene by microorganisms. *J Chem Technol Biot* **81**: 237-256.

Shigematsu, T., Hanada, S., Eguchi, M., Kamagata, Y., Kanagawa, T., and Kurane, R. (1999) Soluble methane monooxygenase gene clusters from trichloroethylene-degrading *Methylomonas* sp. strains and detection of methanotrophs during in situ bioremediation. *Appl Environ Microbiol* **65**: 5198-5206.

Shinagawa, E., Matsushita, K., Adachi, O., and Ameyama, M. (1982) Purification and Characterization of D-Sorbitol Dehydrogenase from Membrane of Gluconobacter suboxydans var. α. *Agric Biol Chem* **46**: 135-141.

Shinagawa, E., Matsushita, K., Adachi, O., and Ameyama, M. (1984) D-gluconate dehydrogenase, 2-keto-D-gluconate yielding, from *Gluconobacter dioxyacetonicus*: purification and characterization. *Agric Biol Chem* **48**: 1517-1522.

Shingler, V., Franklin, F.C.H., Tsuda, M., Holroyd, D., and Bagdasarian, M. (1989) Molecular analysis of a plasmid-encoded phenol hydroxylase from *Pseudomonas* CF600. *J Gen Microbiol* **135**: 1083-1092.

Silverman, L., and Shideler, M.E. (1958) Determination of biphenyl in the presence of polyphenyls : Water solubility method. *Anal Chim Acta* **18**: 540-546.

Simon, R., Priefer, U., and Pühler, A. (1983) A broad host range mobilization system for *in-vivo* genetic engineering - Transposon mutagenesis in Gram-negative bacteria. *Bio-Technology* **1**: 784-791.

Sluis, M.K., and Ensign, S.A. (1997) Purification and characterization of acetone carboxylase from *Xanthobacter* strain Py2. *Proc Natl Acad Sci USA* **94**: 8456-8461.

Sluis, M.K., Sayavedra-Soto, L.A., and Arp, D.J. (2002) Molecular analysis of the soluble butane monooxygenase from *Pseudomonas butanovora*. *Microbiology* **148**: 3617-3629.

Smith, C.A., O'Reilly, K.T., and Hyman, M.R. (2003a) Characterization of the initial reactions during the cometabolic oxidation of methyl *tert*-butyl ether by propane-grown *Mycobacterium vaccae* JOB5. *Appl Environ Microbiol* **69**: 796-804.

Smith, C.V., Huang, C.C., Miczak, A., Russell, D.G., Sacchettini, J.C., and Honer zu Bentrup, K. (2003b) Biochemical and structural studies of malate synthase from *Mycobacterium tuberculosis*. *J Biol Chem* **278**: 1735-1743.

Smith, C.V., Huang, C.-c., Miczak, A., Russell, D.G., Sacchettini, J.C., and Höner zu Bentrup, K. (2003c) Biochemical and structural studies of malate synthase from *Mycobacterium tuberculosis*. *J Biol Chem* **278**: 1735-1743.

Smith, T.J., Slade, S.E., Burton, N.P., Murrell, J.C., and Dalton, H. (2002) Improved system for protein engineering of the hydroxylase component of soluble methane monooxygenase. *Appl Environ Microbiol* **68**: 5265-5273.

Solórzano, L. (1969) Determination of ammonia in natural waters by the phenol hypochlorite method. *Limnol Oceanogr* **15**: 799-801.

Sperl, G.T., Forrest, H.S., and Gibson, D.T. (1974) Substrate specificity of the purified primary alcohol dehydrogenases from methanol-oxidizing bacteria. *J Bacteriol* **118**: 541-550.

Springer, A.L., Morris, C.J., and Lidstrom, M.E. (1997) Molecular analysis of *mxbD* and *mxbM*, a putative sensor-regulator pair required for oxidation of methanol in *Methylobacterium extorquens* AM1. *Microbiology* **143**: 1737-1744.

Springer, A.L., Auman, A.J., and Lidstrom, M.E. (1998) Sequence and characterization of *mxaB*, a response regulator involved in regulation of methanol oxidation, and of *mxaW*, a methanol-regulated gene in *Methylobacterium extorquens* AM1. *FEMS Microbiol Lett* **160**: 119-124.

Stafford, G.P., Scanlan, J., McDonald, I.R., and Murrell, J.C. (2003) *rpoN, mmoR and mmoG*, genes involved in regulating the expression of soluble methane monooxygenase in *Methylosinus trichosporium* OB3b. *Microbiology* **149**: 1771-1784.

Stainthorpe, A.C., Murrell, J.C., Salmond, G.P.C., Dalton, H., and Lees, V. (1989) Molecular analysis of methane monooxygenase from *Methylococcus capsulatus* (Bath). *Arch Microbiol* **152**: 154-159.

Stainthorpe, A.C., Lees, V., Salmond, G.P.C., Dalton, H., and Murrell, J.C. (1990) The methane monooxygenase gene cluster of *Methylococcus capsulatus* (Bath). *Gene* **91**: 27-34.

Starai, V.J., and Escalante-Semerena, J.C. (2004) Acetyl-coenzyme A synthetase (AMP forming). *Cell Mol Life Sci* **61**: 2020-2030.

Steffan, R., McClay, K., Vainberg, S., Condee, C., and Zhang, D. (1997) Biodegradation of the gasoline oxygenates methyl *tert*-butyl ether, ethyl *tert*-butyl ether, and *tert*-amyl methyl ether by propane-oxidizing bacteria. *Appl Environ Microbiol* **63**: 4216-4222.

Stein, L.Y., Yoon, S., Semrau, J.D., DiSpirito, A.A., Crombie, A., Murrell, J.C. et al. (2010) Genome sequence of the obligate methanotroph *Methylosinus trichosporium* strain OB3b. *J Bacteriol* **192**: 6497-6498.

Stephens, G.M., and Dalton, H. (1986) The role of the terminal and subterminal oxidation pathways in propane metabolism by bacteria. *J Gen Microbiol* **132**: 2453-2462.

Steudler, P.A., Bowden, R.D., Melillo, J.M., and Aber, J.D. (1989) Influence of nitrogen fertilization on methane uptake in temperate forest soils. *Nature* **341**: 314-316.

Sticher, P., Jaspers, M., Stemmler, K., Harms, H., Zehnder, A., and van der Meer, J. (1997) Development and characterization of a whole-cell bioluminescent sensor for bioavailable middle-chain alkanes in contaminated groundwater samples. *Appl Environ Microbiol* **63**: 4053-4060.

Stirling, D.I., and Dalton, H. (1978) Purification and properties of an $NAD(P)^+$-linked formaldehyde dehydrogenase from *Methylococcus capsulatus* (Bath). *J Gen Microbiol* **107**: 19-29.

Stirling, D.I., and Dalton, H. (1979) The fortuitous oxidation and cometabolism of various carbon compounds by whole-cell suspensions of *Methylococcus capsulatus* (Bath). *FEMS Microbiol Lett* **5**: 315-318.

Stottmeister, U., Aurich, A., Wilde, H., Andersch, J., Schmidt, S., and Sicker, D. (2005) White biotechnology for green chemistry: fermentative 2-oxocarboxylic acids as novel building blocks for subsequent chemical syntheses. *J Ind Microbiol Biotechnol* **32**: 651-664.

Strobel, B.W. (2001) Influence of vegetation on low-molecular-weight carboxylic acids in soil solution--a review. *Geoderma* **99**: 169-198.

Tamura, K., Dudley, J., Nei, M., and Kumar, S. (2007) MEGA4: Molecular evolutionary genetics analysis (MEGA) software version 4.0. *Mol Biol Evol* **24**: 1596-1599.

Tanaka, Y., Yoshida, T., Watanabe, K., Izumi, Y., and Mitsunaga, T. (1997) Characterization, gene cloning and expression of isocitrate lyase involved in the assimilation of one-carbon compounds in *Hyphomicrobium methylovorum* GM2. *Eur J Biochem* **249**: 820-825.

Taylor, D.G., Trudgill, P.W., Cripps, R.E., and Harris, P.R. (1980) The microbial metabolism of acetone. *J Gen Microbiol* **118**: 159-170.

Taylor, I.J., and Anthony, C. (1976) Acetyl-CoA production and utilization during growth of the facultative methylotroph *Pseudomonas* AM1 on ethanol, malonate and 3-hydroxybutyrate. *J Gen Microbiol* **95**: 134-143.

Taylor, S.C., Dalton, H., and Dow, C.S. (1981) Ribulose-1,5-bisphosphate carboxylase/oxygenase and carbon assimilation in *Methylococcus capsulatus* (Bath). *J Gen Microbiol* **122**: 89-94.

Taylor, S.W., Sherwood Lollar, B., and Wassenaar, I. (2000) Bacteriogenic ethane in near-surface aquifers: Implications for leaking hydrocarbon well bores. *Environ Sci Technol* **34**: 4727-4732.

Textor, S., Wendisch, V.F., De Graaf, A.A., Muller, U., Linder, M.I., Linder, D., and Buckel, W. (1997) Propionate oxidation in *Escherichia coli*: evidence for operation of a methylcitrate cycle in bacteria. *Arch Microbiol* **168**: 428-436.

Theisen, A.R. (2006) Regulation of methane oxidation in the facultative methanotroph *Methylocella silvestris* BL2. *PhD Thesis*. Coventry: University of Warwick.

Theisen, A.R., and Murrell, J.C. (2005) Facultative methanotrophs revisited. *J Bacteriol* **187**: 4303-4305.

Theisen, A.R., Ali, M.H., Radajewski, S., Dumont, M.G., Dunfield, P.F., McDonald, I.R. et al. (2005) Regulation of methane oxidation in the facultative methanotroph *Methylocella silvestris* BL2. *Mol Microbiol* **58**: 682-692.

Thiemer, B., Andreesen, J.R., and Schräder, T. (2001) The NADH-dependent reductase of a putative multicomponent tetrahydrofuran mono-oxygenase contains a covalently bound FAD. *Eur J Biochem* **268**: 3774-3782.

Thiemer, B., Andreesen, J.R., and Schräder, T. (2003) Cloning and characterization of a gene cluster involved in tetrahydrofuran degradation in *Pseudonocardia* sp. strain K1. *Arch Microbiol* **179**: 266-277.

Thomason, M.K., and Storz, G. (2010) Bacterial antisense RNAs: how many are there, and what are they doing? *Annu Rev Genet* **44**: 167-188.

Tinberg, C.E., and Lippard, S.J. (2011) Dioxygen Activation in Soluble Methane Monooxygenase. *Accounts of Chemical Research* **44**: 280-288.

Torres Pazmiño, D.E., Winkler, M., Glieder, A., and Fraaije, M.W. (2010) Monooxygenases as biocatalysts: Classification, mechanistic aspects and biotechnological applications. *J Biotechnol* **146**: 9-24.

Tovanabootr, A., and Semprini, L. (1998) Comparison of TCE transformation abilities of methane- and propane-utilizing microorganisms. *Bioremediation J* **2**: 105-124.

Toyama, H., Anthony, C., and Lidstrom, M.E. (1998) Construction of insertion and deletion *mxa* mutants of *Methylobacterium extorquens* AM1 by electroporation. *FEMS Microbiol Lett* **166**: 1-7.

Toyama, H., Furuya, N., Saichana, I., Ano, Y., Adachi, O., and Matsushita, K. (2007) Membrane-bound, 2-keto-D-gluconate-yielding D-gluconate dehydrogenase from *Gluconobacter dioxyacetonicus* IFO 3271: molecular properties and gene disruption. *Appl Environ Microbiol* **73**: 6551-6556.

Trotsenko, Y.A., and Murrell, J.C. (2008) Metabolic aspects of aerobic obligate methanotrophy. In *Adv Appl Microbiol*. Allen I. Laskin, S.S., and Geoffrey, M.G. (eds): Academic Press, pp. 183-229.

Tuiskunen, A., Leparc-Goffart, I., Boubis, L., Monteil, V., Klingstrom, J., Tolou, H.J. et al. (2010) Self-priming of reverse transcriptase impairs strand-specific detection of dengue virus RNA. *J Gen Virol* **91**: 1019-1027.

Valentine, D.L., Kessler, J.D., Redmond, M.C., Mendes, S.D., Heintz, M.B., Farwell, C. et al. (2010) Propane respiration jump-starts microbial response to a deep oil spill. *Science* **330**: 208-211.

van Beilen, J.B., and Funhoff, E.G. (2005) Expanding the alkane oxygenase toolbox: new enzymes and applications. *Curr Opin Biotechnol* **16**: 308-314.

van Beilen, J.B., Kingma, J., and Witholt, B. (1994) Substrate specificity of the alkane hydroxylase system of *Pseudomonas oleovorans* GPo1. *Enzyme Microb Technol* **16**: 904-911.

Van Beilen, J.B., Li, Z., Duetz, W.A., Smits, T.H.M., and Witholt, B. (2003) Diversity of alkane hydroxylase systems in the environment. *Oil Gas Sci Technol* **58**: 427-440.

van Beilen, J.B., Funhoff, E.G., van Loon, A., Just, A., Kaysser, L., Bouza, M. et al. (2006) Cytochrome P450 alkane hydroxylases of the CYP153 family are common in alkane-degrading eubacteria lacking integral membrane alkane hydroxylases. *Appl Environ Microbiol* **72**: 59-65.

Vangnai, A.S., and Arp, D.J. (2001) An inducible 1-butanol dehydrogenase, a quinohaemoprotein, is involved in the oxidation of butane by *Pseudomonas butanovora*. *Microbiology* **147**: 745-756.

Vangnai, A.S., Arp, D.J., and Sayavedra-Soto, L.A. (2002) Two distinct alcohol dehydrogenases participate in butane metabolism by *Pseudomonas butanovora*. *J Bacteriol* **184**: 1916-1924.

Veenstra, T.D., Conrads, T.P., and Issaq, H.J. (2004) What to do with "one-hit wonders"? *Electrophoresis* **25**: 1278-1279.

Vestal, J.R., and Perry, J.J. (1969) Divergent metabolic pathways for propane and propionate utilization by a soil isolate. *J Bacteriol* **99**: 216-221.

Vogel, T.M., Criddle, C.S., and McCarty, P.L. (1987) ES Critical Reviews: Transformations of halogenated aliphatic compounds. *Environ Sci Technol* **21**: 722-736.

Vorholt, J. (2002) Cofactor-dependent pathways of formaldehyde oxidation in methylotrophic bacteria. *Arch Microbiol* **178**: 239-249.

Vorholt, J.A., Chistoserdova, L., Stolyar, S.M., Thauer, R.K., and Lidstrom, M.E. (1999) Distribution of tetrahydromethanopterin-dependent enzymes in methylotrophic bacteria and phylogeny of methenyl tetrahydromethanopterin cyclohydrolases. *J Bacteriol* **181**: 5750-5757.

Wackett, L.P. (2002) Mechanism and applications of Rieske non-heme iron dioxygenases. *Enzyme Microb Technol* **31**: 577-587.

Wackett, L.P., Brusseau, G.A., Householder, S.R., and Hanson, R.S. (1989) Survey of microbial oxygenases: trichloroethylene degradation by propane-oxidizing bacteria. *Appl Environ Microbiol* **55**: 2960-2964.

Walti, A. (1934) Action of *Aspergillus Niger* on normal 1,2-diols. *J Am Chem Soc* **56**: 2723-2726.

Wang, Z.X., Bramer, C.O., and Steinbuchel, A. (2003) The glyoxylate bypass of *Ralstonia eutropha*. *FEMS Microbiol Lett* **228**: 63-71.

Watanabe, S., and Takada, Y. (2004) Amino acid residues involved in cold adaptation of isocitrate lyase from a psychrophilic bacterium, *Colwellia maris*. *Microbiology* **150**: 3393-3403.

Wegener, W.S., Reeves, H.C., Rabin, R., and Ajl, S.J. (1968) Alternate pathways of metabolism of short-chain fatty acids. *Bacteriol Rev* **32**: 1-26.

West, A.E., and Schmidt, S.K. (1999) Acetate stimulates atmospheric CH_4 oxidation by an alpine tundra soil. *Soil Biol Biochem* **31**: 1649-1655.

White, O., Eisen, J.A., Heidelberg, J.F., Hickey, E.K., Peterson, J.D., Dodson, R.J. et al. (1999) Genome sequence of the radioresistant bacterium *Deinococcus radiodurans* R1. *Science* **286**: 1571-1577.

Whiticar, M.J. (1994) Correlation of natural gases with their sources. In *The petroleum system - from source to trap*. Magoon, L.B., and Dow, W.G. (eds). Tulsa: AAPG, pp. 261-283.

Wieczorek, A.S., Drake, H.L., and Kolb, S. (2011) Organic acids and ethanol inhibit the oxidation of methane by mire methanotrophs. *FEMS Microbiol Ecol* **77**: 28-39.

Wierenga, R.K., Terpstra, P., and Hol, W.G.J. (1986) Prediction of the occurrence of the ADP-binding βαβ-fold in proteins, using an amino acid sequence fingerprint. *J Mol Biol* **187**: 101-107.

Wood, A.P., Aurikko, J.P., and Kelly, D.P. (2004) A challenge for 21st century molecular biology and biochemistry: what are the causes of obligate autotrophy and methanotrophy? *FEMS Microbiol Rev* **28**: 335-352.

Wood, W.A., Fetting, R.A., and Hertlein, B.C. (1962) Gluconic dehydrogenase from *Pseudomonas fluorescens*. *Methods Enzymol* **5**: 287-291.

Woods, N.R., and Murrell, J.C. (1989) The metabolism of propane in *Rhodococcus rhodochrous* PNKb1. *J Gen Microbiol* **135**: 2335-2344.

Wuebbles, D.J., and Hayhoe, K. (2002) Atmospheric methane and global change. *Earth-Sci Rev* **57**: 177-210.

Xin, J.-Y., Cui, J.-R., Chen, J.-B., Li, S.-B., Xia, C.-G., and Zhu, L.-M. (2003) Continuous biocatalytic synthesis of epoxypropane using a biofilm reactor. *Process Biochem* **38**: 1739-1746.

Xu, H.H., Janka, J.J., Viebahn, M., and Hanson, R.S. (1995) Nucleotide sequence of the *mxcQ* and *mxcE* genes, required for methanol dehydrogenase synthesis in *Methylobacterium organophilum* XX: a two-component regulatory system. *Microbiology* **141**: 2543-2551.

Yoon, S., Im, J., Bandow, N., DiSpirito, A.A., and Semrau, J.D. (2010) Constitutive expression of pMMO by *Methylocystis* strain SB2 when grown on multi-carbon substrates: implications for biodegradation of chlorinated ethenes. *Environ Microbiol Rep*: (in press) doi:10.1111/j.1758-2229.2010.00205.x.

Yu, Y., Ramsay, J.A., and Ramsay, B.A. (2009) Production of soluble methane monooxygenase during growth of *Methylosinus trichosporium* on methanol. *J Biotechnol* **139**: 78-83.

Yum, D.Y., Lee, Y.P., and Pan, J.G. (1997) Cloning and expression of a gene cluster encoding three subunits of membrane-bound gluconate dehydrogenase from *Erwinia cypripedii* ATCC 29267 in *Escherichia coli*. *J Bacteriol* **179**: 6566-6572.

Yurkov, V.V., and Beatty, J.T. (1998) Aerobic anoxygenic phototrophic bacteria. *Microbiol Mol Biol Rev* **62**: 695-724.

Zahn, J.A., Bergmann, D.J., Boyd, J.M., Kunz, R.C., and DiSpirito, A.A. (2001) Membrane-associated quinoprotein formaldehyde dehydrogenase from *Methylococcus capsulatus* Bath. *J Bacteriol* **183**: 6832-6840.

Zamboni, N., and Sauer, U. (2009) Novel biological insights through metabolomics and ^{13}C-flux analysis. *Curr Opin Microbiol* **12**: 553-558.

Zealey, G.R., Loosmore, S.M., Yacoob, R.K., Cockle, S.A., Boux, L.J., Miller, L.D., and Klein, M.H. (1990) Gene replacement in *Bordetella pertussis* by transformation with linear DNA. *Bio/Technology* **8**: 1025-1029.

Zhang, M., and Lidstrom, M.E. (2003) Promoters and transcripts for genes involved in methanol oxidation in *Methylobacterium extorquens* AM1. *Microbiology* **149**: 1033-1040.

Zhou, D., and Yang, R. (2006) Global analysis of gene transcription regulation in prokaryotes. *Cell Mol Life Sci* **63**: 2260-2290.

Zimov, S.A., Schuur, E.A.G., and Chapin, F.S. (2006) Permafrost and the global carbon budget. *Science* **312**: 1612-1613.

Zobell, C.E. (1946) Action of microorganisms on hydrocarbons. *Microbiol Mol Biol Rev* **10**: 1-49.